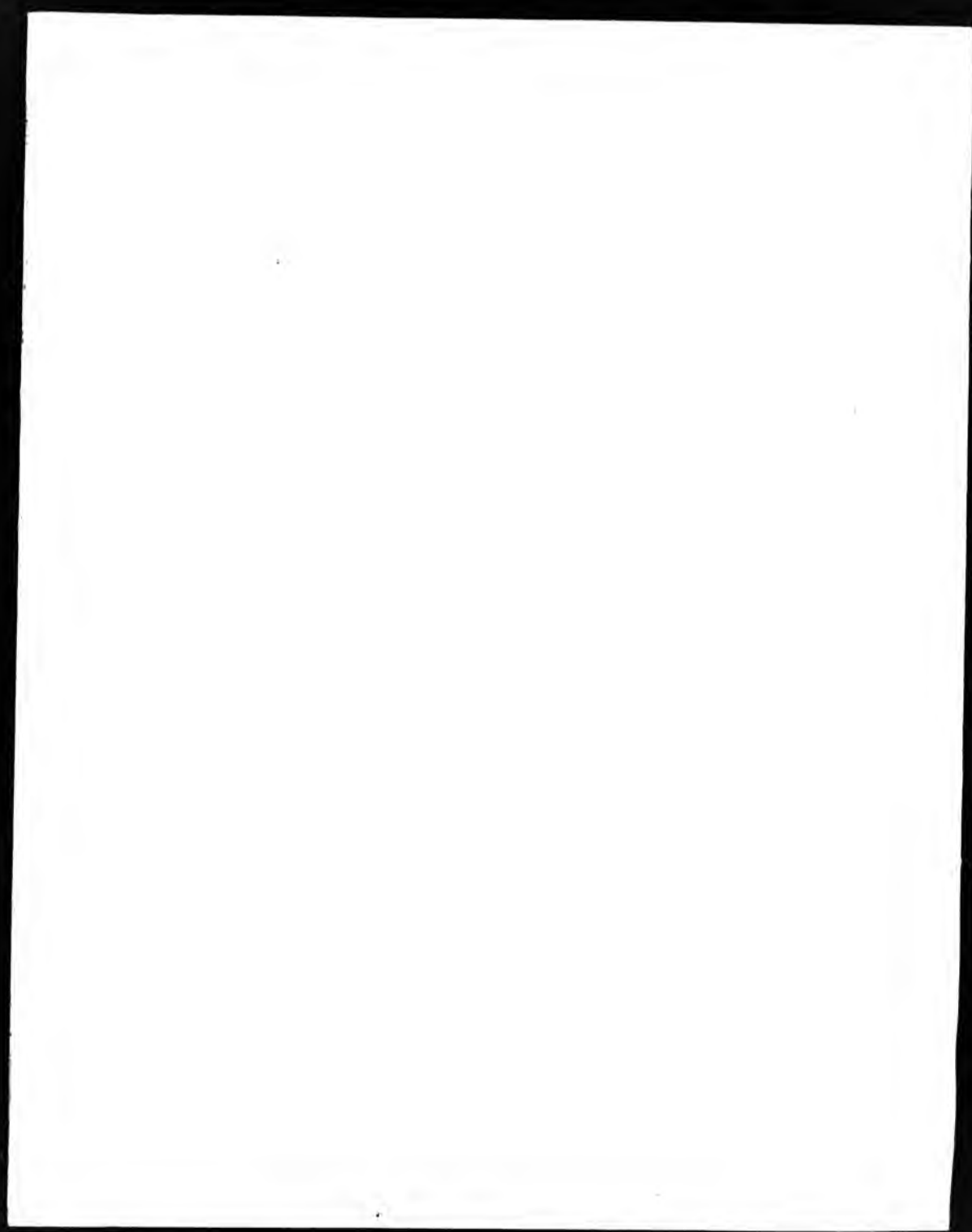
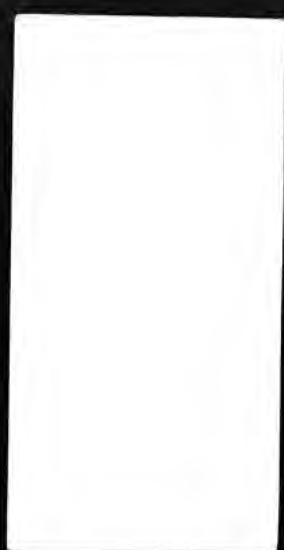


**This PDF was created from the British Library's microfilm copy of the original thesis. As such the images are greyscale and no colour was captured.**

**Due to the scanning process, an area greater than the page area is recorded and extraneous details can be captured.**

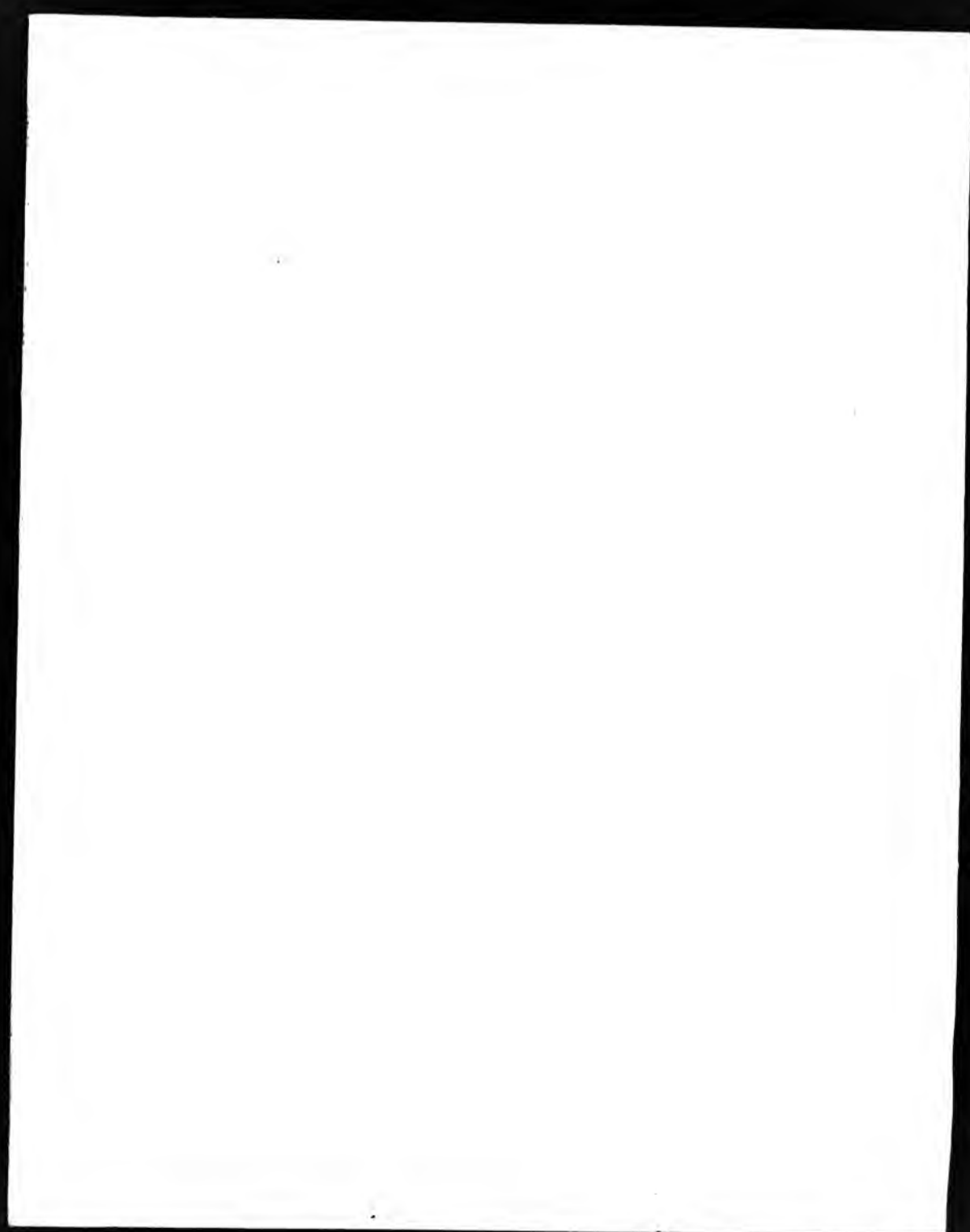
**This is the best available copy**





**DX**

**87720**





**THE BRITISH LIBRARY DOCUMENT SUPPLY CENTRE**

**TITLE** STRUCTURAL BASIS FOR THE DESIGN OF SELECTIVE COMPLEXING  
AGENTS FOR TRANSITION METALS.

**AUTHOR** Laurel .A. Drummord

**INSTITUTION and DATE** NORTH LONDON POLYTECHNIC  
C N A A 1989

Attention is drawn to the fact that the copyright of this thesis rests with its author.

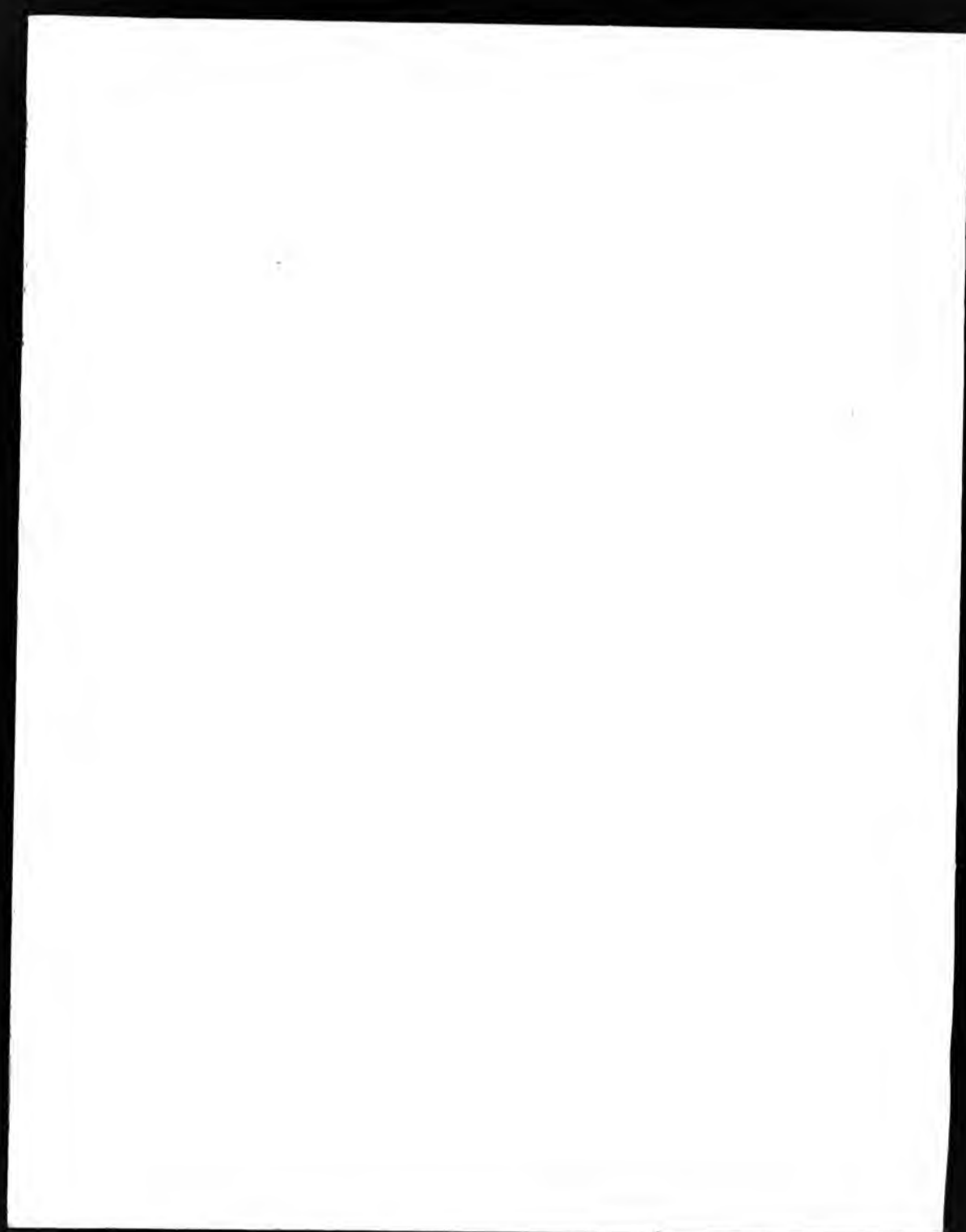
This copy of the thesis has been supplied on condition that anyone who consults it is understood to recognise that its copyright rests with its author and that no information derived from it may be published without the author's prior written consent.

1	2	3	4	5	6
cms					

THE BRITISH LIBRARY  
DOCUMENT SUPPLY CENTRE  
Boston Spa, Wetherby  
West Yorkshire  
United Kingdom

REDUCTION X 20

CAMERA 5



STRUCTURAL BASIS FOR THE DESIGN OF SELECTIVE COMPLEXING  
AGENTS FOR TRANSITION METALS.

A thesis submitted to the  
Council of National Academic Awards  
in partial fulfilment of the requirements  
for the degree of

Doctor of Philosophy

by

Laurel .A. Drummond

April 1989

The work described in this thesis was carried out in the School of  
Chemistry at the Polytechnic of North London, with collaboration from  
ICI Ltd (Organics Division).

1

Structural basis for the design of selective complexing agents  
for transition metals.

L.A. Drummond.

ABSTRACT

X-ray crystallographic analyses of a group of salicylaldehyde ligands, and their copper(II) complexes were carried out. The three of the copper(II) complexes studied, bis-(2-hydroxy-5-methylbenzaldehydeoximate)copper(II),  $[(L1)_2Cu]n$ , bis-(2-hydroxy-5-methylbenzophenoneoximate)copper(II),  $[(L5)_2Cu]$  and bis-(2-hydroxy-3-t-butyl-methylbenzaldehydeoximate)copper(II),  $[(L7)_2Cu]$ , existed as centrosymmetric molecules, with the copper atom at crystallographic inversion centre. Two bidentate ligands produce a planar arrangement of donor atoms around the copper. The molecules resemble macrocyclic systems, due to effective intramolecular hydrogen bonding linking the two ligands.

To correlate chelating properties with intramolecular H-bond strengths an X-ray structural analysis was carried out on one ligand supplied by ICI, and thought to be 3,5-dimethyl-2-hydroxy acetophenone methoxyimine. Unexpectedly the molecule was found to be 3,5-dimethyl-4-hydroxy acetophenone methoxyimine. This was successful in explaining the anomalously low efficiency of extraction for copper(II), shown by the related n-nonyl oxime ligand.

It is thought that the presence of syn and anti isomers in 2-hydroxybenzophenone oximes accounts for the low efficiency of copper extraction shown by reagents which contain this chelating unit. The syn and anti forms, of 2-hydroxy-5-methylbenzophenone oxime (L5H), were prepared separately. Significantly both forms appear to yield  $[(L5)_2Cu]$  when treated with  $Cu(CH_3CO_2)_2 \cdot H_2O$  in a homogeneous solution, although there are indications that formation of the complex from the syn-form is slower.

Selectivity of complexation of metal ions by macrocyclic ligands were investigated. The stability constant data of zinc(II) and cadmium(II) complexes of a series of cyclic quadridentate ligands were compared. For the 15-membered N4 macrocyle L15, the propyl (L15p) and butyl (L15b) C-alkylated derivatives were synthesised for the first time, and the cadmium(II) complex of (L15b) was prepared. X-ray analysis were performed on the free ligand L15b, and the three metal complexes  $[Zn(L15)(NO_3)(H_2O)]NO_3$ ,  $[Cd(L15)(NO_3)]NO_3$ , and  $[Cd(L15b)(NO_3)]NO_3$ . These results were then correlated with the results of stability constant measurements in discussing the probable behaviour of the ligands in the solution environment and hence to provide some insight into the effect of alkylation on the discrimination for zinc(II) over cadmium(II). The discrimination for zinc over cadmium is decreased on alkylation and the reason for this is discussed.



2

"You're not doing it for yourself but for your children....." A.C

Dedicated to Love-brings-happiness, - Ifetayo.

PREFACE.

While registered as a candidate for this degree for which submission is made, the author has not been a registered candidate for another award of the CNNA or of a University during the research programme. The results and conclusions represent original work by the author unless special reference is made.

4

ACKNOWLEDGEMENTS.

I would like to express my deepest gratitude to my supervisors Dr Peter Tasker and Dr Mary McPartlin, for their suggestion of the topic, useful discussions, and for their never lapsing support and encouragement throughout.

I would like to thank Dr Kim Henrick not only for his many hours of patient assistance with the Crystallography, but also for helping me to express myself more fully by creating many "fun periods" during the working day.

I would like to thank my external collaborators such as Drs Ray Price and Ray Dalton from ICI. Professor Len Lindoy and his team of workers at James Cook University, for the many useful discussions and experimental support.

I would like to thank the Polytechnic of North London (PNL), for the Research Assistantship. This thanks is also extended to other academic and non-academic staff in the School of Chemistry for their assistance and the enjoyable moments we shared at PNL.

Many thanks, to my parents without whom this work would not have been possible. To the rest of the family and good friends, in particular Varina for the final stages of proof reading and to Adlin and her mother for family support. Last but by no means least I would like to give a very special thanks to Eden for his encouragement, support and assistance throughout.

## CONTENTS

Chapter 1	Overall introduction to the thesis.	
1.1	Aim of this project.	6
1.2	Naturally occurring metal complexes.	6
1.3	Selective complexation.	7
1.4	Criteria for studying selective binding.	7
1.5	The macrocyclic effect.	8
	1.5.1 The controversy.	10
1.6	Structure activity relationships including the role of hydrogen-bonding.	13
	1.6.1 Ion carriers.	13
	1.6.2 Channel formers.	15
	1.6.3 Molecular models for biological chelating ligands.	15
1.7	Thesis layout.	16
Chapter 2	Hydrometallurgical extraction models.	
2.1	Introduction to salicylaldoxime extraction reagents.	19
	2.1.1 The commercial significance of solvent extraction reagent.	19
	(i) The principle of the solvent extraction process as applied to metal extraction.	20
	(ii) The MAR Process.	21
	2.1.2 Salicylaldoximes as selective extraction reagents.	23

	(i) Requirements of a solvent extraction agent.	25
	(ii) Effects of substitution on extraction ability.	25
	(iii) Marketed reagents.	27
	2.1.3 The effects of substituents on stability constants.	28
	(i) Salicyaldoxime ligands.	29
	2.1.4 Related substituents effects in salicyclic acid donation.	30
	2.1.5 The proposed plan of work.	33
2.2	Results and discussion.	36
	2.2.1 X-Ray diffraction studies.	36
	2.2.2 Preparation of 2-hydroxy-5-methylbenzophenone oxime (L5H).	52
	2.2.2(a) Preparation of the precursor compounds.	55
	2.2.2(b) Preparation of the oxime mixture.	61
	2.2.3 Separation of the isomers of the oxime (L5H).	64
	2.2.3(a) Preston and Lublinska procedure.	64
	2.2.3(b) The method of Blatt.	68
	2.2.4 Preparation of the copper(II) complexes of Isomers A and Isomer B.	73
2.3	Experimental	
	2.3.1 General experimental techniques.	76
	2.3.2 Preparation of 2-hydroxy-5-methylbenzophenone oxime.	77
	(a) 4-Methylphenylbenzoate.	77
	(b) 2-Hydroxy-5-methylbenzophenone.	78
	(c) 2-Hydroxy-5-methylbenzophenone oxime.	78

	2.3.3 Preparation of the copper complexes.	79
2.4	Structure solution and refinement.	
	2.4.1 Bis-(2-hydroxy-5-methylbenzaldehyde-oximato)copper(II) [(L1) <sub>2</sub> Cu].	82
	2.4.2 Bis-(2-hydroxy-5-methylbenzophenone-oximato)copper(II) [(L5) <sub>2</sub> Cu].	84
	2.4.3 Bis-3-tertiarybutyl-(2-hydroxy-5-methylbenzaldehydeoximato)copper(II) [(L6) <sub>2</sub> Cu].	87
	2.4.4 3,5-Dimethyl-2-hydroxyacetophenone methoxyimine 'L7H'.	90
Chapter 3	Metal ion discrimination by macrocyclic ligands.	
3.1	Metal ion discrimination by macrocyclic ligands and its optimisation.	97
	3.1.1 Factors governing selectivity of macrocyclic ligands.	97
	3.1.2 Bonding cavity of rigid cyclic systems.	101
	3.1.3 Discrimination by structural dislocation.	108
	3.1.3(i) The influence of alkyl substituents on discrimination by structural dislocation for ligands with N <sub>2</sub> O <sub>3</sub> -donor sets.	110
	3.1.4 Molecular mechanics calculations.	112
	3.1.5 Aim of this section of the thesis.	113
3.2	Results and discussion.	
	3.2.1 Preparation of C-alkylated derivatives.	117
	3.2.2 Stability constants data for the N <sub>4</sub> -C-alkylated ligands.	121
	3.2.2(i) Further discussions relating to the	

	stability constant data.	129
	3.2.3 Description of X-ray structures.	132
	3.2.3(i) The structure of $[\text{Zn}(\text{L15})(\text{NO}_3)(\text{H}_2\text{O})](\text{NO}_3)$ .	134
	3.2.3(ii) The structure of $[\text{Cd}(\text{L15})(\text{NO}_3)](\text{NO}_3)$ .	139
	3.2.3(iii) The structure of $[\text{Cd}(\text{L15b})(\text{NO}_3)](\text{NO}_3)$ .	139
	3.2.3(iv) The structure of the 'free' ligand L15b.	
	3.2.4 Overall comparison of the structures.	148
	3.2.4(i) The co-ordination geometry of the metal structures.	151
	3.2.4(ii) Nitrate co-ordination to the metals ions.	156
	3.2.4(iii) Torsion angles for these structures.	159
	3.2.4(iv) The 'hole-size'.	161
	3.2.5 Description of the stability results in terms of the structure analyses.	164
	3.2.6 Outstanding X-ray and synthetic results.	168
	3.2.6(i) X-ray analysis of L15 'free' ligand.	168
	3.2.6(ii) Preparation of the ethyl $\text{N}_2\text{O}_2$ 15-membered 'free' ligand.	169
3.3	General methods in the C-alkylation of the 15-membered diimine by the addition of Grignard reagent.	174
	3.3.1 Analytical data for ligand L15p.	174
	3.3.2 Analytical data for ligand L15b.	174
	3.3.3 Preparation of $[\text{Cd}(\text{L15b})(\text{NO}_3)](\text{NO}_3)$ .	175
3.4	Structure solution and refinement.	176
	3.4.1 The 'free' ligand L15b.	176
	3.4.2 $[\text{Cd}(\text{L15b})(\text{NO}_3)](\text{NO}_3)$ .	176

Chapter 4	The X-ray structure determination methods.	
4.1	Data collection.	184
4.2	The phase problem.	186
4.3	Methods used to solve the phase problem.	187
	4.3.1 Patterson synthesis.	188
	4.3.2 Direct methods.	189
4.4	Fourier synthesis.	192
4.5	Refinement.	193
Chapter 5	References.	195
APPENDIX.	Supplementary Crystallographic Data.	214



CHAPTER 1 Overall Introduction to thesis.

## 1. Overall introduction to the thesis.

### 1.1 Aim of this project.

Most work to date on the design of selective complexing agents has involved the study of group IA and IIA metal ions.<sup>1,2</sup> The work in this thesis, is one aspect of work that attempts to redress the balance by considering features of ligand design which lead to selectivity of complexation for d-block metals; it investigates copper(II) selectivity and discrimination between zinc(II) and cadmium(II).

### 1.2 Naturally occurring metal complexes.

Over the last decades investigations paying particular attention to biologically important substances such as proteins show that many of these compounds have co-ordination metal species in their active site. These compounds are collectively known as the metalloproteins. Their behavioural properties and activities are not only dependent on the organic structure present, but are also very dependent on the nature of the attached metal ions. In many cases, such as haemoglobin, the metal ion is held in the cavity of several donor atoms which together define a macrocyclic ligand.

Synthetic macrocycles have been used as models to study the properties of their biologically active counterparts.<sup>3,6</sup> In doing so a whole new area of chemistry has emerged because it has been shown that these synthetic compounds have far greater applications than as models in academic studies. Conjugated systems of the corrin type, for example

phthalocynine complexes, which were used to investigate the activity of vitamin B<sub>12</sub> and its co-enzyme, are now also being developed for use in the next generation of integrated circuits. This is being done because they exhibit unidirectional conduction properties, similar to organic photoconductors.<sup>7-11</sup> It is this property which can be exploited by the electronic industry. It arises due to the planarity of the molecules allowing delocalisation of electrons over a large area.

### 1.3 Selective complexation.

The most important relevance of naturally occurring metal complex to this work is the demonstration of the ability of the bound polydentate ligands to act as selective complexing agents. Selective recognition of metal ions by organic substrates has a wide variety of applications, and there are several areas in which such selectivity is required. Some of these are, ion storage and transport in vivo, treatment of metal poisoning, chemotherapy,<sup>12-15</sup> ion selective electrodes,<sup>16,17</sup> and industrial processes such as hydrometallurgy, the field directly related to this thesis. (see Section 2)

### 1.4 Criteria for studying selective binding.

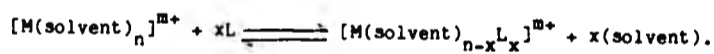
As part of a program to design ligands which show preferential binding to certain metal ions, factors affecting complex formation must be considered. Selectivity can be achieved by varying certain parameters of the ligands, such as atom type, the number of atoms present in forming the chelate or macrocyclic ring (ring size), and the number of atoms donated by the polydentate ligand to the metal ions.<sup>18</sup>

complexation as compared to open chain analogues. This is called the macrocyclic effect and is an extension of the chelate effect.

#### 1.5 The macrocyclic effect.

The origins of the macrocyclic effect are still controversial and the thermodynamics of complexation must be considered.

Formation of metal complexes by displacement of co-ordinated solvent molecules usually occurs in several steps, e.g. for a monodentate ligand L the equilibrium for the first step can be written:-



For the first step when a ligand displaces one molecule of solvent the stepwise stability constant is referred to as  $K_1$ :-

$$K_1 = \frac{[M(\text{solvent})_{n-1}L]^{m+}}{[M(\text{solvent})_n]^{m+} \cdot [L]}$$

and is general for replacement of the nth molecules of solvent the nth stepwise stability constant  $K_n$ :-

$$K_n = \frac{[ML_n]^{m+}}{[M(\text{solvent})_{n-1}]^{m+} \cdot [L]^n}$$

For many of the complexes of interest in this thesis and for those found by ligands responsible for metal ion transport in vivo, macrocyclic ligands are involved and give 1:1 complexes. As a result stabilities for these systems can be compared directly using values of  $K_1$  or  $\log K_1$ .

As mentioned above selectivity is not only based on the nature of the ligand, but is also very dependent on the nature of the metal ions involved. The latter is related to the size and charge of the metal ions, and the type of bonding which occurs on complexation. For transition metals, selectivity by a particular ligand towards those metals carrying the same charge can be predicted by looking at the Irving-Williams series,<sup>19,20</sup> where crystal field stabilisation energy is a contributing factor. The stability of the coordinate bond formed between the Lewis acid and base relates to the electronegative properties of the reacting species. This is commonly summed up in a simplified statement known as the "hard-soft, acid-base"<sup>21-23</sup> generalisation, and can be used as a qualitative method for looking at selectivity of complex formation.

A criterion is required to assess selectivity of the co-ordination species. One major criterion used is to determine the thermodynamic stability of the complex produced by measuring its formation constant ( $B_n$ ). This is the expression of all the stepwise formation constants involved in the production of the complex at equilibrium. This overall stability constant, is:-

$$B_n = K_1 \cdot K_2 \cdot K_3 \cdot K_4 \cdot \dots \cdot K_n$$

A comprehensive guide to relative stabilities based on this criterion is provided by Angelici<sup>24</sup> and Hartley et.al,<sup>25</sup> where the nature of both the metal ions and the ligand parameters are taken into consideration. In these reviews they touch upon a topic which was initially proposed by Cabbiness and Margerum,<sup>26</sup> i.e. enhancement of the thermodynamic stability constant when macrocyclic ligands are involved in

Applying the thermodynamics relating to equilibria:-

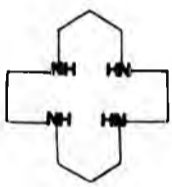
$$\Delta G = -RT \log K = \Delta H - T \Delta S$$

it can be seen from the above equation that both enthalpy( $\Delta H$ ) and entropy( $S$ ) changes during complex formation will affect the stability of the reaction product. A controversy exist as to which of these factors (ie  $H$  or  $S$ ) contributes the most to the macrocyclic effect.

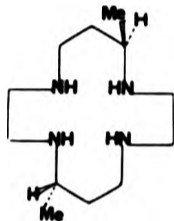
#### 1.5.1 The controversy.

Tetraamines of the type shown in Figure 1.5 (a) and (b) have been subject of much studies. Working on the cyclam systems, Hinz and Margerum<sup>27</sup> found that the stability constant of the macrocycle had increased 106-times greater than its open chain analogue. This increase (the macrocyclic effect), they suggested was due almost entirely with the more favourable enthalpy term associated with the the macrocyclic complex formation, i.e. the enthalpic changes between the cyclic and non-cyclic ligand solvation during complexation. They go on to say that the configurational entropy associated with the macrocyclic complexation reaction, would offset the fact that less solvent will be released by this type of ligand. Kimoda and Kimura<sup>28</sup> from polarographic studies on the cyclic ligand shown in Figure 1.5 (b), suggest that the macrocyclic effect can be accounted for solely from entropy factors. Paoletti, Clay et.al,<sup>29</sup> like Margerum and Hinz, think that the enthalpy term is the significant contributor to the macrocyclic effect, because the enthalpy term varies depending on the size of the cation to which the ligand reacts. Enhanced stability due to enthalpy would relate to the "hole size" provided by the macrocycle and "goodness of fit" when complexation occurs. These two factors have been investigated in the present work and will further be

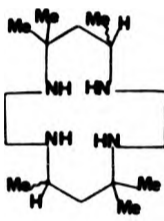
(a) Cyclams



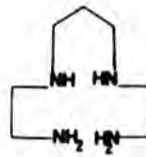
(CYLAM)  
14-ane-0S  
1,4,8,11-tetraazacyclo-  
tetradecane



(Me<sub>2</sub>-CYLAM)  
Hexa-16-12-  
dimethyl-1,4,8,11-tetraazacyclo-  
tetradecane

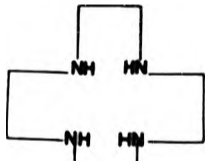


(tot-4/5)  
Hexa/He-5,7,7,10,10,10-  
hexamethyl-1,4,8,11-  
tetraazacyclotetradecane

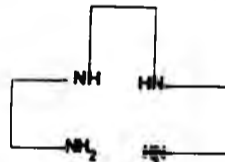


N,N'-bis(2-aminoethyl)-1,3-  
propanediamine

(b) Cyclans

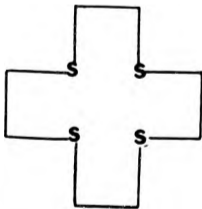


1,4,7,10-tetraazacyclododecane

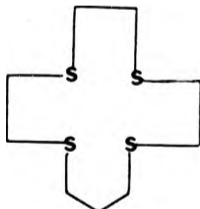


N,N'-bis(2-aminoethyl)-1,2-  
ethanediamine

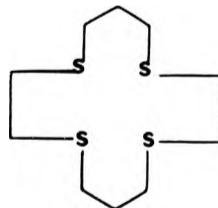
(c) Cyclic Polythia Ethers



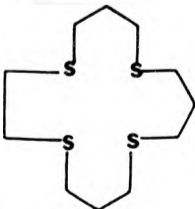
(12-ane 0S)  
1,4,7,10-tetrathia-12-crown-  
4



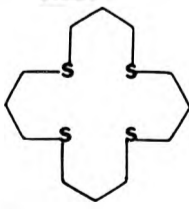
(13-ane 0S)  
1,5,9,10-tetrathia-13-crown-  
5



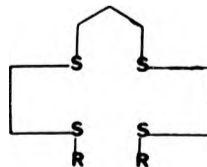
(14-ane 0S)  
1,4,8,11-tetrathia-14-crown-  
6



(15-ane 0S)  
1,4,8,12-tetrathia-15-crown-  
7



(16-ane 0S)  
1,5,10,13-tetrathia-16-crown-  
8



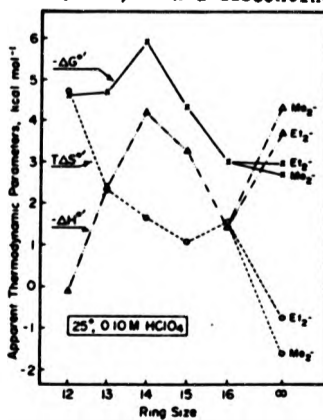
(R<sub>2</sub>-2,3,2 0S)

R = Me:-  
Me-2,5,9,12-tetrathiatridecane  
R = Et:-  
Et-3,6,10,13-tetrathiapentadecane

discussed in Section 3. Paoletti et.al,<sup>29</sup> also suggested that favourable entropy changes would occur both for the cyclic and non-cyclic ligands, but the difference in the solvation enthalpy, for those ligands, was possibly the primary contributor to the macrocyclic effect. Rorabacher<sup>30</sup> has recently applied thermodynamic arguments to thioethers, Figure 1.5 (c), similar to those of the cyclam and cyclen types, to further investigate the origins of the macrocyclic effects. From earlier work<sup>31,32</sup> he had shown that these polythioethers were not easily solvated in aqueous or polar solvents, and so their macrocyclic effect would be less dependent on the nature of the solvent in which their thermodynamic data were collected. In this research a qualitative measure of solvent and hydrogen-bonding effects, which contribute to tetraamine stability can be made by comparing the results for the nitrogen ligands with that from the tetrathioether study.<sup>30</sup> Rorabacher studied each ligand at a range of temperatures, while keeping constant perchlorate ion concentration, maximum stability was produced with the 14-ane Figure 1.5 (c), at all temperatures studied. He then went on to show that  $\Delta S$  decreased for the cyclic ligand as the ring size increased as the difference in entropy between the ligands were compared, with a discontinuity at 16-ane, Figure 1.5 (d).

**Figure 1.5(d)**

Thermo-dynamic parameters for the formation of copper(II) tetrathia ether complexes. Infinite ring size is represented by the open chain tetrathia ethers with terminal alkyl groups.





No difference in enthalpy values were seen between the open chain analogue and that of the most stable complex, 14-ane, Figure 1.5 (c). He concluded that this indicated that the macrocyclic effect is wholly attributable to a more favourable entropy associated with the less flexible cyclic ligand.

#### 1.6 Structure activity relationships including the role of hydrogen-bonding.

In biochemical processes it is well established that enzyme/substrate,<sup>33,34</sup> and antibody/antigen reactions are controlled by structural factors, and a relationship between structure and activity is not a unusual or an insignificant consideration. Studies on many naturally occurring co-ordination species show that their structures have a direct relevance to their biological activity. Many other examples of the importance of subtle features of ligand architecture in biological systems which lead to selectivity in complexation, transport and storage of metal ions, or to selectivity of catalysis by metal ions in metalloenzymes can be found.<sup>33,34</sup>

##### 1.6.1 Ion carriers.

Antibiotics often have complex structures; for example valinomycin, which is selective for potassium cations, is made up of a dodecadeptide sequence consisting of L-valine, L-lactate, and D-isovalerate. Stemyakin<sup>33</sup> and co-workers showed that the slightest change in the structure of the valinomycin molecule would result in loss of its biological activity, as judged by antibiotic or mitochondrial assay. The valinomycin peptide backbone loops to form a

bracelet type of arrangement and hydrogen-bonding is used to create this ordered secondary structure,<sup>35</sup> (see Figure 1.6). This caged structure entraps the cation, the peptide carbonyl groups present hydrogen-bond to the amide protons and this helps to enforce this structure when complexed. In the uncomplexed form some of the amide carbonyl groups, used in ligation, turn outwards and provide a pathway for the cation to enter the cage. The rigid structure conferred by the intra-molecular hydrogen-bonding enforces the specificity of valinomycin. Hence its selectivity towards potassium over sodium, because it has difficulties contracting to encapsulate the smaller sodium ion.

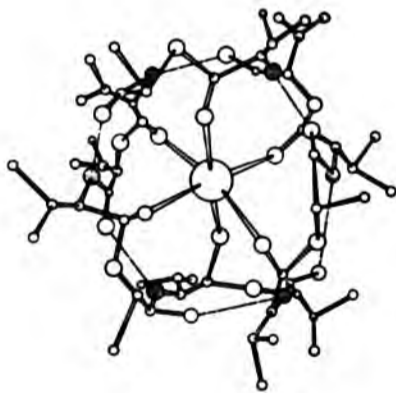


Figure 1.6

The potassium complex of valinomycin. Hydrogen bonds between the peptide carbonyl and the shaded -NH groups are represented by broken lines. The ether carbonyl atoms are octahedrally co-ordinated to the carbonyl atoms.

Secondary hydrogen-bonding is used to stabilize and re-enforce the structure of other ion-carriers such as the carboxylate anionic ionophores, monensin and nigericin.<sup>35</sup> Bonding occurs between the carbonyl groups at one end of the molecule with an hydroxy group at the other. In the above ion-carriers (including valinomycin) all the polar moieties are unavailable for further ligation. They are used either to bond to the metal ion, or are involved in hydrogen-bonding,

thus stabilizing the overall structure of the molecule. The hydrophobic portions of the molecule remain exposed and this increases the lipophilicity of the metal complex.

#### 1.6.2 Channel formers.

Gramicidins A is believed to dimerise<sup>36,37</sup> via hydrogen-bonding to form a helical structure, which runs from one end of a membrane to the other. Carbonyl groups form a channel along the helix and are used to convey cations across the membrane. The carbonyl groups are expected to move so that their oxygen atoms can co-ordinate to the cations in transit. Selectivity is achieved due to structural distortions which must occur during this process, and is greatest for the smallest ions,<sup>36</sup>  $[\text{NH}_4]^+ > \text{K}^+ > \text{Na}^+$  Hydrogen-bonding also occurs across the interior of the molecule, thus preventing multiligand complexation because no ring opening can take place. For this reason the gramicidin are called "channel formers" rather than "ion carriers" because they do not capture the metal ion and carry it across the membrane.

#### 1.6.3 Molecular models for biological chelating ligands.

Ligands such as dimethylglyoxime, phthalocynine, and others are useful models for the sophisticated corrinoids present in vitamin B<sub>12</sub> and its co-enzyme. These ligands emulate the corrinoids in that they are capable of forming cobalt alkyl complexes. Their similarities arise in that they provide planar equatorial sets of four donor atoms, either all N<sub>4</sub> or N<sub>2</sub>O<sub>2</sub> atoms, and are conjugated. The cobalt-carbon bond is formed with an alkyl group which occupies one of the axial positions in both the corrin systems and its models. It has been

suggested<sup>37-41</sup> that the planarity of these ligands provide a strong ligand field, and thus contribute to the kinetic stability of the cobalt-carbon bond. In the conjugate ligand antibonding orbitals may also be utilised in accomodating the extra charge that might be placed on the cobalt. It is also proposed that the property of the metal may be altered by the cobalt-carbon being only slightly polarised due to bonding of the equatorially placed ligand.

#### 1.7 Thesis layout.

The thesis is divided into two Sections, both are concerned with the metathetic reactions between metal and ligand, and a thermodynamic stability approach will be used to investigate the various aspects being studied in each Section.

The first part, Section 2, deals with the models of successfully marketed salicyclaldoxime derivatives which have been used as selective complexing agents in copper hydrometallurgy. The effects of substitution and conformation (syn/anti) isomerisation in the oximes, on their efficiency as extraction reagents, is considered in the light of detailed structural studies in the models by X-ray crystallography.

Factors which lead to discrimination between zinc and cadmium are investigated in the Section 3. Stability constant data are collected for both metals, using a series of structurally related quadridentate ligands. This approach as been used to assess how ligand discrimination varies as a function of a given type of ligand architecture for Zn/Cd cations. Where major differences in stability of the zinc and cadmium complexes are observed, structural analysis is

used in an attempt to understand the origins of such metal ion discrimination. The results may be of future use in attempts to "fine tune" the discrimination shown by a particular ligand type. It may be anticipated that this could then become part of an empirical procedure which would be used in designing selective complexing ligands.

Each Section will be largely self contained, and will include a relevant introduction, the experimental procedure, results and a discussion section.

CHAPTER 2 Hydrometallurgical extraction methods.

## 2.1 Introduction to salicylaldoxime extraction reagents.

The selective solvent extraction ability of a series of salicylaldoxime ligands for copper(II) ions has been investigated in collaboration with ICI Organics Division. The initial phase of the investigation involved some synthesis. An attempt to correlate structure with selective extraction for these ligands has been undertaken in the light of X-ray crystallographic structural analysis results.

### 2.1.1 The commercial significance of solvent extraction reagents.

Solvent extraction techniques for the winning of metals were first used in the 1940's in the production of uranium.<sup>42</sup> Since then these hydrometallurgical processes have become increasingly important in the winning of other metal ions from their ores. The major metals recovered using this process are copper, cobalt, nickel, zinc, uranium and rare earth metals. In 1968 the first commercial solvent extraction operation was used in the recovery of copper,<sup>43</sup> producing over 6000 tons per year, from low grade ores found in the Blue Bird Mines of Arizona. This process now accounts for over 300,000 tons of copper production per year.

With rising energy costs, environmental awareness and the inevitable depletion of high grade ores, hydrometallurgical methods have advantages over the traditional pyrometallurgical methods. In America and Sweden<sup>44</sup> where pollution laws are strictly enforced, hydrometallurgical processes are commercially used in effluent

treatment of mine waters, plating solution, sludges and scrap metals. These secondary sources for metal recovery could also be commercially exploited by other countries. When other new sources for metal recovery, such as Red sea mud, are considered, the old traditional processes for the winning of metals are also less favourable than solvent extraction techniques for the reasons described above. These factors in part account for the rapid expansion in the use of this technique for the winning of base metals. <sup>45-50</sup>

(1) The principle of the solvent extraction process as applied to metal recovery.

The principles involved in the production of metals by hydrometallurgy are based on those of physical, analytical and inorganic chemistry and of electrochemistry, extended to industrial scales.

The first stage is the leaching stage which involves dissolving the metal containing material (ie ore, sludge, etc) into a suitable aqueous phase which could be either water alone, or with added reagent. The metal is then separated by mixing the aqueous phase with an immiscible organic solvent containing an organic reagent. On reacting with the metal a complex is formed which is more soluble in the organic phase. The metal is then recovered by mixing this organic phase with a new aqueous phase known as the strip solution. The composition of the second aqueous phase is such that it cleaves the bonds between the metal and the ligand (organic reagent) releasing the metal back into the aqueous solution in a pure form. This whole stage is known as the stripping phase of the operation. The metal is then removed from the strip liquor using chemical or electrolytic means.

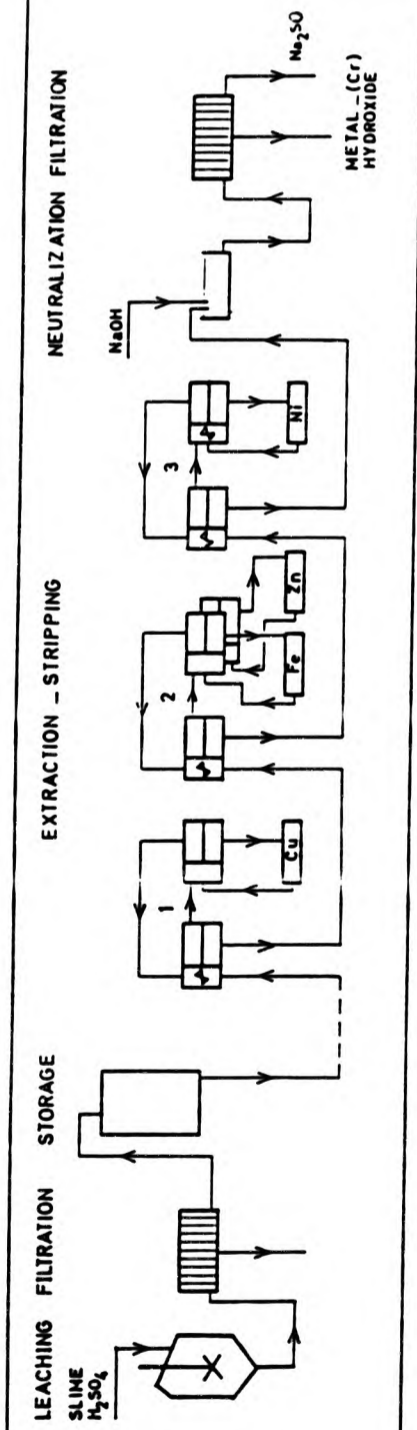


(ii) The MAR process

One commercial process which is used for the recovery of metals is known as the MAR (metal and acid recovery)<sup>51-53</sup> process (see Figure 2.1.1), and is of particular relevance to the work in this project. Using three extraction and stripping steps the metals copper, zinc, iron, nickel and chromium are separated.

Initially a hydroxide slime from differing sources is leached using sulphuric acid to produce a weakly acid metal sulphate solution. The solution is separated from insoluble compounds by filtration. This is followed by extraction and stripping stages, where each metal is in turn separated by changing the organic complexing agents of the kerosene organic phase. Copper is removed in the first stage using a General Mills chemical known as 'LIX 64N' (a mixture of hydroxy aromatic and hydroxy aliphatic oximes). The next stage is the removal of iron and zinc using kerosene containing HDEHP reagent (an organo-phosphoric acid derivative). In varying the stripping process at this stage the separation of these two metal ions is achieved. Next 'MX-200' (a tertiary amine derivative), is added to kerosene. This reagent is selective to nickel over chromium in the absence of copper, iron and zinc. The residual leach liquor would then contain chromium and maybe small amounts of other metals. On neutralisation, these residual metals form hydroxy salts and can then be filtered off, leaving the drainage water free from metal ions. Organic components remaining at this stage are also removed from the drainage water due to adsorption onto the precipitates. Thus most potential pollutants from the drainage water are removed.

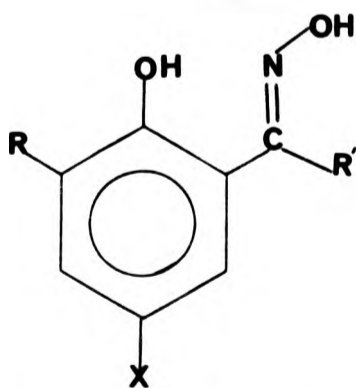
Figure 2.1.1.1 The M A R Process



### 2.1.2 Salicylaldoximes as selective extraction agents.

In view of the advantages of hydrometallurgical methods (see above) there now exists a need for solvent extractants for a wide range of metals. Since most ores contain complex mixtures of metals it is important that these extractants should show a high degree of selectivity towards a particular metal ion. ICI has successfully marketed a range of 5-nonyl-2-hydroxybenzaloxime extractants capable of extracting copper ions from aqueous sulphate leaches, similar to 'LIX 64N' used in the MAR process. These are based on salicylaldoxime ligands of the general type shown below where the nature of the R, R' substituents are varied.

#### Salicylaldoximes Ligand



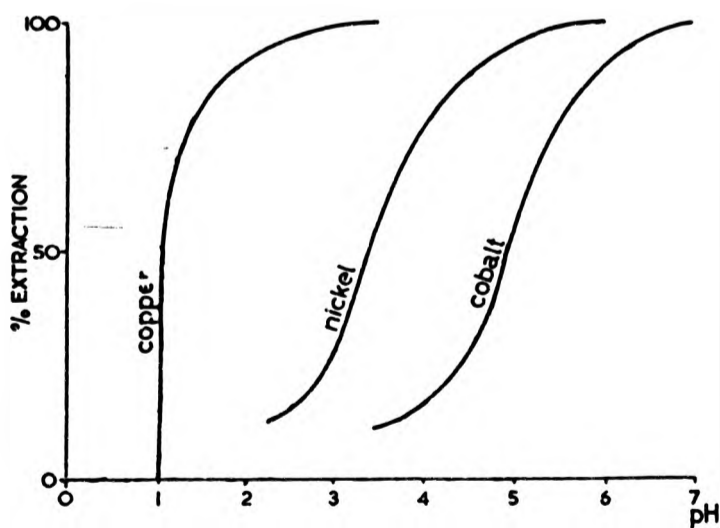
X = C<sub>9</sub>H<sub>19</sub> in ICI ligands.

Separation of the metals can be achieved by the consecutive extraction and stripping exemplified by the MAR process. In the first extraction stage where copper is removed from the leach solution, the factors controlling the selectivity of these extractants towards copper will

be considered below.

ICI and others have shown that the selective extraction ability of their marketed salicyaldoxime reagents towards copper over other metals is very dependent on pH,<sup>54-57</sup> (see Figure 2.1.2 (a)). Copper is extracted between pH 1-2, but other first row transition metals ions are not; by lowering the pH further to less than 1, stripping of the copper back into the aqueous phase, is achieved.

Figure 2.1.2 (a) Extraction of divalent metal ions by 5-nonyl-2-hydroxy-benzaldoximes as a function of pH.



Hydrogen ions concentration is important, but it is by no means the major factor which explains the selective extraction property of the ligands, some others will be discussed in the next section, where the various requirements of an extractants along with those factors which affects the dynamics of an equilibrium will be considered.

(i) Requirements of a solvent extraction agent.

Certain features are desirable in a good extractant and are listed below. It should

- (a) be cheap, readily available and non-toxic simple in chemical composition and pure,
- (b) have good ability to extract, as measured by the up-take at equilibrium, per mole of extractant,
- (c) have a fast rate of loading as measured by the kinetics,
- (d) have a low vapour pressure and low flammability,
- (e) be low in viscosity both alone and when loaded,
- (f) have low solubility in the water phase,
- (g) be resistant to both temperature and chemical degradation,
- (h) readily allow the metal to be stripped from it.

(ii) Effects of substituents on extraction ability

As part of a programme to design improved extraction agents, the effects of substituents in salicylaldoxime ligands on their metal extraction abilities were considered by ICI.

At the start of this project, the effects of substituents on the

equilibrium position for the reaction, in a series of 5-nonyl-salicylaldoxime ligands (Table 2.1.2) were known to vary considerably. The equilibria to be considered for the reaction of these extractants towards copper in acidic conditions (written in a simplified form) is:-

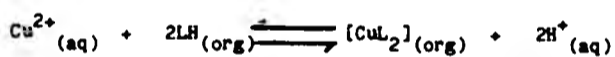
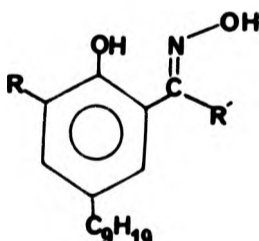
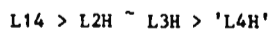


Table 2.1.2 Type of ligands used to study the above equilibrium.

	<u>LH</u>	<u>R</u>	<u>R'</u>
	L1H	H	H
	L2H	H	CH <sub>3</sub>
	L3H	H	C <sub>6</sub> H <sub>5</sub>
	'L4H'	CH <sub>3</sub>	CH <sub>3</sub>

For the series of ligands thought to have the above structures LH1-LH4 (Table 2.1.2) it was found that extraction ability decreased in the order:-

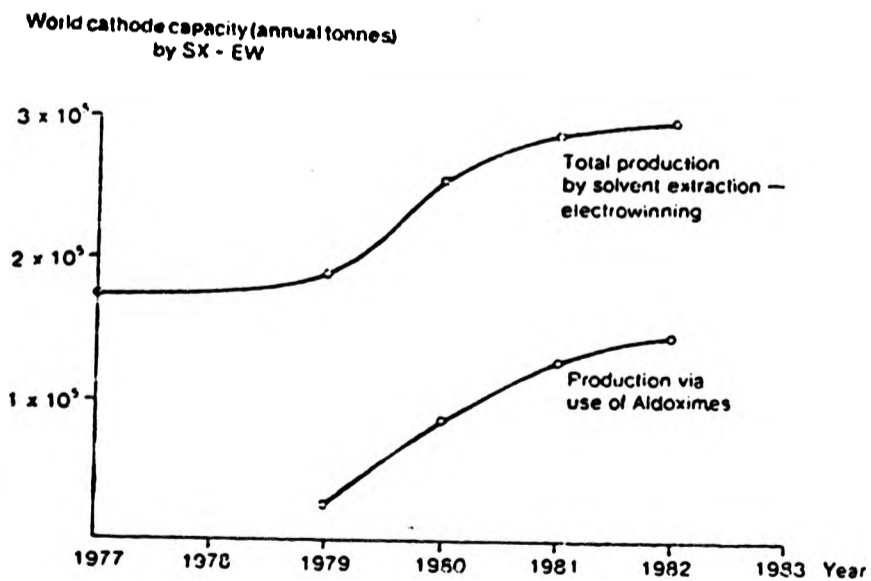


L1H was found to be a good extractant, but L2H L3H and L4H were less effective, and the reason for these marked differences in selectivity were not understood.

(iii) Marketed reagents.

As a result of these studies ICI has marketed <sup>61-63</sup> a new extractant reagent having L1H as the active ingredient. This aldoxime extractant has notable advantages over the original ketoxime reagents such as L1X 64N (active ingredients L3H), and their success is illustrated by Figure 2.1.2 (b), where it can be seen that extraction by this aldoxime ligand has doubled the production of copper.

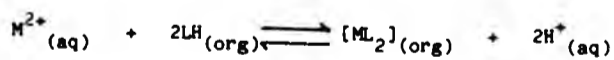
Figure 2.1.2 (b) Growth of world copper production using solvent extraction-electrowinning and compared proportion production by use of aldoxime extractants.



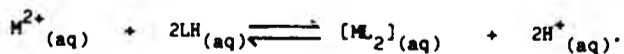
The advantages of using aldoximes of the type (LH, R'=H) rather than ketoximes such as (L3H, R'=C<sub>6</sub>H<sub>5</sub>) were recognised by ICI in the early 1970's. Difficulties were experienced in its commercialization due to its relatively poor stripping performance in the then existing plants; this is measured as the extractant transfer efficiency, defined as the amount of copper transferred between loading and stripping stages, and is expressed as a percentage of the maximum copper loading capacity of the extractant. The transfer efficiency of the ketoxime reagents were of the order 50-60% while those of the aldoxime were only 30%, showing that the aldoximes were being poorly utilized.

### 2.1.3 The effects of substituents on stability constants.

The observed dependence of a solvent extractant's efficiency on the substituents R' in the ligand backbone could involve several different factors. The kinetics and mechanisms of the process have been considered in a number of papers.<sup>64-69</sup> This project is mainly concerned with the influence of substituents on the extraction into the organic phase.



This in turn relates to the stability constant of the formation equilibrium of the metal complex in aqueous solution ie:-

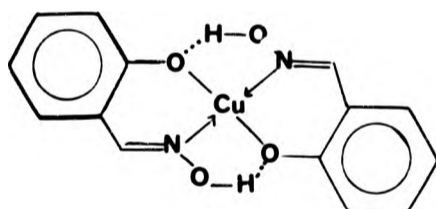


Complex stability is enhanced by the factors mentioned in Section 1.3.



(i) Salicylaldehyde ligands.

From X-ray crystallographic data reported on salicylaldehyde and related copper complexes, <sup>70-73</sup> their structures appear to be planar. They resemble macrocyclic compounds due to intra-molecular hydrogen-bonding thus enhancing the stability of the complex produced due to the "macrocyclic effect" (see section 1.5).

Structure of Bis-salicylaldehydato-copper(II)

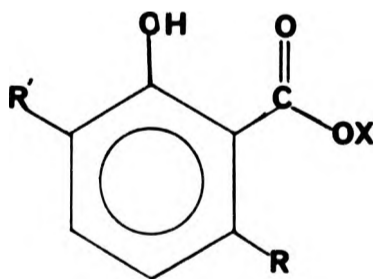
This planar configuration could contribute to the favourable selectivity of extraction of copper by salicylaldehydes. Other metals unable to adopt the planar co-ordination would be unable to benefit from this enhanced stability.

In this project the donor atom types are the same for all the ligands under consideration. Beside the ligand to metal  $\sigma$ -bonds, there exist metal to ligand  $\pi$ -bonds. It might be expected that metal-ligand stability would be affected by the nature of the substituents on the ligand, since changes in electron density on the donor atoms of the ligands would thus affect these bonds. Initial consideration on the effects of substituents and the extraction efficiency of each ligand (reported in Section 2.1.2, (ii)) could only partly be explained in these terms. <sup>74-79</sup>

2.1.4 Related substituents effects in salicylic acid donation.

Consequently it appeared that steric effects were the key factor in explaining the effects of substituents on the extraction ability in terms of the stability constant ( $\log \beta$ ) for the metal complex formation.

The first extensive study of steric effects on ring formation was conducted on a series of salicylic acids and some of their esters,<sup>80-82</sup> using infra-red spectroscopic data.

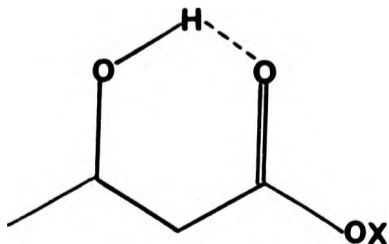


Basic structure

Salicylic acids ( $X = H$ )

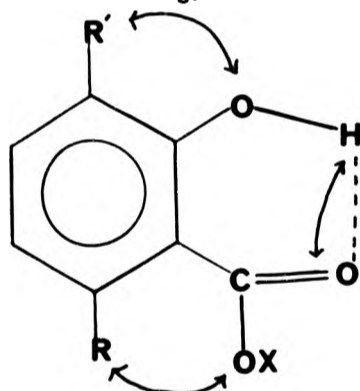
Salicylate esters ( $X = R$ )

The extent of intramolecular hydrogen bonding was judged by the shift (from a higher to lower wavenumber) in the hydroxy stretching



frequency, and is found to be greatly affected by the nature and

position of the substituents on the salicylates. A factor to be considered in interpreting these results is the influence of substituents on the planarity of the proton chelate produced. The conclusions drawn from these results were that bulkier substituents R and R' (ie in the 3 and 6 position of the salicylate) enhance the chelation possibly due to the steric constraints which compresses the bond angles in the chelate ring.



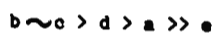
ICI's next step was to apply these results to the salicylaldehyde extraction agents, <sup>60</sup> infra-red studies were conducted on a series of methoxy-salicylaldehyde compounds (methoxyimines) Table 2.1.4.

Table 2.1.4 Series of methoxyimine used in i.r. study.

LH	R	R'	OH/cm <sup>-1</sup>
a	H	H	3250
b	H	CH <sub>3</sub>	3000
c	H	C <sub>6</sub> H <sub>5</sub>	3000
d	CH <sub>3</sub>	H	3210
e	CH <sub>3</sub>	CH <sub>3</sub>	3615

The methoxyimines were chosen because the phenolic hydroxy stretching

absorption could be more easily assigned than in the related oximes for which overlap of the phenolic and oxime OH bands is expected.<sup>83,84</sup> The results showed that the strength of hydrogen-bonding decreased in the order:-



with the dimethyl derivative e not showing any intramolecular hydrogen-bonding.

These results on the methoxyimine series correlated to that observed for the salicylate esters and acids (see above), in that the bulkier substituents at position 3 had lowered the position of the hydroxy stretching frequency, and had thus enhanced chelation. The results obtained from the hydrogen-bonding studies on the methoxyimine were unfortunately not useful in explaining the relative extraction ability of the oxime series discussed in Section 2.1.2 (ii). The methoxyimine analogue of the best extractant (L1H), contrary to expectations, did not form the strongest hydrogen-bond. If it is assumed that chelated hydrogen-bonding is a valid analogue for studying chelating ability, it appears that it is not changes in chelating ability that accounts for the variation in extraction in the oxime series.

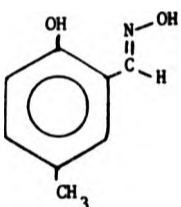
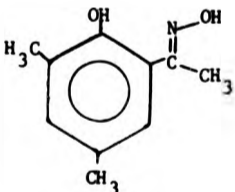
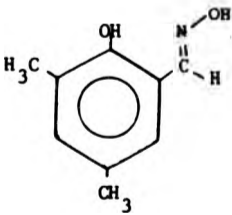
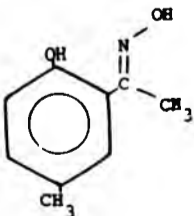
In contrast to substituent in the 3- and 6- positions it has been shown that substituents in the 5-position, (ie para to the phenolic hydroxy group), have no effect on the geometry or chelating properties of the donor atoms. This is exploited in the case of the salicylaldoxime marketed as as solvent extractants, where the long alkyl chain present in this position is used to increase the organic solubility of these compounds.

#### 2.1.5 The proposed plan of work

Variation in extraction ability could be due to minor structural variation resulting from differences in the steric properties of the substituents on the geometry of the chelate rings produced, and the co-ordination sphere of the copper. This work was undertaken to carry out structural determination of some of the ligands, so that effects of substitution on inter- and intramolecular hydrogen bonding could be established. The syn and anti forms of 2-hydroxy-5-methylbenzophenone oxime (L5H), were prepared separately to study the effects of conformation isomerisation on their efficiency as extraction reagents. The other ligands have been prepared previously, and samples were kindly supplied by ICI Organic Division. These materials were required for the preparation of the copper(II) complexes. Crystallisation of samples of ligands and their copper(II) complexes were to be carried out, so that crystals could be obtained which were suitable for X-ray structural analysis.

The Table 2.1.5 shows the range of oximes and related derivatives considered in this thesis.

2.1.5 Table of compounds obtained from ICI and their formal names and abbreviations.

<u>COMPOUND</u>	<u>NAME</u>	<u>CODE</u>
	2-hydroxy-5-methylbenzaldehyde oxime	L1H
	3,5-dimethyl-2-hydroxyacetophenone oxime	L2H
	3,5-dimethyl-2-hydroxybenzaldehyde oxime	L3H
	2-hydroxy-5-methylacetophenone oxime	L4H

## 2.1.5. Table continued

<u>COMPOUND</u>	<u>NAME</u>	<u>CODE</u>
	2-hydroxy-5-methylbenzophenone oxime	L5H
	3-tertiarybutyl-2-hydroxy-5-methylbenzaldehyde oxime	L6H
	3,5-dimethyl-2-hydroxyacetophenone methoxyimine	'L7H'

## 2.2 Results and discussion.

X-ray structure determination was performed on a selection of the O-hydroxy aryl oximes, Figure 2.1.5, copper(II) complexes, and analogous 'free' ligands, with the intention to see if any geometric differences existed between the structures of their copper complexes which might affect their extraction ability (Section 2.1.2). Structural analysis of two of the analogous 'free' ligands (L4H and L7H) were carried out in an attempt to provide evidence to explain the ambiguity in the H-bonding deduced from i.r. data discussed in Section 2.1.4. The X-ray results highlighted questionable factors related to the synthetic routes used for preparing these ligands, and therefore further synthetic work was undertaken. This work was intended to answer the question whether both the syn- and anti- isomer of L5H would complex with copper(II). This is an important consideration since a ligand closely related to L5H is actually used as an active component for a marketed reagent.<sup>85</sup>

### 2.2.1 X-Ray diffraction studies.

The copper complexes of all the ligands shown in Table 2.1.5 (except for 'L4H', L6H, and 'L7H') were prepared as described later in Section 2.3, and characterised by i.r and microanalysis. The results obtained compared favourably with those expected for the neutral 2:1 complexes. Comparison of i.r. spectra of the 'free ligands' and their copper complexes (Section 2.3) showed a decrease in the OH stretch (around  $3400\text{ cm}^{-1}$ ) indicating that the phenolic hydroxy hydrogen had been lost on complex formation. Various attempts to prepare the copper complex of 'L4H' failed, which was in accordance with previous results that 'L4H' formed weak, or no copper complexes with copper(II) ions (see



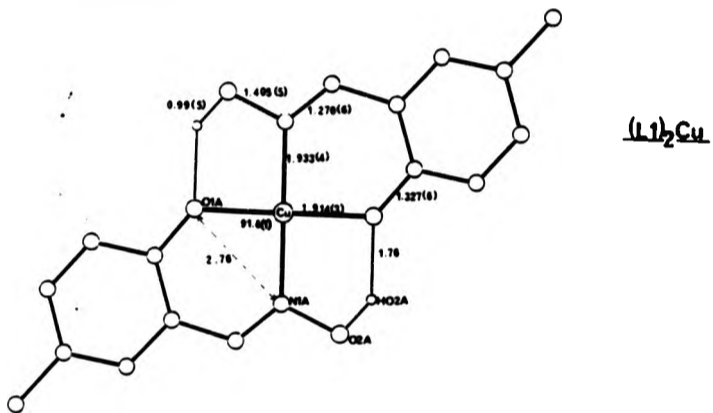
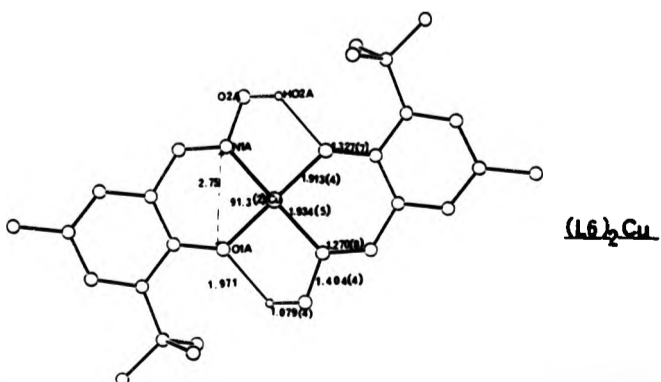
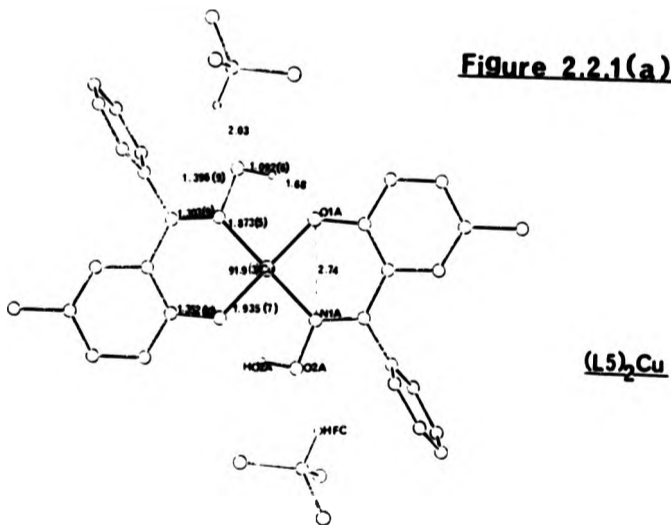


Figure 2.2.1(a)



Section 2.1.2).

The X-ray crystallographic structures of the three recrystallised complexes  $[(L1)_2Cu]n$ ,  $[(L5)_2Cu]$ , and  $[(L6)_2Cu]$  were determined, and the detailed bond length and angles are given in Section 2.3. In all cases the copper atoms occupied crystallographic special positions (inversion centres). Hence each copper complex has a centre of symmetry with two bidentate ligands producing a strictly planar arrangement of donor atoms around the copper atom. In addition to the two six-membered chelate rings in each complex, two five membered rings were also formed due to intramolecular hydrogen bonding (involving the oxime hydrogen approaching the phenolic oxygen) resulting in a pseudo macrocyclic system (see Figure 2.2.1(a)). This was in accordance with similar structures previously reported in the literature, which were discussed earlier in Section 2.1.2.<sup>86-90</sup>

The X-ray structure analyses showed that for  $[(L1)_2Cu]n$  intermolecular bonding between the copper and the oxime oxygen atoms  $[Cu...O(2a') 2.56 \text{ \AA}]$  of other molecules produced a polymeric structure (Figure 2.2.1(b)). The provision of two additional weak bonds to the copper atom thus results in a highly distorted octahedral environment for the copper atom. In the molecule of  $[(L5)_2Cu]$  the phenyl substituents are orientated approximately at right angles to the co-ordination plane around the copper (dihedral angle  $84.7^\circ$ ), a conformation that minimises repulsive interactions (Figure 2.2.1(c)). This would prevent close intermolecular bonding between copper and oxygen to produce the polymeric structure as seen in  $[(L1)_2Cu]n$ . Similarly for  $[(L6)_2Cu]$  the bulky tertiary butyl substituents would also prevent such interactions occurring, Figure 2.2.1(d).

FIGURE 2.2.1(b) Two diagrams showing the polymeric structure produced when copper(II) complexes with LIII

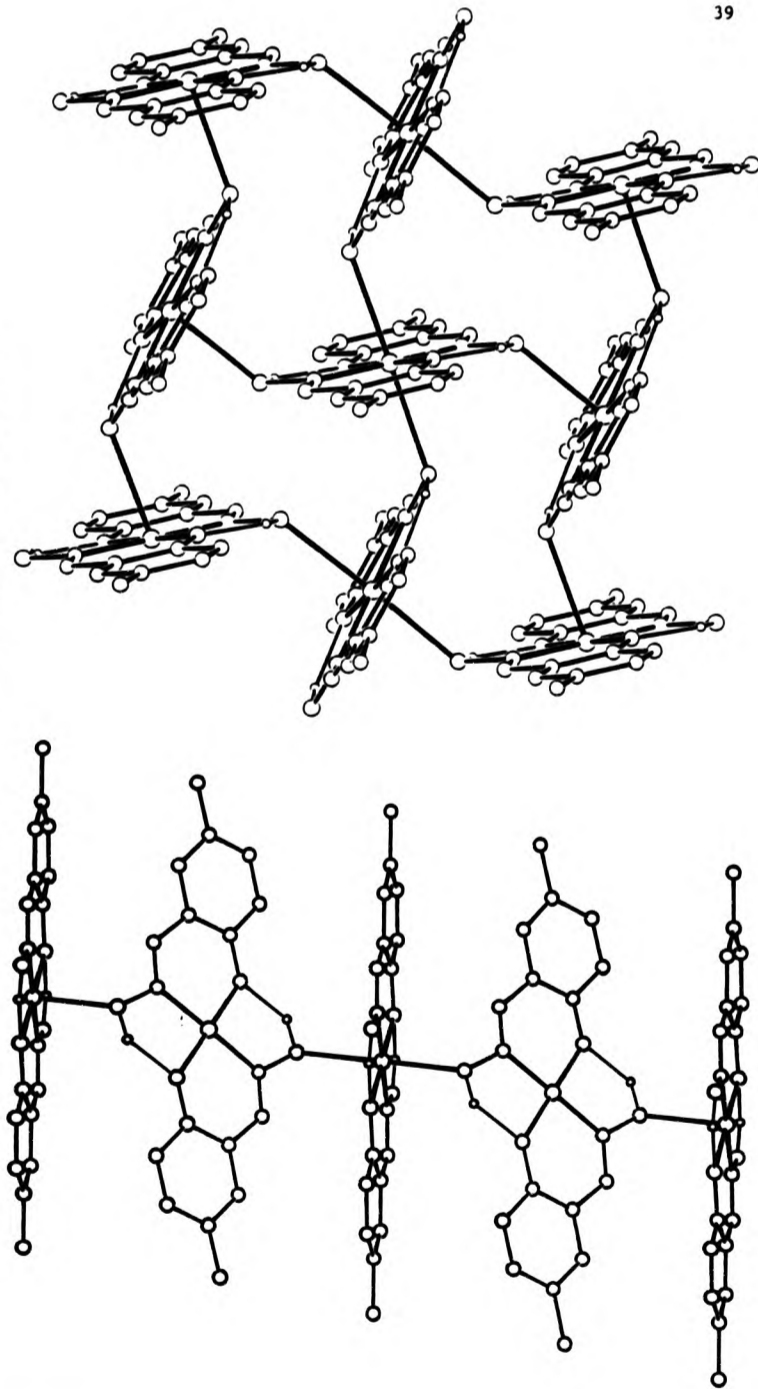
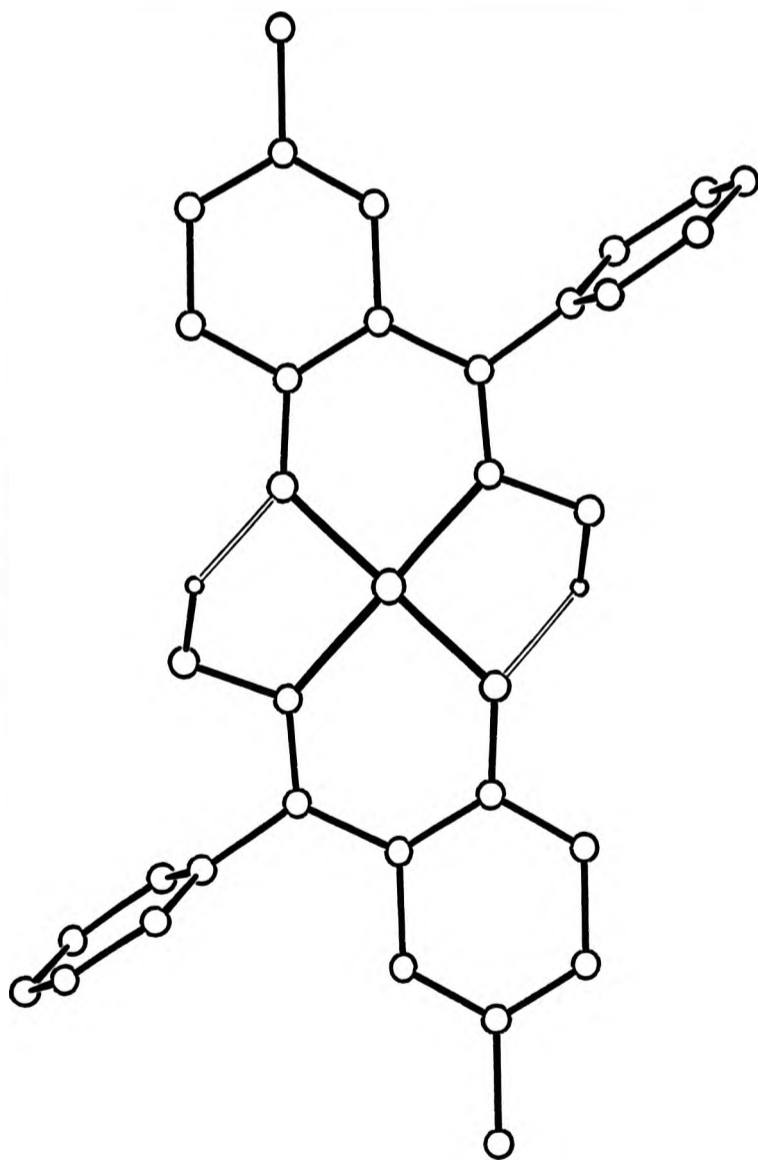
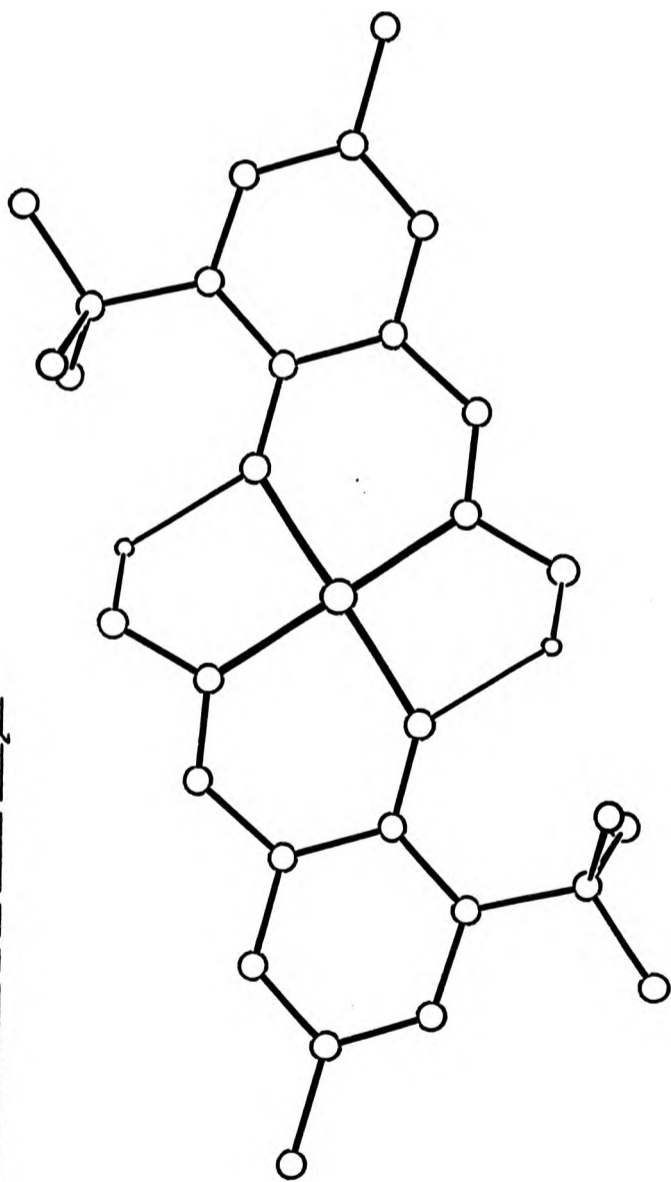


Figure 2.2.1(c) Ortep diagram of the copper(II) complex of LSH oxime





**Figure 2.2.1(d) Diagram of the complex  $[(L6)_2Cu]$**

The crystals of  $[(L5)_2Cu]$  are also solvated with two chloroform molecules which forms intermolecular hydrogen bonds to the hydroxy O-atoms of the ligand on either side of the molecule [O(2b)...H(c) 2.03 Å]. From the view of the unit cell packing shown in Figure 2.2.1(e), it can be seen that the chloroform molecules occupy cavities created by the staggered orientation of the phenyl substituents. The decomposition of the crystals, observed on standing in air is explained due to loss of chloroform.

As outlined in Section 2.1.4 for the series of related salicylic acids and esters, steric constraints of substituents on the benzene ring, have been shown to compress the bond angles in the H-bonded chelate ring. This was shown to enhance the donor abilities, of these ligands, to the proton. It was thought that a similar phenomenon might be applicable when comparing the effects of substituents on chelate formation in the copper complexes for which structural information has been obtained. The co-ordination geometries for the three complexes are illustrated for comparison in Figure 2.2.1(a). The order of decreasing extraction ability of the ligands from which they are prepared is known to be (L1H) > (L5H) > (L6H) for the nonyl analogues used commercially (see Section 2.1.2).

The Cu-N(1a) distances in the three complexes are almost identical, [1.932(4) (L1), 1.935(7) (L5), and 1.934(5) Å (L6)], as are the chelate angle O(1a)-Cu-N(1a) [91.6(1) (L1), 91.9(3) (L5), and 91.3(2)° (L6)]. The Cu-O(1a) distance, in the polymeric  $[(L1)_2Cu]_n$  structure and  $[(L6)_2Cu]$ , are very similar 1.915(3) and 1.913(4) Å respectively, whereas that in  $[(L5)_2Cu]$  is significantly shorter 1.873(5) Å. The phenolic C(2a)-O(1a) bond lengths in (L1) and (L6) complexes are the same, having values 1.327(7) and 1.327(6) Å respectively. These

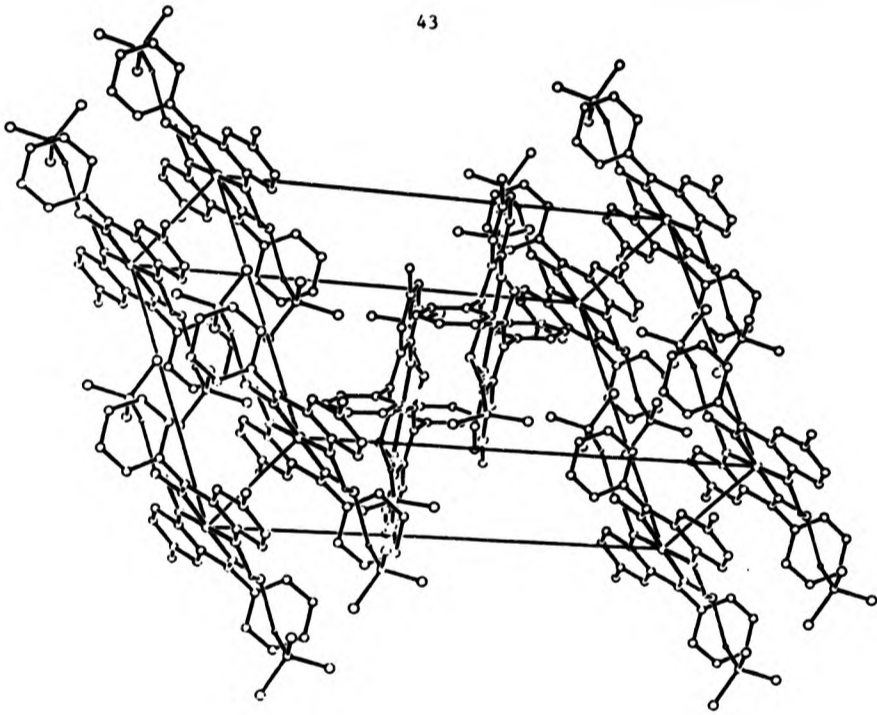
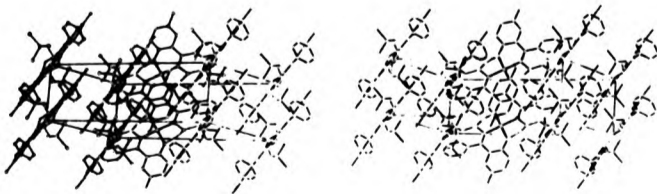


Figure 2.2.1(e) Packing diagram of  $[(L5)_2Cu]$  showing how the chloroform molecules occupy the cavities created by the phenyl substituents; along with a stereoscopic view of the packing arrangement.

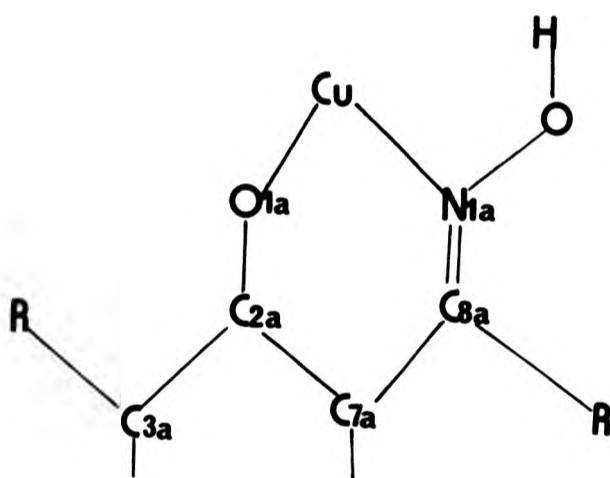


lengths show that the phenolic oxygen atoms must be using  $sp^2$  hybrid orbitals and not  $sp^3$ . The C(2a)-O(1a) bond length in (L5) is slightly longer, 1.352(10) Å, and this along with the shortened Cu-O(1a) bond length, suggests that the phenolic oxygen O(1a) in this case has more  $sp^3$  character than for the same atom in the other complex. This Cu-O(1a) distance is similar to that of 1.888(8) Å observed for the same bond in a related copper complex of salicylaldehyde benzoyl hydrazone (SBH).<sup>91</sup> These are only very small differences in the 'bite' distances in the three complexes, i.e. the distances between the co-ordinating O(1a) and N(1a) atoms, these being 2.76 (L1), 2.75 (L6) and 2.74 Å (L5) (see Figure 2.2.1(a)). As the angles at the copper atom in all three complexes are very similar, and close to the ideal value of  $90^\circ$  for planar co-ordination, [mean O(1a)-Cu-N(1a)  $91.6^\circ$ ], any steric strain in the six membered chelate ring (caused by the bulky substituents) would be expected to show in the other angles. The six-membered chelate rings are almost planar in all three structures with maximum deviations in the range 0.03 to 0.05 Å, and as a result the sum of the interior angles are 719.5, 719.8, 719.9 $^\circ$  respectively (Table 2.2.1a) which is close to the ideal value for a planar hexagon. Although the e.s.d.'s of the angles are rather large some trends in the individual angles may be related to steric factors. For  $[(L1)_2Cu]n$ , (R and R'=H), interaction from substituents R and R', would not be expected to interfere with the alignment of the donor atoms. Hence the angles in  $[(L1)_2Cu]$  may be regarded as optimal, and the other two complex structures may be compared with it.

The key angles to be compared are the exo-angles O(1a)-C(2a)-C(3a) and O(1a)-C(2a)-C(7a) which are most affected by the substituents. The value for these angles in  $[(L1)_2Cu]n$  are 119.3(5) $^\circ$  and 123.7(4) $^\circ$



**Table 2.2.1(a)** Comparison of the chelate bond angles for the three complexes



<u>Angles</u>	<u>Values/°</u>		
	[(L1) <sub>2</sub> Cu]	[(L5) <sub>2</sub> Cu]	[(L6) <sub>2</sub> Cu]
Cu-O1a-C2a	128.0(3)	128.8(5)	130.0(3)
Cu-N1a-C8a	129.3(4)	130.6(6)	128.1(4)
O1a-C2a-C7a	123.7(4)	123.3(7)	121.2(5)
N1a-C8a-C7a	124.1(5)	120.2(7)	125.3(5)
C2a-C7a-C8a	122.8(5)	125.0(7)	123.2(5)
O1a-C2a-C3a	119.3(5)	116.6(7)	121.4(5)
C8a-C7a-C6a	117.4(5)	117.7(7)	115.6(5)

respectively, (Table 2.2.1(a)). In  $[(L6)_2Cu]$  the angle  $O(1a)-C(2a)-C(3a)$  has increased by  $1.7^\circ$  relative to that in  $[(L1)_2Cu]n$ , (Table 2.2.1(a)) due to the bulky *t*-butyl group on  $C(3a)$ , and this in turn reduces the size of  $O(1a)-C(2a)-C(7a)$  by  $2.5^\circ$ . This 'pushing over' of the  $O(1a)-C(2a)$  bond results in an increase of  $2.8^\circ$  in the angle at the  $O(1a)$  donor atom. A 'knock-on-effect' means that the  $C(6a)-C(7a)-C(8a)$  at the other side of the ring has decreased by  $1.8^\circ$ , and the angle at the  $Cu-N(1a)-C(8a)$  at the  $N(1a)$  donor atom has decreased by  $1.2^\circ$ .

In the  $[(L5)_2Cu]$  the largest difference in angles, relative to those in  $[(L1)_2Cu]n$ , in the vicinity of the phenyl substituent is a decrease of  $3.9^\circ$  in the ring angle  $N(1a)-C(8a)-C(7a)$ . This may be attributed to repulsion between the phenyl substituent at  $C(8a)$  and the phenyl ring on one side of it and the  $N-O$  group on the other. Consequently in this case it is the angle at the nitrogen donor,  $C(8a)-N(1a)-Cu$  which shows the largest difference, being  $1.3^\circ$  larger than in  $[(L1)_2Cu]n$ , (Table 2.2.1(a)).

These geometric changes in the structures are clearly related to the position of the substituents, but their subsequent effects on their extraction ability could not be assessed from the structural determination results. The most significant structural result is the ability of  $[(L1)_2Cu]n$  to generate a polymeric unit. Possibly this in some way helps to increase the concentration of copper complexation at the interphase during extraction.

As discussed above all efforts at preparing the copper complex of 'L4H' failed. The decision was then made to determine the structure of the related methoxy-imine 'L7H' since suitable crystals for X-ray

analysis of this compound were available. This methoxy-imine 'L7H' has the same aromatic substitution pattern as 'L4H', and might therefore provide information about the influence of substituents on the orientation of potential donor atoms. Also assignments of hydroxy stretching modes for the analogous salicylate ester is ambiguous (see Section 2.1.4), hence information from the X-ray structure determination might be directly related to the abnormal intramolecular hydrogen bonding observed in that compound.

The X-ray structure determination showed that 'L7H' did not have the expected structure with ortho-substitution shown in Table 2.1.5, instead the compound has the phenolic hydroxy group in the position para to the oxime, (Figure 2.2.1(f)). In the solid state the compound was shown to exist as a polymeric chain which arises from strong intermolecular hydrogen bonding, (Figure 2.2.1(g)) between the phenolic proton and the oxime nitrogen, H(O1a)-N(1a) = 1.98 Å.

Clearly compounds of this type, with donor atoms at opposite ends of the ring, (Figure 2.2.1(f)) cannot form simple chelates, and therefore will not form copper(II) complexes with stabilities comparable to those for the supposed analogous nonyl derivatives mentioned in Section 2.1.2. If this substitution pattern is also present in 'L4H' it clearly explains why no complex could be prepared from the ligand supplied by ICI, as it would not be a potential chelator as originally thought.

Carbon-13 nuclear magnetic resonance studies were conducted on both 'L7H' and 'L4H'. Based on the observed solid state structure of 'L7H' the chemical shifts, at which the carbon atoms would resonate were estimated.<sup>92-98</sup> The observed <sup>13</sup>C n.m.r. spectra, Table 2.2.1(b),

Figure 2.2.1(f) Ortep diagram of the 'free' ligand 'L7H'.

48

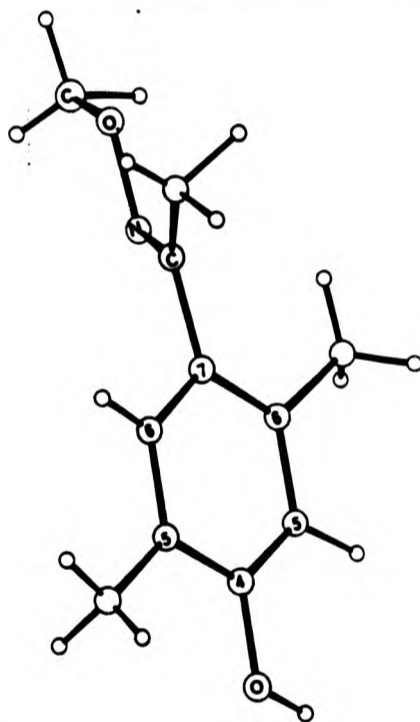


Figure 2.2.1(g) Diagram to show polymeric nature of 'L7H' in the solid state.

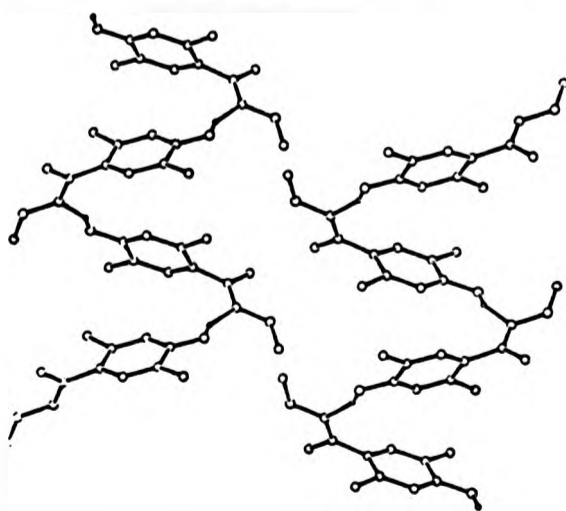
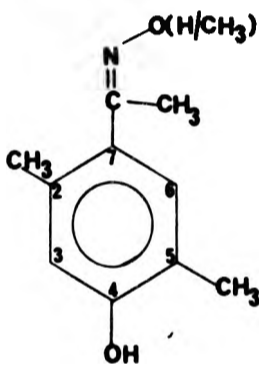


Table 2.2.1(b)  $^{13}\text{C}$  n.m.r. Assignments for 'L4H' and 'L7H' collected in deuterated acetone.

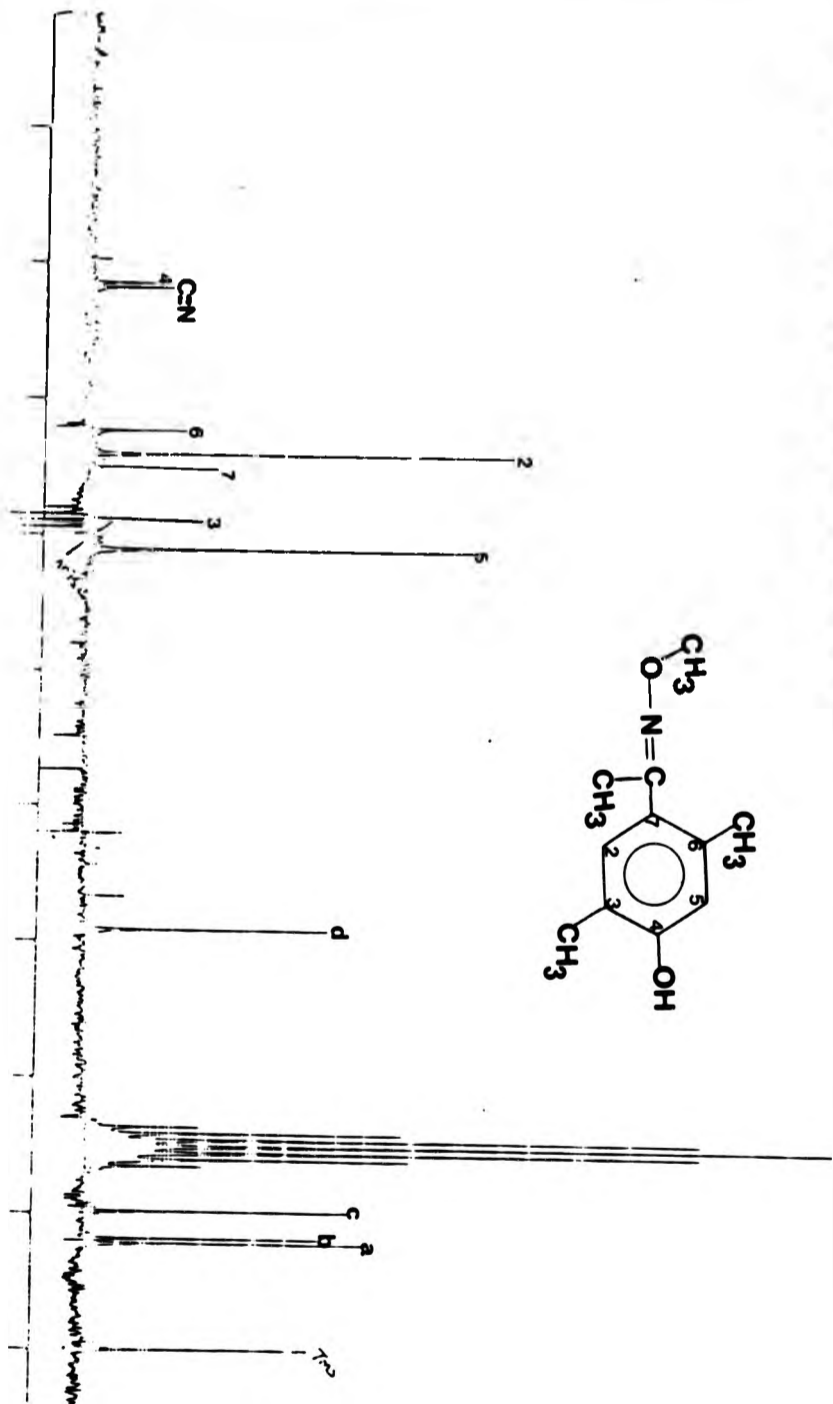


The substitution pattern and numbering scheme for 'L4H' and 'L7H'

<u>Assignment</u>	<u>Chemical Shift/ppm</u>	
	'L7H'	'L4H'
CH3(a)	15.6	15.6
CH3(b)	16.2	15.9
CH3(c)	20.3	20.1
O-CH3(d)	61.6	-
C5	117.7	117.6
C3	122.0	122.1
C7	122.9	130.2
C2	131.8	131.6
C6	135.3	135.0
C=N	156.2	155.9
C4	156.9	157.1

To assist in the assignment of the aromatic carbons the spectra were recorded in the off resonance mode.

Figure 2.2.1(b)  $^{13}\text{C}$  N.M.R. spectrum of the methoxyflavone '17H'



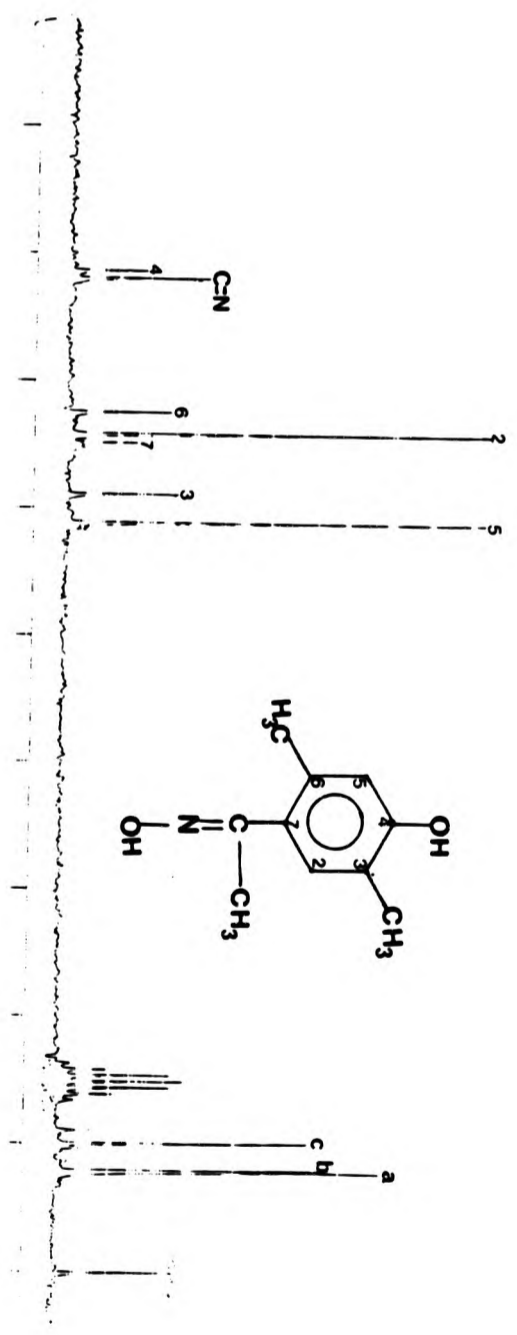


Figure 2.2.1(1)  $^{13}\text{C}$  n.m.r. spectrum of the oxime  $^{14}\text{H}$ .

indicated that the para-substitution was proved to be present in both ligands, Figures 2.2.1(h) and 2.2.1(i). From this it was concluded that 'L4H' also does not have the structure proposed by the earlier workers (shown in Table 2.1.5), but must resemble that of 'L7H' established from the structural analysis carried out in this study.

The implications of these results were important since this new para-formulation explains why 'L4H' was earlier found by ICI to be the weakest extractant for copper as discussed in Section 2.1.2. Therefore because of the unexpected results of this X-ray structure analysis, new attempts to synthesise the oxime L4H were made at ICI but proved unsuccessful. At this stage the ICI workers also recollected the data on the extracting ability of the nonyl series.<sup>99</sup> These newer results changed the order of relative extracting ability, and showed that the L3H analogue is in fact the best extractant for copper of the ligands under study, not L1H as previously thought. This product was never used commercially since it was difficult to remove the copper at the stripping stage (Section 2.1.2).<sup>100</sup>

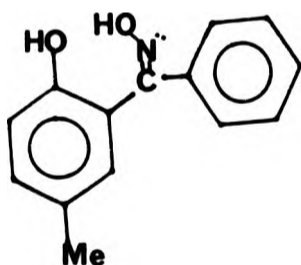
Based on the new extraction data collected at I.C.I the oxime for L6H analogue was found to be the worst extractant for copper. X-ray intensity data was collected for this uncomplexed ligand, but all attempts, to date, to phase the data as failed, and the structure remains unsolved.

#### 2.2.2 Preparation of 2-hydroxy-5-methylbenzophenone oxime (L5H).

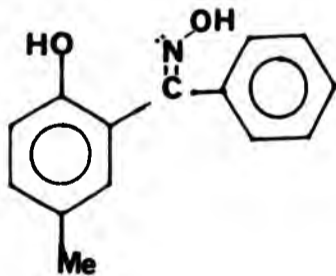
The approach adopted in this preparation was derived from consideration of results of earlier work by Preston and Lublinska.<sup>101</sup> They had reported that the geometric isomers of 2-hydroxy-5-methylbenzophenone oxime were separated by adding copper acetate to



what was considered to be a reaction mixture of isomers. As discussed in Section 2.1 the assumption was made that one isomer, the syn-form (I) would not react with copper, and the anti-form (II) would be removed from the mixture of oximes as the copper complex; on treating the resultant complex with dilute hydrochloric acid, the 'free' anti-oxime would be liberated.

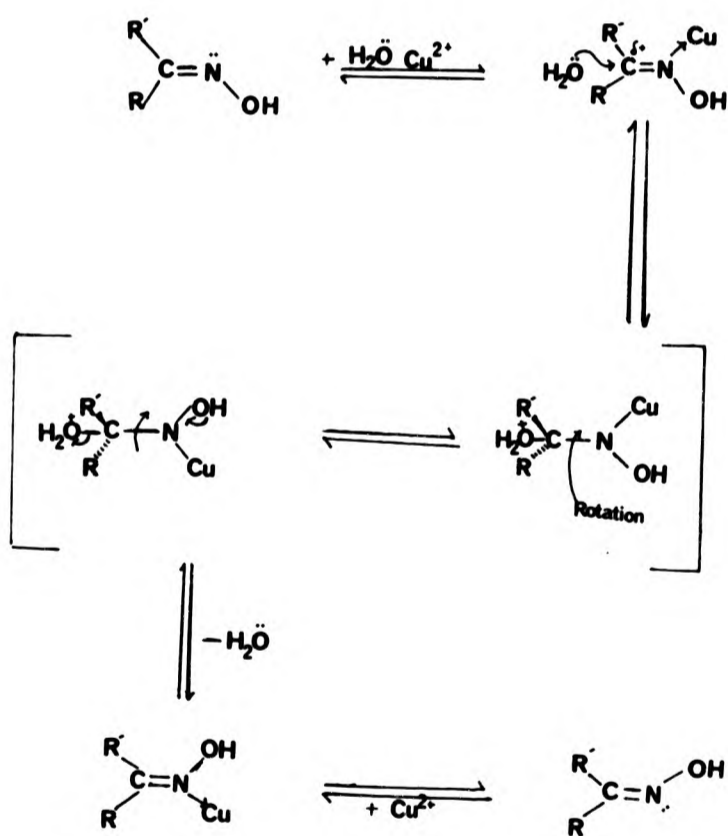


(I):- 'syn'(E)-2-hydroxy-5-methylbenzophenone oxime



(II):- 'anti'(Z)-2-hydroxy-5-methylbenzophenone oxime.

This is a surprising proposal since in the presence, in the reaction mixture, of such a strong Lewis acid as  $\text{Cu}^{2+}$  and a nucleophile such as water, an inter-conversion of the syn- to the anti-isomer during the reaction would be expected Scheme 2.2.2. A possible mechanism involves initially a bond to the copper ion by the oxime nitrogen atom of the syn-form which would facilitate attack at the carbon atom by a

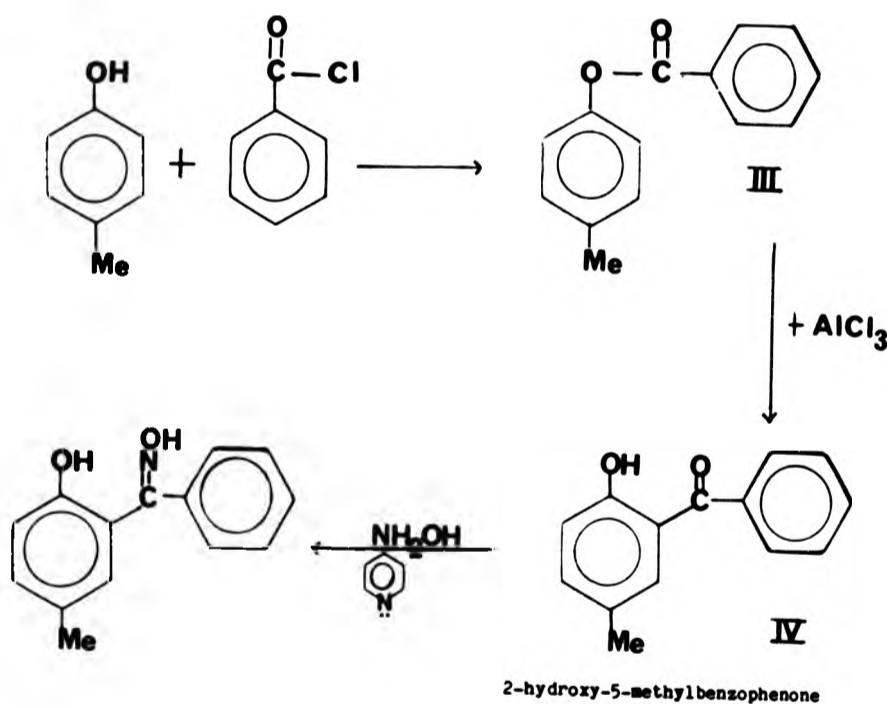


Scheme 2.2.2

water molecule. Free rotation about the C-N bond in the transition state would allow interconversion of the syn- and anti- forms as shown. Consequently the same final copper complex would be formed starting from either of the the two isomeric oximes, viz. that of the favourable bidentate anti-form. The possibility therefore exists that the so-called 'separation' is in fact a conversion of both forms to the anti-form. In the present study preparation of 2-hydroxy-5-methylbenzophenone oxime (L5H) was embarked upon to investigate whether the syn, anti, or any other isomer<sup>102-105</sup> of this compound could be separated from an homogenous organic phase by preferential formation of the copper complex, and to confirm the hypothesis that the preparation of the same Cu(II) complex results from either isomer. The oxime was prepared following the method given by Preston and Luklinska,<sup>101</sup> supplemented with information from ICI.<sup>106</sup>

#### 2.2.2(a) Preparation of the precursor compounds.

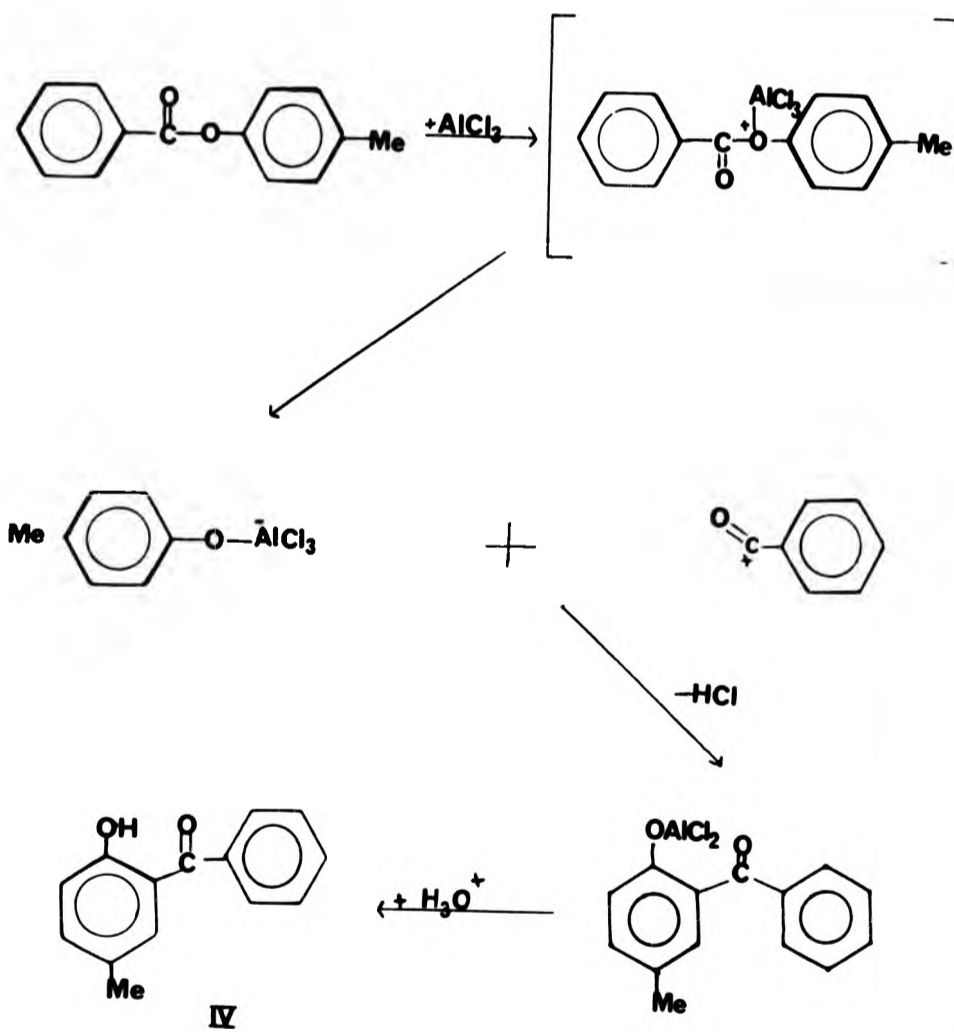
All the precursors were prepared by known reaction routes according to Scheme 2.2.2(Ia). However detailed preparation methods used in this study are recorded in Section 2.3, since detailed reaction procedures have not previously been reported. The required 4-methylphenylbenzoate precursor (III) was prepared using the Schotten-Baumann method. The ester was recrystallised from ethanol, characterisation, using i.r., <sup>1</sup>H n.m.r. and microanalysis (see Experimental Section 2.3) was consistent with the expected structure.

Scheme 2.2.2Ia

The 2-Hydroxy-5-methylbenzophenone precursor (IV), was prepared by the Fries rearrangement of the 4-methylphenylbenzoate (III). The ester was heated under reflux in monochlorobenzene in the presence of anhydrous aluminium chloride, for two hours. Samples of the reaction mixture were analysed by g.l.c. and the reaction was judged to be completed when the ester(III) could no longer be detected.

The mechanism of this reaction is not known. There are two possibilities, one involving intramolecular rearrangement, where the benzoyl group of the ester ( $O=C-Ph$ ) migrates from the phenolic oxygen, directly to the carbon atom giving (IV), (with no ion pair separation). The second possible mechanism {Scheme 2.2.2(IIa)} involves the  $AlCl_3$ -promoted formation of a benzoyl cation(V) and anion (VI). The [phenoxy( $AlCl_3$ )]- substituent in (IV) would direct electrophilic attack to the ortho- and para- positions, but since the para-position is already occupied by the methyl group, attack would occur at the ortho-position. The target ortho-hydroxy ketone (IV) once formed would be stabilised by intra-molecular hydrogen bonding.

To precipitate the ketone as a solid, n-hexane was added to the oil produced after the rearrangement reaction. The mixture was stirred for three hours at ambient temperature, after which a fine yellow powder was obtained. Recrystallisation from ethanol gave flat square shaped yellow crystals. On further evaporation of the n-hexane mother liquor a yellow crystalline solid was obtained, and this was also recrystallised from ethanol producing yellow "needle-like" crystals. The recrystallised products looked different from each other, and the possibility was considered that two isomeric forms of the ketone had been isolated. However the melting point and electronic, i.r. and n.m.r spectra showed no significant difference between the two



2-hydroxy-5-methylbenzophenone oxime

2-hydroxy-5-methylbenzophenone

Scheme 2.2.2. IIa

products; it seems probable that the ketone as a solid exists in two crystalline forms, possibly only differing in their external morphology.

In the i.r. spectrum of the 2-hydroxy-5-methylbenzophenone (IV) prepared, no 'free' hydroxy vibration at  $3500\text{ cm}^{-1}$  was seen. Instead a broad band at  $3220\text{ cm}^{-1}$  which was not very intense was observed. The lowering of the hydroxy vibration from  $3600\text{ cm}^{-1}$  to  $3220\text{ cm}^{-1}$ , plus the lowered intensity indicated the formation of a strong hydrogen bond.

The conclusion that an intramolecular hydrogen bond had been produced, involving the ortho substituted phenolic hydroxide group of this ketone with its carbonyl oxygen atom was further supported by the position observed for the carbonyl stretching vibration. This was found at  $1635\text{ cm}^{-1}$  (compared with the strong broad C=O band in the precursor ester at  $1735\text{ cm}^{-1}$ , and for those reported for other aromatic ketones,<sup>107,108</sup>  $1700\text{-}1680\text{ cm}^{-1}$ ). These observations indicated that a diaryl ketone was present, and that the carbonyl group was conjugated with the aromatic ring. The vibration may have been shifted to this lower frequency of  $1635\text{ cm}^{-1}$ , by the formation of a hydrogen-bond to give a 'chelate'. Peaks seen at  $3072$  and  $2870\text{ cm}^{-1}$  were consistent with the presence of aromatic and methyl C-H stretching modes. The rest of the spectrum were consistent with the formulation as an aromatic hydroxy ketone.

In the  $^1\text{H}$  n.m.r. spectrum the resonance of the methyl group was at  $2.24\text{ ppm}$  due to shielding by the benzene ring. The expected eight aromatic protons signals were found between  $6.89\text{-}7.75\text{ ppm}$ , with the hydroxy group resonance at  $11.8\text{ ppm}$ . This hydroxy proton exchanged

with deuterated water ( $D_2O$ ). The carbonyl chromophore and that of the aromatic ring were also detected in the u.v. spectrum.

The  $^{13}C$  n.m.r. spectrum of the recrystallised 2-hydroxy-5-methylbenzophenone (IV) was obtained so that the purity of the products could be established. Preston et al. have recorded that the 2-hydroxy-5-methylbenzophenone used in their preparation of the oxime crystallised from ethanol as "bright yellow plates."<sup>101</sup> In the present study one of the ketone products resembled that prepared by these workers, both morphological products had identical  $^{13}C$  n.m.r. spectrum, and as mentioned earlier, it appeared that only one single pure product was obtained. The fact that this ketone occurs in two solid state modifications is not altogether surprising since benzophenone also exhibits this phenomenon.<sup>109,110</sup> The crystalline form that resembled that obtained by Preston et al. (the yellow square plates) was used in the later preparation of the oxime to ensure that results relating to isomerism could be compared with those obtained by these workers.

The effects substituents have on chemical shifts, of individual carbons of an aromatic ring are known to be additive.<sup>93</sup> This being the case, using unsubstituted benzene as a standard an approximation of the chemical shift of the proposed compound can be made prior to obtaining the spectrum. In this case, the chemical shifts at which the resonance of the various carbon atom were estimated.

Since the environment of the two pairs of carbon atoms in the phenyl ring were exactly the same (ie C(8),(12) and C(9),(11)), in the aromatic region a total of ten peaks would be expected. The estimated and observed chemical shifts of the aromatic carbons are given in



Table 2.2.2(a), and the agreement observed between them is good, with the exception of C(1), C(2) and C(3), where the combined effects of three substituents on the chemical shifts were greater than expected.

The basicity of the phenolic oxygen, arising from the  $^+I$  effect of the para-methyl substituent, is increased relative to unsubstituted phenol. This is further enhanced by a partial negative charge ( $\delta^-$ ) on the phenolic oxygen atom which would occur if the hydrogen atom of this group is participating in hydrogen bonding, as indicated by the i.r. spectrum. This would decrease the shielding of C(7), causing its signal to resonate further up-field than would be expected, while those of C(2) and C(3) are more shielded hence the increased chemical shift at which they resonate.

#### 2.2.2(b) Preparation of the oxime isomeric mixture.

The 2-hydroxy-5-methylbenzophenone oxime was prepared by reacting 2-hydroxy-5-methylbenzophenone with hydroxylamine hydrochloride, Scheme 2.2.2(b). This condensation reaction occurs in the presence of the organic base, pyridine, whose function is to liberate hydroxylamine from its hydrochloride salt. This is important since the protonated hydroxylamine has no nucleophilic character, and would not attack the ketone.

The oxime produced was extracted several times with ethanol from the excess hydroxylamine hydrochloride solid which remained. The combined organic phase was evaporated down to dryness, leaving a white oily solid. A sample of this was placed under vacuum to remove any excess pyridine and hydroxylamine that might be present. The  $^{13}C$  n.m.r. spectrum of this product was recorded, and estimated chemical shifts were obtained using the procedure outlined above. Once again ten

2.2.2(a) Table showing the estimated and found chemical shifts( $\delta$ /ppm).  
for 2-hydroxy-5-methylbenzophenone  $^{13}\text{C}$  n.m.r

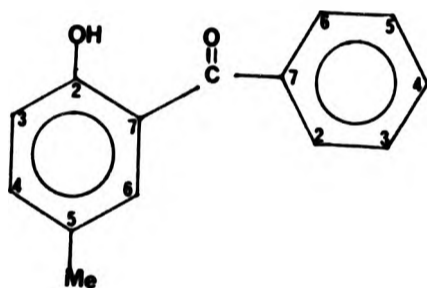
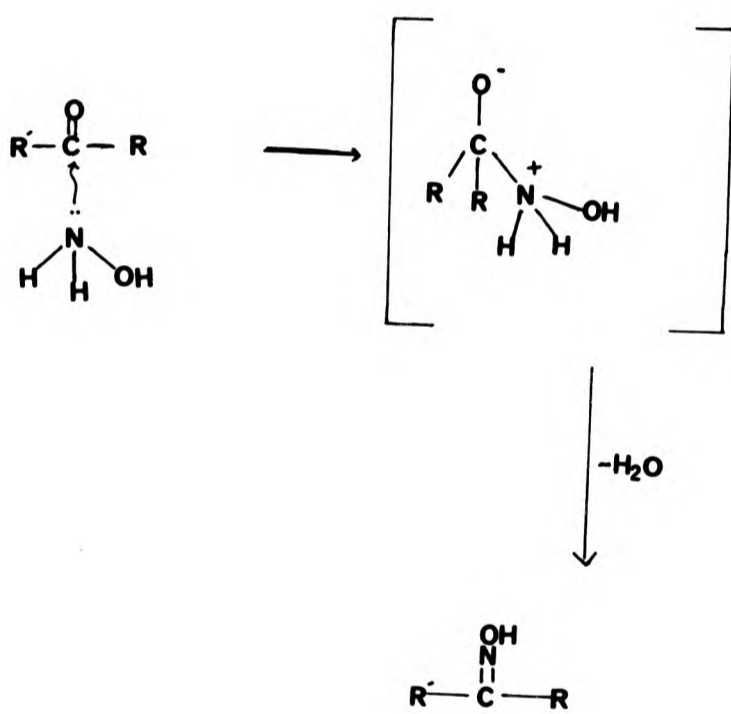
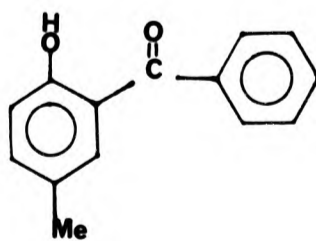


Diagram to show the aromatic carbon labels

<u>Carbon Atom</u>	<u>Estimate</u>	<u>Found <math>\delta</math></u>
C=O	-	201.7
C2	154.0	161.4
C7	137.9	137.5
C4	134.2	133.3
C6	132.2	131.9
C10	132.1	129.3
C8, 12	130.2	128.9
C9, 11	128.3	128.4
C5	129.9	127.9
C1	125.3	119.0
C3	115.5	118.3
CH3	-	20.5



where R'-CO-R is used to represent:-



Scheme 2.2.2(b)

peaks arising from the oxime phenyl rings would be expected. However the spectrum contained several other peaks in the aromatic region, three of which could be assigned to some pyridine impurity, but the three remaining peaks could not be readily assigned.

It is possible that the additional peaks in the  $^{13}\text{C}$  n.m.r. spectrum arise from a second component such as the syn-isomer. However this interpretation is not consistent with the single sharp signal found for the oxime-C (at 160.7 ppm).

### 2.2.3 Separation of the isomers of the oxime (L5H)

Two approaches to separation of the isomers were made. The first following the method of Preston and Lublinska, is reported fully here because no details were published of their original work.<sup>101</sup> The second is the well documented procedure of Blatt for which full details are already published.<sup>111,112</sup> The dangers of wrong assignment of structure based on mere spectroscopic evidence is highlighted by the results obtained earlier in the present study in which X-ray structure analysis shows the structure assigned to 'L7H' by other workers<sup>105</sup> to be wrong (see Section 2.2.1). It is for this reason that the second method, thought to give authentic syn-isomer was used here to check on the results obtained by the controversial approach of Preston and Lublinska.

#### 2.2.3(a) The Preston and Lublinska procedure

Attempts were made to separate the 'syn- and anti-isomers' of L5H following the procedure of Preston and Lublinska. An ethanolic solution containing copper(II) acetate was added to the crude oxime (white oily substance) before recrystallisation, which had been

redissolved in ethanol. After refluxing, a pale green fibrous solid and a dark ethanolic filtrate were obtained. The fibrous material after treatment with dilute HCl produced a fine brown solid.

This solid resembled the copper complex of the authentic 2-hydroxy-5-methylbenzophenone oxime  $[(L5)_2Cu]$  which had been made directly from a sample of L5H (supplied by ICI) and had been structurally characterised by X-ray single crystal analysis (see Section 2.2.1). However unlike  $[(L5)_2Cu]$ , the new brown complex was very soluble in cold toluene and chloroform, whereas the latter was used to recrystallise the complex  $[(L5)_2Cu]$ . This indicated that the product obtained after treatment with acid, was not the copper complex in spite of its appearance. The infra-red spectrum showed a strong hydroxy stretch at  $3359\text{ cm}^{-1}$ , but attempts to obtain the  $^1H$  n.m.r. spectrum failed, probably because some paramagnetic copper compound still remained after treatment with acid.

The dark ethanolic filtrate slowly yielded a second dark brown solid which was relatively insoluble in cold toluene or chloroform, the expected property of  $[(L5)_2Cu]$ . The infra-red spectrum of this solid were consistent with this inference due to absence of the strong phenolic hydroxy stretching mode normally seen in the spectrum of the free ligand (L5H). An additional a peak at about  $3360\text{ cm}^{-1}$  was seen, which suggests that some uncomplexed oxime might also be present.

In an attempt to obtain the oxime, the second brown solid, thought to be  $[(L5)_2Cu]$ , was treated with dilute HCl and no change was observed, even on heating the suspension. However, a saturated solution in  $CHCl_3$  (a bottle green colour) reacted rapidly when shaken with hydrochloric acid giving a pale green aqueous layer. Evaporation of

the organic phase gave a cream solid with an i.r. spectrum containing a broad band at  $3380\text{ cm}^{-1}$  characteristic of a hydrogen atom of an hydroxy group involved in hydrogen bonding.

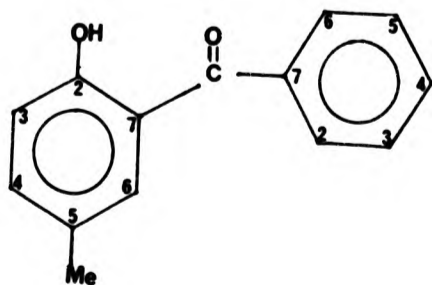
The  $^1\text{H}$  n.m.r. spectrum of this cream solid, thought to be the oxime L5H contained a singlet at 2.4 ppm, which corresponds to the expected three methyl protons. The peaks in the aromatic region of the spectrum integrated to give nine protons. Eight of these would correspond to the protons of the aromatic ring, and possible the ninth to the protons of the oxime hydroxy group, but this did not exchange with deuterium oxide over a period of fifteen minutes. The phenolic hydroxy group was therefore assigned to the peak at 11.6 ppm which rapidly exchanged with deuterated water. The  $^{13}\text{C}$  n.m.r. spectrum of the compound was obtained. Like the precursor ketone ten peaks in the aromatic region were expected and of these the two peaks arising from the pairs of equivalent carbons {C(8),C(12) and C(9),C(11)}, would be expected to be more intense than the other hydrogen substituted benzene carbon atoms {Table 2.2.3(a)}. Only nine peaks were found in the  $^{13}\text{C}$  n.m.r. spectrum in the aromatic region, not the ten expected but a very intense peak at 128.6 ppm corresponds to the two pairs of carbons C(8),(11), and C(9),(12).

The only very marked differences between the observed and calculated  $^{13}\text{C}$  n.m.r. chemical shifts for the oxime are those for the carbon atoms C(1) and C(7) in the vicinity of the oxime group. This discrepancy may be accounted for by the fact that the estimated values for these had been based on the ketone since no values could be found for the effects of an aromatic oxime substituent.

**2.2.3(a) Table showing the expected and found chemical shift ( $\sigma$ /ppm) for 2-hydroxy-5-methylbenzophenone oxime (Isomer A), and its precursor ketone.**

<u>Carbon Atom</u>	<u>Estimated <math>\sigma</math></u>	<u>Ketone</u>	<u>Oxime(L5H).</u>
		<u>Found <math>\sigma</math></u>	<u>Found <math>\sigma</math></u>
C=N or C=O		201.7	162.2
C2	154.4	161.4	155.8
C7	137.9	137.4	131.8
C4	134.2	133.3	131.9
C6	132.3	131.9	130.8
C10	132.1	129.3	130.0
C8,12	130.2	128.9	
			128.6
C9,11	128.1	128.4	
C5	129.9	127.9	128.3
C1	125.1	119.0	118.4
C3	115.5	118.3	117.0
CH3	-	20.5	20.5

Note, the aromatic carbon labels are exactly the same as for the precursor ketone shown below:-



Ebullioscopic molecular weight determinations were carried out to see if the oxime existed in solution as a hydrogen-bonded dimer. The unrecrystallised solid showed a relative molecular mass of 231.3 which can be compared with the value based on the monomeric molecular formula which is 227.26. This shows that the determined mass was correct within experimental error; and that the oxime exists as a monomer in toluene.<sup>113</sup>

From these results it was clear that one pure isomer of the oxime (referred to as Isomer A), presumed to be the active 'anti-form'(I) of Preston and Lublinska,<sup>101</sup> had been obtained. Attempts to isolate the syn-isomer from the residues were unsuccessful. A second preparation was then undertaken to obtain the syn-isomer by a different method.

#### 2.2.3(b) The method of Blatt

Two groups, those of Ashbrook<sup>114,115</sup> and of Blatt,<sup>111,112</sup> both report the isolation and characterisation the two geometric isomers of an o-hydroxybenzophenone oxime. The extraction abilities of each isomer was then tested by shaking an organic phase containing the oxime with an aqueous phase containing copper(II) ions. The relative rate of extraction, and the amount of copper ions extracted from the aqueous phase were compared for the two isomers.

As in these<sup>114</sup> experiments complexation involved two separate phases, the rate at which each isomer complexed to copper would have been greatly affected by the behaviour of the two isomeric forms at the interface.<sup>115,116</sup>

Attempts to prepare the two geometric isomers following the procedure proposed by Blatt were carried out. This was conducted so that the



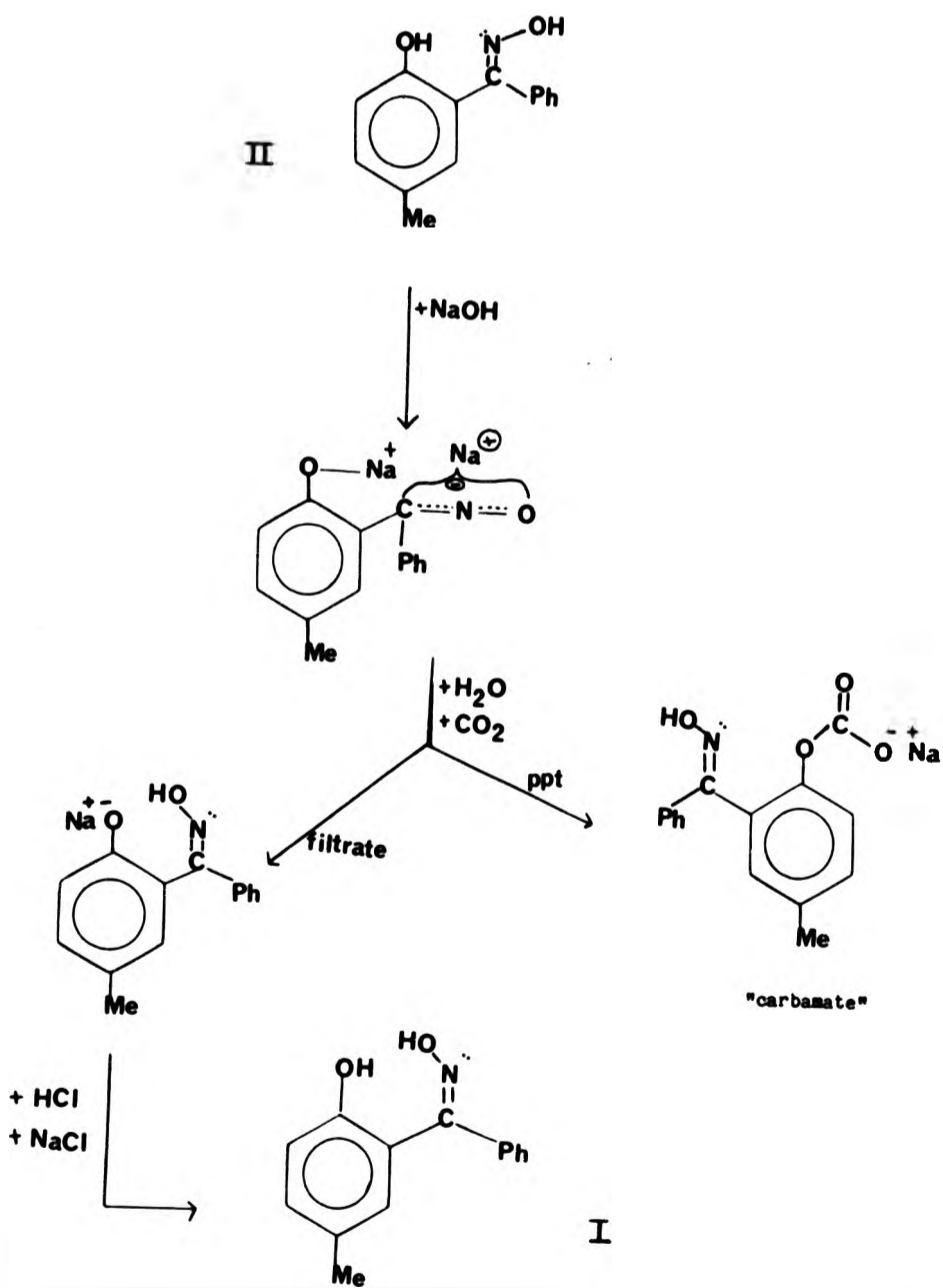
complexing ability of the two geometric isomers of 2-hydroxy-5-methyl-benzophenone oxime to copper(II) ions in an homogenous organic phase could be compared. This was intended to establish whether the assumption made by Preston et.al was not entirely correct, and that both isomer were capable of forming a copper complex.

Starting from the presumable active anti-(I). Isomer (A) discussed in the previous section [Section 2.2.3(a)], the Blatt procedure<sup>111</sup> was followed to produce rearrangement to an Isomer (B) [presumed to be that classified by Blatt as the inactive syn-form (II)]. The Preston method,<sup>101</sup> described above [Section 2.2.3(a)], was first used to obtain isomer (A) which was then boiled in 40% sodium hydroxide solution and after cooling carbon dioxide was blown through the solution. It was assumed that, as reported by Blatt,<sup>111</sup> the unrearranged starting material was in the carbonate precipitate filtered off, and Isomer (A) was liberated from it with hydrochloric acid, [Scheme 2.2.3]. The rearrangement product, Isomer (B), was obtained from the sodium salt left in solution by addition of dilute hydrochloric acid [Scheme 2.2.3].

The products after recrystallisation gave melting points of 135-139°C<sup>111</sup> for Isomer A (lit 136-137°C, for Blatt's 'anti-form'), and 128-132°C for Isomer B (lit 136-137°C, for Blatt's 'syn-form').<sup>111</sup> A mixture of the two solids melted below 115°C, similar to the result obtained by Blatt.<sup>111</sup>

<sup>13</sup>C and <sup>1</sup>H n.m.r. spectra of the two isomers (A) and (B) were obtained. For Isomer (A) only one difference was found in the <sup>1</sup>H spectrum, when compared with the oxime produced following Preston's

## Scheme 2.2.3



method, and used as the starting material. In the spectrum of the recovered Isomer (A) the oxime hydroxy proton showed up as a broad single peak at 7.54 ppm (Table 2.2.3) which readily exchanged with D<sub>2</sub>O after a time lapse of five minutes, whereas the starting material had no distinct singlet at this chemical shift. In the <sup>13</sup>C n.m.r. spectrum no significant difference was found between the recovered oxime and the Isomer A used as the starting material.

For Isomer B major differences were seen in both the <sup>13</sup>C and <sup>1</sup>H n.m.r. compared to Isomer A used as the starting material, and that recovered. In the <sup>13</sup>C spectrum, the oxime carbon resonated further upfield at 158 ppm in Isomer B compared to 162 ppm for Isomer A (Table 2.2.3(b)). The carbons in the aromatic region of Isomer B are all shifted further down-field when compared with Isomer A. (Tables 2.2.3(a) and 2.2.3(b)), the exception to this is C(2), which is shifted further upfield in Isomer B. A significant difference is that, unlike the <sup>13</sup>C spectrum of Isomer A the pairs of carbons C(8),(12) and C(9),(11) resonate at separate chemical shifts of 128.9 and 128.7 ppm respectively. The loss of equivalence is consistent with the effects of the lone pair which would be orientated towards the unsubstituted phenyl ring in a syn-form (I), Section 2.2.2. A lone pair in this orientation would also explain why C(2) resonates at a lower chemical shifts, since it is less shielded in this case than for the same carbon atom in an anti-form. For C(5) in Isomer B the <sup>+</sup>I effect of the p-hydroxy group appears to have increased the shielding of this carbon atom considerably, and it now resonates at 129.8 ppm as compared with Isomer A, (Tables 2.2.3(a) and 2.2.3(b)) and of the precursor ketone (Tables 2.2.3(b)), where the peaks due to C(5) are close to 128 ppm.

Table 2.2.3(b) The chemical shift ( $\sigma$  ppm) for the oxime prepared following Blatt's methods.

<u>Isomer (A)</u>		<u>Isomer (B)</u>	
(So-called anti-oxime)		(So-called syn-oxime)	
C=N	162.0	C=N	158.3
C(2)	155.7	C(2)	153.6
C(4)	131.9	C(7)	135.7
C(7)	131.3	C(4)	133.1
C(6)	130.7	C(6)	131.1
C(10)	129.3	C(10)	130.2
C(8,12 9,11)	128.6		
C(5)	128.3	C(5)	129
		C(8,12)	128.9
		C(9,11)	128.7
C(1)	118.4		
C(3)	117.0	C(1)	120.3
CH3	20.5	C(3)	118.8
CH3	20.4		

The  $^{13}\text{C}$  n.m.r. results for Isomer B ('syn-oxime') are in some ways comparable to those obtained for the precursor ketone, where the orientation of one of the lone pairs of the oxygen atom is also thought to be directed towards the unsubstituted phenyl ring, and where similar chemical shifts for the aromatic carbons are obtained, see Table 2.2.3(a) and 2.2.3(b).

The most unusual feature of the  $^1\text{H}$  spectrum, of the Isomer B assumed to be the Blatt's 'syn-form', was a doublet at around 2 ppm which corresponded to a methyl group. This doublet (coupling constant of 6Hz) would not be expected to have arisen from long range H-H coupling, and is inconsistent with the result expected from a syn-oxime structure. For the remainder of the spectrum, the integration is only consistent with the presence of three protons from one methyl group. In the aromatic region between 7.5-8.5 ppm a very broad band is seen, which on integration is consistent for ten protons being present, and two are readily exchanged with  $\text{D}_2\text{O}$ . It is difficult to explain the splitting of the signal at 2 ppm.

#### 2.2.4 Preparation of the copper(II) complexes of Isomer A and Isomer B.

Attempts were made to form the copper(II) complexes of the two oxime isomers (Isomer A and Isomer B). An ethanol solution of each oxime, which had been obtained by Blatt's method, was mixed with an ethanolic solution of a copper(II) salt. For Isomer A the 'anti-oxime', precipitation occurred immediately producing a sandy brown powder, and for Isomer B the 'syn-oxime', a precipitate was produced, after a time lapse of fifteen minutes, which was dark brown and metallic in appearance. The yields of the complexes were less than 50%, which is

far lower than expected. Characterisation was carried out on the copper complexes using i.r. and microanalysis. The microanalytical results, Table 2.2.4, showed the values are within the expected observed and calculated range. The slight discrepancy seen for the supposedly *syn*-form could be attributed to impurities present. The low yields obtained made it difficult to purify the samples prior to analysis.

Table 2.2.4 Microanalytical data for the two isomers copper(II) complexes.

<u>ATOM</u>	<u>Calculated % for</u> $C_{28}H_{24}N_2O_4Cu$	<u>Found % for ISOMERS</u>	
		A	B
C	65.2	64.9	64.3
H	4.7	4.6	4.0
N	5.4	5.6	4.6
O	12.4	-	-
Cu	12.2	-	-

The mystery remains unsolved whether 'syn'/'anti' isomers of L5H exists. In this work it has not been possible to isolate and separate the syn- and anti-isomers of 2-hydroxy-5-methylbenzophenone, by the method of preferential reaction of the anti-form with copper ions in an homogeneous organic solution using the information given by Preston et.al.<sup>101</sup> The decision, made by Preston and co-workers, that the syn- and anti- oximes could be separated by selective complex formation with copper(II) ion, is disputable. Preston et.al might have come to this conclusion based on evidence<sup>114</sup> which shows that the anti-isomer of this and similar oximes are more reactive in forming a copper complex, than their syn-forms. The former isomer for this reason are often referred to as the "active" form.

## 2.3 Experimental

### 2.3.1 General experimental techniques.

Microanalysis for nitrogen, carbon, and hydrogen were performed at ICI Organics Division.  $^{13}\text{C}$  N.m.r spectra were recorded on a Bruker WP80 spectrometer operating at 20.1 MHz.  $^1\text{H}$  N.m.r were recorded on a Perkin Elmer R12B and a Bruker WP80 operating at 80 MHz. In each case  $\text{CDCl}_3$  was used as the solvent and the data are presented as chemical shifts ( $\delta$ ) expressed in p.p.m. from the internal solvent tetramethylsilane ( $\text{SiMe}_4 = 0.000\text{p.p.m.}$ ). I.r. spectra were obtained using a Pye Unicam SP2000 spectrometer. Hexachlorobutadiene and Nujol mulls of the compound were supported between KBr discs. The spectra were calibrated against the  $1603\text{ cm}^{-1}$  band of polystyrene, and the data are presented as absorption bands expressed in  $\text{cm}^{-1}$ . Uv/visible spectra were recorded using a Pye Unicam SP1800 spectrometer and the data are presented as absorption bands expressed in nm and the log extinction coefficient ( $\log E$ ) is written in parentheses. Molecular mass determination were carried out using a Perkin Elmer 115 apparatus. X-ray crystallographic data were collected on a Philips PW1100 diffractometer with Mo-K radiation.



### 2.3.2 Preparation of 2-hydroxy-5-methylbenzophenone oxime.

#### (a) 4-Methylphenylbenzoate.

p-Cresol (156.3 g, 1.45 mole) was dissolved in NaOH (10%, 2.4 dm<sup>3</sup>) with constant stirring using a mechanical stirrer. To this was added benzoylchloride (340.5 g, 2.42 mole), and the mixture was vigorously shaken mechanically for 30 min. The precipitate produced was collected, washed thoroughly with distilled water, breaking up any solid lumps present. Recrystallisation from I.M.S gave needle-like crystals of 4-methylphenylbenzoate (233.3 g, 76.1%), mp 69-72°C. I.r.: 3070, 3040, 2950, 2920, 2868, 1982, 1925, 1898, 1735(b), 1602, 1590, 1518, 1270, 1223(b), 1209, 1192, 1172 b, 1111, 1090, 1070, 1025, 1009, 941, 880, 810 cm<sup>-1</sup>. Found C, 79.0; H, 5.7 C<sub>14</sub>H<sub>12</sub>O<sub>2</sub> requires C, 79.2; H, 5.7%. <sup>1</sup>H N.m.r. (CDCl<sub>3</sub>): 2.31 (s, 3H, CH<sub>3</sub>), 7.12-8.3 (m, 9H, aryl H) p.p.m.

#### (b) 2-Hydroxy-5-methylbenzophenone.

To a solution of 4-methylphenylbenzoate (106 g, 0.5 mole) in chlorobenzene (500 cm<sup>3</sup>) under nitrogen was added rapidly, powdered anhydrous AlCl<sub>3</sub> (98.6 g, 0.74 mole). The mixture was allowed to reflux for 2h. Completion of the rearrangement reaction was confirmed using gas liquid chromatography (glc), by monitoring the disappearance of the peak produced from the starting material. An EGA Scot capillary column was used, 0.1 ul of reaction mixture was injected into the column at a temperature of 200°C. The carrier gas was nitrogen, and the oven temperature was 160°C.

Concentrated HCl (250 cm<sup>3</sup>) was added slowly, to the reaction mixture, with care, followed by ethylacetate (600 cm<sup>3</sup>). This mixture was washed with water (400 cm<sup>3</sup>) and after separation, the organic layer was dried (MgSO<sub>4</sub>) and evaporated to give an oil (114 g). This was triturated with n-hexane (500 cm<sup>3</sup>), for 2h, when a yellow powder was obtained. Further evaporation of the filtrate yielded a yellow crystalline solid. Total solid obtained from trituration (88 g). Both solids were recrystallised from EtOH, and gave yellow square-plate and needle-like crystals respectively. Total yield (63.0 g 71.6%); mp 81.7-83.9°C, lit 85°C. I.r.: 3220, 3074, 3040, 2949, 2930, 2870, 1972, 1925, 1908, 1881, 1830, 1790, 1745, 1625, 1600(b), 1460, 1440, 1401, 1372, 1332, 1288, 1242, 1225, 1209, 1185, 1150, 1142, 1120, 1072, 1008, 1039, 1021, 995, 955, 913, 885, 819, 799, 782, 752 cm<sup>-1</sup>. Found C, 78.7; H, 5.7 C<sub>14</sub>H<sub>12</sub>O<sub>2</sub> requires C, 79.2; H, 5.7% <sup>1</sup>H N.m.r. (CDCl<sub>3</sub>): 2.24 (s, 3H, CH<sub>3</sub>), 6.89-7.75 (m, 8H, aryl H), 11.8 (s, <sup>1</sup>H, OH, D<sub>2</sub>O exchanged)p.p.m. <sup>13</sup>C N.m.r. (CDCl<sub>3</sub>): 20.5, 118.3, 119.0, 127.9 128.4, 128.9, 129.3, 131.9, 133.3, 137.5, 161.4, 207.7 p.p.m. Electronic spectra max/nm(log E) in 95% EtOH: 258(3.12), 352(2.47).

(c) 2-Hydroxy-5-methylbenzophenone oxime.

To a solution of 2-hydroxy-5-methylbenzophenone (15.8 g, 75 mmole) in EtOH (300 cm<sup>3</sup>), was added pyridine (11.8 g, 0.15 mole) followed by [NH<sub>3</sub>OH]Cl (10.4 g, 0.15 mole). The solution was refluxed for 6h. The resultant white solid was removed, washed with EtOH (100 cm<sup>3</sup>), and the combined filtrate and washing were evaporated to dryness. The resulting oil was dissolved in EtOH (100 cm<sup>3</sup>), Cu(Ac)<sub>2</sub>·H<sub>2</sub>O (11.2 g,

60 mmole) in EtOH (50 cm<sup>3</sup>), was added and the solution refluxed for 15 min. The resulting pale green-blue fibrous precipitate (0.5 g) was collected and treated with dil HCl (2 cm<sup>3</sup>), giving a brownish solid (0.29 g). The EtOH filtrate on evaporation to dryness gave a dark brown solid. This was refluxed in water, and the precipitate was collected and dried, yield 14.9 g. A 6 g sample of this was refluxed in CHCl<sub>3</sub> (800 cm<sup>3</sup>), and the resultant bottle green solution was washed four times with dil HCl (300 cm<sup>3</sup>). The organic layer was evaporated to dryness producing a creamy white solid, (5.2 g). This solid was recrystallised from 80-100° petroleum to give colourless needles yield 4.3 g, 82.4%. mp 134-136°C, lit 137°C. I.r.: 3380, 3078, 2930, 2868, 1911, 1776, 1647, 1625, 1592, 1500, 1402, 1336, 1290, 1258, 1149, 1122, 1078, 1040, 1022, 972, 950, 918, 887, 852, 826, 782, 739 cm<sup>-1</sup>. Found C, 73.5; H, 5.9; N, 5.9 C<sub>14</sub>H<sub>13</sub>O<sub>2</sub>N requires C, 74; H, 5.7; N, 6.2%. <sup>1</sup>H N.m.r. (CDCl<sub>3</sub>): 2.4 (s, 3H, CH<sub>3</sub>), 6.6-7.4 (m, 8H, aryl H and N=OH), 11.6 (b, <sup>1</sup>H, phenolic OH, D<sub>2</sub>O exchanged) p.p.m. <sup>13</sup>C d(CDCl<sub>3</sub>): 20.5, 117.0, 118.4, 128.3, 128.6, 130.0, 131.7, 131.9, 155.8, 162.2 p.p.m. Molar mass/g mole<sup>-1</sup> : 231.3

### 2.3.3 Preparation of the copper complexes.

Samples of the ligands used in preparing these copper complexes were supplied by ICI Organics Division.

Copper acetate (20 mg, 0.1 mmol) was dissolved in warm methanol. To this was added a methanolic solution of the oxime (0.22 mmol in 10 cm<sup>3</sup>). The precipitate was collected and dried in vacuo for 15 mins.

(a) Bis-(2-hydroxy-5-methylbenzaldehydeoximato)-  
copper(II) (L1)<sub>2</sub>Cu.

Found C, 52.7; H, 4.3; N, 7.8  $\text{CuC}_{16}\text{H}_{16}\text{N}_2\text{O}_4$  required C, 52.9; H, 4.4; N, 7.71%. I.r.: 3220, 3110, 3060, 3020, 2930, 2860, 2740, 2560, 2430, 1900, 1840, 1765, 1649, 1612, 1540, 1505, 1402, 1322, 1300, 1270, 1219, 1205, 1155, 1170, 1030, 996, 950, 940, 818, 775, 708  $\text{cm}^{-1}$ .

The fine crystalline powder was recrystallised from dimethylformamide (DMF), giving square "plate-like" bottle green crystals which were suitable for single-crystal X-ray diffraction work

(b) Bis-(3,5-dimethyl-2-hydroxybenzaldehydeoximato)-  
copper(II) (L3)<sub>2</sub>Cu.

Found : C, Found : C, 54.6; H, 4.8; N 7.2  $\text{CuC}_{18}\text{H}_{20}\text{N}_2\text{O}_4$  requires C, 55.2; H, 5.1; N, 7.16%. I.r.: 3120, 3024, 3020, 2980, 2920, 2860, 1930, 1767, 1731, 1645, 1613, 1562, 1516, 1348, 1320, 1280, 1229, 1170, 1050, 1028, 974, 960, 881, 851, 820, 794, 751,  $\text{cm}^{-1}$ .

(c) Bis-(2-hydroxy-5-methylbenzophenoneoximato)-  
copper(II) (L4)<sub>2</sub>Cu.

Found: C, 55.4; H, 5.2; N, 7.3%  $\text{CuC}_{18}\text{H}_{20}\text{N}_2\text{O}_4$  requires C, 55.2; H, 5.1; N, 7.16%. I.r.: 3290, 3210, 3080, 2986, 2660, 1909, 1830, 1750, 1648, 1622, 1553, 1509, 1410, 1322, 1211, 1251, 1151, 1075, 1034, 971, 877, 841, 749, 745  $\text{cm}^{-1}$ .

(d) Bis-(2-hydroxy-5-methylbenzophenoneoximato)-  
copper(II) (L5)<sub>2</sub>Cu.

Found C, 64.9; H, 4.6; N, 5.6  $\text{CuC}_{28}\text{H}_{24}\text{N}_2\text{O}_4$  requires C, 65.2; H, 4.7; N, 5.4%. I.r.: 3070, 2930, 1910, 1760, 1642, 1612, 1551, 1408, 1380, 1322, 1249, 1268, 1150, 1040, 1025, 920, 860, 828, 818, 738  $\text{cm}^{-1}$ . The sandy brown precipitate produced was recrystallised from chloroform giving bottle green "needle-like" crystals suitable for single-crystal X-ray diffraction.

(e) Bis-3-tertiarybutyl-(2-hydroxy-5-methylbenzaldehydeoximato)-  
copper(II) (L6)<sub>2</sub>Cu

This complex was obtained already prepared from ICI and was successfully recrystallised from N,N-dimethyl acetamide, as "brownish-green" plate like crystals, suitable for X-ray crystallographic analysis.

#### 2.4 Structure solution and refinement.

##### 2.4.1 Bis-(-2-hydroxy-5-methylbenzaldehydeoximate)copper(II).



The Dirichlet reduced cell derived before data collection by the computer was converted to a standard orthorhombic unit cell, and gave the required intensity relationships:-

$$I_{hkl} = I_{\bar{h}\bar{k}l} = I_{h\bar{k}l} = I_{hkl} = I_{h\bar{k}\bar{l}} = I_{\bar{h}kl} = I_{h\bar{k}l} = I_{h\bar{k}\bar{l}}$$

From inspection of the corrected intensity data, the following systematic absences were noted:-

- 0k1 when  $k = 2n+1$ ,
- h01 when  $l = 2n+1$ ,
- hk0 when  $h = 2n+1$ ,
- h00 ( $h = 2n+1$ ),
- 0k0 ( $k = 2n+1$ ),
- 001 ( $l = 2n+1$ ).

unambiguously defining the space group as Pbcu (No.61).

The algebraic terms for the equivalent positions for space group Pbcu

from International Tables for Crystallography (Volume I) were:-

$$\begin{array}{r}
 x, \quad y, \quad z \\
 0.5 - x, 0.5 + y, \quad z \\
 0.5 + x, 0.5 - y, \quad -z \\
 0.5 + x, \quad y, 0.5 - z \\
 0.5 - x, \quad -y, 0.5 + z \\
 -x, 0.5 + y, 0.5 - z \\
 x, 0.5 - y, 0.5 + z \\
 -x, \quad -y, \quad -z
 \end{array}$$

the unique terms defining the Patterson maxima derived for vectors between symmetry related atoms were found by systematic subtraction to be:-

$$\begin{array}{r}
 2x, \quad 2y, \quad 2z \\
 0 \quad 0.5 - 2y, \quad 0.5 \\
 0.5 \quad 0 \quad 0.5 - 2z \\
 0.5 - 2x, \quad 0.5 \quad 0 \\
 0.5 \quad 0.5 - 2y, \quad 2z \\
 2x, \quad 0.5 \quad 0.5 - 2z \\
 0.5 - 2x, \quad 2y, \quad 0.5
 \end{array}$$

Ignoring the peak corresponding to the origin, the next three highest peaks observed in the calculated Patterson map had values:-

$$\begin{array}{r}
 0.5 \quad 0.5 \quad 0 \\
 0 \quad 0.5 \quad 0.5 \\
 0.5 \quad 0 \quad 0.5.
 \end{array}$$

Solving the simultaneous equations, derived by relating these to the

algebraic terms for the vectors, the solutions are that  $x, y, z$  are equal to 0, 0, 0. This is a special position corresponding to an inversion centre in space group  $Pbca$ . Therefore the symmetry would only generate a total of four copper atoms at:-

0	0	0
0.5	0.5	0
0	0.5	0.5
0.5	0	0.5

Calculation of the crystal density assuming only four molecules in the unit cell gave a value of  $1.55 \text{ g cm}^{-3}$  which is in the expected density range for this type of compound.

The number of reflections measured were 837 out of which 815 unique reflections, with  $I > 3.0 \sigma(I)$ , were used during refinement. In the final stages of refinement, all the hydrogens atoms were located in a difference-Fourier and were refined; and all the non-hydrogen atoms were given anisotropic thermal parameters, producing a final R-factor of 0.036.

#### 2.4.2 Bis(-2-hydroxy-5-methylbenzophenoneoximate)copper(II)



The crystal of this compound,  $(L5)_2Cu$ , decomposed due to loss of solvent, once they were removed from the mother liquor. Data was therefore collected from a single crystal which had been mounted in a Lindemann glass capillary tube containing some mother liquor. The



Dirichlet reduced cell was converted to a monoclinic cell with the correct intensity relationships were confirmed:-

$$I_{hkl} = I_{\bar{h}k\bar{l}} = I_{h\bar{k}l} = I_{\bar{h}\bar{k}\bar{l}}$$

The number of reflections measured were 1303 of which 1248 were independent reflections with  $I > 3.0 \sigma(I)$ . From inspection of the corrected intensity data, the space group was found to be  $P2_1/c$  (No.14), because the conditions limiting the reflections were  $h0l$  only present when  $l = 2n$  and  $0k0$  when  $k = 2n$ .

The algebraic terms for the equivalent position of  $P2_1/c$ , found from International Tables (Volume I), are:-

$$\begin{array}{ccc} x, & y, & z \\ -x, & 0.5 + y, & 0.5 - z \\ x, & 0.5 - y, & 0.5 + z \\ -x, & -y, & -z \end{array}$$

On subtracting these terms, the corresponding algebraic representation of the vectors for the copper atoms are:-

$$\begin{array}{ccc} 2x, & 2y, & 2z \\ -2x, & 0.5, & 0.5 - 2z \\ 0 & 0.5 - 2y, & 0.5 \end{array}$$

On solving the simultaneous equations, obtained by relating these to the observed Patterson peaks, the atomic coordinates of the copper were found to occupy a special position (centre of symmetry)  $x, y, z = 0, 0, 0$ , with two molecules per unit cell, which corresponded to a reasonable calculated density,  $1.56 \text{ g cm}^{-3}$ . Considering the inherent

difficulties in attempting to phase a Fourier map based on the position of a single copper atom, the Patterson was also solved for a donor atom. For both nitrogen and oxygen, the copper-heteroatom vector would be approximately 2 Å in distance from the origin. A peak of this approximate distance from the origin was looked for in the Patterson Map (see Table 2.4.2), corresponding to the vector:-

$$x_{\text{Cu}} - x_{\text{H}}, \quad y_{\text{Cu}} - y_{\text{H}}, \quad z_{\text{Cu}} - z_{\text{H}}$$

The peak which satisfied this condition was peak 15. This gave the co-ordinates of the heteroatom directly (since the co-ordinates of the copper atom are  $x_1, y_1, z_1 = 0, 0, 0$ ):-

$$\begin{aligned} x_2 &= 0.165 \\ y_2 &= -0.047 \\ z_2 &= 0.058 \end{aligned}$$

For two non-symmetry related atoms, copper and a donor atom, subtraction of the equivalent positions would give the unique vectors:-

$$\begin{array}{lll} x_1 - x_2, & y_1 - y_2, & z_1 - z_2 \\ -(x_1 - x_2), & 0.5 - (y_1 + y_2), & 0.5 - (z_1 - z_2) \\ -(x_1 + x_2), & 0.5 - (y_1 - y_2), & 0.5 - (z_1 + z_2) \\ x_1 + x_2, & y_1 + y_2, & z_1 + z_2 \end{array}$$

The coordinates of the copper atom being 0, 0, 0 means that the above equations are reduced by half since  $x_1 - x_2$  and  $x_1 + x_2$  are now equivalent to each other. A second vector arising from the copper-heteroatom was looked for at 0.165 0.453 0.558 which corresponded to  $x_2, 0.5 - y_2, 0.5 + z_2$ . Peak 71 was found very low down in the

Patterson map and was very inaccurate in the y co-ordinate.

Other higher peaks in the Patterson map, thought to arise from the presence of solvent molecules in the unit cell, complicated the search for a solution. A Fourier map based on the copper and hetero-atoms revealed the presence of the three chlorine atoms associated with the chloroform molecule. Subsequent difference-Fourier syntheses allowed location of all the non-hydrogen atoms. The atomic positions of the hydrogen atoms on the substituted phenyl groups were fixed at calculated positions (C-H 0.95 Å H-C=C 120°). Eight out of the remaining fourteen hydrogens were eventually located and used in refinement. The six which were not found (and not used in calculated positions, during refinement) belonged to the two 5-methyl substituent groups of the molecule.

The number of unique reflections used during refinement were 1129, with  $I > 3.0 \sigma(I)$ . In the final stages of refinement only copper, nitrogen, oxygen and chlorine atoms were refined with anisotropic thermal parameters. The final R-factor was 0.055.

2.4.3 Bis-3-tertiarybutyl-(2-hydroxy-5-methylbenzaldehyde-oximate)copper(II),  $(C_{16}H_{21}NO)_2Cu$ .

The preliminary cell obtained from the peak hunt routine on the PW1100 diffractometer gave a reduced cell matrix which showed relationships indicating that the true cell could be either monoclinic C, or orthorhombic I. Applying the appropriate transformation matrix for the latter gave a cell with a  $\beta$  angle which was not 90°. Similar

application of the monoclinic transformation matrix gave a cell with a B angle as 107.20°. The Laue symmetry reflection relationships for a monoclinic space group were satisfied with  $I_{hkl} = I_{\bar{h}k\bar{l}} = I_{h\bar{k}l} = I_{h\bar{k}\bar{l}}$ . However due to the relatively large B angle, the cell was transformed to a non-standard monoclinic I-centred lattice with a B angle of 92.76°. The data was collected giving a total of 1140 reflections with  $I > 3.0 \sigma(I)$  in the range  $3 < \theta < 25^\circ$ . A calculated density, assuming  $Z=4$ , of  $1.48 \text{ g cm}^3$  was of the magnitude expected for this type of molecule.

Inspection of the corrected intensity data showed limiting conditions in  $h0l$  with  $l=2n$  ( $h=2n$ ). Thus the space group could be either  $Ic$  or  $I2/c$ . Examination of the Patterson map showed that the only major vector peaks were the origin peaks at  $0, 0, 0$  and  $1/2, 1/2, 1/2$ . This was consistent with space group  $I2/c$ , which has 8 equivalent positions, but the copper atom would be required to occupy a special position on an inversion centre, giving  $Z = 4$  as indicated by the calculated density. The space group was assigned as  $I2/c$ , (modified  $C2/c$  No.15) and confirmed by satisfactory refinement.

For the space group  $I2/c$  the algebraic terms defining the equivalent positions are:-

$$\begin{array}{l}
 (0 \ 0 \ 0 ; 1/2 \ 1/2 \ 1/2) + \\
 \begin{array}{lll}
 x & y & z \\
 -x & y & 0.5 - z \\
 x & -y & 0.5 + z \\
 -x & -y & -z
 \end{array}
 \end{array}$$

For a atom in a special position such as  $1/4, 1/4, -1/4$  these reduce to:-

$$(0\ 0\ 0; 1/2\ 1/2\ 1/2) + \\ 1/4\ 1/4\ -1/4; 1/4\ -1/4\ 1/4$$

The Patterson map was examined for vectors arising from copper-oxygen or copper-nitrogen atoms of approximately 2 Å in length. A peak having values  $u = 0.059$ ,  $v = 0.187$  and  $w = -0.041$  was found. This corresponds to the vector  $x_1-x_2, y_1-y_2, z_1-z_2$ . Where the copper atomic co-ordinates are  $x_1, y_1, z_1$  and the heteroatom (oxygen or nitrogen) co-ordinates being at  $x_2, y_2, z_2$ . Substituting in the relevant values for the copper atomic co-ordinates ( $1/4, 1/4, -1/4$ ), the co-ordinates for the metal bonded atom were found to be:-

$$x_2 = 0.191 \\ y_2 = 0.063 \\ z_2 = -0.209$$

A vector corresponding to  $x_1+x_2, y_1-y_2, -1/2+(z_1+z_2)$  was then searched for {this term being derived by subtracting the algebraic terms,  $(-x_2, y_2, 1/2-z_2$  from  $(x_1, y_1, z_1)$ } at the calculated position  $u=0.440$ ,  $v=0.187$  and  $w=-0.959$  in the Patterson map. This was found as  $u=0.443$ ,  $v=0.191$  and  $w=0.042$  (i.e.  $-0.956$ ), confirming the co-ordinates of the first heteroatom.

Another new short vector of the same length (2 Å) was looked for, and was found at  $u = -0.046$ ,  $v = 0.086$  and  $w = 0.160$ . This corresponds to

$x_1-x_3, y_1-y_3, z_1-z_3$ . The second atom was therefore found at:-

$$\begin{aligned}x_3 &= 0.296 \\y_3 &= 0.164 \\z_3 &= -0.410\end{aligned}$$

These positions (i.e. that of the copper and two heteroatoms) were used to calculate structure factors and hence a Fourier synthesis from which the other non-hydrogen atoms were found.

Of the number of reflections recorded 1056 were unique with  $I > 3.0 \sigma(I)$ , and were used during refinement. All the hydrogen atoms were located in difference-Fourier maps and refined, in the last stages, with the exception of those of the 5-methyl groups. All the non-hydrogen atoms were assigned anisotropic thermal parameters. The final R-factor produced was 0.047.

#### 2.4.4 3,5-Dimethyl-2-hydroxyacetophenone methoxy imine, 'L7H'

The unit cell for this structure was found to be orthorhombic having the same intensity relationship as for structure (L1)<sub>2</sub>Cu. Scan mode 1 was used during data collection so that all reflections were recorded giving a total of 1125. From inspection of the corrected data, reflections in h00, 0k0, and 00l, were only present when h, k or l were equal to 2n. No other limiting conditions were found, which defined the space group as P2<sub>1</sub>2<sub>1</sub>2<sub>1</sub> (No.18). This indicates the presence of 4 molecules in the unit cell, for which the calculated density value of 1.193 g cm<sup>-3</sup> was obtained.

From the list of normalised structure factor and alpha values (193, with  $E > 1.2$ ) the starting set of phases were chosen. For this space group  $P2_12_12_1$ , to define the origin, three reflections must be used. These should have high E-values and alpha values, each must have one zero element, none may belong to eee parity group, and no combination of the three should give eee.

The reflections used as the starting set are listed in Table 2.4.4.

Table 2.4.4 Reflections used to initiate phase determination for 'L7H'

	h	k	l	E -value	-value	phase angle ( $^{\circ}$ )
origin	9	2	0	2.833	113.3	90
origin	0	1	6	2.481	74.3	90
origin	12	0	1	2.980	108.7	90
enantiomorph	14	3	3	3.148	217.3	45 135
multisolution	0	2	1	2.785	114.8	0 180
multisolution	0	4	1	2.276	58.8	0 180
multisolution	0	4	6	1.947	39.0	0 180
multisolution	20	0	1	3.014	71.4	0 180
multisolution	15	0	4	2.519	130.7	45 135 225 315
multisolution	14	2	3	2.347	110.8	45 135 225 315

Specifications of the above and recalculations using the tangent formula, an E-map was obtained which had peaks with a feasible arrangement for thirteen out of the fourteen non-hydrogen atoms. The remaining carbon atom and the hydrogen atoms were located from subsequent difference Fourier synthesis.

In the final stages of refinement 544 unique reflections with  $I > 3.0 \sigma(I)$  were used. All atoms of the structure were refined. All the non-hydrogen atoms were given anisotropic thermal parameters, and the final R-factor was 0.048.

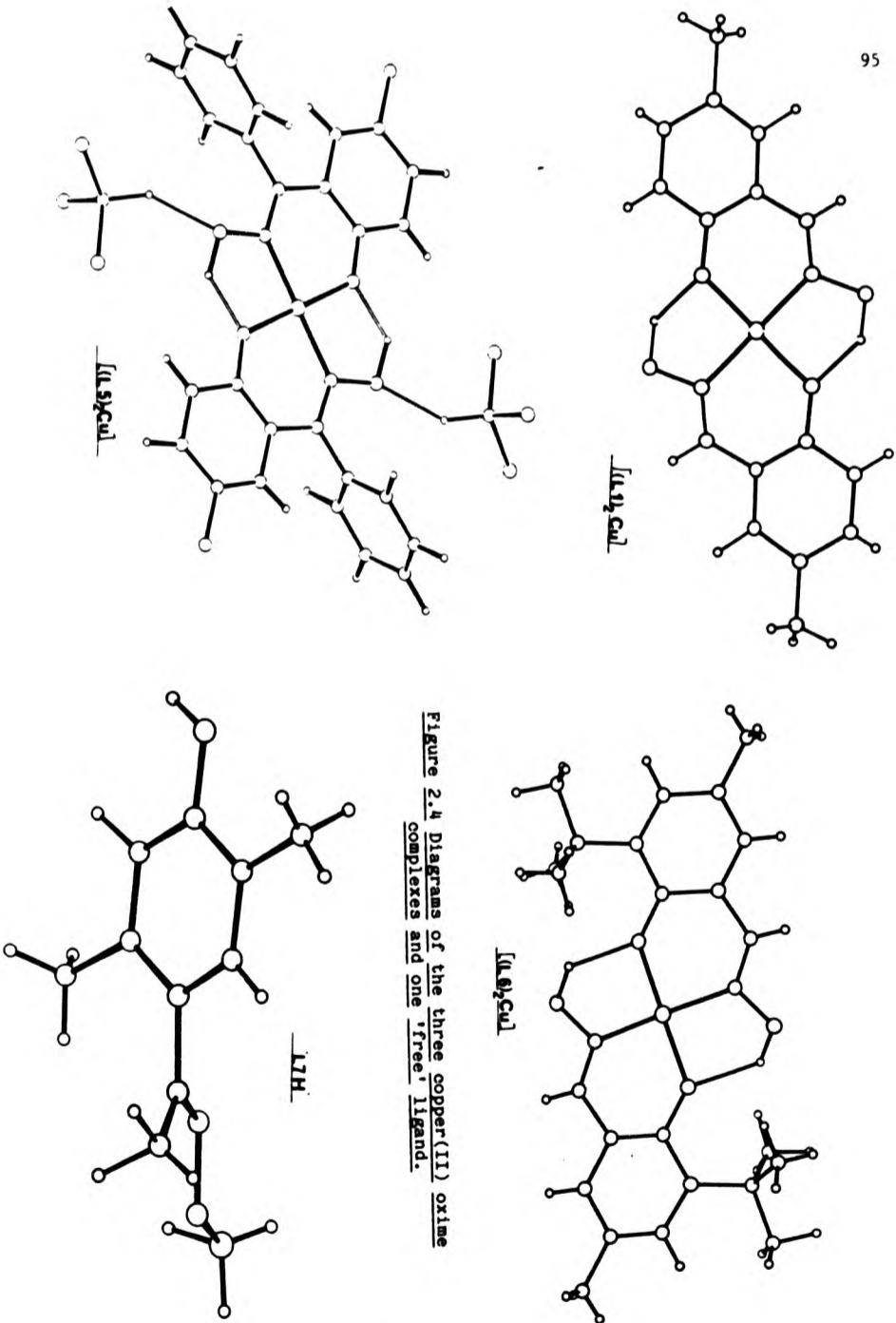


TABLE 2.4 MOLECULAR STRUCTURE DETERMINATION DATA.

	[ (L1) <sub>2</sub> Cu ] <sub>n</sub>	[ (L5) <sub>2</sub> Cu ]	[ (L6) <sub>2</sub> Cu ]	' L/H '
Molecular formula	C <sub>16</sub> H <sub>16</sub> N <sub>2</sub> O <sub>4</sub> Cu	C <sub>30</sub> H <sub>26</sub> N <sub>2</sub> O <sub>4</sub> Cl <sub>6</sub> Cu	C <sub>24</sub> H <sub>32</sub> N <sub>2</sub> O <sub>4</sub> Cu	C <sub>11</sub> H <sub>15</sub> NO <sub>2</sub>
Molecular weight	363.86	754.79	476.07	193.25
Colour	Bottle-green	Bottle-green	Brownish-green	Colourless
Crystal Dimensions/mm	0.176x0.08x0.208	-	0.16x0.048x0.048	0.32x0.16x0.45
Crystal system	Orthorhombic	Monoclinic	Monoclinic	Orthorhombic
Space group	Pbca	P2 <sub>1</sub> /c	I2/c	P2 <sub>1</sub> 2 <sub>1</sub> 2 <sub>1</sub>
a/Å	32.047(2)	6.317(5)	21.631(3)	20.874(5)
b/Å	7.517(2)	11.849(3)	6.678(2)	7.537(1)
c/Å	6.488(1)	21.558(2)	16.088(4)	6.826(2)
β/°	90	93.75(1)	92.76(2)	90
V/Å <sup>3</sup>	1562.94	1610.07	2321.24	1073.92

TABLE 2.4 continued:-

$D_c/\text{gcm}^{-3}$	1.55	1.56	1.48	1.195
$E(\text{000})$	748	766	1004	416
$Z$	4	2	4	4
$\mu(\text{Mo-K}\alpha)\text{cm}^{-1}$	12.74	11.01	8.64	0.48
$\theta$ range, min; max	3;28.5°	2;20°	3;25°	3;25°
Scan mode	2	2	2	1
No. of reflections measured.	837	1303	1140	1141
No. of independent reflections.	835	1248	1129	1125
No. of unique observed reflections $\geq 3\sigma I$ .	815	1129	1056	544
No. of parameters used in refinement.	138	121	153	128
$R$	0.0361	0.0554	0.0470	0.0478
$R_w$	0.0374	0.0605	0.0455	0.0451
$w=1/\sigma^2(I)$				



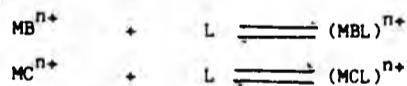
CHAPTER 3 Metal ion discrimination by macrocyclic ligands.

### 3.1 Metal ion discrimination by macrocyclic ligands and its optimisation.

As mentioned in Section 1 synthetic co-ordination compounds have been used as models to study the behaviour of their biological counterparts. Specificity in metal binding is an important topic in such studies. In this section, a structural approach to macrocyclic ligand design will be developed which aims to increase our understanding of how metal ion discrimination could be enhanced.

#### 3.1.1 Factors governing selectivity of macrocyclic ligands.

Selectivity is achieved when competitive complexation of metal ions and a ligand result in a far greater fraction of the ligand forming a complex with one of the ions than with the other. As mentioned in Section 1 selectivity is related to thermodynamic stabilities of the complexes produced, these being compared by complex formation constants (eg  $\log K_1$  values).



The ratio of the  $K_1$  values or the difference between the  $\log K_1$  values defines the ability of the ligand to discriminate between the metal ions.

Since most naturally occurring ligands which show high discrimination ( $\Delta \log K_1$ ) between metal ions are rigid and/or cyclic multidentate systems, related synthetic ligands are used in this study. On closer examination of the overall equilibrium for metal complex formation, (Section 1.5), component  $\Delta G$  terms can be used to describe the overall reaction.<sup>117-126</sup> The properties of the metal or ligand which make these terms more favourable can then be examined. Both the metal ion

and the ligand must undergo a process of desolvation before they can react with each other ( $\Delta G_{\text{desolvation}}$  of ligand and metal). For the metal ion, most or all of the co-ordinated (or associated) solvent molecule must be lost before complex formation.

Normally the ligand will also have to adopt a different configuration to be able to present a donor set with the correct co-ordination geometry for the metal ion ( $\Delta G_{\text{conformational}}$  change for the ligand). On complexation, formation of strong bonds between the metal ion and donor atoms will release free energy ( $\Delta G_{\text{Binding}}$ ). We can now write:-

$$-RT \ln K_1 = \Delta G_{\text{Desol.}} + \Delta G_{\text{Conf.}} + \Delta G_{\text{Bind.}}$$

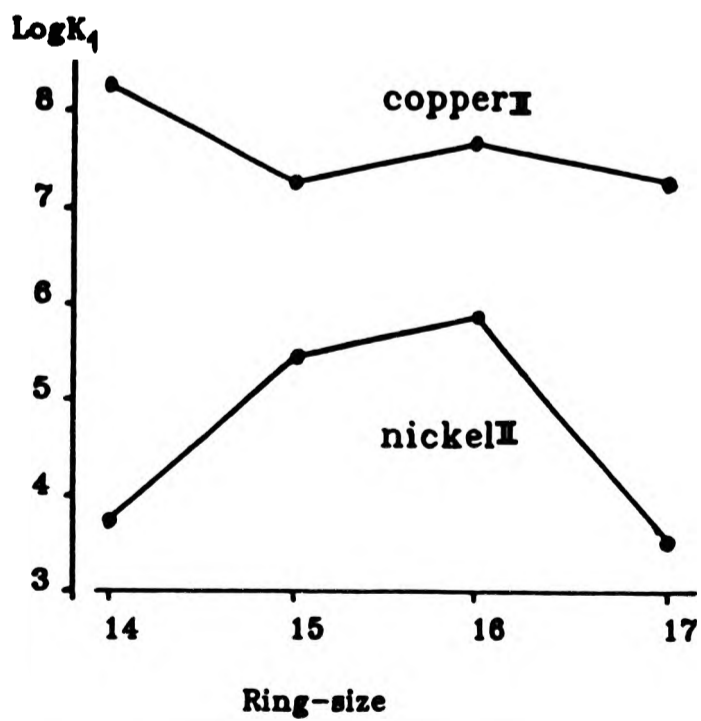
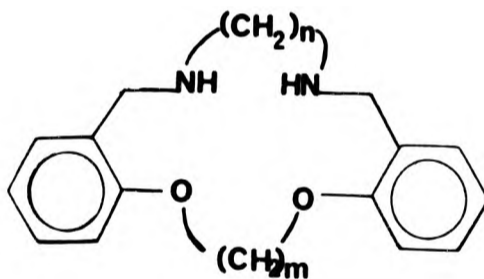
In order to obtain a high stability constant  $K_1$ , the individual  $\Delta G_{\text{terms}}$  should be negative or carry as small positive value as possible.

The most favourable free energy term is usually  $\Delta G_{\text{Bind.}}$ . The magnitude of  $\Delta G_{\text{Bind}}$  depends largely on the strength of the metal bonds formed. This in turn depends on a favourable match between the number, type and geometry of the donor atoms, and the requirements of the metal ion.<sup>127-135</sup> The basicity (pKa) of the donor atoms will be very important in giving favourable  $\Delta G_{\text{Bind.}}$ <sup>135</sup>

The metal ions which are the most solvated will be those with the most unfavourable value of desolvation free energy. This term is related to the ionic radii of the metal, with small ions being most heavily solvated. It would be expected that cyclic ligands will be associated with a more favourable  $\Delta G_{\text{Desolvation}}$  value than a linear analogues,<sup>124,125</sup> because they are less solvated. Here solvation occurs mainly in the polar portion of the molecule which are usually required for formation of the metal ligand bonds. Consequently the

Figure 3.1.1 Plot of  $\log K_1$  against ring size variation for copper and nickel complexes of  $N_2O_2$  macrocycles, structure shown below:-

Ring-size	m	n
14	2	2
15	2	3
16	3	3
17	4	3



ligand must lose most of the solvent molecules associated with it, to be able to participate in complexation.

The  $\Delta G_{\text{Conf}}$  for the ligand is unfavourable if a major change in geometry is required to align donor atom to the metal co-ordination sites. These changes are frequently associated with increased repulsion between the donor atoms which were previously more separated from each other.

Ligand design can be approached to give enhanced discrimination between two metal ions by developing features which lead to more favourable free energies for binding to one of the metal ions and to easier desolvation and ligand conformational changes in setting up the ligand to bond to this metal. Ideally to optimise complex stability the ligand should provide enough atoms to saturate the co-ordination geometry of the metal. In addition an important factor is the "goodness of fit" of the metal in the ligand donor set, ie in the ligands "bonding cavity". The concept of macrocyclic cavity size to achieve metal ion recognition is not new.<sup>136-144</sup> So far it has been studied mainly for alkali and alkaline earth metal complexes.

In a series of quadridentate macrocyclic ligands of the type shown in Figure 3.1.1, a plot of  $\log K_f$  values against ligand ring size for high spin nickel complexes, showed<sup>145-147</sup> that the most stable complex was produced with the 16-membered ring. Structural analyses showed that for this series the 16-membered ring provided the best fit for the nickel although the optimum hole size could well lie between those provided by the 15- 16-membered rings.



To optimise  $\log K_1$ , another structural parameter of the ligand could be altered. Keeping the ring size constant, we could try adding bulky pendant groups to the ligand. This might not only vary the  $pK_a$  of a given donor, but would also restrict the ligand which would affect its hole size.

The effects of such a procedure, and any other structural alteration to the ligand could lead to a "fine-tuning" of the ligand to provide a better fit for a particular metal ion. The information obtained could be expressed as a matrix relationship, and then used to select factors to enhance  $\log K_1$  for this and other metal ions with which this ligand would react.

### 3.1.2 Bonding cavity of rigid cyclic systems.

The fit of a metal for a strain free arrangement of the donor set is of major importance when considering discriminatory effects of a macrocyclic ligand. From X-ray structural results the bonding cavity of the macrocycle can be obtained.<sup>145-146</sup> This method can be applied even if the ligand has an odd number and/or non-planar arrangement of donor atoms<sup>147</sup> Figure 3.1.2(a); giving a more realistic estimate of hole size than the conventional approach of defining the diameter of the cavity as the distance between diametrically opposed donor atoms.<sup>146</sup> First an estimate of the hole size is obtained by finding the mean distance of the donor atoms from their centroid,<sup>145-146</sup> Figure 3.1.2(b). To find the centroid (CE) the mean x,y, and z co-ordinates of the donor atoms are found. The mean distance of the donor atoms from the CE is the ligand hole size  $R_H$ . This is then corrected for the "appropriate covalent radii" of the donor atoms.<sup>147</sup> These "appropriate covalent radii" were obtained by searching Cambridge

Figure 3.1.2(a) Showing the limitation of using the distance between diametrically opposed donor atoms to estimate the radius( $R$ ) of the "hole" defined by a non-planar donor set. In this example the four donor set shows a tetrahedral distortion from planarity. Ce = centroid.

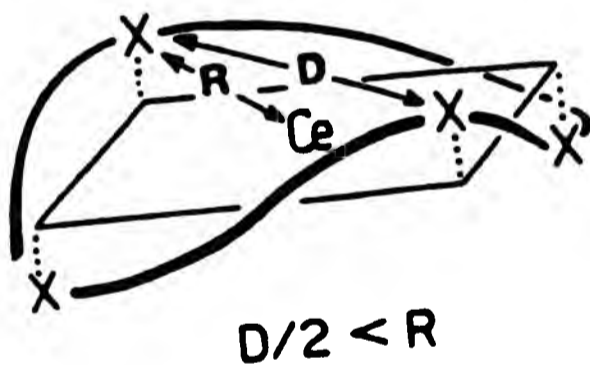
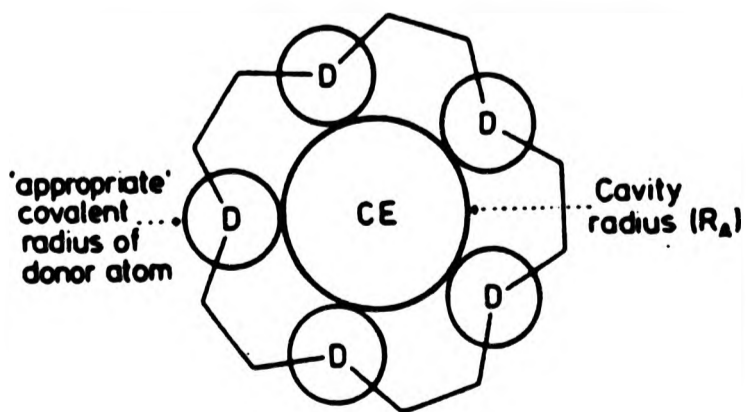


Figure 3.1.2(b) The bonding cavity radius ( $R_A$ ) available to metal ion in a symmetrical macrocyclic ligand.



X-ray Crystallographic data base for all complexes containing the particular metal ion under study, and the relevant donor atoms. The metal-donor bond lengths are found and the Pauling covalent radius for the metal ( $R_p$ ) is subtracted from them. These values are then used to calculate the "available bonding cavity" of the macrocycle ( $R_A$ ).

$$R_A = R_H - \text{mean donor covalent radii.}$$

$R_A$ , is the bonding cavity available to the metal whose covalent radii was used in the calculation above. When the ratio of available bonding cavity and Pauling covalent radius of the metal is unity ( $R_A/R_p = 1$ ), then "goodness of fit" is perfect. This should give the most favourable  $\Delta G_{\text{Bind}}$  for any given series of ligands with the same set of donor atoms.

Work by Tasker et.al.<sup>147</sup> has shown that  $R_H$  is affected not only by ring size variation but also by the degree of unsaturation that is present in the macrocycle. Tasker has shown that for a limited range of planar  $N_4$  ligands incorporation of additional methylene groups into the ring is associated with increase of approximately 0.04 - 0.05 Å in hole size. That is, expanding ring size from nineteen to twenty nine atoms  $R_H$  values can change from 1.90 - 2.35 Å.

Unsaturation tends to reduce ring puckering, increasing planarity. The associated flattening of the ring which increases the hole size is more than offset by the introduction of shorter bonds which reduce the circumference and  $R_H$ . Substituents in an axial or equatorial position of the macrocycle, may also effect the hole size of ligands, especially if interactions occur with the complexed metal ion. These are likely to lead to flattening or puckering of the ring to reduce strain. Clearly, therefore, ring size, unsaturation level and substitution pattern are all likely to have an influence on the size

of the bonding cavity.

For the series of quadridentate  $N_2O_2$  ligands mentioned above, the 16-membered ring has the best hole size, but the optimum could well lie between that of 15- 16-membered ring.

Structural analysis of the precursor 16-member diimine nickel complex showed<sup>145</sup> Figure 3.1.2(c), that only a minor reduction ( $R_H=2.07$ ) in cavity size was achieved by the substitution of two imine for two secondary amine linkages. However the difference is less pronounced when the binding cavities are compared once the data are corrected for the covalent radii for  $sp^2$  and  $sp^3$  nitrogen.

Further studies of macrocyclic hole size, Table 3.1.2, in relation to the above were carried out using a series where the ring size remained constant, but the donor atom types were varied.<sup>146</sup> Detailed structural analysis of their high spin nickel (II) complexes were obtained. For the high-spin nickel(II) ion a relative good fit is provided by all three macrocycles. Even though the radii of the sulphur atoms are much larger than those of nitrogen and oxygen, the cavity presented to the nickel remained near ideal because the four long carbon sulphur bonds increased the overall "circumference" of the inner ring, Figure 3.1.2(d). For this ligand series nickel(II) lies in the plane of the  $N_2O_2$ -donor set, and thus can be said to be completely contained in the cavity of the macrocycle. Copper(II), on the other hand, forms 5-co-ordination complexes, Figure 3.1.2(e),<sup>148-150</sup> in which the Cu(II) ion is displaced towards the attached chloro-group and sits above the hole of the macrocycle.<sup>148</sup> Consequently the stability constants for copper(II) complexes if this series of ligands show a smaller dependence on ring size, Figure 3.1.1.

Figure 3.1.2(c) Comparison of bond length/Å and angle/deg with in the donor atom planes of the of the 16-membered macrocycles:-

- a)  $[\text{Ni}(\text{O}_2\text{N}_2)\text{Br}_2]$  -ie with no imine bonds  
 b)  $[\text{Ni}(\text{O}_2\text{N}_2)\text{Br}_2]$  -ie with two imine bonds  
 along with an ortep diagram of this complex.

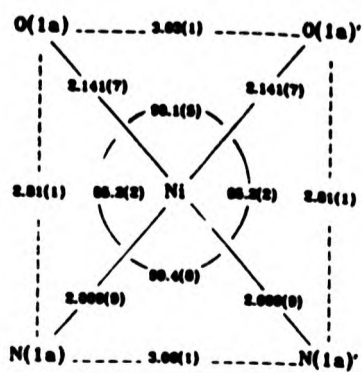
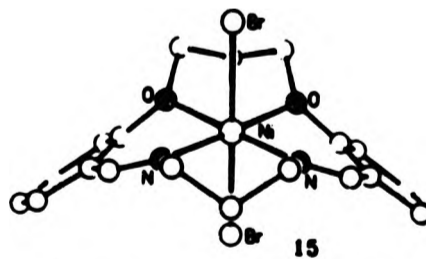
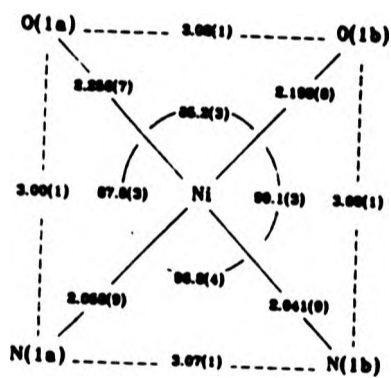


**Table 3.1.2** Calculated values for the hole size of three 15-membered co-ordination macrocycles with nickel(II) ion differing in their donor atom type.

	<u>D/Å diameter of macrocyclic hole</u>	<u>RA/Å apparent radii of metal</u>
$[\text{Ni}(\text{O}_2\text{N}_2)\text{Cl}_2]$	4.18	1.35
$[\text{Ni}(\text{N}_2\text{N}_2)\text{Cl}_2]$	4.22	1.39
$[\text{Ni}(\text{S}_2\text{N}_2)\text{Cl}_2]$	4.54	1.39

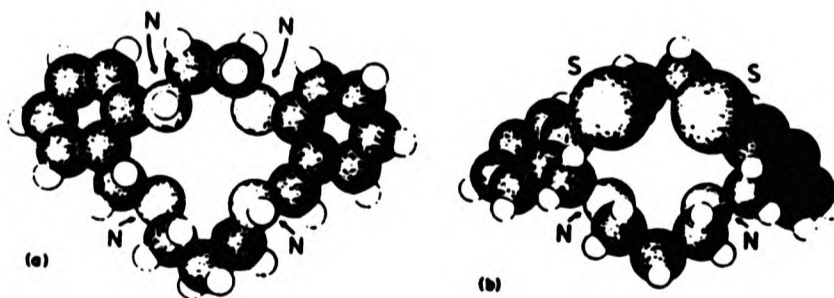
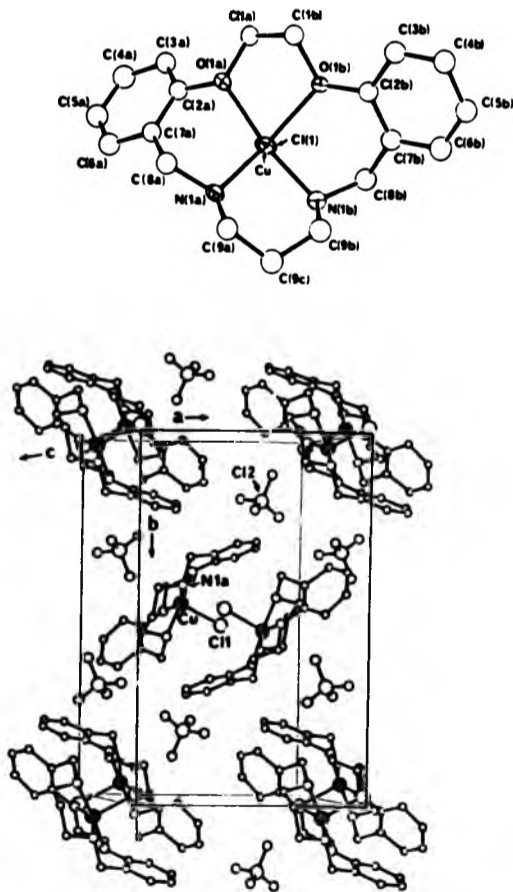


**Figure 3.1.2(d)** Space-filling representation nickel(II) complexes of the 15-membered macrocycles with:-

- a) the  $\text{N}_2\text{N}_2$ -donor and
- b) the  $\text{S}_2\text{N}_2$ -donor set.

Figure 3.1.2(e) Showing the cation  $[\text{Cu}(\text{N}_2\text{O}_2\text{-15-membered}(\text{Cl}))]^+$  viewed down the Cu-Cl bond; along with the contents of the unit cell of this complex viewed down c.



Recent work at PNL<sup>151-152</sup> as also demonstrated that "goodness-of-fit" and complex stability for Ni(II) in  $N_4$ -macrocycles is very dependent on whether high or low spin nickel(II) is present.

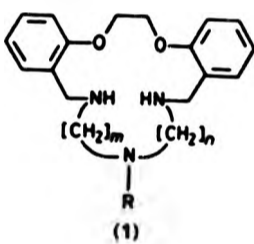
### 3.1.3 Discrimination by structural dislocation.

Systematic variation of a structural feature such as ring-size within a series of ligands can lead to a gross change in geometry of complexes with a given metal ion at a particular point along the ligand series. Such a "structural dislocation"<sup>153-156</sup> may occur at a different point in the series for complexes of another metal ion and hence may have important consequences for the discrimination between the two metal ions. An example of this type of behaviour has been found for the Zn(II) and Cd(II) complexes of the quinquedentate ligands<sup>156</sup> shown in Figure 3.1.3. The plot of  $\log K_1$  values, Figure 3.1.3, shows that along the series of 17- to 19-membered ring ligands there is a sudden change from the unusual discrimination in favour of Cd(II) ( $\log K_1 \sim 1.0$ ) shown by the 17- and 18-membered ligands, to the normal discrimination in favour of Zn(II) ( $\log K_1 \sim 1.0$ ) shown by the 19-membered ring. This is brought about by a major decrease in stability of the Cd(II) complexes of the ligands as the ring size increases from 18 to 19. X-ray structural analysis has confirmed<sup>155, 156</sup> that there is a "structural dislocation" at this point.

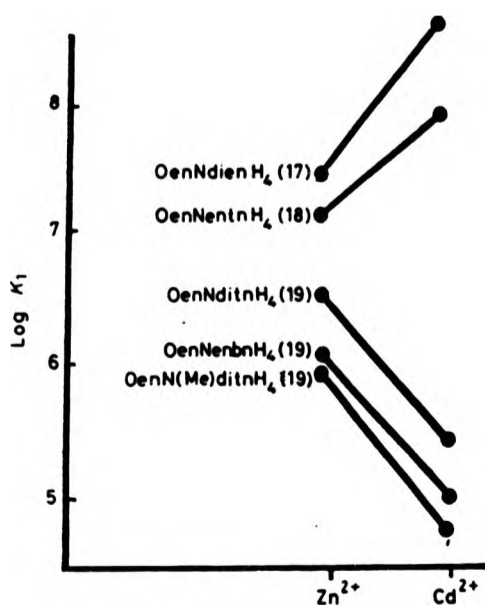
For the smaller rings the five donors in the macrocycle interact with Cd(II) to give an approximately planar equatorial  $N_3O_2$ -donor set. In the 19-membered ring the ether oxygens are no longer bonded, and the Cd(II) is displaced from the centroid and the least squares plane of the  $N_3O_2$ -donor set. Co-ordination is through the three nitrogen atoms



Figure 3.1.3 A plot of logK values for zinc(II) and cadmium(II) complexes of the quinquedentate macrocycles shown below:-



Ring size	m	n	R	Abbreviation
17	2	2	H	OenNdienH <sub>4</sub>
18	2	3	H	OenNentnH <sub>4</sub>
19	3	3	H	OenNditnH <sub>4</sub>
19	2	4	H	OenNenbnH <sub>4</sub>
19	3	3	Me	OenN(Me)ditnH <sub>4</sub>



only.

In contrast, in the Zn(II) series there is no "dislocation" and structural analysis has established the tridentate mode of co-ordination is already present in the smallest size ligand,<sup>156</sup> Figure 3.1.3. The assumption can therefore be made that this arrangement occurs in all the Zn(II) complexes of the ligand with ring size variation.

3.1.3(i) The influence of alkyl substituents on discrimination by structural dislocation for ligands with N3O2-donor sets.

It has already been shown above that a "structural dislocation" can occur in a series of quinquedentate ligands by varying the ring size. This phenomenon can also be imposed on these ligands by systematic variation in the numbers and sites of alkyl substituents, Table 3.1.3(i).<sup>157-159</sup>

An X-ray structure determination has established that the unsubstituted 17-membered ligand of the above series, Figure 3.1.3i(a), defines five vertices of a co-ordination octahedron in the complex  $[\text{Ni}\{3.1.3(i)\}\text{H}_2\text{O}](\text{ClO}_4)_2$ , with a *fac*-arrangement of the three nitrogen atoms. This type of arrangement cannot be adopted by the symmetrically substituted dimethyl derivative, ligand 3.1.3(i)c, as computer-calculated models show,<sup>157</sup> the methyl groups would be found to be either in close proximity of the adjacent ethane bridges or to the adjacent benzyl chelate rings, Figure 3.1.3(i)b. Structure analysis has shown that this dimethyl substituted ligand forces a very irregular five co-ordination geometry on Ni(II) in the complex  $[\text{Ni}\{3.1.3(i)c\}](\text{NCS})_2$ , with the two oxygen atoms of the ligand at non-bonding distances.

Figure 3.1.31(a) Ortep diagram of the X-ray structure of  $\text{fac-}[\text{Ni}(\text{3.1.3(1)a})(\text{H}_2\text{O})](\text{ClO}_4)_2$ .

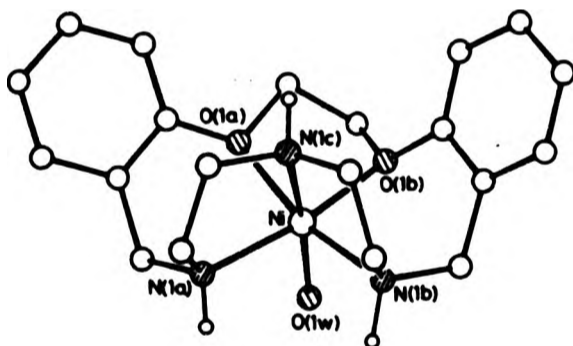
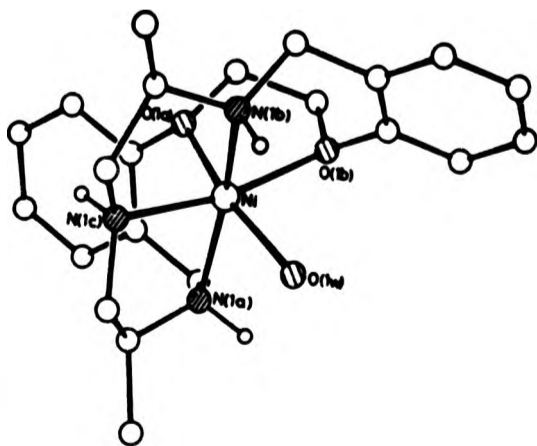


Figure 3.1.31(b) The structure of  $\text{mer-}[\text{Ni}(\text{3.1.3(1)c})(\text{H}_2\text{O})]^{2+}$  predicted by the molecular mechanic calculation.



The "structural dislocation" imposed by the methyl groups produces a marked drop in the stability of the Ni(II) compounds. The overall effect of this is that the methyl substitution has greatly enhanced the discrimination in favour of Cu(II), ( $\Delta \log K_1$  4.3 for 3.1.3(i)a and 7.3 for 3.1.3(i)c). Since negligible differences in stability occur for the copper complexes, presumably due to its ability to adopt a different geometry.

#### 3.1.4 Molecular mechanics calculations.

The significance of conformational differences on metal ion discrimination can be examined by using force field calculations, based on the method described by Allinger<sup>160, 161</sup> for purely "organic" molecules. Dr Adams at James Cook University (JCU), has developed a new series of programs, (MOLMIN), to perform such calculations on metal complexes. The method requires force-field parameters which define how the overall energy of the molecule varies as bonds stretch or compress from normal lengths, bond-angles deform from normal values, intra-molecular contacts vary (Van der Waals forces) and molecular dipole-dipole interactions are changed.

In collaboration with Lindoy, Leong et.al at JCU, MOLMIN has been used to investigate different behaviour of the quinquedentate ligands in Figure 3.1.3(i), towards Ni(II) ions. Starting from the X-ray atomic co-ordinates for the  $[\text{Ni}\{3.1.3(i)a\}(\text{H}_2\text{O})]^{2+}$  the structure was minimised and its "strain" energy recorded. The geometry of the minimised structure differed in only minor detail from the X-ray structure. Such differences are to be expected since no account of crystal packing is incorporated in the molecular mechanics procedure. The hypothetical (meridional) isomer atomic co-ordinates were

estimated, using molecular models as a guide, and was minimised using the molecular mechanics procedure. The structure produced was found to be 9.0 kJ/mol less stable than the corresponding minimised facial structure.<sup>157</sup> A similar procedure was carried out on the dimethyl substituted complexes,<sup>157</sup>  $[\text{Ni}\{3.1.3(i)c\}(\text{H}_2\text{O})](\text{NCS})_2$ , for the corresponding meridional and facial forms. The results showed a reversal of stability order. The meridional isomer was predicted to be 7.2 kJ/mol more stable than its facial form, and corresponded to that observed experimentally. In the calculations it was assumed that the *meso*-isomer was present, as was observed to occur in the related complex  $[\text{Ni}\{3.1.3(i)a\}(\text{H}_2\text{O})](\text{ClO}_4)_2$ .<sup>157</sup> In this complex the  $\text{N}_3$ -donor fragment also assumes a meridional arrangement.

This investigation demonstrated that molecular mechanics calculations could be applied successfully to model "dislocation" discrimination of the type described above. Further, it appears feasible that such calculations may be used predictively for the design of new metal-ion discriminating reagents.

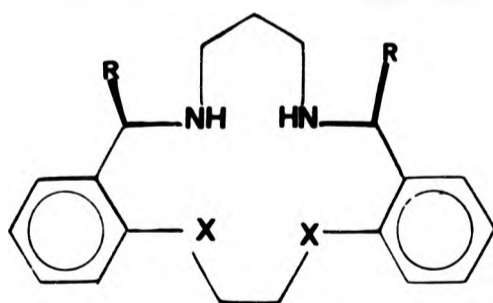
#### 3.1.5 Aim of this section of the thesis.

Any investigation involving the stability of metal complexes of macrocyclic ligands is made easier if  $\log K$  values are in a range which is accessible by pH titration methods. For  $\text{N}_4$  macrocycles of the type shown in Figure 3.1.4  $\log K_1$  values are convenient for Zn(II) and Cd(II) complexes. Similarly, for  $\text{N}_2\text{O}_2$  ligands, stability data for Ni(II) and Cu(II) can also be considered.

The present investigation will be mainly concerned with Zn/Cd discrimination. This is very challenging because the chemical properties and solution chemistry of these two metal ions are very

similar. The potential practical application<sup>162-164</sup> of systems which can discriminate between these metal ions are far reaching since both these metal ions are commonly found in the same ores. In biochemical systems, zinc ions are required in many enzymic reactions. Many examples exist which show that cadmium ions displace those zinc ions from such metalloprotein, leading to cadmium toxicity. Detoxification by selective removal of cadmium from systems in which it has been incorporated instead of zinc is thus of some considerable interest.

Figure 3.1.4 Showing the types of ligands used in this used in this investigations, where X is O or N.



<u>Ligand</u>	<u>R</u>	<u>Ring size</u>
L15e	Et	15
L15p	n-Pr	15
L15b	n-Bu	15

### 3.2 Results and discussion

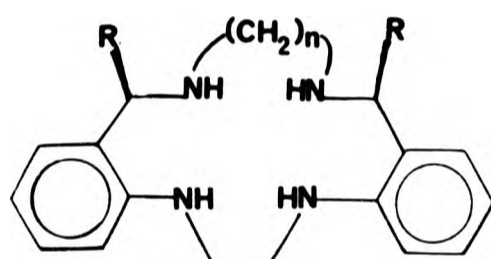
The ability of a given macrocyclic ligand to discriminate between two metal ions, can be assessed by comparing the relative stabilities of its 1:1 complex with the two metals, and this has been discussed in Section 3.1.1.

Systematic alteration of ligand structural parameters, such as variation in ring size and donor atom type, which changes the "goodness-of-fit", have been extensively studied by measuring  $\log K$  for suitable series of metal complexes.<sup>146,155</sup>

In particular stability constant have been measured for  $Zn^{2+}$  and  $Cd^{2+}$  complexes with a range of  $N_4$ -macrocycles Figure 3.2 with ring size variation.<sup>153,154</sup> A marked difference in stability between the  $Zn(II)$  and  $Cd(II)$  complexes were discovered for the 15-membered ring.<sup>153,154</sup>

As part of this project the structures of the zinc and cadmium complexes of the unsubstituted 15-membered ring, L15, were studied in an attempt to establish the origin of this discrimination.

In the later stage of the project a new approach to achieving discrimination has been attempted. In this the ring size is kept constant at 15-membered, and a new ligand parameter, the nature of an alkyl substituent, has been varied. This is of particular relevance to development of solvent extractants where it has been shown<sup>164</sup> that bulky organic substituents enhance the solubility of the metal complex in the organic phase. This is also useful in that the variation of another parameter (bulk of alkyl substituent) provides an extension of the "matrix approach" to fine tuning of metal ion discrimination (Section 3.1.1).



<u>Ligand</u>	<u>R</u>	<u>n</u>	<u>Ring size</u>
L14	H	2	14
L15	H	3	15
L15e	Et	3	15
L15p	n-Pr	3	15
L15b	n-Bu	3	15
L16	H	4	16

Figure 3.2 A general diagram of the macrocycles for which zinc(II) and cadmium(II) stability constants were measured.

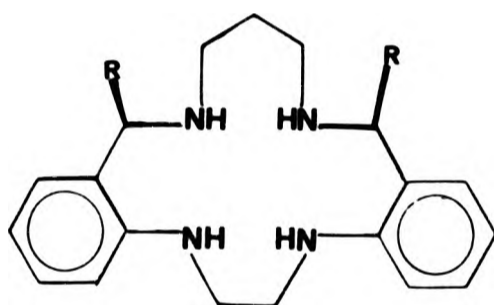


In discussing these results, the first section will deal with the synthetic route to the alkyl substituted ligands, and the later section gives an account of the effects of alkyl substitution on logK and structure.

### 3.2.1 Preparation of C-alkylated derivatives.

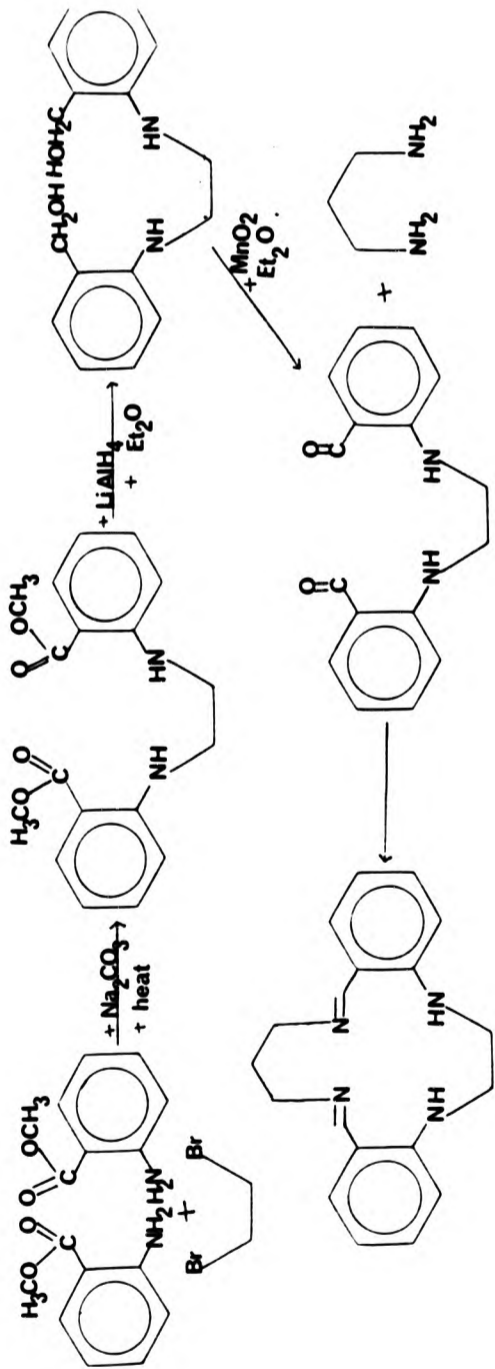
A series of 15-membered ligands with N4-donor sets and different alkyl substituents (Figure 3.2.1) were prepared by stereoselective C-alkylation of the diimine, Scheme 3.2.1(a). All the precursors leading up to the preparation of the diimine were synthesised and characterised, these are not reported here since they were prepared by previously reported routes, Scheme 3.2.1(b).<sup>165-167</sup>

Alkyl substitution at the benzylic carbon atoms was achieved by reacting the diimine with the appropriate freshly prepared Grignard reagent. In ether solution these alkyl magnesium halides normally form tetrahedral molecules with two co-ordinated ether molecules,<sup>168-171</sup> which reduces the carbanion character of the carbon attached to the magnesium atom. In an attempt to increase the effective nucleophilic character of this carbon atom, the reaction was carried out in 1:1 benzene/petroleum-ether mixture. It was hoped that the reaction would be more likely proceed via formation of the carbanion. The possible mechanism proposed for the C-alkylation is shown in Scheme 3.2.1(a). Addition of the alkyl substituents at the azomethine<sup>172</sup> carbon atom results in the formation of the two chiral centres, giving the possibility that meso and racemic forms of the molecule could be obtained.

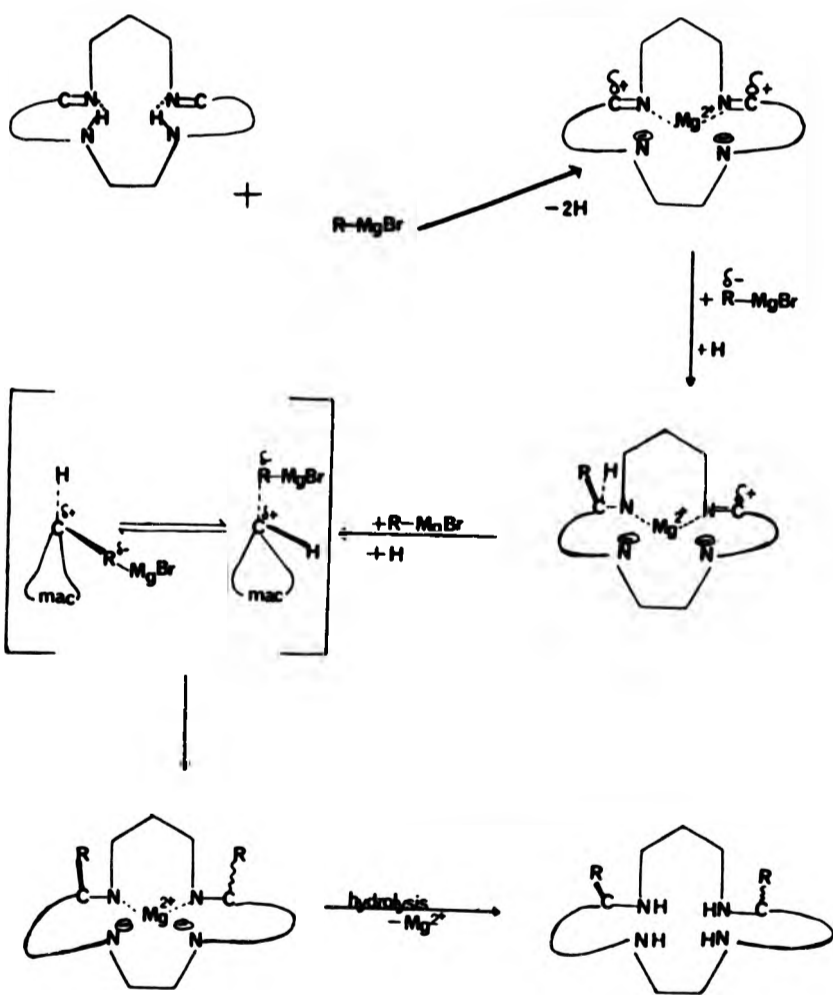


<u>Ligand</u>	<u>R</u>	<u>n</u>	<u>Ring size</u>
L15e	Et	3	15
L15p	n-Pr	3	15
L15b	n-Bu	3	15

Figure 3.2.1 General diagram of 15-membered ligands with different alkyl substituents used in this study.



L15 Diimine



Scheme 3.2.1(b)

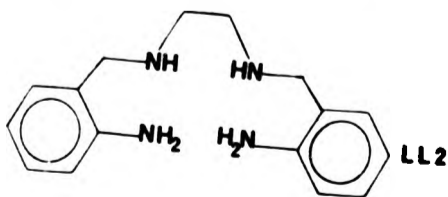
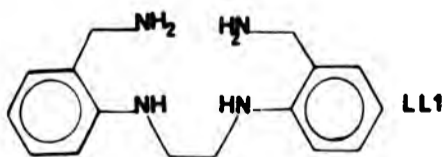
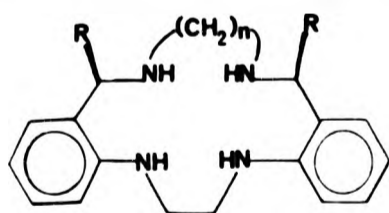
However the  $^1\text{H}$  and  $^{13}\text{C}$  n.m.r. spectra have consistently shown that only one isomeric product has been obtained, and other related C-alkylated compounds have been shown to exist also as the meso isomer.<sup>167,172-175</sup> The proposed mechanism is based on the idea that the magnesium ion is small enough to lie centrally in the cavity of these ligands. Their geometry would then be fixed, and polarization of the azomethine carbon due to the presence of the bonded magnesium would therefore enhance the attack by additional Grignard reagents in which there is considerable carbanion character. This conclusion is supported by the results of the X-ray structural analysis carried out in this work (Section 3.2.3)

### 3.2.2 Stability constant data for the N<sub>4</sub> C-alkylated ligands.

Study on the N<sub>4</sub> quadridentate macrocyclic ligands involved obtaining stability constant data for their  $\text{Zn}^{2+}/\text{Cd}^{2+}$  complexes. The stability constant measurements were kindly performed by our collaborating team at JCU. The results are shown in Table 3.2.2. which contains the logK values for the ligands and also the logK for the complexes with zinc and cadmium. A graphical representation of these results can be seen in Figure 3.2.2(a), in which the stability constants, logK, are plotted against ring size variation for both metals. The stability constants for the C-alkylated complexes are also incorporated in this graph for the 15-membered ring size. Examination of the data in Figure 3.2.2(a), in which the only difference in the ligands was ring size, shows that unlike the results obtained for the  $\text{N}_3\text{O}_2$  quinquedentate systems discussed in Section 3.1.3, the 'natural' stability order of  $\text{Zn(II)} > \text{Cd(II)}$  for the complexes is observed throughout. This behaviour is typical of the results found for simple polyamine ligands,<sup>176</sup> where with increase in the chain length

**Table 3.2.2 Stability constants for 1:1 complexes of the dibenzo ligands with zinc and cadmium measured in 95% methanol at 25.**

Ligand	R	n	Ring size	logK		$\Delta\log K$
				Zn(II)	Cd(II)	
L14	H	2	14	8.60	7.77	0.8
L15	H	3	15	8.64	5.40	3.2
L15e	Et	3	15	6.30	4.08	2.2
L15p	n-Pr	3	15	5.99	3.86	2.1
L15b	n-Bu	3	15	5.80	4.12	1.7
L16	H	4	16	6.43	6.18	0.3
LL1	-	-	-	8.57	8.12	0.5
LL2	-	-	-	7.92	7.66	0.3



stability is always maintained in the order  $Zn(II) > Cd(II)$ .

As discussed earlier, Section 3.2, the largest difference in  $\log K$  for unsubstituted ligands for the zinc and cadmium metals occurred with ligand L15,  $\Delta \log K = 3.24$ . Looking at Figure 3.2.2(a) it can be seen that in the case of the zinc that there is only a small difference of 0.04 between the  $\log K$  values moving from the 14- to the 15-membered complex, whereas for the cadmium complexes this difference is very large, 2.37. This is the cause of the maximum  $\Delta \log K$  value for zinc and cadmium occurring at L15. Contrary to what had been hoped for the substituted 15-membered derivatives all appeared to show relative lowering of  $\log K$  for zinc and cadmium.

In order to take a closer look at what is happening to the stability constants when the C-alkylated compounds are introduced into the series,  $\Delta \log K$  has been plotted against ring size in Figure 3.2.2(b). This clearly shows that for the unsubstituted ligand L15  $\Delta \log K$  is at a maximum not only with regards to ring size, but it is also greater than that for the ethyl, propyl, butyl substituted ligands. The substituent effect is seen more clearly in Figure 3.2.2(c) where  $\log K$  values for the 15-membered ligand complexes of zinc and cadmium are plotted against substitution pattern. As might be expected from steric considerations, the addition of the bulky substituents adjacent to the "aliphatic" amine donors, results in a drop in stability for both metals relative to the parent L15. The presence of the ethyl substituents lowers  $\Delta \log K$  from 3.24 to 2.22, but addition of the more bulky alkyl groups produces much smaller changes in  $\Delta \log K$  for the metals, as can be seen in Figure 3.2.2(d) where  $\Delta \log K$  is plotted against the substitution pattern. The loss in discrimination (as assessed by  $\Delta \log K$ ), on substitution of the ligands arises principally

Figure 3.2.2 (a)

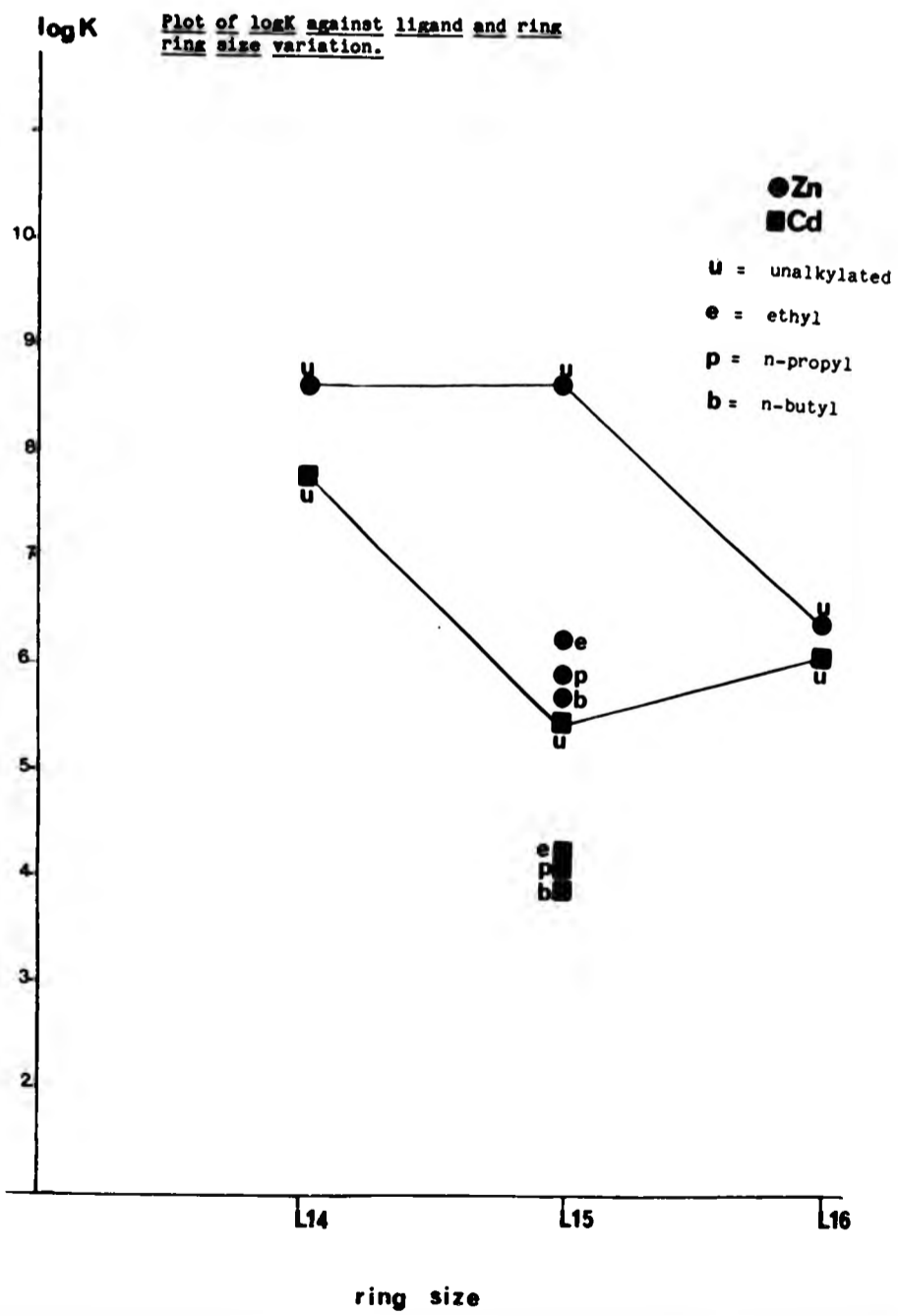




Figure 3.2.2 (b)

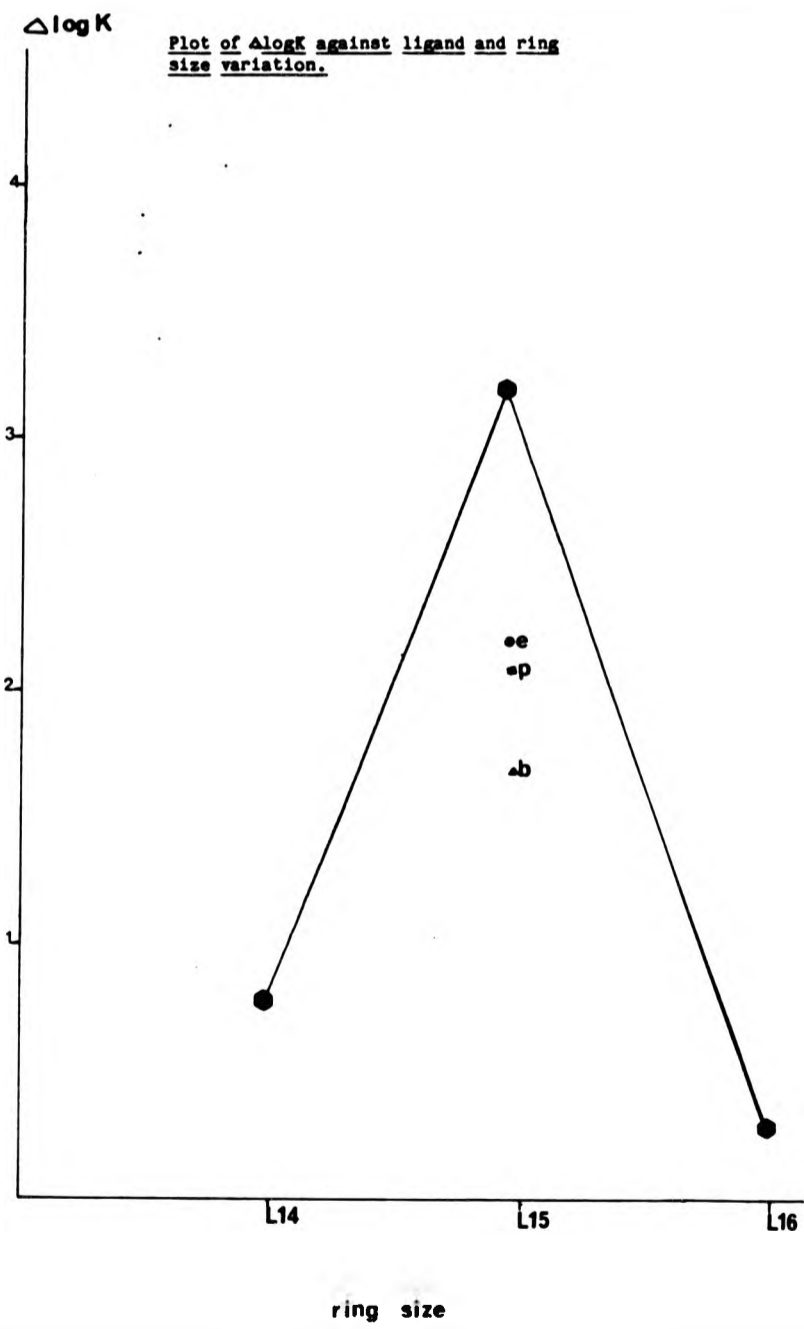
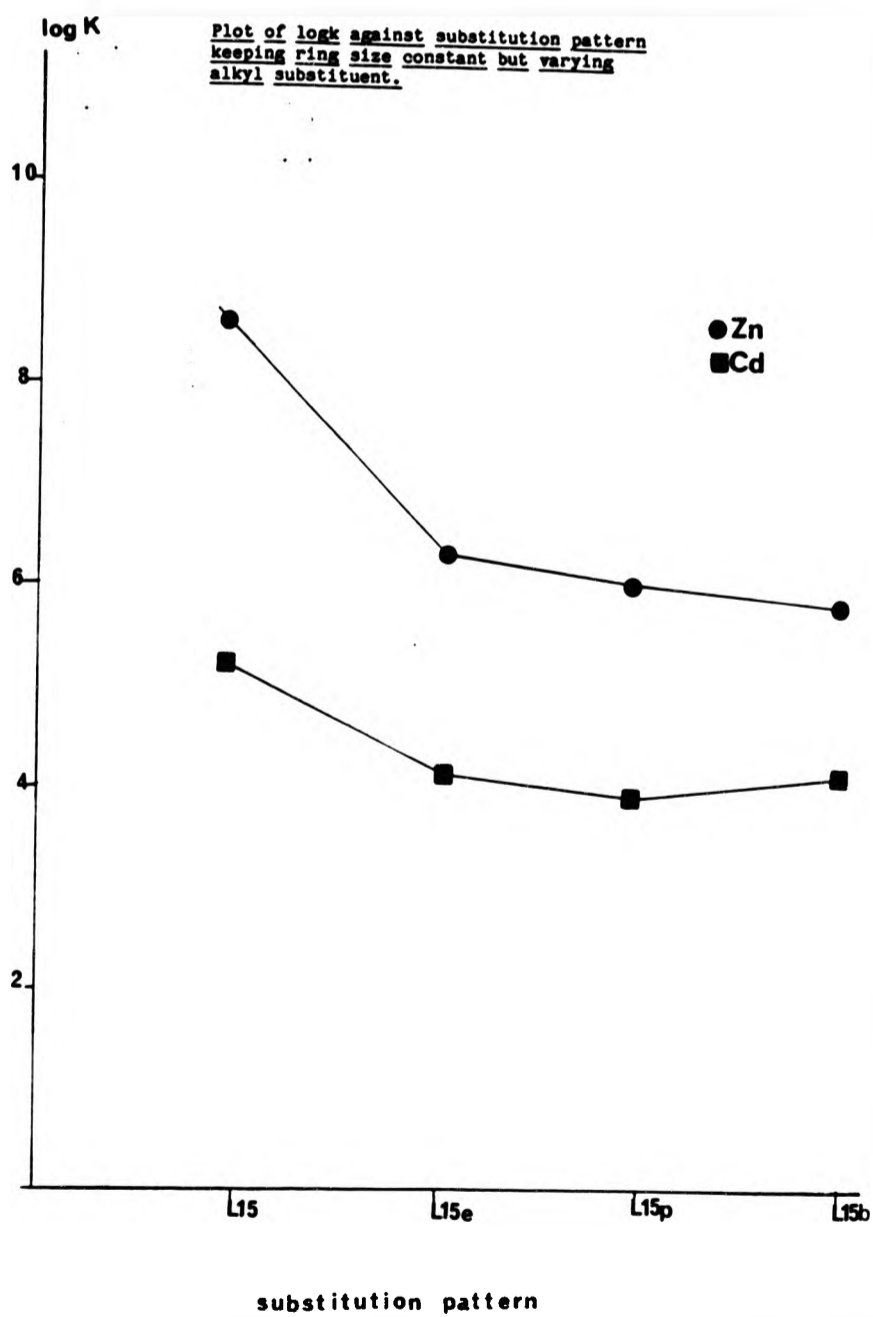
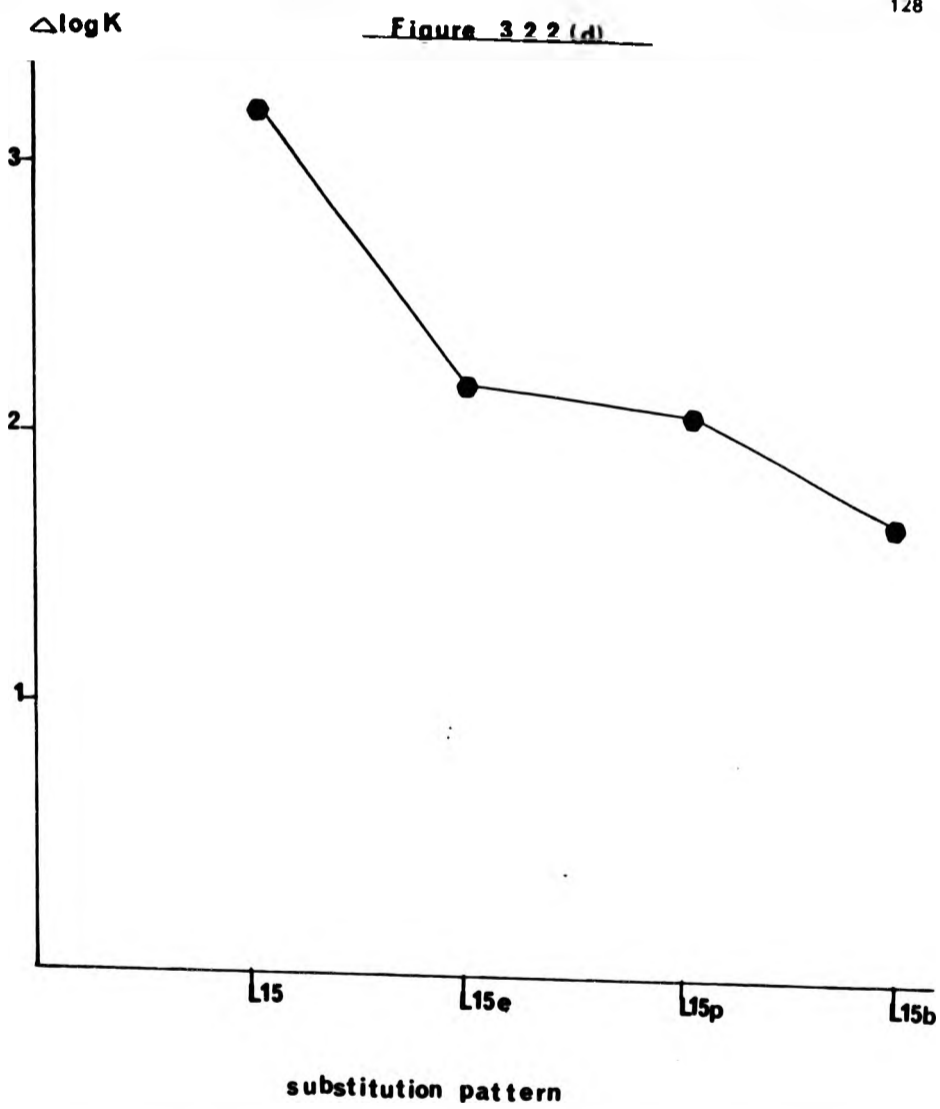


Figure 3.2.2(c)



**PAGINATION  
ERROR**



Plot of  $\Delta \log K$ , keeping ring size constant but changing substituent.

from a sharp drop in stability of the zinc complexes which is slightly greater in each case than of the corresponding cadmium complexes, Figure 3.2.2(c).

The purpose of introducing bulky substituents on the ligand of maximum discrimination for zinc over cadmium (L15), was to attempt to enhance the discrimination. This as proved not to be the case, all the substituted ligands have produced a lowering in discrimination than the parent unsubstituted L15. In fact, as can be seen in Figure 3.2.2(c) there continues to be a drop in discrimination as the size of the substituent is increased. Alkylation has had a more marked effect on the stability of the cadmium complexes than that of the zinc. Thus the discrimination observed for the parent 15-membered ring is markedly decreased for its alkylated derivatives.

If the observed trend for the 15-membered ring on C-alkylation were to be observed for the 16-membered ring, where for the unsubstituted there is a very small  $\Delta \log K$ , it is possible that the stability of the zinc complexes would fall below those of the cadmium, thus reversing the discrimination to favour cadmium.

#### 3.2.2(1) Further discussion relating to the stability constant data.

From these results various assumptions could be made. Firstly that for L14 and L15 macrocycles, similar co-ordination geometries might exist for the zinc complexes, since there is only a slight increase in the  $\log K$  values, Figure 3.2.2(a). Their geometries would then be expected to be similar to that of the open-chain ligands complexes, LL1 and LL2,<sup>177,178</sup> both may be considered to be analogue for the parent macrocycle L15. The structure would presumably be trans octahedral.<sup>178-180</sup>

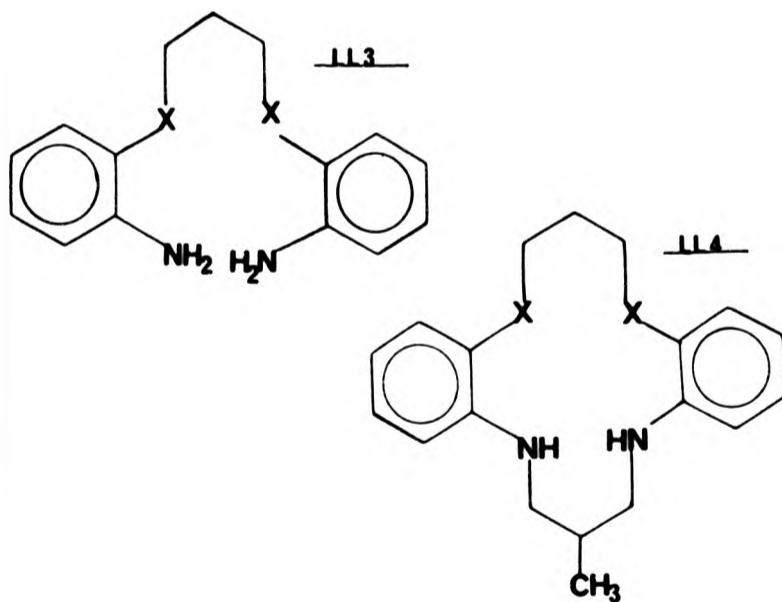
For the 14-membered cadmium compound the corresponding logK value, for its analogous open chain complex, is of the same order as that obtained for the zinc complex, Table 3.2.2. The deduction could then be made that the geometries for these two compounds would be the same. The marked difference, in logK values observed for the 15-membered ring is associated with the macrocyclic systems since it is not observed for the  $N_4$  open chain analogues. The changes in logK values in the case of the cadmium complexes is more complicated than a simple 'fit not-fit' picture. If the 14-member ligand gives a logK value of 7.7 for cadmium, then it would not have been expected that the value would drop markedly for the 15-membered ring. More likely the strain in one ring system brings about a change to a new geometry relative to the zinc complex. The lowering of logK values for the alkyl derivatives, as mentioned above, are presumably a steric hinderance effect.

For the 16-membered macrocycles logK values is much lower for zinc but higher for cadmium. Although the presence of a 7-membered chelate in these systems might be expected to lower logK values, the effect for the zinc seems too big to be due solely to this source. In the case of cadmium the value increases, and this climb perhaps is due to a similar geometry being presented as for the 15-membered ring, but with less strain in the 16-membered system.

These stability constant measurements could not be explained purely by considering the hole size offered by the ligands to these metal ions. The form of the logK against ring size plot, Figure 3.2.2, appear to be like that expected for a dislocation situation, see Section 3.1.3. Thus providing further evidence of structural dislocation similar to that observed for the quinquedentate  $N_2O_3$  series discussed in Section

## 3.1.3.

In a parallel study, the co-ordinating ability of the anilino nitrogens in related dibenzo ligands was investigated,<sup>178</sup> The logK values for their zinc and cadmium complexes of the open chain ligand LL3 and related macrocyclic species, LL4, were determined, Table 3.2.2<sup>178</sup> diagrams of these molecules are given below:-



The results indicated that all four ligands formed weak complexes with these metals, clearly due to the presence of all anilino nitrogens with their weaker base strengths. This suggests that the anilino nitrogen atoms have the same affinity for the metals and these are not greatly different from those of ether oxygens. These findings are important in that the dislocation behaviour may involve a change in the mode of complexation, relating to the way in which the metals interact with all four nitrogen donors. The metal may interact with

all four donors of the macrocycle, while in other cases there remains a strong interaction with the more basic benzylamine nitrogen atoms while those of the poorer anilino nitrogen donors are rejected in favour of solvent molecules. This *exo*-structure has already been observed for the  $N_3O_2$  quinquedentate system mentioned above, Section 3.1.3. This behaviour is also consistent with the similarities of the stabilities observed for the complexes of L16, both of which might have similar non co-ordination of the macrocyclic anilino nitrogen atoms.

Structural analysis were then carried out which included the two key structures of zinc and cadmium complexes of L15 (these structures elucidation were performed by Dr K.P.Dancey). The cadmium complexes of L15(b) and the corresponding 'free' ligand were also determined.

### 3.2.3 Description of X-ray structures.

The full X-ray structural analysis of the butyl substituted 'free' ligand L15b, its cadmium(II) complex, and the zinc(II) and cadmium(II) complexes of the unsubstituted ligand L15 had been carried out. The molecular structure of these compounds are discussed individually, then a comparison is made in Section 3.2.4. To aid these discussions the previously determined<sup>167</sup> related ethylated compound L15e is also included.

Tables of bond lengths and angles for all the structures studied in this thesis can be found in Section 3.4. Selective bond lengths and angles for the structures discussed here are given in Table 3.2.3.



Table 3.2.3 Selected bond lengths/ Å and angles/deg. for the metal complexes.

<u>Bond Lengths/ Å</u>	<u>Zn(L15)</u>	<u>Cd(L15)</u>	<u>Cd(L15b)</u>
M - N1a	2.227(5)	2.412(6)	2.310(7)
M - N1b	2.168(4)	2.387(6)	2.418(7)
M - N2a	2.104(5)	2.275(6)	2.274(7)
M - N2b	2.089(5)	2.257(6)	2.251(7)
M - O(N1a)	2.410(5)	2.360(9)	2.325(7)
M - O(N1b)	-	2.544(8)	2.633(8)
M - Ow	2.151(4)	-	-
M ... O(N2)		2.893(9)	2.721(8)

Angles/°

N1a - M - N1b	80.1(2)	72.2(2)	75.0(2)
N2a - M - N2b	97.8(2)	99.2(2)	100.0(3)
N1a - M - N2a	90.2(2)	85.4(2)	89.0(3)
N1b - M - N2b	90.0(2)	87.5(2)	86.4(2)
ON' - M - ON	-	49.4(3)	49.8(3)

3.2.3(i) The structure of  $[Zn(L15)(NO_3)(H_2O)](NO_3)$ .

The stereochemical arrangement of atoms around the zinc in this complex may be described as distorted octahedral, Figure 3.2.3i(a). The four nitrogen donor atoms of the macrocycle defines the equatorial sites, with one molecule of water and a nitrate group occupying the axial sites of the octahedron. The zinc atom lies 0.12 Å away from the plane defined by the nitrogen donors, towards the water molecule. The co-ordinated nitrate and water groups form lines, O(1) - Zn and O(w) - Zn to the  $N_4$ -plane at angles of  $13.0^\circ$  and  $2.57^\circ$  respectively. The bond from the nitrate is very much longer than that from the water molecule, Zn - O(N1a) 2.410(5) and Zn - O(w) 2.151(4) Å respectively. A weak interaction also occurs between the metal and a second oxygen atom of the co-ordinated nitrate, giving a close contact distance between these two atoms Zn...O(N2) 3.55 Å.

Two oxygen atoms, of the unco-ordinated nitrate group, are involved in hydrogen bonding. One occurs between this group and one of the benzylic nitrogen hydrogen atoms, O(6)...H(N2b) 2.13 Å. This unco-ordinated nitrate anion is located just below the water molecule giving an O(4)...H(Ow1) distance of 1.81 Å. which is consistent with strong H-bond formation.

The phenylene groups are folded towards the axial site which is occupied by the co-ordinated water molecule. This 'saddle shape' conformation, results in a dihedral angle between the phenylene rings and the nitrogens least square plane of  $48.6^\circ$  and  $46.6^\circ$  for the rings (a) and (b) respectively. This contrasts with the structure produced by this same macrocycle with nickel(II) chloride,  $[Ni(L15)Cl_2]$ ,<sup>153</sup> where the phenylene rings adopt a step conformation, and the overall structure has pseudo- $C_2$  symmetry, Figure 3.2.3(i)b.

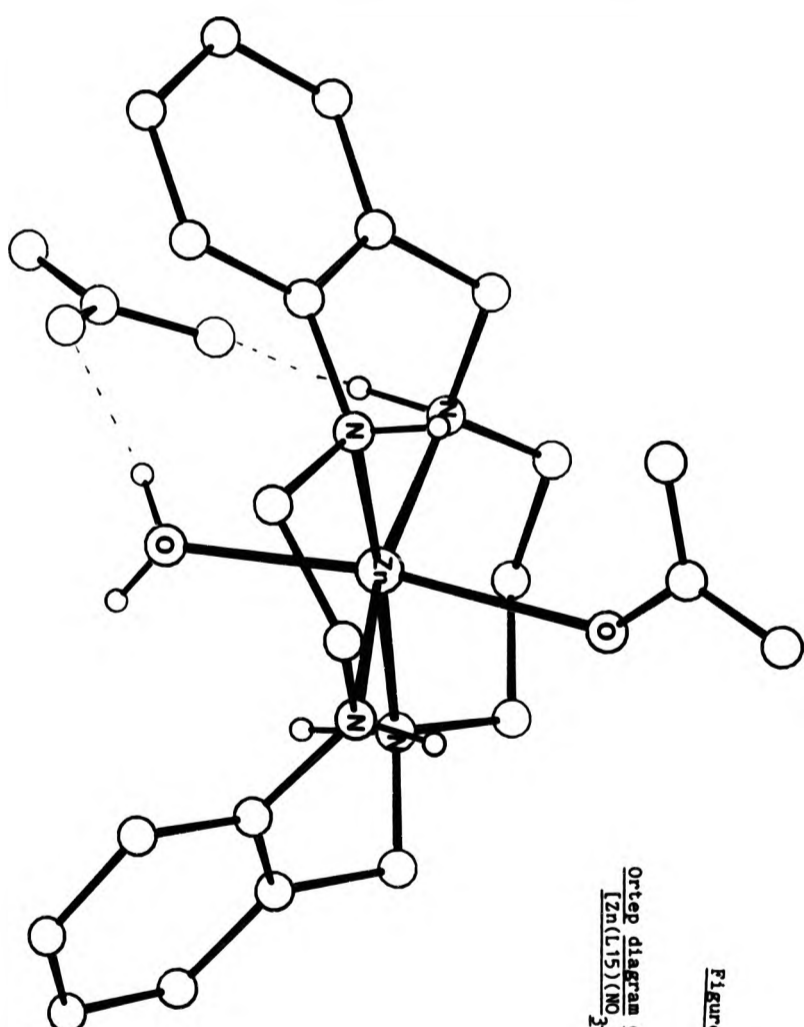
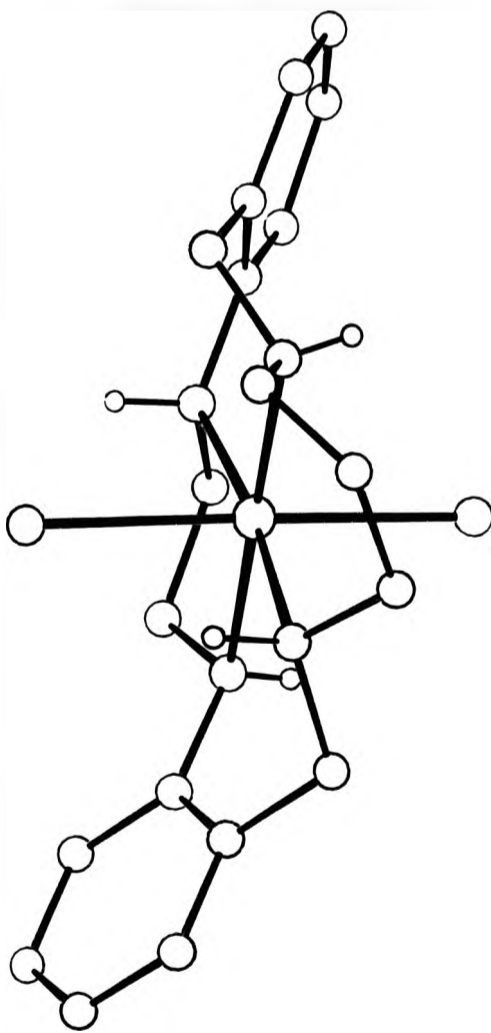


Figure 3.2.3(1)a

Ortep diagram of the structure of  
 $[Zn(L15)(NO)_2(H_2O)](NO_3)_2$ .

Figure 3-2-3(1)b Diagram of the N4 15-membered ligand L15 in the nickel(II) chloride structure, showing pseudo-two fold geometry.

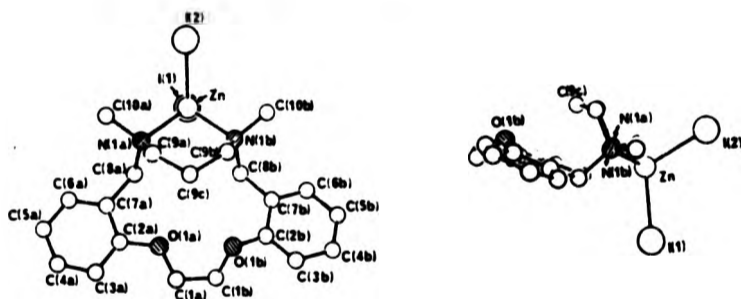


One important observation is the variation of metal to nitrogen bond lengths, Table 3.2.3. Three of the Zn-N distances appear to be unremarkable having values Zn - N(1b) 2.168(4) Å, an anilino nitrogen, Zn - N(2a) 2.089(5) and Zn - N(2b) 2.104(5) Å for the benzylic nitrogens. However that of Zn-N(1a), the second anilino nitrogen distance is significantly longer, Zn-N(1a) 2.227(5) Å. Overall the zinc ion interaction appears greater with the benzylic nitrogen atoms than the anilino nitrogen atoms. There is a marked difference in the chelate angles N(2a)-Zn-N(2b) 97.8(2) and N(1a)-Zn-N(1b) 80.1(2)°, which may be related to the difference in the bond lengths for the anilino nitrogen atoms, Table 3.2.3.

For two previously studied structures of zinc-L15 complexes, [Zn(L15)(I)](I) and [Zn(L15)(ClO<sub>4</sub>)<sub>2</sub>],<sup>184</sup> different co-ordination are adopted. In the case of the iodine complex with L15, the structure was found to be square pyramidal with the co-ordinated iodine atom occupying the axial site that lies in the fold created by the phenylene rings. The anionic iodine atom is located diametrically opposite to the co-ordinated iodine, on the other side of the zinc at a distance of 3.6 Å. The metal ion is displaced from the best plane through the macrocyclic donor atoms towards the bonded iodine. This is thought to arise, not because there is a mismatch between diameters of the 'hole' of macrocycle and the radius of the zinc ion, but because of the interaction between the metal and the axial iodine.<sup>184</sup> This is similar to the present results of the structure determination of [Zn(L15)(NO<sub>3</sub>)(H<sub>2</sub>O)](NO<sub>3</sub>), where the zinc lies 0.12 Å, away from the best plane through the N<sub>4</sub>-donor sets of the macrocycle towards the strongly co-ordinated water ligand. The results reported here correlate with a partial structure determination carried out on

$[\text{Zn}(\text{L}15)(\text{ClO}_4)_2]$ ,<sup>184</sup> in that the zinc lies in an environment which has six co-ordination overall, in this latter compound the perchlorates occupying the axial sites.

In contrast to the above zinc complexes, the structure of the related N-dimethyl substituted 15-membered  $\text{N}_2\text{O}_2$  zinc(II) iodide complex<sup>185</sup> adopts a very different geometry, shown below:-



Diagrams of  $\text{N}_2\text{O}_2$  15-membered dimethylated zinc(II) iodide complex.

Substituting oxygen for nitrogen, in two of the donor sites, has a profound effect on this systems configuration. Here a distorted tetrahedral co-ordination is formed, and the macrocycle is folded with the zinc atom lying completely outside the macrocyclic cavity, and only two benzylic nitrogen atoms of the macrocycle are co-ordinated, while the ether oxygens remain unco-ordinated. These two different structural patterns for the zinc 15-membered  $\text{N}_4$  and  $\text{N}_2\text{O}_2$  systems is undoubtedly a reflection of the low affinity of the ether donors relative to the corresponding saturated nitrogen donors for this metal ion. This finding is comparable to the results reported for the zinc(II) and cadmium(II) complexes formed with some members of the  $\text{N}_2\text{O}_3$  quinquidentate macrocyclic systems discussed in Section 3.1.4,

where the ether oxygens in are not involved in co-ordination to the metal ions.

3.2.3(ii) The structure of  $[Cd(L15)(NO_3)](NO_3)$

The co-ordination of the cadmium atom may best be envisaged as a distorted square pyramidal, where the nitrogen atoms of the unsubstituted macrocycle defines the square base, with a co-ordinated nitrate group occupying the fifth axial site, Figure 3.2.3(ii). Cd - O distances from this nitrate Cd-O(N1a) 2.360(9) and Cd-O(N1b) 2.544(8) Å may also be regarded as weakly bonding in character giving the nitrate a bidentate bonding mode. The line made by Cd-N(1) makes an angle of  $9.9^\circ$  to the plane defined by the four nitrogen donors of the macrocycle.

The cadmium atom here is displaced 0.61 Å away from the least square plane defined by the nitrogen donor atoms in the direction of the co-ordinated nitrate in the fifth site which occupies the cavity created by the folded phenylene rings. The 'saddle shape' conformation of the ligand results in dihedral angles between the two rings (a) and (b) and the nitrogen donor least square plane of  $46.9^\circ$  and  $42.1^\circ$  respectively. There is a relatively close contact between the metal and an oxygen, Cd...O(4) 2.89 Å, of the unco-ordinated nitrate counter anion which is located on the opposite side to the co-ordinated nitrate ligand.

3.2.3(iii) The structure of  $[Cd(L15b)(NO_3)](NO_3)$

Structural analysis of the cadmium complex of the butyl substituted ligand illustrated in Figure 3.2.3(iii), showed it may be regarded as having a square pyramidal co-ordination. The four nitrogen donors of

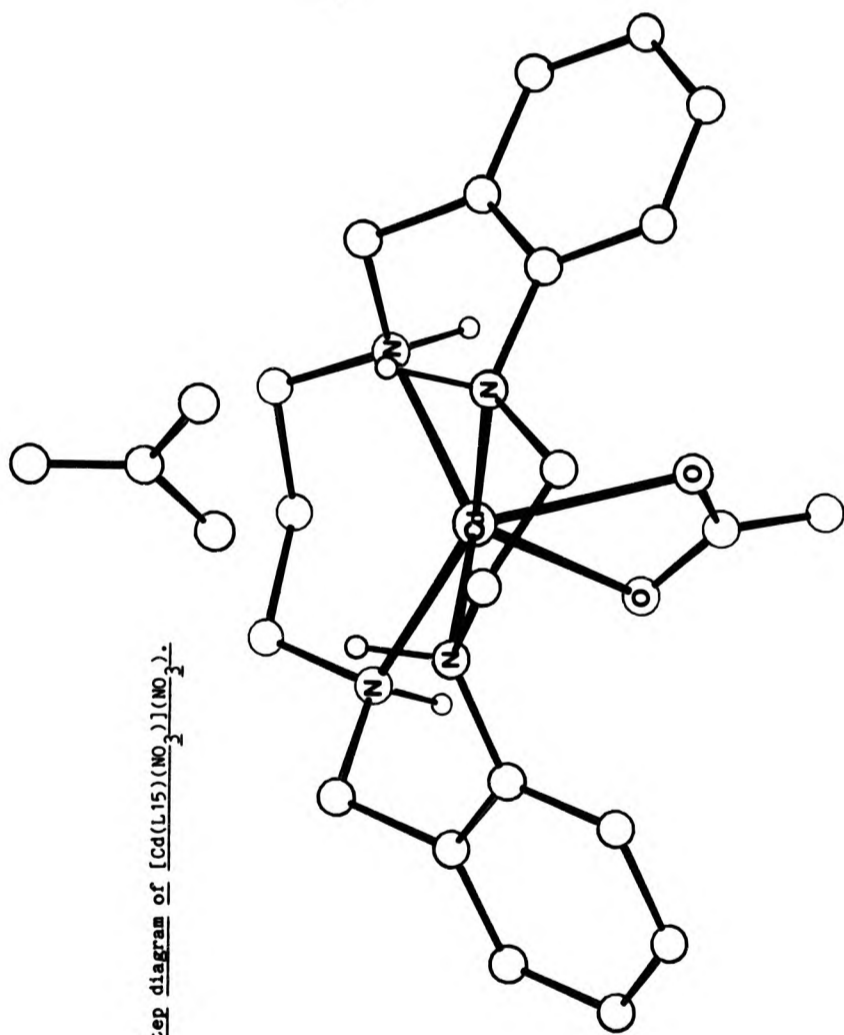


Figure 3.2.3(11) Ortep diagram of  $[Cd(L15)(NO_3)](NO_3)$ .



the macrocycle form the square base with a co-ordinated nitrate group in the apical position. The metal ion is located 0.49 Å above the least square plane through the four nitrogen atoms, towards the co-ordinated nitrate group. The nitrate group occupying the axial site is bonded to the metal in a bidentate mode, Cd - O(N1a) 2.325(7), Cd - O(N1b) 2.633(8) Å. The Cd-N(1) line intersects the plane of the donor atoms at an angle of 10.5°. The phenylene rings of the molecule are folded to the same side as the axial nitrate group. This gives the ligand a 'saddle shape' similar to those of the other complexes described above; the angles between the rings and the least squares plane defined by the nitrogen donors are 52.7° and 61.3°, for rings (a) and (b) respectively. These larger angles as compared to the those of the unalkylated complex, mean 44.5° for the latter, has caused the butylated macrocyclic cadmium complex to adopt a generally less planar conformation than the corresponding cadmium unalkylated species.

The second nitrate ion is located on the other side of the cavity produced by the phenylene rings, with Cd...O(N2) distance of 2.72 Å, slightly shorter than that observed in the case of the unalkylated cadmium complex [Cd(L15)(NO<sub>3</sub>)](NO<sub>3</sub>) discussed above. The 'saddle shape' distortion of the macrocycle from planarity is more marked in this case than in the related two unalkylated zinc and cadmium complexes of L15. It may be concluded that due to the molecular arrangement, in this structure, closer contact between the cadmium and the unco-ordinated nitrate can be made than in the corresponding unalkylated cadmium complex.

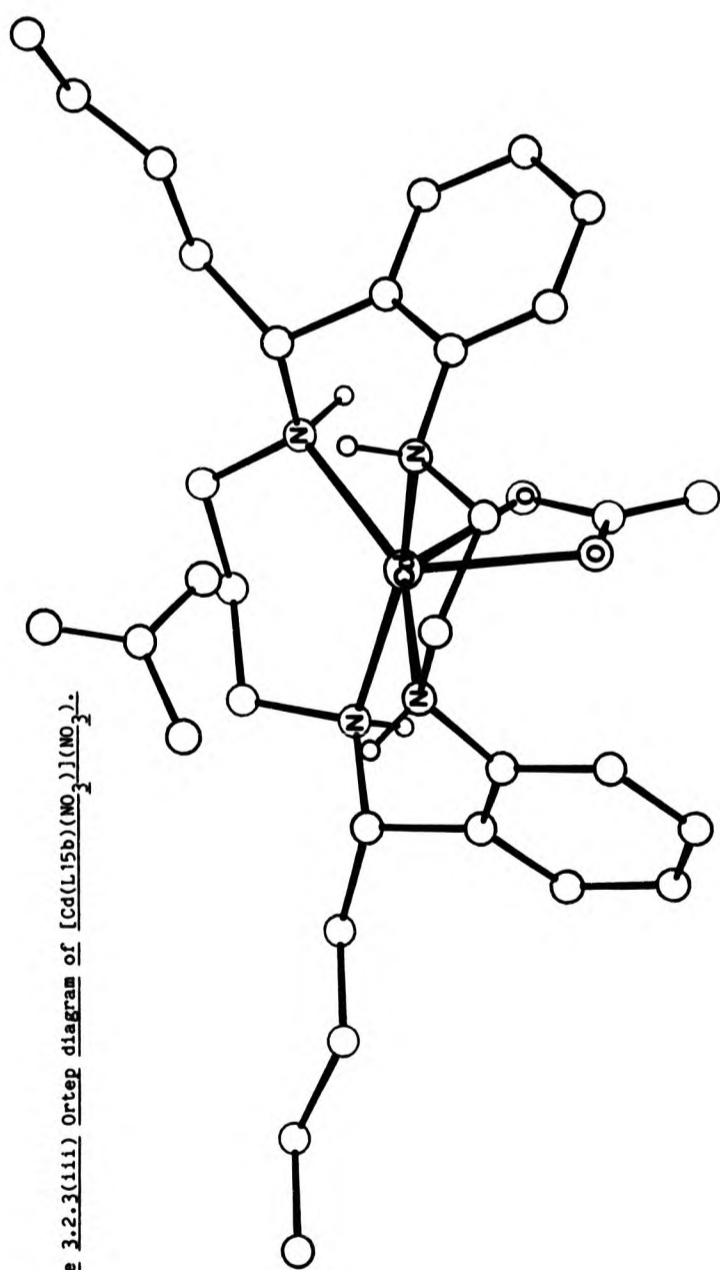


Figure 3.2.3(iii) Ortep diagram of  $[Cd(L15b)(NO_3)_2] \cdot (NO_3)_2$ .



**PAGINATION  
ERROR**

3.2.3(iv) The structure of the butyl substituted 'free' ligand, L15b.

The structure of L15b, Figure 3.2.3(iv)a, confirmed the stereoselectivity assumed in the the strategy by which the  $N_4$ -alkylated macrocycle was synthesised, the butyl substituents giving the *meso* isomer, as observed for similar alkylated structures,<sup>167</sup> (Section 3.2.1).

The related ethyl substituted ligand, L15e, Figure 3.2.3(iv)b, appears to have virtual mirror plane symmetry ( $C_s$ ), passing through the centre carbon atom of the trimethylene bridge C(9c) and the mid-point of the ethylene bridge C(1a)-C(1b). The  $-HN-[CH_2]_3-NH-$  chelating fragment adopts a partial chair like conformation. In contrast the butyl substituted 15-membered ligand molecule, L15b, appears to have localised pseudo  $C_2$  symmetry in the vicinity of the trimethylene bridge. The "two-fold axis" passing through the central carbon atom C(9c). The fragment  $-NH-[CH_2]_3-NH-$  therefore does not adopt the partial chair like conformation, (observed in the case of the ethyl substituted ligand), C(9a) and C(9b) lying on opposite sides of the plane defined by N(2a), C(9c) and N(2b), deviations being  $-0.87$ , and  $0.83$  Å, respectively. The carbon atoms of the ethylene bridge attached to the anilino nitrogens lie above and below the plane defined by the four potential donor nitrogen atoms, (deviations C(1a)  $0.35$  C(1b)  $-0.41$  Å. This compares to the ethylene bridge of the ethyl substituted ligand L15e where the deviations of the corresponding atoms are  $-0.46$  and  $0.48$  Å respectively. The  $N_4$  potential donor atoms in L15b are planar to within  $0.014$  Å.

Overall the molecule may be described as 'saddle shaped'. The dihedral angles between the two phenylene rings, (a) and (b), and the

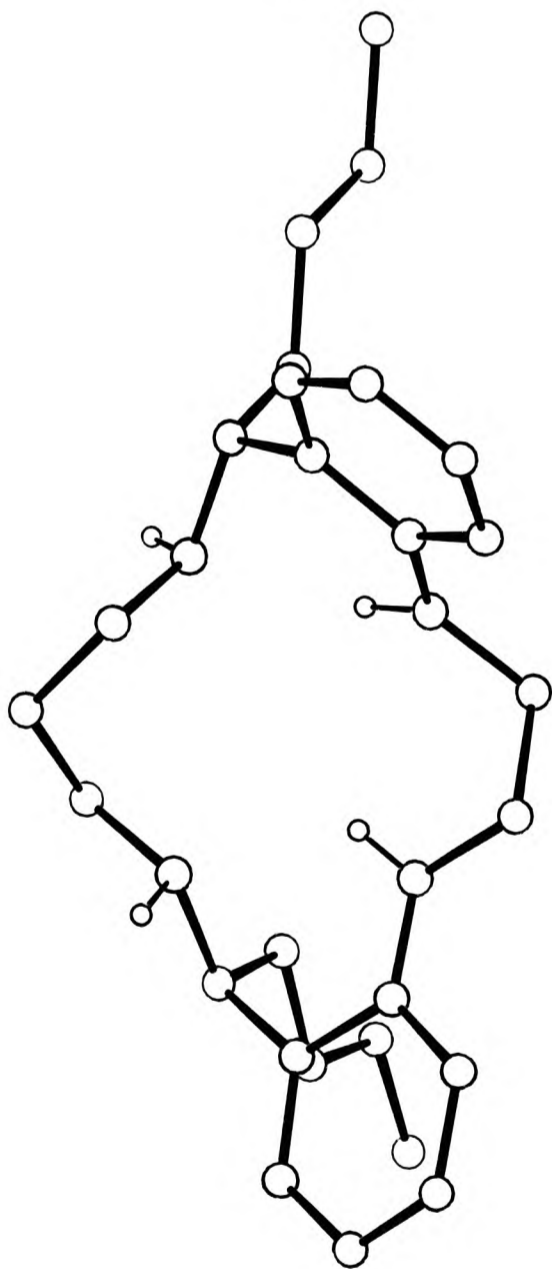


Figure 3.2.3(iv) a Diagram of the 'free' ligand L15b.

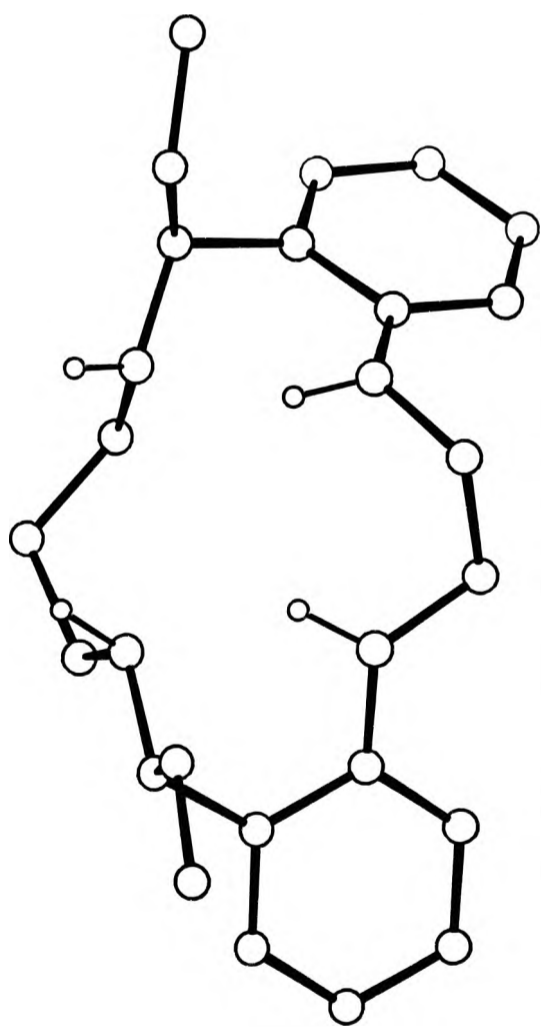


Figure 3.2.3(iv) b Diagram of the 'free' ligand L15e.

plane defined by the nitrogen atoms are  $28.3^\circ$  and  $58.1^\circ$  respectively thus the folding of the phenylene groups away from this plane is asymmetric. When this ligand, L15b, is bonded to cadmium(II), a more symmetrical 'saddle shape' arrangement of the molecule is observed, Section 3.2.3(iii), with angles between the  $N_4$  plane and the (a) and (b) phenylene groups being  $52.7^\circ$  and  $61.3^\circ$ , respectively. The same angles for the corresponding ethyl substituted 'free' ligand L15e have values of  $37.1^\circ$  and  $49.0^\circ$  for (a) and (b) respectively.

The 'hole size' for the 'free' ligand L15b was calculated as described in Section 3.1.2, and  $R_H = 2.14 \text{ \AA}$ . The corresponding value for L15e is  $2.10 \text{ \AA}$ .<sup>147</sup> Comparing the values obtained for L15b and L15e it appears that increasing length of alkyl substituent has produced an opening of the macrocyclic cavity. Ring substituents have previously been shown<sup>155</sup> to have an influence on hole size in related ligands of the type with  $N_2O_3$  donor sets, especially when such substituents often lead to changes in the macrocycle conformation, Section 3.1.3. This is the first time it has been studied for the  $N_4$ -ligands and such changes would be expected to occur more readily in the more flexible saturated ring system.

In the structure of the ethyl substituted ligand L15e hydrogen bond formation occurs between the anilino hydrogens and the lone pairs of the nitrogen atoms of the benzylic nitrogens, H(N1a)...N(2a)  $1.989 \text{ \AA}$  and H(N1b)...N(2b)  $1.997 \text{ \AA}$ . For the structure of the butyl substitution ligand, L15b, H(N1a)...N(2a) and H(N1b)...N(2a), distances of  $2.202 \text{ \AA}$  and  $2.049 \text{ \AA}$  respectively are also consistent with intra-molecular hydrogen bonding. The difference in these interactions may be relevant to the increase of  $0.04 \text{ \AA}$  in the L15b hole size, relative to the ethylated species L15e. It is well

established that H-bonding is important in determining the conformation of such unco-ordinated macrocyclic species.<sup>167</sup> The general overall rather distorted molecular structure adopted by this 'free' ligand, L15b, compared to the more ordered structural arrangement of the overall molecule of the ethyl substituted ligand, L15e, must be produced by steric effects. This would be expected to be related to differences in H-bonding. The molecule of L15e is less folded than that found here for L15b, the mean value of the angles between the planes defined by the phenylene rings and the donor atoms, in L15e is  $43.0^\circ$  and in L15b is  $43.2^\circ$ .

#### 3.2.4 Overall comparison of the four structures discussed above.

In all three complexes, the  $N_4$ -donor atoms show a slight tetrahedral distortion from exact planarity, Figure 3.2.4(a). The two trans donor atoms, such as N(1a) and N(2b) are displaced in the same direction as each other, deviations/ Å being:-

	<u>Zn(L15)</u>	<u>Cd(L15)</u>	<u>Cd(L15b)</u>
N(1a)	-0.13	0.08	0.16
N(2b)	-0.12	0.06	0.13
N(1b)	0.13	-0.08	-0.16
N(2a)	0.12	-0.06	-0.13

The six membered chelate rings with the propyl bridge may be regarded as adopting a 'chair' conformation in the case of the zinc complex. However for the cadmium complexes of L15b a distorted 'chair' conformation is observed, while a distorted 'boat' conformation is adopted in the cadmium complex of the unalkylated ligand L15. The central part of the chelate rings, defined by N(2a), C(9a), C(9b),



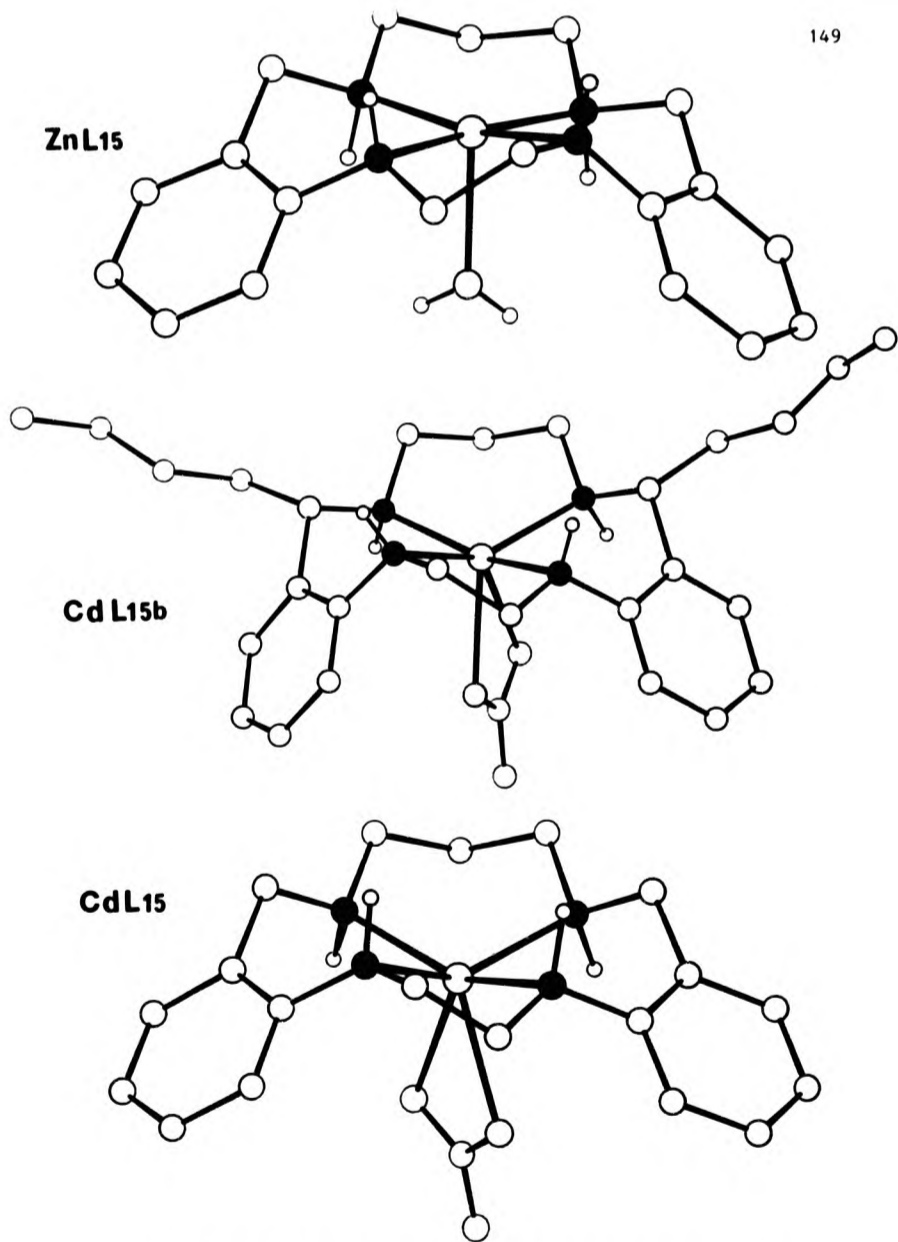
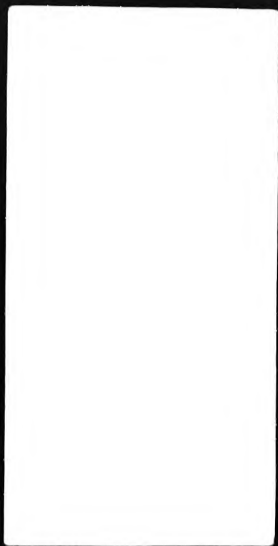


Figure 3.2.4(a) Side views of the three metal complexes to show the non-planarity of the shaded nitrogen donor atoms. The weakly bonding counter ion is removed for clarity.

N(2b), are close to planar in the three complexes, as shown below:-

Deviations for the atoms used in the calculations of the plane/ Å.

	<u>Zn(L15)</u>	<u>Cd(L15)</u>	<u>Cd(L15b)</u>
N(2a)	0.00	0.01	-0.02
C(9a)	0.00	-0.02	0.03
C(9b)	0.00	0.02	-0.03
N(2b)	0.00	-0.01	0.02

The metal atoms lie 0.74, 0.35, -0.61 Å from this plane respectively for Zn(L15), Cd(L15) and Cd(L15b), and the centre carbon atom C(9c) lies at -0.75, 0.78 and 0.74 Å respectively to this plane.

The five membered chelate ring with the ethylene bridge adopt distorted conformations. In the case of the two cadmium complexes both the two carbon atoms of the -CH<sub>2</sub>-CH<sub>2</sub>- bridge, C(1a) and C(1b) lie on the same side as N-M-N, towards the co-ordinated nitrate (N1), deviations 0.26 and 0.86 Å for Cd(L15) and for Cd(L15b), 0.74 and 0.09 Å respectively. In the case of the zinc complex, which has octahedral geometry, although C(1b) lies markedly out of the N-M-N plane, towards the strongly co-ordinated water molecule, the second carbon atom C(1a) lies on the opposite side to the plane, deviations 0.64 and -0.07 Å respectively.

In all the structures studied here the observed molecular configuration is 'saddle shaped', as may be seen from a comparison of the dihedral angles between the phenylene rings and the plane defined by the nitrogen donor atoms. The mean value of the two dihedral angles for both cadmium complexes, are 44.5° for [Cd(L15)] and 57.0°

for [Cd(L15b)], Figure 3.2.4(b). It thus appears that in the unsubstituted complex the phenylene rings are less bent away from the plane defined by the donor atoms as compared to the alkylated cadmium complex, where the phenylene ring are bent further away from the  $N_4$  plane. In contrast to the cadmium complex of L15b the corresponding 'free' ligand L15b, has a very uneven displacement of phenylene rings, Figure 3.2.4(b), once this ligand is bonded to the metal, a more symmetrical configuration results Figure 3.2.4(b).

#### 3.2.4(i) The co-ordination geometry of the metal complexes.

The most striking difference between the zinc and the two cadmium complexes is the overall co-ordination geometries. The zinc is octahedrally co-ordinated and the two cadmium complexes have square pyramidal geometry.

In marked contrast to the two cadmium complexes, in the zinc complex, [Zn(L15)(NO<sub>3</sub>)(H<sub>2</sub>O)](NO<sub>3</sub>), metal lies quite close to the plane defined by the macrocycle donor atoms, deviation 0.12 Å, Section 3.2.3(i). The sum of the angles at Zn in this equatorial plane is very close to 360°, are as expected for a octahedrally co-ordinated metal atom. Those of the two six membered chelate, N(1a)-Zn-N(2a) and N(1b)-Zn-N(2b), have a mean value of 91.1°, Figure 3.2.4(i). The angle N(1a)-Zn-N(1b) is 81.1°, the smaller value being expected for a five membered chelate. Compensation for this small angle occurs at the third six membered chelate, where the N(2a)-Zn-N(2b), angle is enlarged to 97.8°, Figure 3.2.4(i).

The angles at the metal in the other two cadmium complexes comply with the fact that the metals lies below the plane of the macrocycle

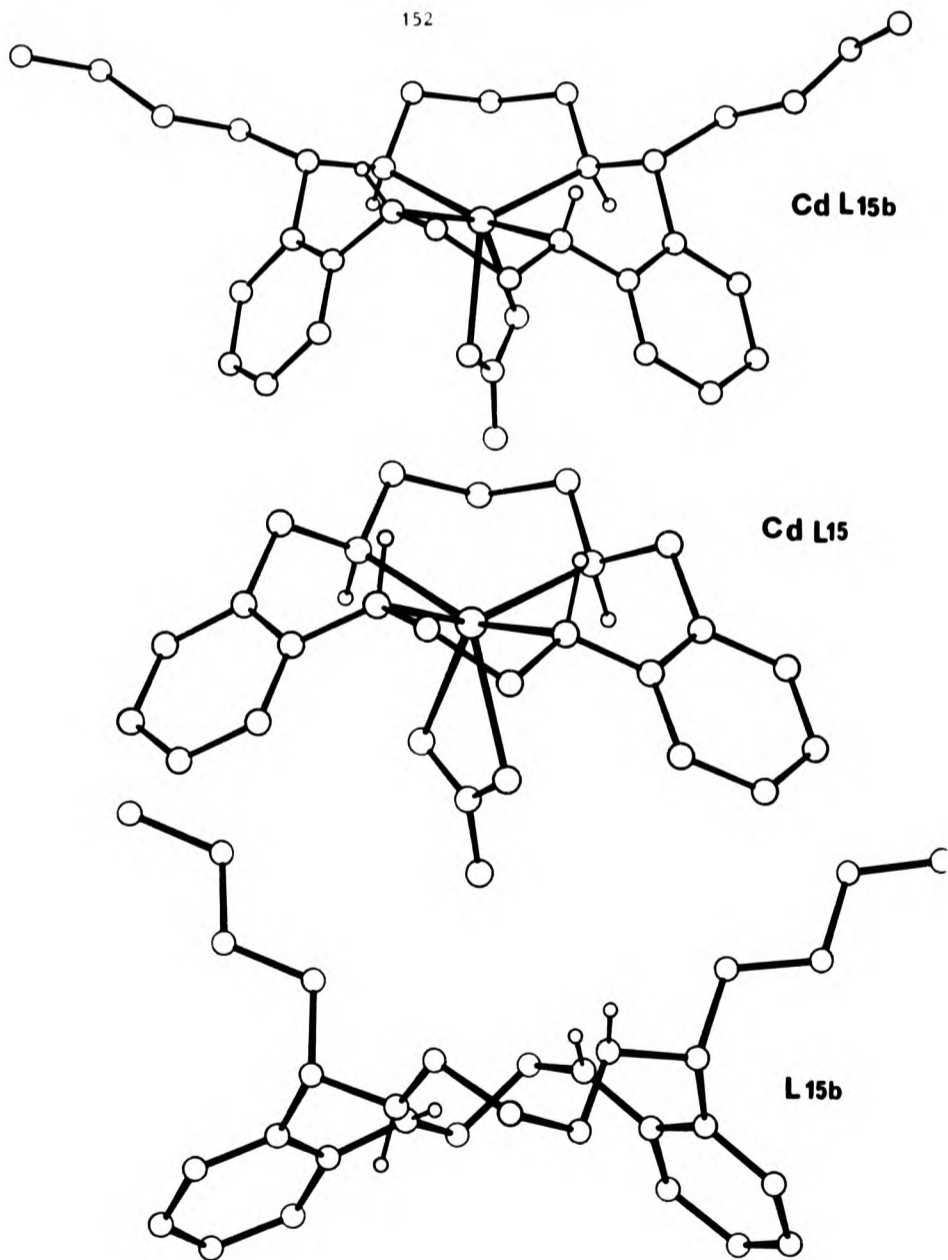
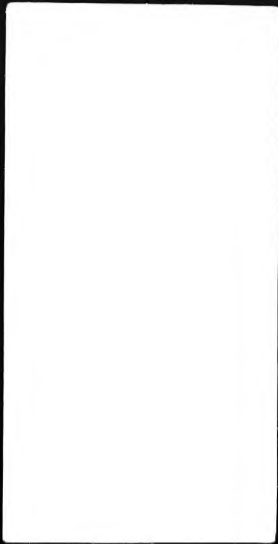


Figure 3.2.4(b) Showing side views of the two metal complexes and the 'free' ligand L15b, to show the orientations of the phenylene rings.

defined by its donor atoms towards the fifth ligand, the sum of the angles being  $344.3^\circ$  for the unalkylated complex when the metal is  $0.61 \text{ \AA}$ , out of the plane and  $350.5^\circ$  for the n-butylated species when the metal is  $0.49 \text{ \AA}$ , out of the plane. Similarly the angles  $N(1a)-M-N(1b)$  are smaller than for zinc than the corresponding angles, and  $N(2a)-M-N(2b)$  are larger, values for  $[Cd(L15)]$  being  $72.2^\circ$  and  $99.2^\circ$  respectively and for  $[Cd(L15b)]$   $75.5^\circ$  and  $100.0^\circ$  respectively, Figure 3.2.4(i).

In all three complexes the chemically equivalent pairs of angles  $N(1a)-M-N(2a)$  and  $N(1b)-M-N(2b)$  are the closest to  $90^\circ$ , Figure 3.2.4(i). For the two cadmium complexes of L15 and L15b the mean value of these angles two angles are  $86.5^\circ$  and  $87.8^\circ$  respectively. The value for the angle in the five membered chelate ring,  $N(1a)-M-N(1b)$  is  $81.0^\circ$ ,  $72.2^\circ$  and  $75.0^\circ$  for  $[Zn(L15)]$ ,  $[Cd(L15)]$  and  $[Cd(L15b)]$  respectively. The value in the third six membered ring,  $N(2a)-M-N(2b)$  is  $97.8^\circ$ ,  $99.2^\circ$  and  $100.0^\circ$  for the zinc complex and cadmium complexes of L15 and L15b respectively, Figure 3.2.4(i). All the other angles of the three complexes are similar. The angles at the benzylic nitrogens  $N(2a)$  and  $N(2b)$  are consistent with  $sp^3$  hybridisation at these atoms, the mean value of these angles being  $111.5^\circ$ , which is close to the ideal tetrahedral angle of  $109^\circ$ . In contrast to this the anilino nitrogens do not appear to involve  $sp^3$  hybridisation as judged by the angles around these nitrogen atom which are very distorted but add up to  $360^\circ$  in each. In all cases the angles  $C(2a)-N(1a)-C(1a)$  and  $C(2b)-N(1b)-C(1b)$  on the two sides of the macrocycles are relatively large, the mean value being  $116.7^\circ$  and  $118.5^\circ$  respectively, for the three complexes, but are less than  $120^\circ$ . This is consistent with the fact that an angular value close to  $90^\circ$  is

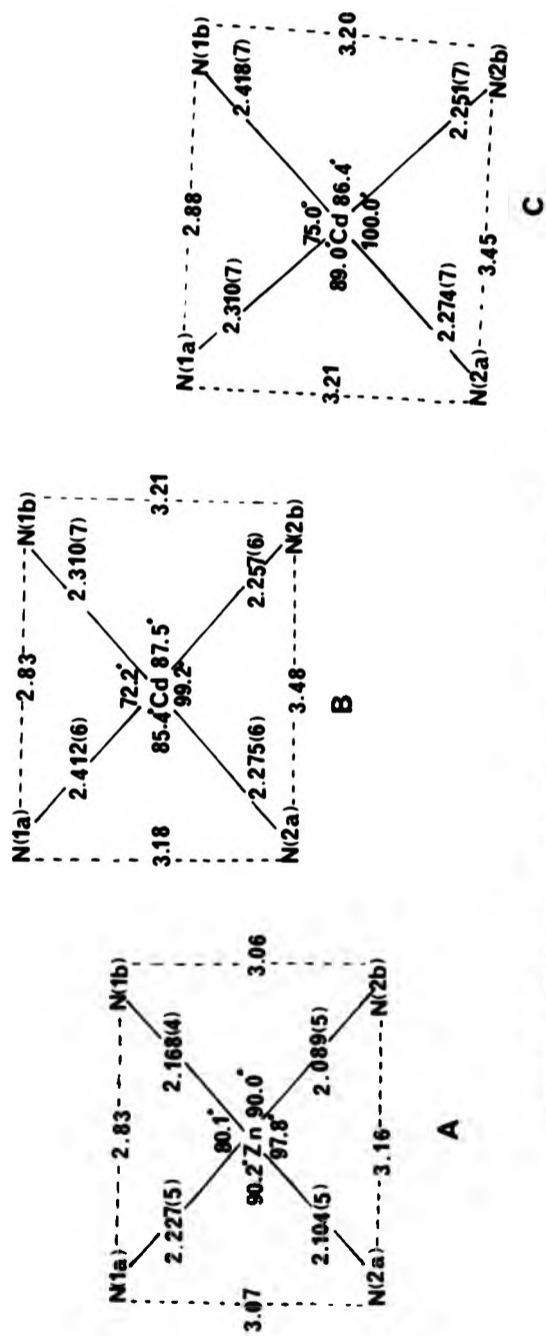


Figure 3.2.4(i) Comparison of bond lengths/A and angles/ $^{\circ}$  within the donor atom planes of the macrocycles:-

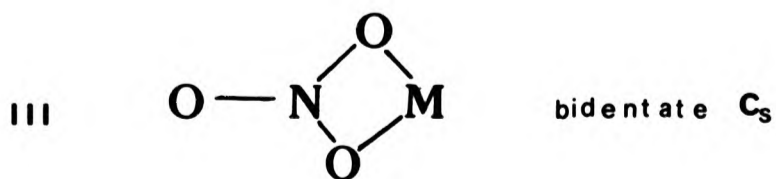
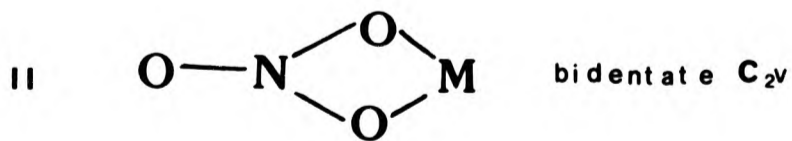
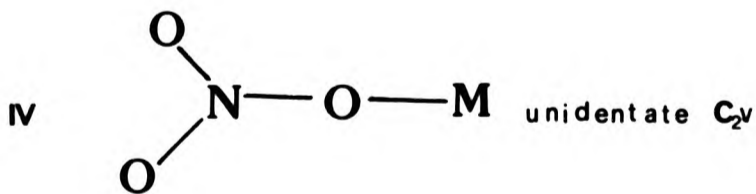
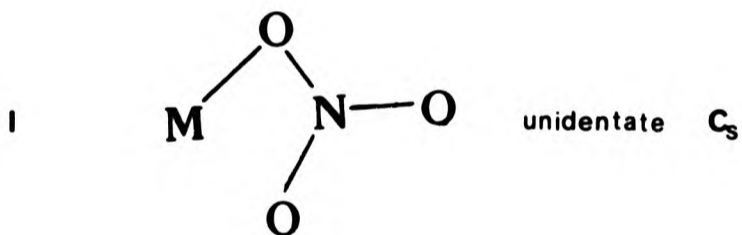
- a)  $[\text{Zn}(\text{L15})(\text{NO}_3)(\text{H}_2\text{O})](\text{NO}_3)$
- b)  $[\text{Cd}(\text{L15})(\text{NO}_3)](\text{NO}_3)$
- c)  $[\text{Cd}(\text{L15b})(\text{NO}_3)](\text{NO}_3)$

being maintained about the metal atom, this is followed by a contraction of the angles C(2a)-N(1a)-M and C(2b)-N(1b)-M, the mean values of these two type of angles being  $106.5^\circ$  and  $108.9^\circ$  respectively in the three complexes. As a consequence the third angle at this nitrogen is very large in all three metal complexes. If these angles are compared with the equivalent angles in L15b, the 'free' ligand, we find that in these structures these angles are closer to  $120^\circ$ . This is also consistent with the the anilino nitrogen of the 'free ligand' having more ideal  $sp^2$  hybrid orbitals, and the shorter C(2)-N(1) bond lengths, mean value is  $1.382 \text{ \AA}$ , supports this. These anilino C(2)-N(1) bond lengths in the complexes are rather longer with a mean of  $1.436 \text{ \AA}$ , which is still consistent with some double bond character. In contrast the benzylic nitrogen to carbon distances C(8)-N, are in the range  $1.496 - 1.526 \text{ \AA}$ , which are more consistent with non-conjugated carbon nitrogen bond distances.<sup>186</sup>

Comparison of the bond lengths from the nitrogen donor atoms to the metal in all cases show them to be fairly similar in pattern. Those arising from the benzylic nitrogen to the metal atom, N(2)-M, are in all cases shorter than the corresponding anilino nitrogen, N(1)-M,  $2.198$  [Zn(L15)],  $2.361$  [Cd(L15)] and  $2.364 \text{ \AA}$  [Cd(L15b)]; N(2)-M,  $2.097$  for the zinc and  $2.266$  for the L15 cadmium complex and  $2.263 \text{ \AA}$  for L15b cadmium complex. Figure 3.2.4(1). This suggests that the benzylic nitrogens have formed stronger bonds to the metal than those arising from the anilino nitrogen atoms, has been observed in other macrocycles.<sup>178</sup>

3.2.4(ii) Nitrate co-ordination the metal ions.

There are at least four ways in which the nitrate ion can co-ordinate to a metal, of which only three are relevant to this study.





From the number of structures studied by 1971 the preferred mode of co-ordination appears to be the symmetrical bidentate structure(II). In this structure with the zinc complex  $[\text{Zn}(\text{L15})(\text{NO}_3)(\text{H}_2\text{O})](\text{NO}_3)$  the sixth axial site is occupied by a unidentate nitrate group of the type shown above as structure(I), and this mode of co-ordination was deemed to be less common.<sup>187</sup> From this monodentate nitrate the Zn-O(N1a) length is 2.410 Å, with the corresponding N-O(N1a) bond length, being 1.271(6) Å, which is slightly longer than the other N-O lengths in this nitrate structure, the mean value is 1.290(6) Å. The mean unco-ordinated N-O lengths in this compound is 1.225(7) Å.

In contrast to the zinc complex,  $[\text{Zn}(\text{L15})(\text{NO}_3)(\text{H}_2\text{O})](\text{NO}_3)$ , in both the cadmium complexes,  $[\text{Cd}(\text{L15})(\text{NO}_3)](\text{NO}_3)$  and  $[\text{Cd}(\text{L15b})(\text{NO}_3)](\text{NO}_3)$  the mean N-O bond lengths in the bidentate co-ordinated nitrate is 1.20 Å. This distance is shorter than that obtained in the case of the zinc. For the cadmium complexes, a lengthening of the N-O bond, involved in complexation, also occurs. For the complex of L15 and L15b the increase lengths from 1.2 Å, are 0.03 and 0.06 Å respectively. The mean unco-ordinated N-O for all the structures studied here is 1.225 Å, and are close to the value 1.22 Å<sup>187</sup> for an unco-ordinated nitrate anion.

In both the cadmium complexes, no significant distances could be detected between the metal atom and the second unco-ordinated nitrate group, because of the relatively larger esd's associated to these structures. These groups were also considered to be too far away to be within significant bonding distances. The closest contact from this group to the metal ions is Cd ...O(N2) 2.89 Å for  $[\text{Cd}(\text{L15})(\text{NO}_3)](\text{NO}_3)$  and Cd ...O(N2) 2.72 Å in  $[\text{Cd}(\text{L15b})(\text{NO}_3)](\text{NO}_3)$ , Table 3.2.3.

In contrast to the zinc complex,  $[\text{Zn}(\text{L15})(\text{NO}_3)(\text{H}_2\text{O})](\text{NO}_3)$ , in both the cadmium complexes  $[\text{Cd}(\text{L15})(\text{NO}_3)](\text{NO}_3)$  and  $[\text{Cd}(\text{L15b})(\text{NO}_3)](\text{NO}_3)$ , as mentioned previously it is observed that bidentate co-ordination of the nitrate ligand to the cadmium atom takes place. For the unalkylated cadmium complex  $[\text{Cd}(\text{L15})(\text{NO}_3)](\text{NO}_3)$ , Cd-O(N1a) is 2.360(9) and Cd-O(N1b) is 2.544(8) Å. The difference between these bond lengths (0.18 Å) is in the range classified as the symmetrical bidentate mode of nitrate co-ordination. The difference, (0.31 Å), in metal to nitrate oxygen lengths are more marked in the case of the butyl alkylated complex, Cd-O(N1a) being 2.325(7) and Cd-O(N1b) 2.633(8) Å. This means that this would be classified as an unsymmetrical bidentate nitrate mode of bonding. The criterion used by the authors of the review is that a small but real difference (0.2 - 0.7 Å)<sup>187</sup> between the two M-O bonding being classified as unsymmetrical, differences less than 0.2 Å as symmetrical. In this study the difference in the unalkylated complex is 0.184 Å as compared to 0.308 Å for the alkylated species so that the bonding mode for these complexes belongs to these two categories. The authors have suggested two factors which may lead to asymmetrical bidentate bond formation. The first arises from the electronic configuration of the metal being asymmetrical with respect to the two co-ordinated oxygen of the bidentate nitrate group. Secondly the presence of a ligand with a strong trans influence, situated in a position trans to only one of the two co-ordinated oxygen atoms of the bidentate nitrate group, which produces this asymmetry. It might be expected from this explanation that the asymmetrical bidentate co-ordination in the complex,  $[\text{Cd}(\text{L15b})(\text{NO}_3)](\text{NO}_3)$ , occurred due to the first explanation since the electronic configuration of the metal would be asymmetrical in this square pyramidal form.

For the complexes, in all cases the hydrogens attached to the nitrogen donor atoms all adopt a trans tetrahedral arrangement around these atoms. That is H(N1a) and H(N2b) are situated on the opposite side to the metal atoms, where as H(N2a) and H(N1b) are situated on the same side as the metal atoms.

3.2.4(iii) Torsion angles in these structures.

A general comparison of the key torsion angles for the three metal complex structures and the 'free' ligand L15e and L15b is layed out in Table 3.2.4(iii), which shows only the major torsion angles of the inner great rings of these systems, from which the conformation adopted can be defined. In the case of the three metal complexes the signs on the torsion angles of both halves of the inner great ring suggests that they all possess a virtual mirror plane of symmetry. The most significant part of the inner great ring from which the conformation of the structures can be determined involves the regions containing the aliphatic propylene bridge. Here there is more molecular flexibility and by looking at the torsion angles associated with this region:-

1. N(1)-C(2)-C(7)-C(8)
2. C(2)-C(7)-C(8)-N(2)
3. C(7)-C(8)-N(2)-C(9)
4. C(8)-N(2)-C(9)-C(9c)
5. C(1)-C(9)-C(9c)-C(9)'

the conformation adopted by the structures can be determined. The values of the torsion angles and the signs they have corresponding to both parts (A) and (B) should be equal and have opposite signs to be classified as having mirror plane symmetry. In the case of the cadmium complex of L15b we find that the sign on the angle

**Table 3.2.4(iii) Torsion angles/ $^{\circ}$  in the inner great rings of the free ligands L15e and L15b and the three metal complexes.**

PART	<u>L15e</u>		<u>L15b</u>	
	A	B	A	B
C(1)'-C(1)-N(1)-C(2)	-174	-76	166	82
C(1)-N(1)-C(2)-C(7)	-179	-173	-176	177
N(1)-C(2)-C(7)-C(8)	-2	0	-3	-5
C(2)-C(7)-C(8)-N(2)	50	-49	-52	50
C(7)-C(8)-N(2)-C(9)	67	-67	-174	64
C(8)-N(2)-C(9)-C(9c)	170	-154	160	154
N(2)-C(9)-C(9c)-C(9)'	65	-86	60	54

PART	<u>[Zn(L15)]</u>		<u>[Cd(L15)]</u>		<u>[Cd(L15b)]</u>	
	A	B	A	B	A	B
C(1)'-C(1)-N(1)-C(2)	-94	18	109	178	-176	88
C(1)-N(1)-C(2)-C(7)	-177	-177	169	175	178	180
N(1)-C(2)-C(7)-C(8)	-1	4	0	0	2	-6
C(2)-C(7)-C(8)-N(2)	-67	64	73	-71	-77	81
C(7)-C(8)-N(2)-C(9)	-175	168	176	-174	-174	-174
C(8)-N(2)-C(9)-C(9c)	178	-178	172	-172	-170	178
N(2)-C(9)-C(9c)-C(9)'	74	-75	-84	86	81	-87

Primes denote the atoms from the alternative part of the molecule.

Atom C(9c) is the central atom of the trimethylene bridge.

C(7)-N(2)-C(9) are the same for both parts of the molecule and does not conform entirely to the rule. The 'free' ligand L15e can be classified as having virtual mirror plane symmetry, however for the n-butyl L15b ligand this is not the case, and this structure could not be described as possessing a virtual mirror plane symmetry. As mentioned in Section 3.2.3(iv) portions of the inner great ring appears to have localised pseudo two-fold symmetry.

#### 3.2.4(iv) The 'hole-size' $R_H$ .

In Table 3.2.4(iv) is a list of values for hole sizes  $R_H$  (see Section 3.1.2 for the method of calculation) for the structures studied in this project, and also for some related  $N_4$  'free' ligands studied by other workers. No successful molecular mechanics study of these ligands has yet been completed by the James Cook group, so it has not been possible to do a complete comparative study of MOLMIN structures, Section 3.1.4, with the X-ray structures studied here. In the absence of a well defined structure of the 'free' ligand L15, predictions based on the calculated minimised structure would have provided another way to get a  $R_H$  value and comparisons could then have been made with the other 'free' ligands in the series and the corresponding metal complexes. Examination of the limited structural data available for the free ligands, that is  $R_H$  2.02 Å for L14 and  $R_H$  2.06 Å for L16 it might seem that the hole size would increase steadily with the number of atoms in the great ring. However with the greater flexibility introduced by the lengthening of the alkyl bridge different conformations may occur, possibly produced by steric effects of the alkyl substituents causing different intramolecular H-bonding patterns. The very recent synthesis and structure determination of the analogous 17-membered  $N_4$ -ligand by P. Baillie show a very large

Table 3.2.4(iv) Hole Sizes ( $R_H / \text{\AA}$ ) in these compounds.

<u>Hole Size</u>	<u><math>R_H / \text{\AA}</math></u>
L14	2.02 <sup>a</sup>
L15	?
L15e	2.10
L15b	2.14
L16	2.06 <sup>b</sup>
Zn(L15)	2.14
Cd(L15)	2.24
Cd(L15b)	2.25

<sup>a</sup> The value for this ligand was obtained from reference 147.

<sup>b</sup> The value for this ligand was obtained from P. Baille (PNL) unpublished work.

$R_H$  of 2.41 Å with a very non-planar arrangement of the four nitrogen atoms. It is possible that measurement of hole size in the free ligand may not directly give a measure of the cavity available once a metal atom is present to constrain the donor atoms to be more planar.

The  $R_H$  values for the cadmium complexes show a slight increase on alkylation 2.24 Å for L15 and 2.25 Å for L15b. It is of interest that the  $R_H$  values in the two cadmium complexes are at least 0.1 Å larger than those of the only 15-membered ligands that have been studied {L15e 2.10 and L15b 2.14 Å, Table 3.2.4(iv)}. Conclusions about the relationship between hole sizes would be of limited meaning here because the metal atoms are well out of the plane of the ligands, but it does seem as if the metal is bringing the two values of  $R_H$  much closer than they would be for the free ligand. The very small difference of 0.01 Å, seen between the  $R_H$  values for the two cadmium complexes, although of low significance, seems to correspond to a slight expansion produced as the metal gets closer to the plane of the four nitrogen donors in the butyl substituted complex Cd(L15b).

The values of hole size observed for the two metal complexes of the unsubstituted 15-membered ligand L15 is 0.1 Å greater for the cadmium than for the zinc complex. The smaller  $R_H$  value for the zinc structure is not only associated to the fact that the covalent radii for this metal atom is smaller than that of cadmium, but also that it lies very much in the plane defined by the  $N_4$ -donors (deviation 0.12 Å). Interestingly the  $R_H$  value here of 2.14 Å is also equal to that found for the 'free' ligand L15b, and is 0.04 Å larger than that of the ethyl substituted 'free' ligand. Although it did not prove possible to get a direct measure of the hole size of the unsubstituted L15 ligand it might be expected to be slightly smaller than L15e which

is smaller than L15b, this suggests that it would have a value which would lie in the range 2.03 Å (the value for the 15-membered diimine ligand) and 2.10 Å (for L15e). As the  $R_H$  for the [Zn(L15)] complex is bigger than this estimated range it would seem that an expansion has occurred on complexing, as was noticed for the cadmium complexes of both L15 and L15b.

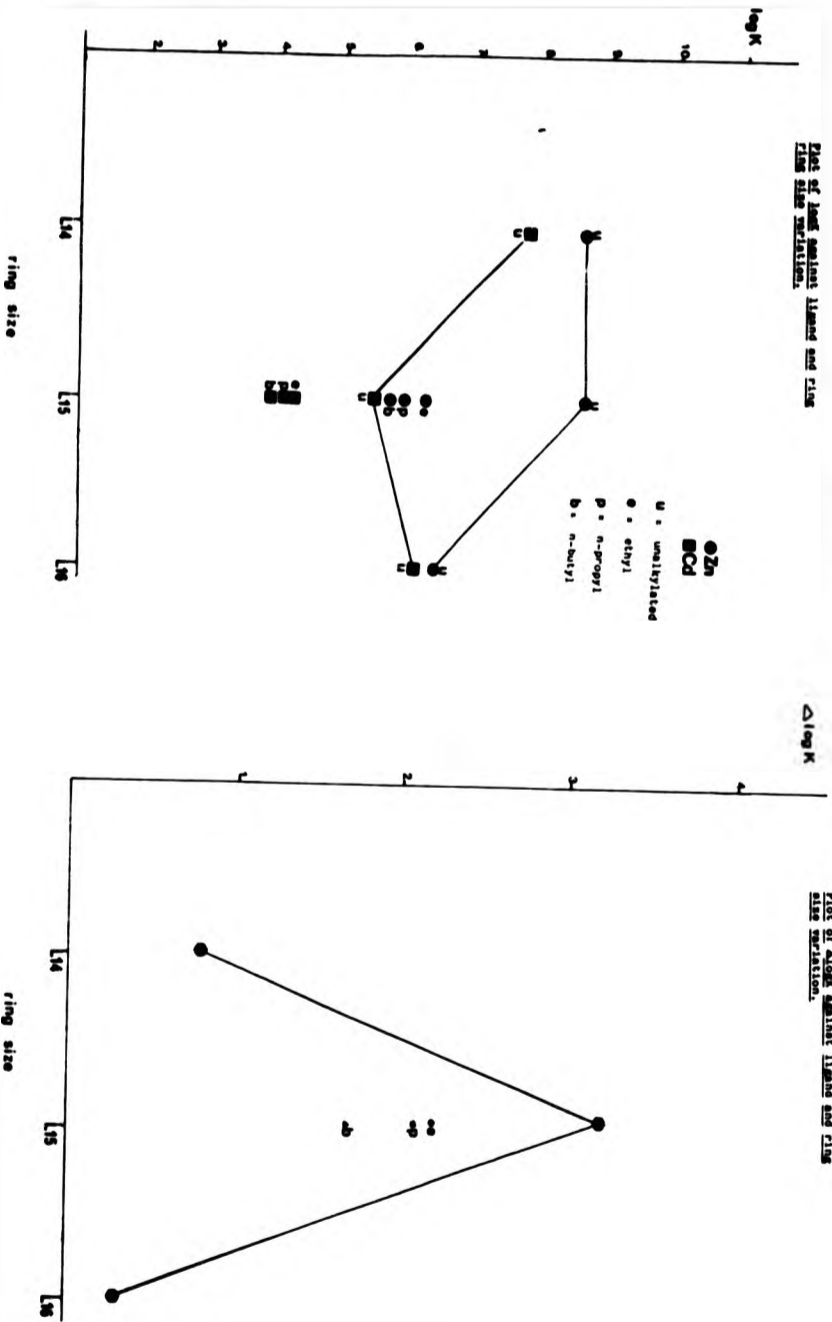
### 3.2.5 Discussion of the stability results in terms of the structure analysis results.

The results of the stability constant measurements on the metal complexes made in this project and related compounds were discussed in Section 3.2.2 where they were correlated with number of atoms in the ligand great ring for 14, 15, and 16-membered macrocycles. The results were summarised in Figure 3.2.2(a) and this is reproduced here as Figure 3.2.5 to allow the correlation to be extended to the observed structures.

The plot of  $\log K$  against ring size, Figure 3.2.5(a), shows the stability order is that the complexes of the zinc are more stable than the corresponding cadmium complexes. This observation conforms with that suggested by the Irvin-Williams series. The largest discrimination, as assessed by  $\Delta \log K$ , is found at the 15-membered ring. The structure determinations of the Cd(II) and Zn(II) complexes of L15 has produced some insight into why such a large  $\Delta \log K$  is obtained at this point in the series. As discussed above for the zinc and cadmium complexes of the unsubstituted ligand L15, the zinc is octahedrally co-ordinated while the cadmium is square pyramidal. This might suggest that co-ordination geometry has a large influence on the discrimination for zinc over cadmium,  $\Delta \log K$  3.24, shown by the ligand L15. It appears that this could be regarded as a 'hole-size' effect;



Figure 3.2.5 Reproduced stability constant graphs.



L15 being large enough to accommodate the smaller zinc atom but the cadmium sits well below the plane of the donor atoms (see Section 3.2.3).

What is of considerable interest is the fact that in all the complexes, the most strongly co-ordinated ligand lies in the cavity created by the folded phenylene groups. For the zinc complex this site is occupied by water, and by the nitrate group for the cadmium complexes. In a related zinc complex,  $[\text{Zn}(\text{L15})(\text{I})](\text{I})$ ,<sup>184</sup> the metal has five co-ordination geometry and the bonding iodine atom also occupies the axis which lies in the cavity produced by the phenylene rings, Section 3.2.3(i). This finding is contrary to what might have been expected, i.e. the axial ligand is in the apparently sterically hindered site between the phenylene rings.

C-alkylation of the most discriminating ligand L15 was carried out not only to see if enhancement of discrimination would occur, but also because the industrial applications of the ligands require that they should have high a degree of solubility in organic solvents. Discrimination for zinc over cadmium stability, for the substituted ligand complexes show in all cases that stability decreases with substitution and with alkyl chain length. Unfortunately this decline in stability is greater for zinc than for the cadmium and therefore a decrease in discrimination occurs instead of the desired increase.

On the basis of these results it is interesting to attempt to envisage what may occur in the actual environment under which the stability constant data is measured. Firstly it seems reasonable to assume that the the macrocycles are approached by solvated metal in the direction that is less sterically hindered. That is, the approach occurs from

the side of the macrocycle away from the folded phenylene rings, shown to be present in all the free ligands studied. The observed structures would therefore suggest that the metal in attaching to the macrocycle produces an inversion of the molecule. This results in the metal and its co-ordinated axial ligand being encapsulated into the cavity formed by the folding of the phenylene groups during complex formation.

In the case of the zinc nitrate complex,  $[\text{Zn}(\text{L15})(\text{NO}_3)(\text{H}_2\text{O})](\text{NO}_3)$ , the zinc ion is located almost in the equatorial plane of the macrocycle, so on the less sterically hindered side a nitrate group can approach the sixth axial site giving the observed octahedral co-ordination. For the cadmium complex where the metal atom lies well out of the  $\text{N}_4$ -donors atoms plane in the direction of the phenylene rings approach by a sixth axial ligand to the cadmium from the other side appears to be ruled out.

The alkyl chain in the substituted ligands, which have meso conformations, have been shown to lie on the side of the molecule away from the phenylene rings. In these structures this side of the molecule can no longer be described as being less sterically hindered. The reason for the relatively greater drop in stability for the zinc complexes compared to the cadmium compounds when the ligand are alkylated then may readily be attributed to the alkyl groups preventing co-ordination at the sixth site. The lowering of the stability in the alkylated complexes could therefore be associated with the fact that a five co-ordinated geometry is being adopted for both metal ions; and the observed discrimination can mainly be attributed to the Irvin-Williams order.

### 3.2.6 Outstanding X-ray and synthetic results.

A brief discussion on work which was initially undertaken as part of this project but for a number of reasons has not been completed is outlined below. This includes the important structure related to the uncompleted 'free' ligand L15 and synthetic routes for preparing the related C-alkylated ligands for the corresponding  $N_2O_2$  15-membered ligands.

#### 3.2.6(1) X-ray analysis of L15 'free' ligand.

Pale yellow crystals of this 15-membered unalkylated 'free' ligand were found to be monoclinic in its crystal system, having the non-centric space group Cc (No. 9 from International Tables Volume I). However it proved difficult to phase the data using crystallographic routines involving direct methods. Vector peaks obtained from a Patterson synthesis showed that the possibility of some kind of heavy atom being present. From the experimental conditions under which this molecule was made it was deduced that the possible atoms which could produce such high Patterson peaks might have arisen from halogen atoms. Solving the Patterson for the atomic positions of this atom produced a reasonable arrangement of some of the macrocyclic atoms. A great deal of time was spent in attempting to completely locate the atoms and achieve a refinement of this structure but it proved to be unsuccessful and it was not even clear which halide counterion was present as the electron density appeared to be intermediate between that expected for chlorine and bromine. The presence of the halide anion indicated that there must have been in a deprotonated form of the ligand in the crystal.

It is interesting to note that the X-ray structural analysis of the corresponding  $N_2O_2$  15-membered macrocyclic analogue of this compound also existed as a deprotonated molecule.<sup>188, 189</sup> This  $N_2O_2$  species was prepared using a similar synthetic technique where hydrogenation on the precursor diimine, was carried out, using sodium tetrahydroborate. The deprotonated  $N_2O_2$  molecule was liberated after successive reaction with nitric acid. This is part of the preparation procedure normally carried out so that the reduced diimine can be liberated.

3.2.6(ii) Preparation of the ligand ethyl  $N_2O_2$  15-membered 'free' ligand.

Studies involving stability constant measurements are well documented<sup>155</sup> for the series of  $N_2O_2$  unalkylated ligands with varying ring size, which are analogous to the  $N_4$ -macrocyclic series discussed in, Section 3.2. In the reported work the data was collected on the formation of the copper and nickel complexes, of the  $N_2O_2$  ligand, since measurement of the equivalent stability date for those of zinc and cadmium were too high. Furthermore X-ray analysis<sup>155</sup> of a zinc(II) complex of the 15-membered unalkylated species, showed it to behave as a bidentate ligand, with only the benzylic nitrogen atoms of the macrocycle co-ordinated to the metal, thus making it unsuitable for macrocyclic studies. For a series of nickel complexes of these  $N_2O_2$  unalkylated ligands, the optimum stability was shown to lie between the 15- and 16-membered rings (Section 3.1.1) where as no definite trend was observed for the related copper complex. In this work it was intended to extend the studies carried out on the  $N_4$ -ligands to the preparation of the corresponding  $N_2O_2$  15-membered ethyl C-alkylated ligand, and to compare the results with known stabilities of the unsubstituted  $N_2O_2$  ligands with copper and nickel.

Preparation of  $N_2O_2$  15-membered ethyl derivative, was carried out using the same procedure described above for the preparation of the  $N_4$ -alkylated species (Section 3.2.1). Once again the corresponding precursors required to make the diimine were made following already reported synthetic routes.<sup>190-193</sup> Alkylation of the diimine was conducted using the same synthetic route outlined in Figure 3.2.1, where the diimine is reacted with the corresponding Grignard reagent, and this produced a creamy white solid.

The  $^1H$  n.m.r spectrum for this solid was obtained. For the expected structure a total of 32 peaks should be present, corresponding to 6 methyls, these should appear as a triplet resonating at around 1ppm. Signals arising from the 4 protons of the ethane group occurring between 1-2 ppm. A quartet should occur, arising from the trimethylene bridge of the macrocycle, giving 6 protons. A singlet between 3-4 ppm, integrating to 6 protons, due to the resonance of the protons of the benzylic carbon and the ethane ether bridge of the molecule. The phenyl hydrogen occurring at around 7 ppm while those of the benzylic nitrogen atoms can occur any where on the spectrum. What was actually found showed that a mixture of isomers were present, as judged by the resonance of the benzylic hydrogen and those of the methyl group, Figure 3.2.6(ii). The relative intensities of the signals also indicates that these isomers are not present in equal amounts.

It has been reported that the corresponding 15-membered  $N_2O_2$  unalkylated saturated 'free' ligand exist as two independent molecules with different conformations.<sup>144</sup> They differ only in the conformation at the benzylic carbon and nitrogen bonds, one having gauche and the other an anti arrangement, see below:-

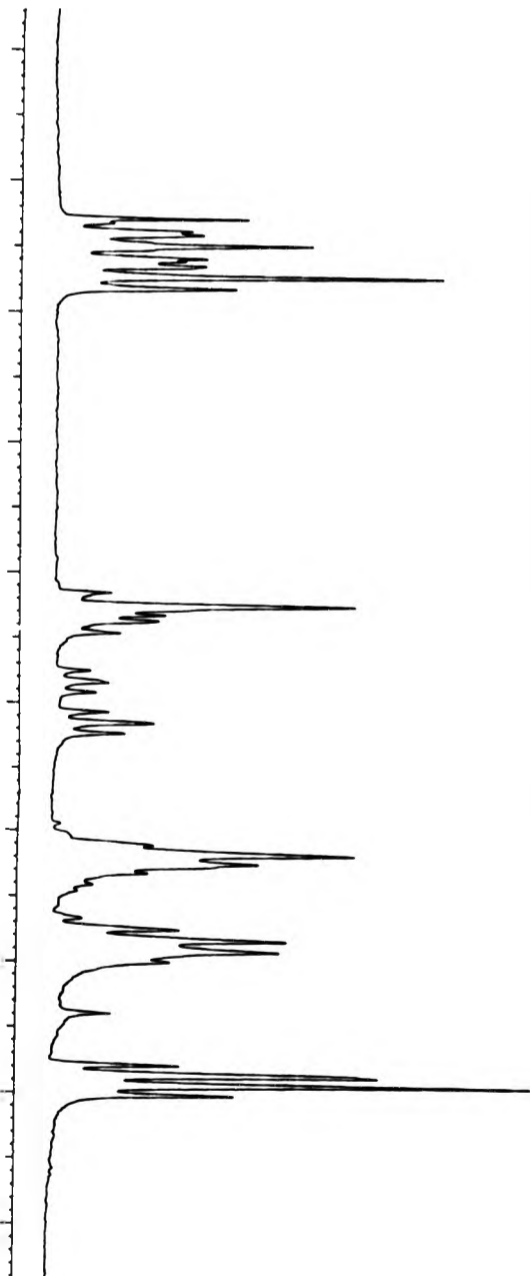
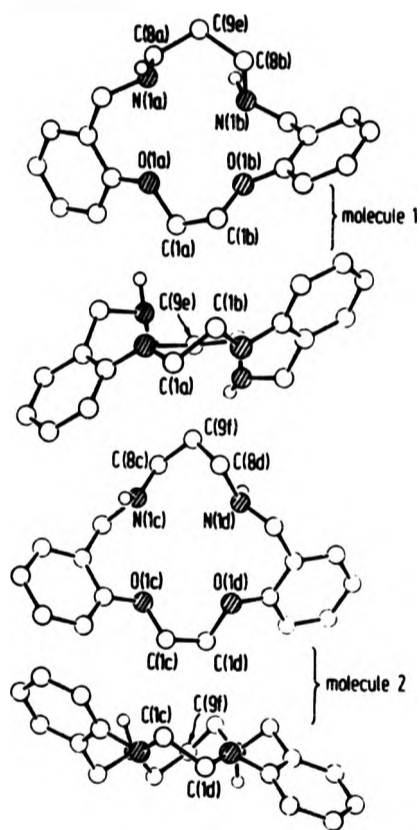


Figure 3.2.6(11)  $^1\text{H}$  n.m.r. spectrum of  $\text{N}_2\text{O}$  L15e, showing that an isomeric mixture is present.



The conformations of molecules 1 and 2 of (1b), showing the approximate 2-fold symmetry of each.

In solution the  $^1\text{H}$  n.m.r. suggest that only one compound exist at  $30^\circ\text{C}$ .<sup>144</sup> Therefore rapid interchange between these forms must occur in solution at this temperature. The possibility therefore exists that the alkylated species follows the same pattern but interchange between the two forms is very slow at  $30^\circ\text{C}$ . The formation of an isomeric mixture is perhaps not a suprising result when the proposed mechanism for forming these alkyl substituted compounds are considered.



X-ray structural analysis of the zinc complex<sup>155</sup> of the unalkylated reduced  $N_2O_2$  15-membered ligand as been reported. The zinc is found bonded solely to the nitrogen atoms of the macrocycle and the ether oxygen atoms are not co-ordinated. The metal forms a pseudo-tetrahedral arrangement of atoms, with the iodine atoms occupying the other two tetrahedral sites. The ethylene bridge portion of the molecule distorted away from this coordination sphere, and the trimethylene bridge lying back over the cavity of the macrocycle, Section 3.2.3(i).

In the attempted synthesis of the ethylated  $N_2O_2$  ligand assuming that an isomeric mixture were present, one might expect that in solution the magnesium would form a similar species and hence the precursor diimine molecule would be held less rigidly. Thus formation of the resultant isomeric mixture of alkyl substituted macrocycle is produced; since the bonding of the magnesium with the macrocycle has little or no effect on the stereochemistry of the products.

In the absence of high performance liquid chromatography equipment (HPLC),<sup>194</sup> isolation of a single isomer of this product was attempted, by forming the perchlorate salt of the alkyl ligand. This was conducted as an iterative procedure where-by the loss of one isomer is achieved during the protonation/deprotonation of the reaction mixture, ie. using solubility and dilution techniques for removing one isomer. From the n.m.r study, some loss was achieved, as evident from the intensity of peak ratios. However after several repetitions of this process, no significant amount of a single isomer was isolated. Progression to the preparation of the corresponding copper or nickel complex was not attempted due to the ambiguity in the structure of the prepared  $N_2O_2$  L15e compound.

3.3 General method in the C-alkylation of 15-membered Diimines by the addition of Grignard reagents.

N-alkylmagnesium bromide was freshly prepared by reacting alkylbromide (150 mmol) in  $\text{Et}_2\text{O}$  ( $100 \text{ cm}^3$ ) with magnesium metal (150 mmol) in 1:1  $\text{Et}_2\text{O}$ /benzene ( $200 \text{ cm}^3$ ). The corresponding diimine (7.76 mmol) was added in small portions. Each addition of the diimine was followed by effervescence, and in some cases a transient yellow colour. The mixture was refluxed for 30 min. After cooling  $\text{NH}_4\text{Cl}$  ( $200 \text{ cm}^3$ ) was added then the mixture was extracted three times using  $\text{CH}_2\text{Cl}_2$  (total volume  $300 \text{ cm}^3$ ). The organic layer was combined and dried using  $\text{MgSO}_4$ . On, evaporated under pressure, cooling a solid was obtained.

3.3.1 Analytical data for ligand L15p.

Recrystallisation from MeOH/Pet.ether (60:40<sup>o</sup>) mixture gave colourless white needles of L15p. Yield 2.4g, 79.9% mp  $132 - 132^\circ\text{C}$ . Found: C, 75.7; H, 10.5; N, 13.6,  $\text{C}_{22}\text{H}_{38}\text{N}_4$  requires C, 76.1; H, 9.7; N, 14.2%. Ir.:  $\nu$  3260, 3050, 2978, 2380, 1610, 1594, 1523, 1385, 1332, 1285, 1256, 1221, 1200, 1150, 1105, 1090, 1050, 1020, 928, 856, 828, 806, 785,  $742 \text{ cm}^{-1}$ .  $^{13}\text{C}$  n.m.r (CDCl<sub>3</sub>):  $\delta$  14.2, 20.3, 31.4, 34.6, 41.8, 45.8, 65.9, 109.6, 115.4, 125.4, 128.0, 129.5, 147.4, p.p.m. Mass Spectrum : m/e 3394 ( $m^+$  = 19.9%).

3.3.2 Analytical data for ligand L15b.

Recrystallisation from MeOH/Pet.ether (60:80<sup>o</sup>) mixture gave colourless white needles of L15b. Yield 2.33g, 71.2%, mp  $97-99^\circ\text{C}$ . Found: C, 75.8; H, 10.1; N, 14.2;  $\text{C}_{27}\text{H}_{42}\text{N}_4$  requires: C, 76.8; H, 10.3; N, 13.3%. Ir.:  $\nu$  : 3280, 3230, 3078, 3040, 2930, 2860, 2800, 2700, 1603, 1585, 1512, 1328, 1280, 1250, 1240, 1220, 1190, 1161, 1149, 1100,

1082, 1049, 1022, 972, 955, 935, 912, 900, 860, 830, 810, 791, 765, 740 $\text{cm}^{-1}$ .  $^{13}\text{C}$  n.m.r (CDCl<sub>3</sub>):  $\delta$  14, 22.7, 29.2, 31.4, 32.1, 41.7, 45.6, 65.9, 109.4, 115.2, 125.3, 127.8, 129.3, 147.3. Mass spectrum: m/e 422 ( $m^+$  - 33.1%).

### 3.3.3 Preparation of Cd[(L15b)(NO<sub>2</sub>)](NO<sub>2</sub>).

N-butyl ligand (0.1439g, 0.341 mmol) was added to a warmed CH<sub>3</sub>CN (50 $\text{cm}^3$ ) solution of CdNO<sub>3</sub>·4H<sub>2</sub>O (0.1275g, 0.413 mmol). The mixture was allowed to reflux for 30 min. after which water was added, dropwise, to precipitate the complex. The precipitate was dried and refluxed again in excess CH<sub>3</sub>CN (50 $\text{cm}^3$ ). The volume of solution was reduced under vacuum, and on cooling, long colourless needlelike crystals were obtained. Yield 0.168g, 76.7%. Found: C, 57.2; H, 6.1; N, 12.7; Cd C<sub>27</sub> H<sub>42</sub> N<sub>6</sub> O<sub>6</sub> requires C, 57.2; H, 6.40; N, 12.7%. Ir.:  $\nu$ : 3422, 3370, 3220, 3050, 2960, 2890, 1595, 1570, 1510, 1340, 1320, 1270, 1210, 1185, 1170, 1090, 1070, 1040, 1010, 970, 850, 782, 767 $\text{cm}^{-1}$ .

### 3.4 Structure solution and refinement.

#### 3.4.1 The 'free' ligand L15b.

From the diffractometer Dirichlet reduction a triclinic space group was indicated. A reasonable calculated density of  $1.096 \text{ g cm}^{-3}$  was obtained when it was assumed that there were two molecules per unit cell. This indicated that the space group was  $P\bar{1}$  (No2), which was confirmed by satisfactory refinement of the structure.

The structure was solved using the automatic centrosymmetric routine EEES of the Shelx program. The starting origin and multisolution chosen by the program to initiate calculation of the phases for the normalised structure factors are given in Table 3.4.1.

The first calculated E-map indicated the positions of all the non-hydrogen atoms. The N-H hydrogen atoms were located from a difference Fourier synthesis, while those of the carbon atoms were included in calculated positions (C-H,  $1.08 \text{ \AA}$ ). The carbon atoms of the two phenyl rings and the hydrogen atoms bonded to nitrogen were refined with isotropic thermal parameters. The four nitrogen donor atoms, and the remaining non-phenyl carbon atoms were refined with anisotropic thermal parameters.

In the final stages of full-matrix refinement 2159 unique reflections with  $I > 3.0 \sigma(I)$  were used, and the final R-factor was 0.074.

#### 3.4.2 $[\text{Cd}(\text{L15b})(\text{NO}_2)](\text{NO}_2)$ .

A preliminary data obtained from the diffractometer showed the crystal system to be monoclinic with intensity data:-

$$I_{hkl} = I_{\bar{h}\bar{k}l} = I_{h\bar{k}l} = I_{\bar{h}kl}$$

Table 3.4.1 Showing the reflections and their corresponding E-value used to phase the structure factors for the 'free' ligand L15b.

	<u>H</u>	<u>K</u>	<u>L</u>	<u>E</u>
Origin	7	4	6	3.743
Origin	-1	-5	4	2.834
Origin	-2	-2	4	2.653
Multisolution	-3	4	0	2.511
Multisolution	0	-1	9	2.917
Multisolution	-3	7	2	2.987
Multisolution	-7	-3	5	3.145
Multisolution	-2	4	0	2.087
Multisolution	2	0	2	3.354
Multisolution	2	2	0	2.496
Multisolution	7	2	8	2.866
Multisolution	0	-2	3	2.144
Multisolution	10	-4	5	2.801
Multisolution	1	-3	10	2.401

The calculated density of  $1.46 \text{ gcm}^{-3}$  was a reasonable value assuming four molecules being present in the unit cell. Inspection of the corrected intensity data showed systematic absences in

$$\begin{aligned} h0l & \text{ when } h + l = 2n + 1 \text{ and} \\ 0k0 & \text{ when } k = 2n + 1 \end{aligned}$$

This defined the space group as  $P2_1/n$ , a special case of  $P2_1/c$  (No. 14). The algebraic terms for  $P2_1/c$ , from the International Tables, had to be modified for  $P2_1/n$  symmetry giving:-

$$\begin{aligned} x, & \quad y, & \quad z \\ -x, & \quad -y, & \quad -z \\ 0.5 - x, & 0.5 + y, & 0.5 - z \\ 0.5 + x, & 0.5 - y, & 0.5 + z \end{aligned}$$

subtracting the equivalent positions for this space group, the unique terms defining the maxima in the Patterson for vectors between symmetry related atoms were:-

$$\begin{aligned} 2x, & \quad 2y, & \quad 2z \\ 0.5 - 2x, & 0.5, & 0.5 - 2z \\ 0.5, & 0.5 - 2y, & 0.5 \end{aligned}$$

These were used to find the position of the zinc atoms in the Patterson map which had the following principle peaks:-

	<u>Height</u>	<u>u</u>	<u>v</u>	<u>w</u>
1	999	0	0	0
2	404	0.224	0.5	0.246
3	404	0.5	0.045	0.5
4	201	0.276	0.455	0.257
5	68	0.078	0	0.333

From the first four peaks shown above, the position of the cadmium atom was readily found to be at:-

$$x = 0.138$$

$$y = 0.288$$

$$z = 0.128$$

The metal position was used to phase the structure factors to calculate an electron density map from which the positions of twelve atoms of two the phenyl groups were located. These positions along with that of the metal atom was used in further Fourier synthesis and subsequently revealed the positions of the other non-hydrogen atoms, with the exceptions of the two adjacent terminal carbon atoms of one of the n-butyl substituents. These proved to be difficult to locate, but where reasonable peaks, ca.  $2e\text{\AA}^{-3}$ , occurring in pairs, were located corresponding to a 1:1 distortion of this part of the group. The carbon atoms C(12a) and C(13a) were treated as disordered and were assigned half-occupancy.

Further difference maps calculations, after six cycles of refinement the positions of the found atoms, revealed the position of the four hydrogen atoms bonded to the nitrogen donor atoms. The remaining hydrogen atoms were included at calculated positions (C-H, 1.08 Å).

In the final stages of refinement the metal, non-phenyl carbon, six oxygen and six nitrogen atoms were refined with anisotropic thermal parameters. The other atoms were assigned isotropic thermal parameters parameters, and final structure refinement using 2506 unique reflections with  $I > 3.0 \sigma(I)$  to a final R-factor of 0.048.

TABLE 3.4. MOLECULAR STRUCTURE DETERMINATION DATA

	$[\text{Zn}(\text{L15})(\text{NO}_3)(\text{H}_2\text{O})](\text{NO}_3)$	$[\text{Cd}(\text{L15})(\text{NO}_3)](\text{NO}_3)$	$[\text{Cd}(\text{L15B})(\text{NO}_3)](\text{NO}_3)$	L15b
Molecular formula	$\text{C}_{19}\text{H}_{28}\text{N}_6\text{O}_7\text{Zn}$	$\text{C}_{19}\text{H}_{26}\text{N}_6\text{O}_6\text{Cd}$	$\text{C}_{27}\text{H}_{42}\text{N}_6\text{O}_6\text{Cd}$	$\text{C}_{27}\text{H}_{42}\text{N}_4$
Molecular weight	517.8	546.8	659.1	422.7
Colour	White	White	White	Colourless
Crystal/system	Monoclinic	Monoclinic	Monoclinic	Triclinic
Space group	C2/c	$\text{P2}_1/\text{c}$	$\text{P2}_1/\text{n}$	$\text{P1}$
$a/\text{\AA}$	19.628(3)	8.310(4)	16.437(4)	11.305(2)
$b/\text{\AA}$	7.679(2)	18.965(3)	23.196(2)	11.031(2)
$c/\text{\AA}$	29.153(2)	14.352(2)	7.965(2)	10.947(1)
$\alpha/^\circ$	90	90	90	109.441(1)
$\beta/^\circ$	99.28(1)	100.09(2)	98.79(1)	84.66(1)
$\gamma/^\circ$	90	90	90	87.13(1)
$V/\text{\AA}^3$	433.42	2224.53	2987.62	1276.97
$D/\text{gcm}^{-3}$	1.588	1.633	1/465	1.096
$F(000)$	2160	1292	1368	464
$Z$	8	4	4	2
$\mu(\text{Mo-K}\alpha)/\text{cm}^{-1}$	2.52	9.48	6.97	0.34
$\theta$ range, min: max	3:25	3:25	3:25	3:25
Scan mode	2	2	2	1



TABLE 3.4 continued:-

No. of reflections measured	2424	2020	2648	2325
No. of unique observed reflections >3 $\sigma$ I.	2424	2013	2640	1752
No. of parameters used in refinement	382	367	289	229
$\bar{R}$	0.043	0.044	0.048	0.074
$\bar{R}_w$	0.045	0.055	0.048	0.074
$w=1/\sigma^2(F)$				

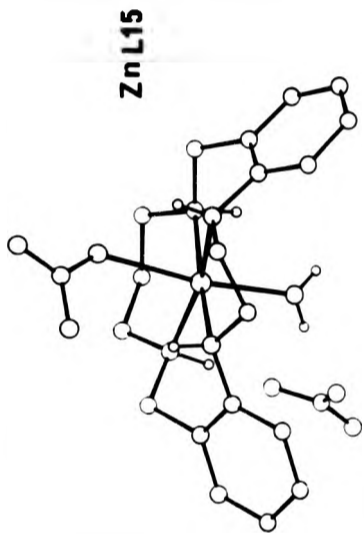
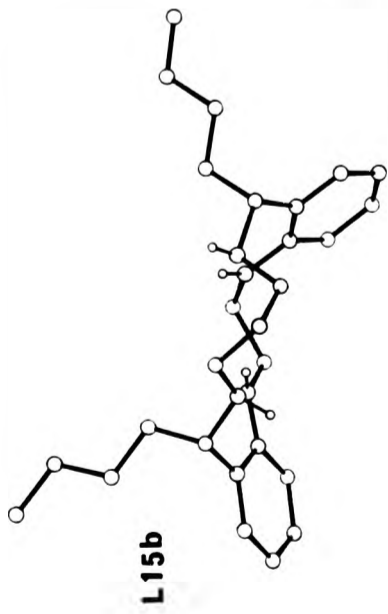
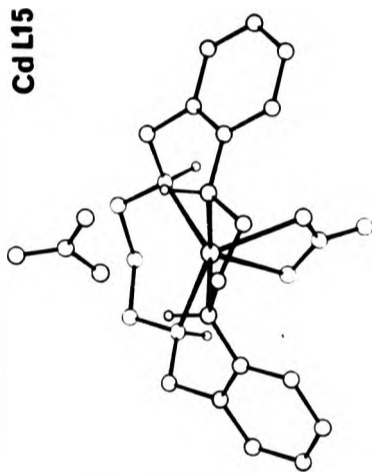
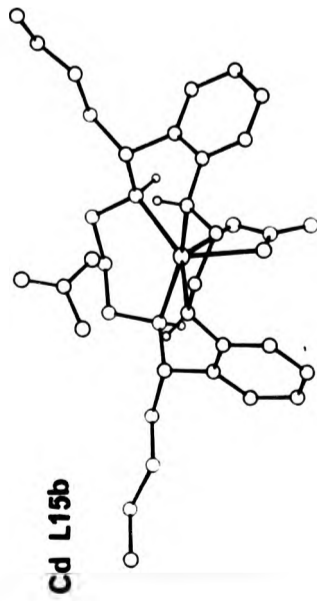


Figure 3.4 Diagrams of the three metal complexes and the free ligand L15b.



CHAPTER 4 The X-ray structure determination methods.

#### 4 The X-ray structure determination method

##### 4.1 Data Collection

In each case the single crystal to be analysed was mounted on a goniometer head and was centred on a Philips PW1100 four circle diffractometer controlled by a computer. X-Rays from a Mo-K $\alpha$  ( $\lambda = 0.71069 \text{ \AA}$ ) source, monochromated by a single graphite crystal, were used throughout. A Dirichlet reduced cell, which was converted to a standard unit cell, was obtained after an initial peak hunt. In this search the four circles of the diffractometer were systematically incremented by the diffractometer until 25 strong, low angle reflections had been detected and their setting angles ( $\theta$ ,  $2\theta$ ,  $\chi$ , and  $\phi$ ) optimised and recorded. Least squares analysis was then then carried out on the setting angles of 25 higher reflections with  $\theta$  ca.  $10^\circ$  and counts ( $I/s^{-1}$ )  $>1000$ , which produced more accurate unit cell dimensions. The intensity relationships were checked at this stage by driving to a range of reflections, to confirm the crystal system.

All intensity data were collected, in the unique volume corresponding to the crystal Laue symmetry, at ambient temperature. Two different scanning procedures were used when measuring these intensities, with speed  $0.05^\circ \text{ sec}^{-1}$  in  $\omega$ . The type of scan mode used was dependent on the type of method which would be used to solve the structure, which varied with the nature of the crystal. When scan mode 1 was used, all reflections were recorded. When scan mode 2 was used reflections were

not recorded when:-

$$I_t - 2 / I_t < I_b$$

$I_t$  = count rate at the top of the reflection peak.

$I_b$  = the mean count rate of two preliminary  
5s background measurements on either  
side of the peak,

and reflections with  $I_t < 500 \text{ s}^{-1}$  were rescanned to increase their accuracy. The scan width varied for each structure (see Table 2.4 and 3.4 for summaries of crystal data).

The raw intensity data ( $I_{hkl}$ )<sub>raw</sub> and the estimated standard deviation for each reflection were obtained. These were corrected for Lorentz (L) and polarisation (p) factors, using the formula:-

$$(I_{hkl}) = (I_{hkl})_{\text{raw}}(Lp)^{-1}.$$

These correction for the loss in intensity of the X-ray beam as a result of polarisation and geometric factors are:-

$$p = (1 + \cos^2 2\theta) / 2 \text{ and } (L = 1 / \sin^2 \theta).$$

The estimated standard errors,  $\sigma(I)$ , of the intensities ( $I_{hkl}$ ) were obtained from the expression:-

$$\sigma(I) = [\sigma^2(I) + (0.04I)2]^{1/2}$$

where K is an 'instability' constant and a value of  $0.04^{195}$  was assigned to it.

Equivalent reflections were averaged, and the number of reflections collected and the number used during refinement are recorded in the relevant Tables for the structure determination data in Sections 2.4 and 3.4.

#### 4.2 The Phase Problem

Diffraction of X-rays occurs after initial scattering by the electrons associated with the atoms within the unit cell. The electron density ( $\rho_{xyz}$ ) at any point  $x, y, z$  throughout the unit cell may be expressed as a three dimensional Fourier series:-

$$(4a) \rho_{xyz} = V^{-1} \sum_{hkl} F_{hkl} e^{-2\pi i(hx + ky + lz)}$$

where  $V$  is the unit cell volume.

To be able to find the positions of the atoms electron density maps must be calculated over the unique part of the unit cell. The problem is that the phase of the structure factor  $F_{hkl}$  cannot be experimentally measured. If the positions and type of the  $N$  atoms in the unit cell were known the structure factor could be calculated:-

$$(4b) F_{hkl} = \sum_{n=1}^{n=N} (f_n)_{hkl} e^{2\pi i(hx_n + ky_n + lz_n)}$$

where  $f_n$  is the scattering factor of the  $n$ th atom, whose value is a function of  $\sin\theta$  and the number of electrons in the atom.  $F_{hkl}$  is a complex number and so can be written as the sum of a real and imaginary portion.

$$F_{hkl} = A_{hkl} + iB_{hkl}$$

$$(4c) F_{hkl} = |F_{hkl}| \cos\phi_{hkl} + i(|F_{hkl}| \sin\phi_{hkl})$$

To be able to solve the structure under analysis some way of obtaining preliminary values of the structure factors  $F_{hkl}$  must be found. The value of  $F_{hkl}$  cannot be calculated directly since it is the squared modulus  $|F_{hkl}|^2$  that equals the intensity measured  $I_{hkl}$ . The unknown

angle,  $\phi_{hkl}$ , associated with  $|F_{hkl}|$  must be estimated before any electron density map can be calculated, and this is known as the phase problem. Solving the phase problem is determining the phase of  $F_{hkl}$ , and this is the first stage of any structural analysis.

For centrosymmetric structures, for every atom at  $x, y, z$ , there is an equivalent atom at  $-x, -y, -z$ . Only  $N/2$  independent atoms are then present in the unit cell, the remaining  $N/2$  atoms being related to these by the inversion centre. It can be shown that the phase angles  $\phi_{hkl}$  for centrosymmetric crystals are restricted to having one of two values, 0 or  $180^\circ$ . Substituting these values into (4c) gives:-

$$F_{hkl} = |F_{hkl}| \cos 0 \text{ or } F_{hkl} = |F_{hkl}| \cos 180.$$

As  $\cos 0$  is  $+1$  and  $\cos 180$  is  $-1$ , the phase problem is reduced to a matter of finding the signs of the  $F_{hkl}$  values. The equation to calculate the structure factor for centrosymmetric crystals can be simplified to:-

$$(4d) \quad F_{hkl} = 2 \sum_{n=1}^{n=N/2} f_n \cos\{2\pi(hx_n + ky_n + lz_n)\}$$

Although for centrosymmetric structures the phase problem is reduced to finding the sign (+ or -) of the structure factor  $F_{hkl}$ , for non-centrosymmetric structures this is not the case and the value of the phase angle, which can be between  $0$  and  $360^\circ$ , must be determined.

#### 4.3 Methods used to solve the phase problem.

Two main methods are usually used to solve the phase problem, either via the Patterson or by direct methods. Both these procedures have been used in this present work

#### 4.3.1 Patterson Synthesis.

A Patterson vector map can be obtained directly from the observed intensity synthesis using the equation:-

$$4(e) \quad P_{uvw} = |F_{hkl}|^2 \cos 2\pi(hu + kv + lw)$$

This is a three dimensional map which has a peak for every pair of atoms within the real unit cell. These peaks are situated in a particular direction and distance from the origin, which corresponds to the vector between the pair of atoms in the real unit cell. Each peak is at position (u, v, w) related to the atomic coordinates,  $x_1, y_1, z_1$  and  $x_2, y_2, z_2$  of the two atoms by:-

$$(a) \quad u = x_1 - x_2$$

$$(b) \quad v = y_1 - y_2$$

$$(c) \quad w = z_1 - z_2$$

The height of each peak in a Patterson map is proportional to the product of the atomic numbers of the atoms involved. Therefore the highest peaks usually corresponds to the vectors of the heaviest atoms in the unit cell. The highest peaks in the Patterson map always occurs at the origin and all atoms contribute to it. The next highest can be assigned to the vectors arising from the heaviest atom in the unit cell. Taking these u, v, w values, the position x, y, z of the heaviest atom in the real unit cell can then be found algebraically. This position can then be used to calculate preliminary structure factors and hence an electron density map from which more atoms can be obtained.



#### 4.3.2 Direct Methods.

Direct methods is a statistical procedure which is used to determine the phases of a structure. There are comprehensive texts<sup>196,197</sup> available to describe how direct methods is used in phase determination. The key formulae used in the application of direct methods are included in Table 4.3.2. An outline of the procedures used in this work will be given here.

- (i) Normalised structure factors<sup>198</sup> are calculated for every reflection in the data.
- (ii) Reflections above a specific minimum E-value (normalised structure factor), are sorted according to their magnitudes.
- (iii) All the possible combinations of these reflections are listed to see if their indices satisfy the  $\Sigma_2$  relationship.<sup>199-201</sup>
- (iv) After the relationships have been generated the, evaluation of the structure factor phases is started.
- (v) A few reflections (usually two or three) in any data set may be allocated arbitrary phase values, which are subject to certain restrictions depending on the space group. These reflections determine the starting set and are used to define the origin uniquely<sup>202</sup> at a site within the unit cell. Only reflections whose phases vary with the origin position can be used for this purpose.

In the automatic centrosymmetric routine EEES203 the origin defining, and any other starting reflections, are chosen by the SHELX '76 program.<sup>204</sup>

With the routine TANG, within SHELX '76 the origin defining

normalised structure factor<sup>198</sup>  $|E_h|^2 = |F_h|^2 / c \sum_{j=1}^N f_j^2$

where  $|F_h|$  is the structure factor magnitude,  $f_j$  is the atomic scattering factor for the  $j$ th atom in a unit cell containing  $N$  atoms, and  $c$  is a number which corrects for space group extinctions.

sigma-two relationship ( $L_2$ ):  $sE_h = s|E_h, E_{h-h}$ ,

where  $s$  means 'sign of'.

associated probability:  $P_{\pm h} = \frac{1}{2} \pm \tanh \sigma_3 \sigma_2^{-3/2} |E_h| |E_h, E_{h-h}|$

where  $\sigma_n = \sum_{j=1}^N Z_j^n$ , and  $Z_j$  is the atomic number of the  $j$ th atom in a unit cell containing  $N$  atoms. <sup>199-201</sup>

tangent formula: <sup>205</sup>  $\tan \phi = \frac{\sum |E_h, E_{h-h}| \sin(\phi_h + \phi_{h-h})}{\sum |E_h, E_{h-h}| \cos(\phi_h + \phi_{h-h})}$

associated probability:  $P_{\phi_h} = \{2\pi I_0(\kappa)\}^{-1} \exp\{\kappa \cos(\phi_h - \phi_h, -\phi_{h-h})\}$  <sup>201</sup>

where  $I_0$  = Bessel function <sup>13</sup>, and  $\kappa = \kappa_{hh} = 2\sigma_3 \sigma_2^{-3/2} |E_h, E_{h-h}|$ , in which the kappa value ( $\kappa$ ) is a measure of reliability of the phase ( $\phi$ ) determined using the tangent formula. <sup>207</sup>

convergence map:  $\alpha_h^2 = \{\sum \kappa_{hh} \cos(\phi_h + \phi_{h-h})\}^2 + \{\sum \kappa_{hh} \sin(\phi_h + \phi_{h-h})\}^2$ , in which the alpha value ( $\alpha$ ) is a measure of the variance of the determined phase angle ( $\phi$ ). <sup>200</sup>

reliability equations: <sup>208, 209</sup>

$$R_{R_1} \sim \frac{\sum \alpha_h - \sum (\alpha_h^2)_r}{\sum \alpha_h^2} \frac{1/2}{\sum (\alpha_h^2)_e} \frac{1/2}{\sum (\alpha_h^2)_r} \frac{1/2}{\sum (\alpha_h^2)_r}$$

$$R_{R_A} \sim \{\sum (E_o - kE_c)^2 / \sum (E_o)^2\}^{1/2}$$

<sup>20</sup> based on

where  $r$  and  $e$  are random and estimated phases respectively,  $o$  and  $c$  are observed and calculated normalised structure factors respectively, and  $k$  is a scale factor.

Table 4 Key formulae used in direct methods of phase determination.

and the other starting reflections must be specified by the user. The choice is made after examination of a convergence map,<sup>205</sup> calculated by the program, which estimates the alpha values for each reflection in the data set above a specified minimum E-value. In the calculation of the convergence map the reflection with the smallest alpha value is eliminated from the data set together with all the phase relationships in which the reflection is involved. The alpha<sup>205</sup> values for all reflections involved are then re-estimated and once more the reflection with the lowest estimated alpha is eliminated. This process converges onto a group of reflections that are linked with a large number of strong phase relationships and these constitute the convergence map. From this map the origin defining and starting reflections can be selected and it is possible to evolve a possible path of phase determination using the tangent formula. The reflections with the highest alpha values are the most important in the subsequent application of the tangent formula as they contribute to the largest number of reflections.

- (vi) The arbitrarily assigned phases which constitute the starting set are subsequently used with the  $\sum_2$  relationship<sup>199</sup> or the tangent formula<sup>206</sup> to derive the phases of all those reflections in the  $\sum_2$  sign expansion pathway with E-values above the specified minimum.
- (vii) The phased reflections are then used to calculate an E-map,<sup>204</sup> which is a three dimensional Fourier synthesis, and uses normalised structure factors in the calculations rather than the structure factors themselves. The result is a map with sharpened peaks.
- (viii) From the E-map,<sup>204</sup> co-ordinates of peaks (representing

atoms positions) are used in structure factor calculations and attempted refinement to test for satisfactory solution.

#### 4.4 Fourier synthesis

Once the position of some of the atoms are found, either from a Patterson map or from direct method, they are then used to calculate an electron density map. First the co-ordinates of the found atoms are used to calculate  $F_{hkl}$  values ( $F_c$ ), and so, assign phases to  $F_o$  values for all  $hkl$ . If the atoms of the partial solution contribute significantly to the diffracting power of the structure being studied the phase determination will be almost correct. An electron density map is then calculated from the three dimensional Fourier series:-

$$\rho_{xyz} = V^{-1} \sum_{hkl} F_{hkl} e^{-2\pi i(hx+ky+lz)}$$

Positions of the unfound atoms within the asymmetric unit cell are obtained by employing two alternative methods of calculating Fourier maps. The first involves applying the phases of all  $F_c$  values to the experimentally obtained structure amplitudes  $F_o$  in the above equation. This method is particularly useful if the partial solution contributes in a non-random way to the total diffraction, (i.e. if atoms are in a special position or one of pseudo-symmetry). For centrosymmetric space groups the Fourier maps are produced by a simplified equation:-

$$\rho_{xyz} = 2V^{-1} \sum_{hkl} S_c |F_o| \cos[2\pi(hx+ky+lz)]$$

where ( $S_c$ ) is the calculated sign of each  $F_{hkl}$

From the observed Fourier map the fractional co-ordinates of other

atoms may be obtained. These are used to calculate a new set of  $F_c$  values and the new phases used to calculate a better Fourier map. Once the position of most of the non-hydrogen atoms are found a difference-Fourier synthesis can be used in calculating a new map in which corresponding to the H-atoms may be located. In this Fourier calculation the calculated phases are applied to the difference between the observed structure amplitude  $F_o$  and the calculated structure factor  $F_c$ , and for centrosymmetric space groups the expression used is:-

$$\Delta \rho_{xyz} = 2V^{-1} \sum_{hkl} S_c ( |F_o| - |F_c| ) \cos[2\pi(hx+ky+lz)]$$

These are iterative procedures and successive use slowly builds up the structure contained in the asymmetric unit of the unit cell, from which the whole crystal structure may be generated.

#### 4.5 Refinement.

The atomic parameters are refined using a three dimensional least-square procedure. The function  $\sum w ( |F_o| - K |F_c| )^2$  is minimised during refinement where  $w$  is the weight assigned to each reflection ( $w=1/\sigma^2|F_o|$ ), and  $K$ , the overall scale factor =  $|F_o|/|F_c|$

The reliability of the results obtained from the final refinement is expressed by the R-factor.

$$R = \frac{\sum_{hkl} |K|F_o| - |F_c||}{\sum_{hkl} K|F_o|}$$

CHAPTER 5 References.

## References.

1. J.M. Lenh, *Structure and Bonding*, 1973, 16, 1.
2. J.J. Christensen, *Science*, 1971, 174, 4008.
3. J.H. Wang, *Accounts Chem. Res.*, 1970, 3, 90.
4. A. Eschenmoser, *Q. Revs.*, 1970, 24, 366.
5. P.A. Frey, *J. Am. Chem. Soc.*, 1970, 92, 4488.
6. P.A. Frey, *J. Am. Chem. Soc.*, 1971, 93, 1242.
7. F. Fan and L.R. Faulkner, *J. Am. Chem. Soc.*, 1979, 101, 4779.
8. B.M. Hoffmann, J.A. Ibers, and T.J. Marks, *J. Am. Chem. Soc.*, 1980, 102, 6702.
9. B.M. Hoffmann J.A. Ibers., *J. Am. Chem. Soc.*, 1982, 104, 83.
10. R.A. Palmer and W.E. Hatfield *Structural Inorganic Chemistry*, Benjamin, New York.
11. M. Hanack, *Material Sci.*, 1981, 7, 185.
12. P.M. May and D.R. Williams, *Nature*, 1979, 278, 581.
13. A.D. Canty and R. Kishimoto, *Nature*, 1975, 253, 123.
14. N. Dennis Chasteen, *Co-ord. Chem. Revs.*, 1977, 22, 1.

15. J.E.F. Reynolds and A.B. Prasad, *The Extra Pharmacopoeia*, 1982, The Pharmaceutical Press, London.
16. R. Frank, *Science.*, 1970, 167, 987.
17. E. Eyal, G.A. Rechnitz, *Anal. Chem.*, 1971, 43, 1090.
18. F.A. Cotton and G. Wilkinson, *Advanced Inorganic Chemistry* see how Pat sets up ref for books.
19. H. Irving and R.J.P. Williams, *Nature.*, 1948, 162, 746.
20. M.N. Hughes, *The Inorganic Chemistry of Biological Processes*, 1981.
21. R.P. Hanzlik, *Inorganic Aspects of Biological Processes* 1981.
22. R.G. Pearson, *J. Chem. Ed.*, 1968, 45, 643. (Parts III)
23. J.E. Huheey, *Introduction to Advanced Inorganic Chemistry* 1983.
24. R.J. Angelic, *Inorganic Biochemistry*, 1969.
25. D. Hartley, *Solution Equilibria*.
26. D.K. Cabbiness and D.W. Mergerum, *J. Am. Chem. Soc.*, 1969, 91, 6540.
27. F.P. Hinz and D.W. Mergerum, *Inorg. Chem.*, 1974, 13, 294.
28. M. Kodama and K. Kimura, *J. Chem. Soc., Chem. Comm.*, 1975, 891, 327.



29. R.M. Clay, M. Michlelonis, P. Paoletti, and W.V. Steele, *J. Am. Chem Soc.*, 1977, 22, L25.
30. L.S.W.L. Sokol, L.A. Ochrymowycz, and D.B. Rorabacher, *Inorg. Chem.*, 1981, 20, 3189.
31. T.E. Jones, L.L. Zimmer, L.L. Diaddario, D.B. Rorabacher, and L.A. Ochrymowycz, *J. Am. Chem. Soc.*, 1975, 97, 7163.
32. L.L. Zimmer, T.E. Jones, L.L. Diaddario, L.S. Sokol, R.B. Cruz, G.L. Yee, L.A. Ochrymowycz and D.B. Rorabacher, *J. Am. Chem. Soc.*, 1979, 101, 3511.
33. M.M. Shemyakin, Y.A. Ovchinnikov, V.T. Ivanov, A.V. Evstrator, *Nature.*, 1967, 213, 412.
34. F. Wold, *Macromolecules: Structure and Function*, Foundation of Modern Biochemistry Series, Prentice Hall, Inc., Englewood Cliff New Jersey.
35. M.R. Trater, *Structure and Bonding*, 1973, 16, 71.
36. P.M. Harison and R.J. Hoare, *Metals in Biochemistry*, Outline Studies in Biology, 1980, Chapman and Hall Ltd. London.
37. E. Ochiai, *Inorganic Biochemistry* vol 2.
38. D.H. Bush, E. Ochiai, K.M. Long and C.R.Sperati, *J. Am. Chem. Soc.*, 1969, 11, 3201.

39. D. Day, Co-ord. Chem. Revs., 1967, 2, 523.
40. M.M. Fung, J. Am. Chem. Soc., 1970, 92, 2966.
41. L.L. Ingraham and H. Johansen, J. Ther. Biol., 1969, 23, 199.
42. J. Dasher, Paper 199, International Solvent Extraction Conference 1972.
43. D.S. Flett, Rep. Prog. Appl. Chem., 1970, 55, 365.
44. M. Hughes, Chem. and Ind., 1975, 104.
45. C.A. Flemings and A.J. Nonhemius, Hydrometallurgy, 1979, 4, 159.
46. F. Vernon, N.A. Banja and M.O.B. Karrer, J. Chem. Res. (S.), 1982, 90.
47. J.S. Preston, D.M. Muir and A.J. Parker, Hydrometallurgy, 1980, 5, 227.
48. J.S. Preston, Hydrometallurgy, 1983, 10, 187.
49. M.J. Hudson, Hydrometallurgy, 1982, 9, 149.
50. H.M. Irving, Q. Revs., 1953, 3192.
51. H. Reinhardt, Chem. and Ind., 1975, 210.
52. A. Tucker, Mining and Metallurgy, 1982, 2, 126.

53. Technology, Chem and Eng., 1985, 58.
54. R. Price and J.A. Tumilty, I. Chem. E. Symposium Series No. 42., 1975, 18.1.
55. I. Dahl, Anal. Chim. Acta., 1968, 48, 9.
56. D.S. Flett, D.N. Okuhara and D.R. Spink, J. Inorg. Nucl. Chem., 1973, 35, 2471.
57. A.W. Asbrook, Co. Chem. Rev., 1975, 16, 296.
58. S.B. Syzmanowski, Rudy, Met, Neizelaz, Reagent improved solvent extraction of copper, 1980, 25, 62.
59. A.S. Van der Zeeuw, R. Kok, Cim. Spec. Proc. Int. Solvent Extr. Conf., 1977, 21, 17.
60. R.F. Dalton and R. Price, The Chemistry of Copper Extraction of O-Hydroxy aryl Oximes, 1976.
61. J. S. Preston and Z. B. Luklinska, J. Inorg. Nucl. Chem., 1980, 42, 431.
62. R.J. Whewell, M.A. Hughes and C. Hanson, J. Inorg. Nucl. Chem., 1975, 37, 2303.
63. M.A. Hughes, J.S. Prseton and R.J. Whewell, J. Inorg. Nucl. Chem., 1976, 38, 2067.
64. D.S. Flett, D.N. Okuhara and Spink, J. Inorg. Nucl. Chem., 1976, 35, 2471.

65. S.P. Carter and H. Freiser, *Anal. Chem.*, 1980, 52, 511.
66. W.J. Albery, R.A. Choudheryand, R.P. Frisk, *Faraday Discuss. Chem. Soc.*, 1984, 77, 53
67. R.F. Dalton and G. W. Seward, *The Institute of Mining and Metallurgy conference* 1984.
68. G.M. Ritcey, *Hydrometallurgy*, 1980, 5, 97.
69. J.M. Tumility, G.W. Seward and F.P. Messam, *Canadian Institute of Mining and Metallurgy*, 1979, 21, 40.
70. C.E. Pluger and R.L. Harlow, *Acta Cryst.*, 1973, B29, 2608.
71. B. Jersley, *Nature*, 1950, 741, 4226.
72. E.C. Lingafelter and M.A. Jarski, *Acta Cryst.*, 1964, 17, 1109.
73. E.C. Lingafelter, P.L. Orioli and B.W. Brow, *Acta Cryst.*, 1964, 17, 1113.
74. K. Burger, I. Ruff, and F. Ruff, *J. Inorg. Nucl. Chem.*, 1965, 27, 179
75. K. Burger and I. Egyed, *J. Inorg. Nucl. Chem.*, 1965, 27, 2361.
76. K. Burger, F. Ruff and I. Egyed, *Acta Chem. Hung. Tomus.*, 1965 45, 2.

77. K. Burger, F. Ruff, I. Ruff and I. Egyed, *Acta Chem. Acad. Hung.*, 1965, 46, 1
78. K. Burger and I. Ruff, *Talanta*, 1963, 10, 329.
79. H.S. Maslen and T.N. Walkers, *Co-ord. Chem. Revs.*, 1976, 16, 1137.
80. C.J.W. Brooks, G. Eglington and J.F. Morman, *J. Chem. Soc.*, 1961, 661.
81. A.W. Ashbrook, *Co-ord. Chem. Revs.*, 1975, 16, 285.
82. D. Hadzi and I. Premru, *Spectrochimica Acta*, 1967, 23A, 35.
83. S.N. Linnell, *Hydrogen Bonding*, 1971, New York.
84. B.N. Laskorin, and V.V. Yaksin, *The Society of Chemical Industry London*, 1974, 1775.
85. A.W. Ashbrook, *Co-ord. Chem. Revs.*, 1975, 16, 124.
86. H.E. Ungnade, L.W. Kissinger, A.N. Narath and D. Barham, *J. Org. Chem.*, 1962, 28, 134.
87. E.G. Cox, W. Wardlow and K.C. Webster, *J. Inorg. Chem.*, 1980, 53.
88. B. Jersley, *Nature*, 1964, 17, 1109.
89. E.C. Lingafelter and M.A. Jarski, *Acta Cryst.*, 1964, 17, 1109.

90. E.C. Lingafelter, P.L. Orioli and B.W. Brow, *Acta Cryst.*, 1964, 17, 1113.
91. A.A. Aruffo, T.B. Murphy, D.K. Johnson, N.J. Rose, and V. Schomaker, *Inorg. Chim. Acta.*, 1982, 67, L25.
92. J.S. Decourcy and T. Neil-Waters, *J.C.S. Chem. Comm.*, 1977, 572.
93. G.C. Levy, R.L. Litcher and G.L. Nelson, *Nuclear magnetic resonance spectroscopy*, ed 2. R.J. Abraham and P. Loftus, *Proton and Carbon-13 NMR Spectroscopy an integrated approach*, Heyden and Son Ltd.
94. G.J. Karabatsos, R.A. Taller, F.M. Vane, *J. Org. Chem.*, 1964, 85, 2326.
95. E. Lustig, *J. Org. Chem.*, 1961, 65, 491.
96. G. Slomp and W.J. Wechter, *Chemistry and Industry*, 1962, 41.
97. G.G. Kleinspehn, J.A. Jung and S.A. Studriarz, *J. Magnetic Resonance*, 1966, 32, 460.
98. H. Gunther, *NMR Spectroscopy*, John Wiley and Sons, ed 2.
99. Private Communication ICI Organics Division.
100. E. Uhlig, *Co-ord., Chem., Revs.*, 1982, 43, 299.
101. J.S. Preston and Z.B. Lunclinska, *J. Inorg. Nucl. Chem.*, 1975, 37, 2303.

102. J.D. McCullough, Jr., D.Y. Curtis and I.C. Paul, J. Am. Chem. Soc., 1972, 94, 874.
103. J.D. McCullough, Jr., I.C. Paul and D.Y. Curtis J. Am. Chem. Soc., 1972, 94, 883.
104. W.A. Mosher, R.N. Hirely and F.H. Dean, J. Org. Chem., 1970, 35, 3689.
105. T.M. Gorrie and N. F. Haley, J. C. Soc. Chem. Comm., 1972, 1081.
106. Private communications from ICI.
107. L.S. Bellamy, The infra-red spectra of complex molecules, Volumes I and II, Edition 2.
108. A. Chakraworty, Co-ord. Chem. Revs., 1974, 13, 1.
109. I.L. Finar, Organic Chemistry Vol I, 1975, Ed 6
110. I.L. Finar, Organic Chemistry Vol (II), 1975 Ed 6
111. A.H. Blatt and R.P. Barces, J. Am. Chem. Soc., 1939, 58, 1900
112. A.H. Blatt, J. Am. Chem. Soc., 1939, 61, 214.
113. E.G. Cox, K.C. Webster, J. Inorg. chem, 1980, 53.
114. A.W. Ashbrook, J. Chromatogr., 1975, 105, 141.
115. A.W. Ashbrook, Co-ord. Chem. Revs., 1975 16, 285.

116. A.W. John, R.A. Choudhery, R.A. Fisk, and R. Peters, Faraday Discuss. Chem. Soc., 1984, 77, 53.
117. J.J. Christensen, D.J. Eatough, and R.M. Izatt, Hand book of metal ligand heats and related thermodynamics quantities., 1975, Dekker, 2nd Ed.
118. F.P. Hinz and D.W. Margerum, J. Am. Chem. Soc., 1974, 96, 4993.
119. F.P. Hinz and D.W. Margerum, Inorg. Chem., 1974, 13, 2841.
120. M. Michelio and P. Paoletti, Inorg. Chim. Acta., 1980, 43, 109.
121. R.J. Motekaitis, A.E. Martell and D.A. Nelson, Inorg. Chem., 1984, 22, 275
122. D.P. Graddon, M. Micheloni and P. Paoletti, J. Chem. Soc. Dalton., 1981, 337, 1.
123. A. Ekstrom, L.F. Lindoy and R.J. Smith, Inorg. Chem., 1980, 19, 727.
124. J.J. Christensen, D.J. Eatough and R.M. Izatt, Chem. Rev., 1974, 74, 366.
125. R.M. Izatt, J.S. Bradshaw, S.A. Nielsen, J.D. Lamb, D. Sen and J.J. Christensen, Chem. Rev., 1985, 85, 271.
126. G.F. Smith and D.W. Margerum, J. Chem. Soc. Chem. Comm., 1975, 807.



127. S. Ahrland, J. Chatt and N.R. Davis, *Q. Revs.*, 1958, 12i.
128. S. Ahrland, *Struc. Bonding.*, 1968, 5, 118.
129. S. Ahrland, *Struc. Bonding.*, 1973, 15, 167.
130. R.F. Hudson, *Struc. Bonding.*, 1966, 1, 221.
131. R.G. Pearson and J. Songstad, *J. Am. Chem. Soc.*, 1967, 89, 87.
132. R.G. Pearson and J. Songstead, *Chem. Revs.*, 1975, 75, 1.
133. R.W. Jones and R.H. Staley, *J. Am. Chem. Soc.*, 1982, 104, 2296.
134. R.W. Jones and R.H. Staley, *J. Phys. Chem.*, 1982, 86, 1387.
135. J.E. Huheey, *Inorg. Chem. Principle of structure and reactivity*, 1983, Ed.3.
136. J.H. Lehn, *Struc. Bonding.*, 1973, 16, 1.
137. N.K. Dalley in *Synthetic multidentate macrocyclic compounds.*, 1978, Academic press, New York.
138. J.D. Lamb, R.M. Izatt, J.J. Christensen and D.J. Eatough, *Co-ord. Chem. of macrocyclic compounds.*, 1979, 147.
139. G. Shoham, W.N. Lipscomb and U. Olsher, *J. Chem. Soc. Chem. Comm.*, 1983, 208.

140. A. Ekstrom, L.F. Lindoy and R.J. Smith, *Inorg. Chem.*, 1980, 19, 724.
141. L.P. Battaglia, A. Bonamartini Corradi and A. Mangia, *Inorg. Chim. Acta.*, 1980, 39, 211.
142. A. Ekstrom, L.F. Lindoy, H.C. Lip, R.J. Smith, H.J. Goodwin, M. McPartlin, and P.A. Tasker, *J. Chem. Soc. Dalton. Trans.*, 1979, 1027.
143. K. Henrick, L.F. Lindoy, M. McPartlin, P.A. Tasker and M. Wood, *J. Am. Chem. Soc.*, 1984, 106, 1641.
144. P.A. Tasker, J. Trotter, L.F. Lindoy, *J. Chem. Research.*, 1981, 3834.
145. H.J. Goodwin, K. Henrick, L.F. Lindoy, M. McPartlin and P.A. Tasker, *Inorg. Chem.*, 1982, 21, 3261.
146. L.A. Drummond, K. Henrick, M.J.L. Kanagasundaram, L.F. Lindoy, M. McPartlin and P.A. Tasker, *Inorg. Chem.*, 1982, 21, 3923.
147. K. Henrick, P.A. Tasker and L.F. Lindoy, *Prog. Inorg. Chem.*, 1985, 33, 1.
148. K.R. Adam, G. Anderegg, L.F. Lindoy, H.C. Lip, M. McPartlin, J.H. Rea, R.J. Smith and P.A. Tasker, *Inorg. Chem.*, 1980, 19, 2956.
149. K.R. Adam, A.J. Leong, L.F. Lindoy and A. Anderegg, *J. Chem. Soc. Dalton. Trans.*, 1988, 1733.

150. L.F. Lindoy, *Prog. Macrocyclic Chem.*, 1987, 3, 1.
151. P.B. Donaldson, P. Haria, P.A. Tasker, *J.Chem. Soc. Daltons Trans.*, 1976, 2382. D.K. Uppal, PhD Thesis., 1986, P.N.L.
152. C.W. Ansell, M.F.H.Y. Chung, M. McPartlin and P.A. Tasker, *J. Chem. Soc. Daltons Trans.*, 1982, 2113.
153. L.A. Drummond, K.P. Dancey, A.J. Jones, L.F. Lindoy, M. McPartlin and P.A. Tasker, Paper presented at 3rd European Symposium on Macrocyclic chemistry, Sterlin, 1984.
154. K.R. Adam, C.W. Ansell, L.A. Drummond, K.P. Dancey, A.J. Leong, L.F. Lindoy and P.A. Tasker, *J. Chem. Soc. Chem Comm.*, 1986, 1011.
155. L.F. Lindoy, *Current Topics in Macrocyclic Chemistry*, 1987, 78.
156. K.R. Adam, K.P. Dancey, B.A. Harrison, A.J. Leong, L.F. Lindoy M. McPartlin and P.A. Tasker, *J. Chem. Soc. Chem. Comm.*, 1983, 1351.
157. K.R. Adams, L.G. Brigden, K. Henrick, L.F. Lindoy, M. McPartlin, B. Mimmagh and P.A. Tasker, *J. Chem. Soc. Chem. Comm.*, 1985, 710.
158. K.R. Adam, L.F. Lindoy, H.C. Lip, J.H. Rea, B.W. Skelton and A.H. White, *J. Chem. Soc. Daltons Trans.*, 1981, 75.

159. P.A. Harding, K.Henrick, L.F. Lindoy, M. McPartlin and P.A. Tasker, J. Chem. Soc. Chem. Comm., 1983, 1300.
160. D.H. Wertz and N.L. Allinger, Tetrahedron, 1977,30, 1579.
161. N.L. Allinger, Adv. Phys. Org. Chem., 1976, 13, 1.
162. J.H. Barnes, C. Bates and F.R. Hartley, Hydrometallurgy., 1983, 10, 205.
163. Perspectives, Chemistry in Britian, July 1983.
164. J. Monhemius, Chemistry and Industry, June 1981, 412 look up rest of info.
165. M. Green, J. Smith and P.A. Tasker, Inorg. Chemica Acta., 1971, 17.
166. G.A. Melson, Co-ordination chemistry of macrocyclic compounds., 1972, Pleum Press.
167. R. Peters PhD thesis 1981. P. Judd PhD thesis 1980.
168. J.E. Richmans, T.S. Atkins, J. Am. Chem. Soc., 1974, 96, 2268.
169. F.R. Muller and H. Handel, Tetrahedron Lett., 1982, 23, 2769.
170. S. Pasynkiewicz, S. Maciaszek, J. Organomet. Chem., 1968, 15, 301.

171. R.E. Dessy and R.M. Salinger, *J. Am. Chem. Soc.*, 1961, 3530.
172. P.G. Owston, R. Peters, E. Ramsamy, P.A. Tasker, and J. Trotter, *J. Chem. Soc. Chem. Comm.*, 1980, 1218. L.A. Drummond, B.Sc Thesis, 1981.
173. A.J. Greenwood, K. Henrick, P.G. Owston and P.A. Tasker, *J. Chem. Soc. Chem. Comm.*, 1980, 88.
174. N.W. Alcock, P. Moore and K.F. Mok, *J. Chem. Soc., Perkins(II)*, 1980, 1186.
175. K. Henrick, P.M. Judd, P.G. Owston, R. Peters, P.A. Tasker and R.W. Turner, *J. Chem. Soc. Chem. Comm.*, 1983, 1253.
176. R.M. Smith and A.E. Martell, 'Critical Stability Constants Amines' 1975, 2, Pleum, New York.
177. C.W.G. Ansell, M. McPartlin, P.A. Tasker and A. Thambythura, *Polyhedron*, 1983, 2, 83.
178. K.R. Adams, A.J. Leong, L.F. Lindoy, C.W.G. Ansell K.P. Dancey, L.A. Drummond, K.M. Henrick, M. McPartlin D.K. Uppal and P.A.Tasker, To be published.
179. E.C. Constable, *Co-ord. Chem. Review*, 1982, 45, 329.
180. D.G. Tuck, *The Stereochemistry of Co-ordination Compounds of Cadmium(II)*, 1978.

181. T. Ito, M. Kato, H. Ito, Bull. Chem. Soc. Jpn., 1984, 57, 2634.
182. L.F. Lindor and D.H. Busch, Inorg. Chem., 1974, 10, 2494.
183. N.W. Alcock, N.Herron and P. Moore, J. Chem. Soc. Dalton Trans., 1978, 1282.
184. C.W.G. Ansell, K.P. Dancey L.F. Lindoy, M. McPartlin and P.A. Tasker, J. Chem. Soc. Dalton Trans., 1983, 1789.
185. L.F. Lindoy, H.C. Lip, J. H. Rea, R.J. Smith, K. Henrick, M. McPartlin and P.A. Tasker, Inorg. Chem, 1980, 19, 3360.
186. L. Pauling, "The Nature Of The Chemical Bond" 3rd ed., Cornell University Press Ithaca New York, 1960.
187. C.C. Addison, N. Logan, S.C. Wallwork and C.D. Garner, Q. Revs, 1971, 25, 289.
188. A. Mangia and C Tiripicchio, Cryst. Struct. Comm., 1979, 8, 699.
189. J. Lindgren and I Olousson, Act. Cryst., 1968, b24, 554.
190. L.G. Armstrong, P.G. Grimsely, L.F. Lindoy, H.C. Lip, V.A. Norris and R.J. Smith, Inorg. Chem., 1978, 9, 2350.
191. P.G. Grimsley, L.F. Lindoy, H.C. Lip, R.J. Smith and J.T. Baker, Aust. J. Chem., 1977, 30, 2095.

192. L.G. Armstrong, L.F. Lindoy, M. McPartlin, G. M. Mockler, and P.A. Tasker, *Inorg. Chem.*, 1977, 1, 1665
193. L.F. Lindoy, *Q. Revs.*, 1971, 3, 379.
194. H. Veering and B.R. Willeford, *HPLC in Organomet. and Co-ord. Chem.*, 1979, 3, 282.
195. P.W.R. Cornfield, R.J. Doedens and J.A. Ibers, *Inorg. Chem.* 1967, 6, 197.
196. P.B. Hitchcock and R. Mason, *Chemistry in Britain*, 1971 17, 511.
197. J. Karle, *International tables of X-ray crystallography*, 1974, 4, Kynoc Press Birmingham.
198. J. Karle and H. Hauptman, *Acta Cryst.*, 1959, 12, 93.
199. D. Sayre, *Acta Cryst.*, 1952, 5, 60.
200. J. Karle and I.L. Karlye, *Acta Cryst.*, 1966, 21, 841.
201. W. Cochran, M.M. Woolfson, *Acta Cryst.*, 1955, 8, 1.
202. J. Karle and H. Hauptman, *Acta Cryst.*, 1961, 14, 217.
203. I.L. Karle, H. Hauptman, J. Karlye and A.B. Wing, *Acta Cryst.*, 1958, 11, 257.
204. G.M. Sheldrick, *SHELX 1976*, University of Cambridge England. Unpublished programs for solving and refining crystal structures, (EELS and TANG are routines within the program).

205. J. Karle and I.L. Karle, *Acta Cryst.*, 1966, 21, 849.
206. J. Karle and H Hauptman, 1956, 9, 635.
207. G.N. Watson, *Theory of Bessel function*, 1945, Cambridge University Press, Cambridge.
208. G. Germain, P. Main, M.M. Woolfson, *Acta Cryst.*, 1971, A27, 368.
209. P.J. Roberts, R.C. Petterson, G.M. Sheldrick, N.W. Isaacs and O Kennard, *J. Chem. Soc. Perkins, Trans. (II)*, 1973, 1978.





213

APPENDIX

APPENDIXSupplementary Crystallographic data.

This section includes all the atomic co-ordination, anisotropic thermal parameters bond lengths, angles, and contact distances for all the structures.

CONTENTS.

A1	Table for $[(L1)_2Cu]$ .
A2	Tables for $[(L5)_2Cu]$ .
A3	Tables for $[(L6)_2Cu]$ .
A4	Tables for 'L7H'.
A5	Tables for $[Zn(L15)(NO_3)(H_2O)](NO_3)$ .
A6	Tables for $[Cd(L15)(NO_3)](NO_3)$ .
A7	Tables for $[Cd(L15b)(NO_3)](NO_3)$ .
A8	Tables for L15b.

A1 Table for [(L1)<sub>2</sub>Cu].

X-ray structure determination of  $[(L1)_2Cu]_2$

Crystal data:  $C_{16}H_{16}N_2O_4Cu$  Mwt = 363.7 orthorhombic

Bis-[2-hydroxy-5-methylbenzaldehydeoximate]copper(II).

space group Pbc<sub>2</sub>a, a = 32.047(2) Å, b = 7.517(2) Å,

c = 6.488(1) Å. Beta = 90.0°, U = 1562.94 Å<sup>3</sup>,

D<sub>c</sub> = 1.55 gm<sup>-3</sup>, F<sub>000</sub> = 748.

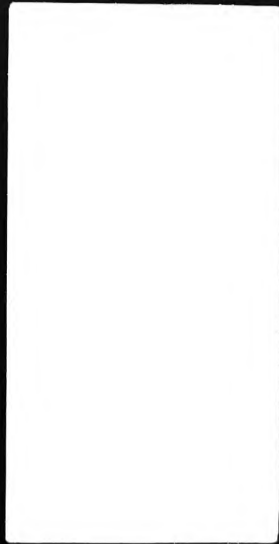
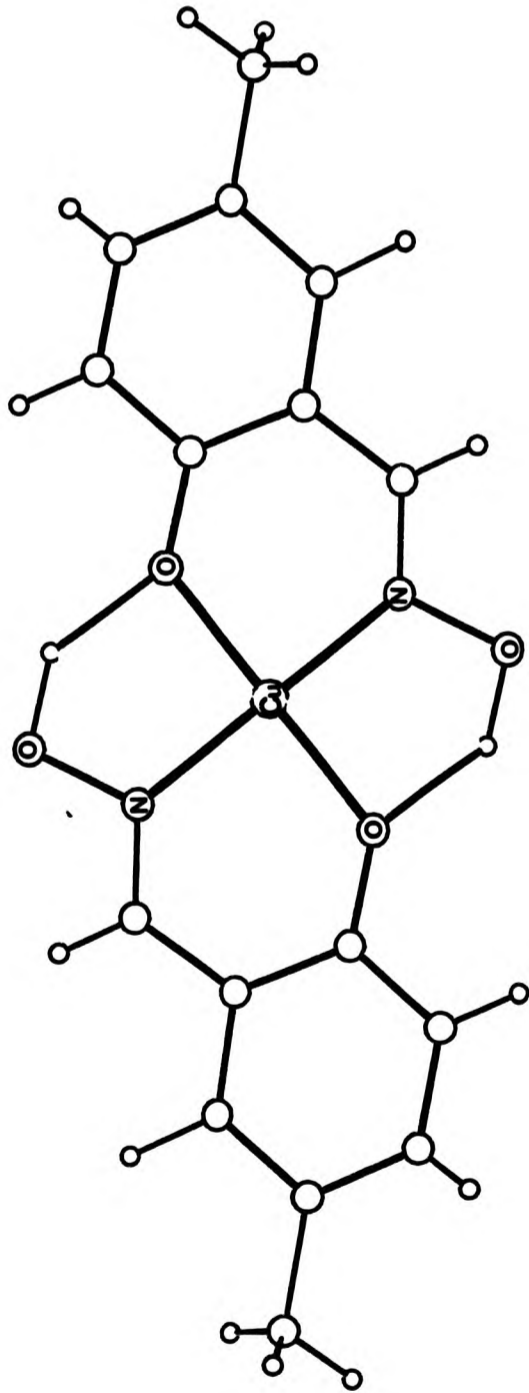


TABLE 1 Fractional atomic coordinates and thermal parameters ( $\text{\AA}^2$ )

Atom	x	y	z	$U_{\text{iso}}$ or $U_{\text{eq}}$
Cu	0.00000	0.00000	0.00000	0.0292(3)
O(1a)	-0.0551(1)	-0.0433(4)	0.1023(5)	0.036(2)
O(2a)	0.0078(1)	0.1742(4)	-0.3886(5)	0.034(2)
N(1a)	-0.0217(1)	0.1014(5)	-0.2523(6)	0.029(2)
C(2a)	-0.0911(1)	-0.0256(5)	0.0030(9)	0.032(2)
C(3a)	-0.1281(2)	-0.0790(7)	0.1016(9)	0.043(3)
C(4a)	-0.1664(2)	-0.0560(7)	0.0061(11)	0.053(3)
C(5a)	-0.1704(2)	0.0192(8)	-0.1897(9)	0.049(3)
C(6a)	-0.1340(2)	0.0707(7)	-0.2871(8)	0.043(3)
C(7a)	-0.0946(1)	0.0483(6)	-0.1983(8)	0.032(3)
C(8a)	-0.0591(1)	0.1086(6)	-0.3164(8)	0.035(3)
C(9a)	-0.2128(2)	0.0466(9)	-0.2910(11)	0.078(5)

TABLE 2 Fractional atomic coordinates for the hydrogen atoms

Atom	x	y	z	$U_{\text{iso}}$ or $U_{\text{eq}}$
H(02a)	0.035(2)	0.146(7)	-0.326(8)	0.08(2)
H(3a)	-0.124(1)	-0.149(7)	0.234(9)	0.07(2)
H(4a)	-0.187(2)	-0.088(7)	0.062(9)	0.10(2)
H(6a)	-0.136(1)	0.126(5)	-0.429(6)	0.02(1)
H(8a)	-0.064(1)	0.153(5)	-0.442(6)	0.04(1)
H(9a1)	-0.231(2)	-0.054(8)	-0.240(10)	0.15(2)
H(9a2)	-0.208(2)	0.012(8)	-0.434(10)	0.14(2)
H(9a3)	-0.226(2)	0.146(10)	-0.280(11)	0.21(3)

TABLE 3 Anisotropic thermal parameters (Å<sup>2</sup>)

Atom	U <sub>11</sub>	U <sub>22</sub>	U <sub>33</sub>	U <sub>23</sub>	U <sub>13</sub>	U <sub>12</sub>
Cu	0.0294(3)	0.0327(4)	0.0256(3)	0.0057(5)	0.0033(5)	0.0037(4)
O(1a)	0.031(2)	0.045(2)	0.032(2)	0.013(2)	0.003(2)	0.004(1)
O(2a)	0.034(2)	0.039(2)	0.029(2)	0.010(2)	0.004(1)	-0.002(1)
N(1a)	0.035(2)	0.029(2)	0.023(2)	0.002(2)	0.004(2)	0.003(2)
C(2a)	0.035(2)	0.025(3)	0.037(2)	-0.002(3)	0.016(3)	0.003(2)
C(3a)	0.037(3)	0.046(3)	0.045(3)	0.009(3)	0.008(3)	0.001(3)
C(4a)	0.035(2)	0.061(3)	0.064(4)	0.004(5)	0.002(3)	-0.006(2)
C(5a)	0.035(3)	0.051(4)	0.061(4)	0.001(3)	-0.005(3)	-0.001(3)
C(6a)	0.046(3)	0.040(3)	0.043(3)	-0.001(3)	-0.011(3)	0.002(2)
C(7a)	0.031(2)	0.029(3)	0.037(3)	-0.001(2)	0.002(2)	-0.001(2)
C(8a)	0.044(3)	0.034(3)	0.027(2)	-0.002(2)	-0.004(2)	0.000(2)
C(9a)	0.037(3)	0.110(6)	0.085(5)	0.014(5)	-0.010(3)	-0.004(3)

TABLE 4 Bond lengths (Å)

Cu -O(1a)	1.914(3)	Cu -N(1a)	1.933(4)
O(1a) -C(2a)	1.327(6)	O(2a) -N(1a)	1.405(5)
N(1a) -C(8a)	1.270(6)	C(2a) -C(3a)	1.406(7)
C(2a) -C(7a)	1.422(8)	C(3a) -C(4a)	1.385(8)
C(4a) -C(5a)	1.395(9)	C(5a) -C(6a)	1.381(8)
C(5a) -C(9a)	1.522(8)	C(6a) -C(7a)	1.399(7)
C(7a) -C(8a)	1.443(7)		
O(2a) -H(02a)	.99(5)	C(3a) -H(3a)	1.01(5)
C(4a) -H(4a)	.78(6)	C(6a) -H(6a)	1.01(4)
C(8a) -H(8a)	.89(4)	C(9a) -H(9a1)	1.01(6)
C(9a) -H(9a2)	.98(7)	C(9a) -H(9a3)	.86(7)

TABLE 5 Bond angles (°)

N(1a) -Cu -O(1a)	91.6(1)	C(2a) -O(1a) -Cu	128.1(3)
O(2a) -N(1a) -Cu	116.3(2)	C(8a) -N(1a) -Cu	129.2(3)
C(8a) -N(1a) -O(2a)	114.4(4)	C(3a) -C(2a) -O(1a)	119.0(5)
C(7a) -C(2a) -O(1a)	123.5(4)	C(7a) -C(2a) -C(3a)	117.5(4)
C(4a) -C(3a) -C(2a)	120.6(5)	C(5a) -C(4a) -C(3a)	122.5(5)
C(6a) -C(5a) -C(4a)	116.9(5)	C(9a) -C(5a) -C(4a)	121.9(5)
C(9a) -C(5a) -C(6a)	121.2(5)	C(7a) -C(6a) -C(5a)	122.7(5)
C(6a) -C(7a) -C(2a)	119.7(4)	C(8a) -C(7a) -C(2a)	123.2(4)
C(8a) -C(7a) -C(6a)	117.1(5)	C(7a) -C(8a) -N(1a)	123.8(5)

Table 5 continued

H(02a)-O(2a) -N(1a)	105(3)	H(3a) -C(3a) -C(2a)	115(3)
H(3a) -C(3a) -C(4a)	124(3)	H(4a) -C(4a) -C(3a)	119(4)
H(4a) -C(4a) -C(5a)	118(4)	H(6a) -C(6a) -C(5a)	118(2)
H(6a) -C(6a) -C(7a)	119(2)	H(8a) -C(8a) -N(1a)	119(3)
H(8a) -C(8a) -C(7a)	118(3)	H(9a1)-C(9a) -C(5a)	106(4)
H(9a2)-C(9a) -C(5a)	103(4)	H(9a2)-C(9a) -H(9a1)	102(5)
H(9a3)-C(9a) -C(5a)	121(5)	H(9a3)-C(9a) -H(9a1)	110(6)
H(9a3)-C(9a) -H(9a2)	113(6)		



TABLE 6 Intermolecular distances (Å)

Cu ...Cu	4.96	3	0.0	-1.0	-1.0
O(2a) ...Cu	2.56	3	0.0	0.0	-1.0
N(1a) ...Cu	3.47	3	0.0	0.0	-1.0
C(8a) ...Cu	3.69	3	0.0	0.0	-1.0
H(O2a)...Cu	3.10	3	0.0	0.0	-1.0
H(8a) ...Cu	3.34	3	0.0	0.0	-1.0
O(2a) ...O(1a)	2.59	-1	0.0	0.0	0.0
N(1a) ...O(1a)	2.68	-1	0.0	0.0	0.0
H(O2a)...O(1a)	1.76	-1	0.0	0.0	0.0
O(2a) ...O(1a)	2.95	3	0.0	0.0	-1.0
C(8a) ...O(1a)	3.31	-3	0.0	1.0	0.0
H(8a) ...O(1a)	2.96	-3	0.0	1.0	0.0
O(2a) ...O(2a)	3.03	-1	0.0	0.0	-1.0
N(1a) ...O(2a)	3.15	-1	0.0	0.0	-1.0
C(8a) ...O(2a)	3.30	-1	0.0	0.0	-1.0
N(1a) ...O(2a)	3.37	3	0.0	-1.0	-1.0
N(1a) ...O(2a)	3.05	-3	0.0	1.0	1.0
H(O2a)...C(2a)	2.90	-1	0.0	0.0	0.0
C(8a) ...C(2a)	3.50	-3	0.0	1.0	0.0
H(8a) ...C(2a)	2.95	-3	0.0	1.0	0.0
H(8a) ...C(7a)	2.96	-3	0.0	1.0	0.0
H(8a) ...C(8a)	3.02	-3	0.0	1.0	0.0

TABLE 7 Intramolecular distances (Å)

O(2a) ...Cu	2.85	C(2a) ...Cu	2.93
C(3a) ...Cu	4.20	C(7a) ...Cu	3.31
C(8a) ...Cu	2.91	H(O2a)...Cu	2.63
H(8a) ...Cu	3.71	N(1a) ...O(1a)	2.76
C(3a) ...O(1a)	2.35	C(7a) ...O(1a)	2.42
C(8a) ...O(1a)	2.95	H(3a) ...O(1a)	2.50
C(8a) ...O(2a)	2.25	H(8a) ...O(2a)	2.33
C(2a) ...N(1a)	2.93	C(7a) ...N(1a)	2.40
H(O2a)...N(1a)	1.91	H(8a) ...N(1a)	1.87
C(4a) ...C(2a)	2.42	C(5a) ...C(2a)	2.85
C(6a) ...C(2a)	2.44	C(8a) ...C(2a)	2.52
H(3a) ...C(2a)	2.05	C(5a) ...C(3a)	2.44
C(6a) ...C(3a)	2.76	C(7a) ...C(3a)	2.42
H(4a) ...C(3a)	1.89	C(6a) ...C(4a)	2.37
C(7a) ...C(4a)	2.77	C(9a) ...C(4a)	2.55
H(3a) ...C(4a)	2.12	H(9a1)...C(4a)	2.61
H(9a3)...C(4a)	3.07	C(7a) ...C(5a)	2.44
H(4a) ...C(5a)	1.89	H(6a) ...C(5a)	2.06
H(9a1)...C(5a)	2.04	H(9a2)...C(5a)	1.98
H(9a3)...C(5a)	2.10	C(8a) ...C(6a)	2.43
C(9a) ...C(6a)	2.53	H(4a) ...C(6a)	3.06
H(8a) ...C(6a)	2.54	H(9a2)...C(6a)	2.59
H(9a3)...C(6a)	3.00	H(6a) ...C(7a)	2.09
H(8a) ...C(7a)	2.02	H(O2a)...C(8a)	3.03
H(6a) ...C(8a)	2.59	H(4a) ...C(9a)	2.64
H(6a) ...C(9a)	2.67		

A2      Tables for [(L5)<sub>2</sub>Cu].

X-ray structure determination of  $[(L5)_2Cu]$ .

Bis-[2-hydroxy-5-methylbenzophenoneoximate]copper(II).

Crystal data:  $C_{30}H_{26}N_2O_4Cl_6Cu$  Mwt = 754.8 monoclinic,  
space group  $P2_1/c$ ,  $a = 6.317(5) \text{ \AA}$ ,  $b = 11.849(3) \text{ \AA}$ ,  
 $c = 21.558(2) \text{ \AA}$ . Beta =  $93.8(1)^\circ$ ,  $U = 1610.07 \text{ \AA}^3$ ,  
 $D_c = 1.56 \text{ g cm}^{-3}$ ,  $F_{000} = 766$ .

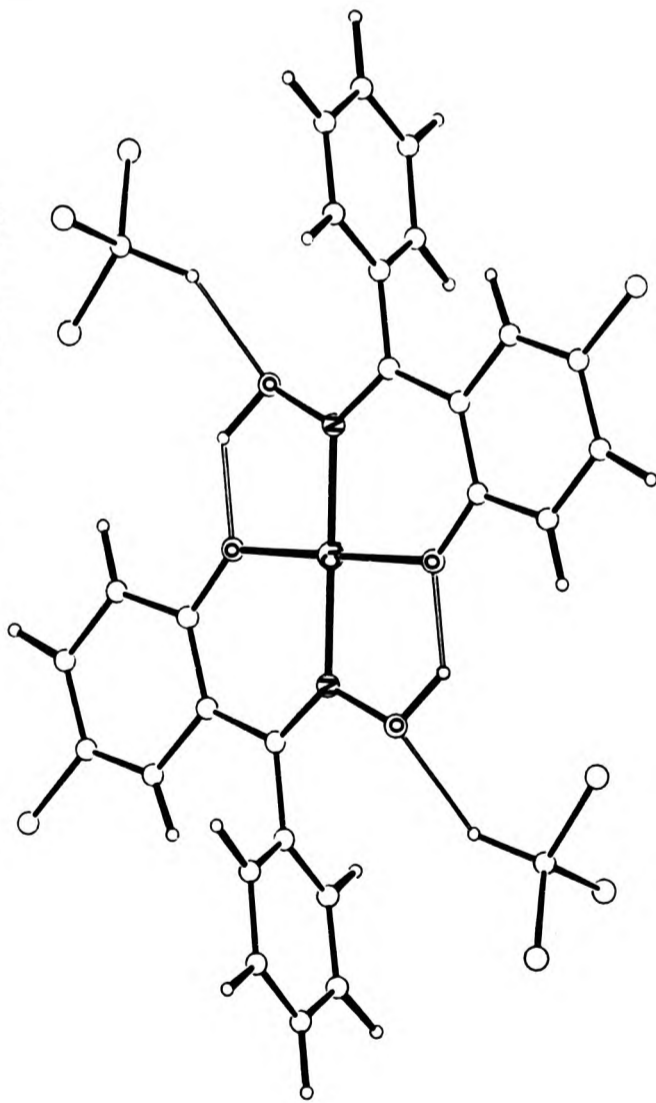


TABLE 1 Fractional atomic coordinates and thermal parameters ( $\text{\AA}^2$ )

Atom	x	y	z	$U_{\text{iso}}$ or $U_{\text{eq}}$
Cu	0.00000	0.00000	0.00000	0.0387(10)
O(1a)	0.1948(8)	0.1188(5)	-0.0023(3)	0.044(4)
N(1a)	0.1581(9)	-0.0693(6)	0.0699(3)	0.039(4)
O(2b)	0.0660(8)	-0.1659(5)	0.0937(3)	0.054(4)
C(fc)	0.8457(15)	0.0817(9)	0.3761(6)	0.070(8)
C1(1)	0.6583(5)	-0.0012(4)	0.4131(2)	0.114(3)
C1(2)	0.8557(6)	0.0399(4)	0.3002(2)	0.119(3)
C1(3)	1.0891(5)	0.0699(3)	0.4172(2)	0.110(3)
C(8a)	0.3329(13)	-0.0379(7)	0.1007(4)	0.036(2)
C(7a)	0.4482(12)	0.0615(7)	0.0809(4)	0.035(2)
C(2a)	0.3789(13)	0.1338(7)	0.0324(4)	0.037(2)
C(3a)	0.4968(13)	0.2297(7)	0.0195(4)	0.043(2)
C(4a)	0.6955(13)	0.2518(8)	0.0542(4)	0.047(2)
C(5a)	0.7688(13)	0.1799(7)	0.0999(4)	0.040(2)
C(6a)	0.6507(12)	0.0874(7)	0.1139(4)	0.038(2)
C(9a)	0.9776(14)	0.2064(7)	0.1383(4)	0.048(2)
C(7b)	0.4078(13)	-0.1028(7)	0.1572(4)	0.038(2)
C(6b)	0.3210(14)	-0.0801(8)	0.2115(4)	0.055(3)
C(5b)	0.3843(16)	-0.1377(9)	0.2659(5)	0.067(3)
C(4b)	0.5372(15)	-0.2214(9)	0.2634(5)	0.064(3)
C(3b)	0.6211(16)	-0.2439(10)	0.2091(5)	0.074(3)
C(2b)	0.5618(15)	-0.1850(8)	0.1544(5)	0.059(3)
H(fc)	0.80710	0.18310	0.37870	0.0800

TABLE 2 Fractional atomic coordinates for the hydrogen atoms

Atom	x	y	z
H(6b)	0.1999	-0.0159	0.2124
H(5b)	0.3158	-0.1180	0.3092
H(4b)	0.5898	-0.2677	0.3047
H(3b)	0.7349	-0.3116	0.2073
H(2b)	0.6371	-0.2015	0.1118
H(3a)	0.4442	0.2835	-0.0159
H(4a)	0.7638	0.3286	0.0379
H(6a)	0.6716	0.0308	0.1484
H(02b)	-0.0301	-0.1917	0.0521

TABLE 3 Anisotropic thermal parameters ( $\text{\AA}^2$ )

Atom	$U_{11}$	$U_{22}$	$U_{33}$	$U_{23}$	$U_{13}$	$U_{12}$
Cu	0.025 (1)	0.044 (1)	0.047 (1)	0.005 (1)	-0.009 (1)	-0.005 (1)
O (1a)	0.029 (3)	0.049 (4)	0.054 (4)	0.007 (3)	-0.018 (3)	-0.012 (3)
N (1a)	0.024 (4)	0.037 (4)	0.054 (5)	0.003 (4)	-0.005 (4)	-0.008 (4)
O (2b)	0.038 (4)	0.054 (4)	0.069 (5)	0.019 (4)	-0.016 (3)	-0.017 (3)
C (c)	0.048 (6)	0.059 (7)	0.101 (9)	-0.010 (7)	-0.007 (6)	0.002 (6)
C1 (1)	0.077 (2)	0.147 (3)	0.118 (3)	-0.008 (3)	0.021 (2)	-0.033 (2)
C1 (2)	0.103 (3)	0.148 (4)	0.106 (3)	-0.002 (2)	0.017 (2)	-0.026 (2)
C1 (3)	0.063 (2)	0.090 (2)	0.176 (4)	0.015 (2)	-0.038 (2)	-0.004 (2)

TABLE 4 Bond lengths (Å)

Cu -O(1a)	1.873(5)	Cu -N(1a)	1.935(7)
O(1a) -C(2a)	1.352(9)	N(1a) -O(2b)	1.397(9)
N(1a) -C(8a)	1.304(10)	C(8a) -C(7a)	1.464(12)
C(8a) -C(7b)	1.492(12)	C(7a) -C(2a)	1.398(11)
C(7a) -C(6a)	1.455(11)	C(2a) -C(3a)	1.397(12)
C(3a) -C(4a)	1.442(11)	C(4a) -C(5a)	1.360(12)
C(5a) -C(6a)	1.371(12)	C(5a) -C(9a)	1.542(12)
C(7b) -C(6b)	1.351(13)	C(7b) -C(2b)	1.381(13)
C(6b) -C(5b)	1.393(14)	C(5b) -C(4b)	1.388(14)
C(4b) -C(3b)	1.344(15)	C(3b) -C(2b)	1.399(15)
C(fc) -C1(1)	1.768(11)	C(fc) -C1(2)	1.716(13)
C(fc) -C1(3)	1.728(10)		



TABLE 5 Bond angles (°)

N(1a) -Cu -O(1a)	91.9(3)	C(2a) -O(1a) -Cu	128.8(5)
O(2b) -N(1a) -Cu	115.3(4)	C(8a) -N(1a) -Cu	130.6(6)
C(8a) -N(1a) -O(2b)	114.0(6)	C(7a) -C(8a) -N(1a)	120.2(7)
C(7b) -C(8a) -N(1a)	118.7(7)	C(7b) -C(8a) -C(7a)	121.1(7)
C(2a) -C(7a) -C(8a)	125.0(7)	C(6a) -C(7a) -C(8a)	117.7(7)
C(6a) -C(7a) -C(2a)	117.3(7)	C(7a) -C(2a) -O(1a)	123.3(7)
C(3a) -C(2a) -O(1a)	116.6(7)	C(3a) -C(2a) -C(7a)	120.1(7)
C(4a) -C(3a) -C(2a)	120.1(7)	C(5a) -C(4a) -C(3a)	120.3(8)
C(6a) -C(5a) -C(4a)	119.8(7)	C(9a) -C(5a) -C(4a)	119.9(7)
C(9a) -C(5a) -C(6a)	120.2(7)	C(5a) -C(6a) -C(7a)	122.3(7)
C(6b) -C(7b) -C(8a)	118.6(8)	C(2b) -C(7b) -C(8a)	121.0(8)
C(2b) -C(7b) -C(6b)	120.4(8)	C(5b) -C(6b) -C(7b)	121.4(9)
C(4b) -C(5b) -C(6b)	119(1)	C(3b) -C(4b) -C(5b)	119(1)
C(2b) -C(3b) -C(4b)	122(1)	C(3b) -C(2b) -C(7b)	117.7(9)
Cl(2) -C(fc) -Cl(1)	109.7(6)	Cl(3) -C(fc) -Cl(1)	108.9(6)
Cl(3) -C(fc) -Cl(2)	112.2(6)		

TABLE 6 Intermolecular distances (Å)

C(4a) ...Cu	3.78	1	1.0	0.0	0.0
C(5a) ...Cu	3.43	1	1.0	0.0	0.0
C(6a) ...Cu	3.56	1	1.0	0.0	0.0
C(9a) ...Cu	3.87	1	1.0	0.0	0.0
N(1a) ...O(1a)	2.65	-1	0.0	0.0	0.0
O(2b) ...O(1a)	2.54	-1	0.0	0.0	0.0
H(2b) ...O(1a)	2.83	-1	1.0	0.0	0.0
H(02b)...O(1a)	1.68	-1	0.0	0.0	0.0
H(2b) ...O(2b)	2.79	1	1.0	0.0	0.0
C(fc) ...O(2b)	3.10	2	1.0	0.0	0.0
Cl(3) ...O(2b)	3.28	2	1.0	0.0	0.0
H(fc) ...O(2b)	2.03	2	1.0	0.0	0.0
Ho(2b)...C(2a)	2.85	-1	0.0	0.0	0.0
H(2b) ...C(3a)	2.92	-1	1.0	0.0	0.0
Cl(1) ...C(3a)	3.66	2	1.0	-1.0	0.0
Cl(1) ...C(4a)	3.78	2	1.0	-1.0	0.0
H(4b) ...C(6a)	2.95	2	1.0	-1.0	0.0
H(5b) ...C(9a)	3.05	2	1.0	-1.0	0.0
H(4b) ...C(9a)	2.94	2	2.0	-1.0	0.0
H(fc) ...C(7b)	2.96	2	1.0	0.0	0.0
Cl(2) ...H(6b)	3.05	1	1.0	0.0	0.0
Cl(2) ...H(3b)	3.14	2	2.0	0.0	0.0
Cl(3) ...H(3b)	3.29	2	2.0	0.0	0.0
H(fc) ...C(2b)	2.86	2	1.0	0.0	0.0
Cl(3) ...H(2b)	3.30	2	2.0	0.0	0.0

table 6 continued

C1(3) ...C1(1)	3.98	-1	2.0	0.0	1.0
H(3a) ...C1(1)	3.33	-2	0.0	1.0	0.0
H(4a) ...C1(1)	3.41	-2	0.0	1.0	0.0
C1(3) ...C1(3)	4.16	-1	2.0	0.0	1.0
H(4a) ...C1(3)	3.14	2	2.0	0.0	0.0
H(02b)...C1(3)	2.93	2	1.0	-1.0	0.0
H(3a) ...C1(3)	3.12	-2	-1.0	1.0	0.0

TABLE 7 Intramolecular distances (Å)

O(2b) ...Cu	2.83	C(8a) ...Cu	2.96
C(7a) ...Cu	3.31	C(2a) ...Cu	2.92
C(3a) ...Cu	4.15	Ho(2b)...Cu	2.55
N(1a) ...O(1a)	2.74	C(8a) ...O(1a)	2.98
C(7a) ...O(1a)	2.42	C(3a) ...O(1a)	2.34
H(3a) ...O(1a)	2.54	C(7a) ...N(1a)	2.40
C(2a) ...N(1a)	2.92	C(7b) ...N(1a)	2.41
C(6b) ...N(1a)	3.16	C(2b) ...N(1a)	3.33
H(O2b)...N(1a)	1.90	C(8a) ...O(2b)	2.27
C(7b) ...O(2b)	2.59	C(6b) ...O(2b)	3.09
C(2b) ...O(2b)	3.32	C(2a) ...C(8a)	2.54
C(6a) ...C(8a)	2.50	C(6b) ...C(8a)	2.45
H(6b) ...C(8a)	2.62	C(2b) ...C(8a)	2.50
H(2b) ...C(8a)	2.73	H(6a) ...C(8a)	2.45
H(O2b)...C(8a)	3.06	C(3a) ...C(7a)	2.42
C(4a) ...C(7a)	2.82	C(5a) ...C(7a)	2.47
C(7b) ...C(7a)	2.57	C(6b) ...C(7a)	3.42
C(2b) ...C(7a)	3.38	H(6a) ...C(7a)	1.99
C(4a) ...C(2a)	2.46	C(5a) ...C(2a)	2.83
C(6a) ...C(2a)	2.44	H(3a) ...C(2a)	2.11
C(5a) ...C(3a)	2.43	C(6a) ...C(3a)	2.77
H(4a) ...C(3a)	2.07	C(6a) ...C(4a)	2.36
C(9a) ...C(4a)	2.51	H(3a) ...C(4a)	2.15
H(4a) ...C(5a)	2.21	H(6a) ...C(5a)	2.16
C(9a) ...C(6a)	2.53	C(7b) ...C(6a)	2.91

table 7 continued

C(2b) ...C(6a)	3.40	H(4a) ...C(9a)	2.87
H(6a) ...C(9a)	2.86	H(6b) ...C(7b)	2.10
C(5b) ...C(7b)	2.39	C(4b) ...C(7b)	2.76
C(3b) ...C(7b)	2.38	H(2b) ...C(7b)	2.15
H(6a) ...C(7b)	2.32	H(5b) ...C(6b)	2.16
C(4b) ...C(6b)	2.39	C(3b) ...C(6b)	2.72
C(2b) ...C(6b)	2.37	H(6a) ...C(6b)	2.98
C(5b) ...H(6b)	2.14	H(4b) ...C(5b)	2.15
C(3b) ...C(5b)	2.36	C(2b) ...C(5b)	2.78
C1(2) ...C(5b)	3.68	C(4b) ...H(5b)	2.15
C1(1) ...H(5b)	3.31	H(3b) ...C(4b)	2.09
C(2b) ...C(4b)	2.40	C1(2) ...C(4b)	3.75
C(3b) ...H(4b)	2.10	H(2b) ...C(3b)	2.17
C(2b) ...H(3b)	2.14	H(6a) ...C(2b)	2.66
C1(2) ...C1(1)	2.85	C1(3) ...C1(1)	2.84
H(fc) ...C1(1)	2.51	C1(3) ...C1(2)	2.86
H(6a) ...C1(2)	3.40	H(c) ...C1(2)	2.43
H(fc) ...C1(3)	2.34		

A3 Tables for  $[(L6)_2Cu]$ .

X-ray structure determination of  $[(L6)_2Cu]$ .

Bis-[2-hydroxy-5-methylbenzaldehydeoximate]copper(II)

Crystal data:  $C_{24}H_{32}N_2O_4Cu$  Mwt = 476.1, monoclinic,  
space group  $P2_1/c$ ,  $a = 21.631(3) \text{ \AA}$ ,  $b = 6.678(2) \text{ \AA}$ ,  
 $c = 16.088(4) \text{ \AA}$ . Beta =  $92.76(2)^\circ$ ,  $U = 2321.2 \text{ \AA}^3$ ,  
 $D_c = 1.48 \text{ g cm}^{-3}$ ,  $F_{000} = 766$ .

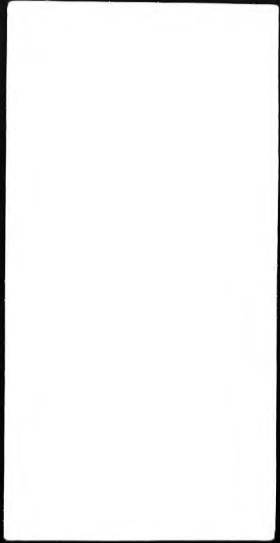
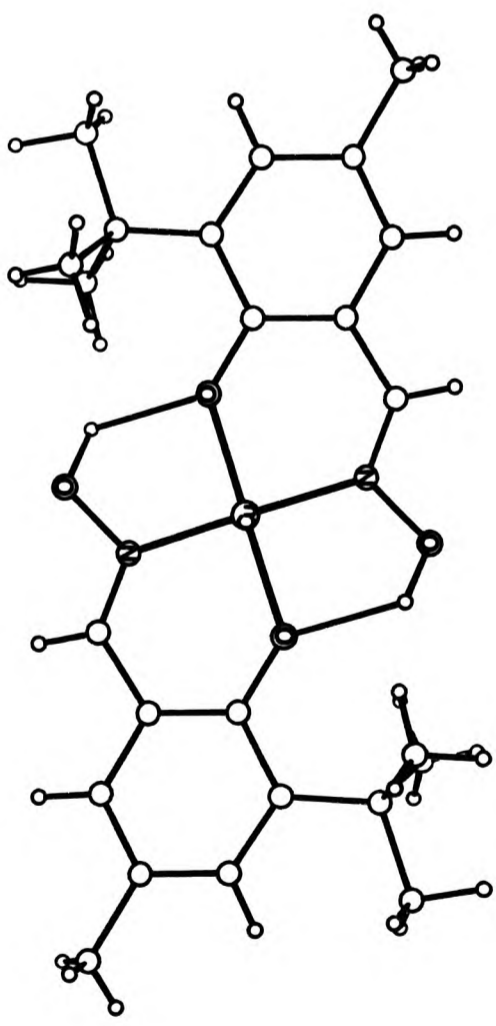


TABLE 1 Fractional atomic coordinates and thermal parameters ( $\text{\AA}^2$ )

Atom	x	y	z	$U_{\text{iso}}$ or $U_{\text{eq}}$
Cu	0.25000	0.25000	-0.25000	0.0375(6)
O(1a)	0.1904(2)	0.0703(6)	-0.2073(2)	0.038(2)
N(1a)	0.2552(2)	0.0914(7)	-0.3500(3)	0.039(3)
O(2a)	0.2940(2)	0.1599(6)	-0.4116(3)	0.056(3)
C(2a)	0.1655(2)	-0.0959(9)	-0.2394(3)	0.034(4)
C(3a)	0.1195(2)	-0.2035(8)	-0.1979(3)	0.033(4)
C(4a)	0.0965(3)	-0.3792(9)	-0.2338(4)	0.036(4)
C(5a)	0.1160(3)	-0.4585(9)	-0.3092(4)	0.038(4)
C(6a)	0.1597(3)	-0.3541(10)	-0.3492(4)	0.039(4)
C(7a)	0.1846(3)	-0.1745(9)	-0.3164(4)	0.034(4)
C(8a)	0.2286(3)	-0.0737(9)	-0.3676(3)	0.036(4)
C(9a)	0.0874(4)	-0.6489(11)	-0.3456(5)	0.054(5)
C(10a)	0.0941(2)	-0.1261(9)	-0.1159(4)	0.038(4)
C(1b)	0.0428(3)	-0.2632(13)	-0.0837(4)	0.060(5)
C(2b)	0.1458(3)	-0.1219(11)	-0.0473(4)	0.051(5)
C(3b)	0.0660(3)	0.0830(10)	-0.1278(4)	0.057(5)



TABLE 2 Fractional atomic coordinates for the hydrogen atoms

Atom	x	y	z
H(91)	0.1183	-0.7375	-0.3462
H(92)	0.0573	-0.6141	-0.3829
H(93)	0.0667	-0.7195	-0.3143
H(1b1)	0.0099	-0.2502	-0.1195
H(1b2)	0.0583	-0.3847	-0.0675
H(1b3)	0.0265	-0.1692	-0.0305
H(2b1)	0.1548	-0.2508	-0.0301
H(2b2)	0.1867	-0.0587	-0.0617
H(2b3)	0.1334	-0.0473	-0.0059
H(3b1)	0.0929	0.1859	-0.1487
H(3b2)	0.0342	0.0611	-0.1602
H(3b3)	0.0459	0.1436	-0.0752
H(4a)	0.0635	-0.4483	-0.2094
H(6a)	0.1735	-0.4165	-0.3989
H(8a)	0.2356	-0.1420	-0.4162
H(02a)	0.3316	0.2418	-0.3810

TABLE 3 Anisotropic thermal parameters ( $\text{\AA}^2$ )

Atom	$U_{11}$	$U_{22}$	$U_{33}$	$U_{23}$	$U_{13}$	$U_{12}$
Cu	0.039(1)	0.044(1)	0.030(1)	-0.006(1)	0.010(1)	-0.007(1)
O(1a)	0.038(2)	0.041(3)	0.034(2)	-0.007(2)	0.012(2)	-0.011(2)
N(1a)	0.043(3)	0.036(3)	0.037(3)	-0.006(3)	0.014(3)	-0.009(3)
O(2a)	0.063(3)	0.063(3)	0.043(3)	-0.007(2)	0.027(2)	-0.027(2)
C(2a)	0.030(3)	0.040(4)	0.031(3)	-0.000(3)	0.004(3)	0.000(3)
C(3a)	0.030(3)	0.038(5)	0.032(3)	0.002(3)	0.004(3)	0.002(3)
C(4a)	0.032(4)	0.037(4)	0.040(4)	0.003(3)	0.002(3)	-0.002(3)
C(5a)	0.038(4)	0.043(4)	0.034(3)	-0.001(3)	-0.005(3)	-0.001(3)
C(6a)	0.044(4)	0.037(4)	0.035(4)	-0.003(3)	0.008(3)	0.005(3)
C(7a)	0.034(3)	0.038(4)	0.031(3)	0.002(3)	0.003(3)	-0.002(3)
C(8a)	0.039(4)	0.039(4)	0.030(3)	-0.006(3)	0.002(3)	0.004(3)
C(9a)	0.056(5)	0.048(4)	0.059(5)	-0.007(4)	0.001(4)	-0.015(5)
C(10a)	0.028(3)	0.050(4)	0.037(4)	-0.001(3)	0.011(3)	-0.004(3)

table 3 continued

C(1b)	0.055(4)	0.074(5)	0.052(4)	-0.001(5)	0.022(4)	-0.007(5)
C(2b)	0.060(5)	0.056(5)	0.037(4)	-0.004(4)	0.008(3)	-0.002(4)
C(3b)	0.055(5)	0.060(5)	0.056(5)	-0.002(4)	0.017(5)	0.007(4)

TABLE 4 Bond lengths (Å)

Cu -O(1a)	1.913(4)	Cu -N(1a)	1.934(5)
O(1a) -C(2a)	1.327(7)	N(1a) -O(2a)	1.404(6)
N(1a) -C(8a)	1.270(8)	C(2a) -C(3a)	1.420(8)
C(2a) -C(7a)	1.425(8)	C(3a) -C(4a)	1.390(8)
C(3a) -C(10a)	1.542(8)	C(4a) -C(5a)	1.407(8)
C(5a) -C(6a)	1.361(9)	C(5a) -C(9a)	1.518(9)
C(6a) -C(7a)	1.407(9)	C(7a) -C(8a)	1.454(8)
C(10a) -C(1b)	1.548(9)	C(10a) -C(2b)	1.534(8)
C(10a) -C(3b)	1.531(9)		

TABLE 5 Bond angles (°)

N(1a) -Cu -O(1a)	91.3(2)	C(2a) -O(1a) -Cu	130.8(3)
O(2a) -N(1a) -Cu	118.0(3)	C(8a) -N(1a) -Cu	128.1(4)
C(8a) -N(1a) -O(2a)	113.9(5)	C(3a) -C(2a) -O(1a)	121.4(5)
C(7a) -C(2a) -O(1a)	121.2(5)	C(7a) -C(2a) -C(3a)	117.5(5)
C(4a) -C(3a) -C(2a)	118.5(5)	C(10a) -C(3a) -C(2a)	121.3(5)
C(10a) -C(3a) -C(4a)	120.2(5)	C(5a) -C(4a) -C(3a)	124.1(5)
C(6a) -C(5a) -C(4a)	117.3(6)	C(9a) -C(5a) -C(4a)	120.9(6)
C(9a) -C(5a) -C(6a)	121.7(6)	C(7a) -C(6a) -C(5a)	121.5(6)
C(6a) -C(7a) -C(2a)	121.2(5)	C(8a) -C(7a) -C(2a)	123.2(5)
C(8a) -C(7a) -C(6a)	115.6(5)	C(7a) -C(8a) -N(1a)	125.3(5)
C(1b) -C(10a) -C(3a)	112.3(5)	C(2b) -C(10a) -C(3a)	110.1(5)
C(2b) -C(10a) -C(1b)	106.3(5)	C(3b) -C(10a) -C(3a)	110.7(5)
C(3b) -C(10a) -C(1b)	107.2(5)	C(3b) -C(10a) -C(2b)	110.2(5)

TABLE 6 Intermolecular distances (Å)

C(4a) ...Cu	4.16	1	0.0	-1.0	0.0
C(5a) ...Cu	3.58	1	0.0	-1.0	0.0
C(6a) ...Cu	3.61	1	0.0	-1.0	0.0
C(9a) ...Cu	3.83	1	0.0	-1.0	0.0
H(91) ...Cu	3.18	1	0.0	-1.0	0.0
H(6a) ...Cu	3.61	1	0.0	-1.0	0.0
H(91) ...O(1a)	2.96	1	0.0	-1.0	0.0
N(1a) ...O(1a)	2.69	-1	0.5	0.5	-0.5
O(2a) ...O(1a)	2.64	-1	0.5	0.5	-0.5
H(O2a)...O(1a)	1.97	-1	0.5	0.5	-0.5
H(2b2)...O(2a)	2.73	-1	0.5	0.5	-0.5
H(3b1)...O(2a)	2.78	-1	0.5	0.5	-0.5
H(O2a)...C(2a)	3.06	-1	0.5	0.5	-0.5
H(2b3)...C(8a)	3.07	-2	0.0	0.0	1.0
H(O2a)...C(10a)	3.03	-1	0.5	0.5	-0.5
H(O2a)...C(2b)	2.84	-1	0.5	0.5	-0.5
H(O2a)...C(3b)	2.50	-1	0.5	0.5	-0.5

TABLE 7 Intramolecular distances (Å)

O(2a) ...Cu	2.87	C(2a) ...Cu	2.96
C(7a) ...Cu	3.32	C(8a) ...Cu	2.90
H(8a) ...Cu	3.74	H(02a)...Cu	2.81
N(1a) ...O(1a)	2.75	C(3a) ...O(1a)	2.40
C(7a) ...O(1a)	2.40	C(8a) ...O(1a)	2.91
C(10a)...O(1a)	2.92	C(2b) ...O(1a)	3.07
H(2b2)...O(1a)	2.50	C(3b) ...O(1a)	3.03
H(3b1)...O(1a)	2.47	C(2a) ...N(1a)	2.97
C(7a) ...N(1a)	2.42	H(8a) ...N(1a)	1.92
H(02a)...N(1a)	2.02	C(8a) ...O(2a)	2.24
H(8a) ...O(2a)	2.38	C(4a) ...C(2a)	2.41
C(5a) ...C(2a)	2.86	C(6a) ...C(2a)	2.47
C(8a) ...C(2a)	2.53	C(10a)...C(2a)	2.58
C(2b) ...C(2a)	3.14	H(2b2)...C(2a)	2.88
C(3b) ...C(2a)	3.11	H(3b1)...C(2a)	2.89
C(5a) ...C(3a)	2.47	C(6a) ...C(3a)	2.81
C(7a) ...C(3a)	2.43	C(1b) ...C(3a)	2.57
H(1b1)...C(3a)	2.76	H(1b2)...C(3a)	2.81
C(2b) ...C(3a)	2.52	H(2b1)...C(3a)	2.79
H(2b2)...C(3a)	2.75	C(3b) ...C(3a)	2.53
H(3b1)...C(3a)	2.79	H(3b2)...C(3a)	2.65
H(4a) ...C(3a)	2.04	C(6a) ...C(4a)	2.36
C(7a) ...C(4a)	2.74	C(9a) ...C(4a)	2.55
H(91) ...C(4a)	3.05	H(92) ...C(4a)	2.96
H(93) ...C(4a)	2.68	C(10a)...C(4a)	2.54

table 7 continued

C(1b) ...C(4a)	2.84	H(1b1)...C(4a)	2.82
H(1b2)...C(4a)	2.84	C(7a) ...C(5a)	2.41
H(91) ...C(5a)	1.96	H(92) ...C(5a)	1.99
H(93) ...C(5a)	2.04	H(4a) ...C(5a)	2.01
H(6a) ...C(5a)	1.97	C(8a) ...C(6a)	2.42
C(9a) ...C(6a)	2.52	H(91) ...C(6a)	2.71
H(92) ...C(6a)	2.85	H(8a) ...C(6a)	2.46
H(6a) ...C(7a)	2.10	H(8a) ...C(7a)	2.00
H(6a) ...C(8a)	2.62	H(4a) ...C(9a)	2.64
H(6a) ...C(9a)	2.60	H(1b1)...C(10a)	2.00
H(1b2)...C(10a)	2.06	H(1b3)...C(10a)	2.07
H(2b1)...C(10a)	2.04	H(2b2)...C(10a)	2.19
H(2b3)...C(10a)	2.00	H(3b1)...C(10a)	2.15
H(3b2)...C(10a)	1.91	H(3b3)...C(10a)	2.20
H(4a) ...C(10a)	2.69	C(2b) ...C(1b)	2.47
H(2b1)...C(1b)	2.53	H(2b3)...C(1b)	2.69
C(3b) ...C(1b)	2.48	H(3b2)...C(1b)	2.49
H(3b3)...C(1b)	2.72	H(4a) ...C(1b)	2.43
C(3b) ...H(1b1)	2.54	C(2b) ...H(1b2)	2.59
C(2b) ...H(1b3)	2.63	C(3b) ...H(1b3)	2.48
C(3b) ...C(2b)	2.51	H(3b1)...C(2b)	2.83
H(3b3)...C(2b)	2.81	C(3b) ...H(2b2)	2.93
C(3b) ...H(2b3)	2.54		

A4     Tables for 'L7H'.



X-ray structure determination of 1,7H-  
3,5-dimethyl-4-hydroxyacetophenone.

Crystal data:  $C_{11}H_{15}N_2O_2$ , Mwt = 476.1,  
orthorhombic,  $P2_12_12_1$ ,  $a = 20.874(5) \text{ \AA}$ ,  
 $b = 7.537(1) \text{ \AA}$ ,  $c = 6.826(2) \text{ \AA}$ .  $\beta = 90^\circ$ ,  
 $U = 1073.9 \text{ \AA}^3$ ,  $D_c = 1.20 \text{ gm}^{-3}$   $F_{000} = 416$ .

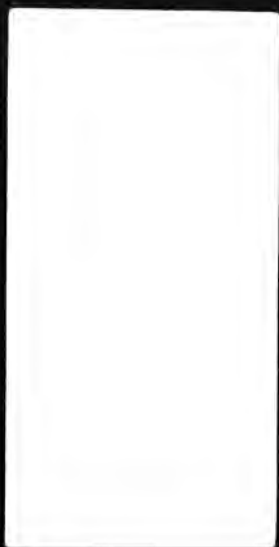
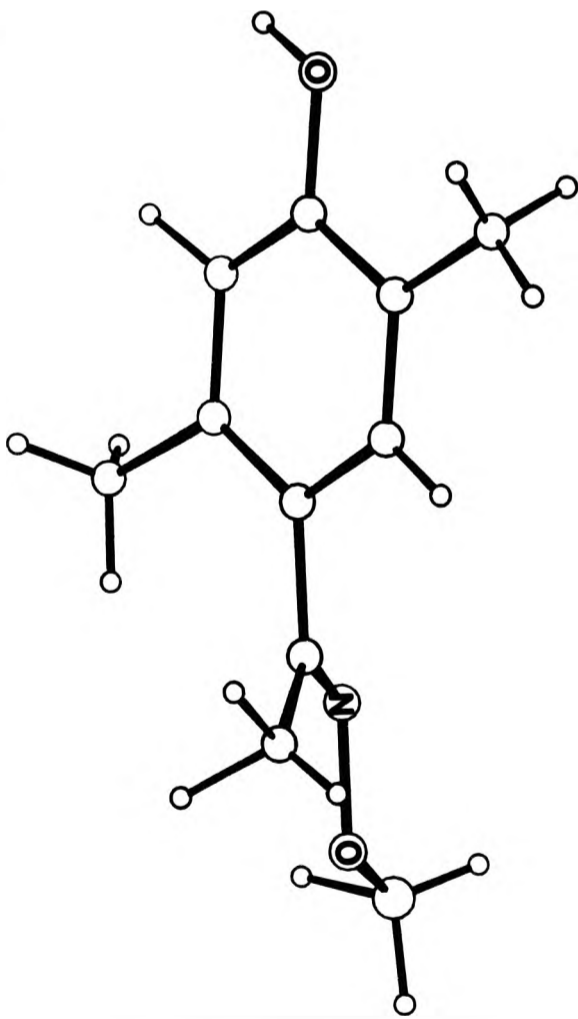


TABLE 1 Fractional atomic coordinates and thermal parameters ( $\text{\AA}^2$ )

Atom	x	y	z	$U_{\text{iso}}$ or $U_{\text{eq}}$
O(1a)	0.6060(2)	-0.1224(9)	0.0313(9)	0.050(4)
N(1a)	0.3347(2)	0.2288(8)	0.1268(9)	0.040(4)
O(2b)	0.2713(2)	0.2933(7)	0.0939(8)	0.051(3)
C(2a)	0.4383(3)	-0.0546(11)	0.1757(10)	0.037(5)
C(3a)	0.5018(4)	-0.1088(11)	0.1804(12)	0.041(5)
C(4a)	0.5433(3)	-0.0710(9)	0.0281(10)	0.035(4)
C(5a)	0.5228(3)	0.0233(9)	-0.1356(9)	0.033(4)
C(6a)	0.4590(3)	0.0756(10)	-0.1385(11)	0.039(5)
C(7a)	0.4163(3)	0.0414(10)	0.0169(10)	0.035(4)
C(8a)	0.3505(3)	0.1152(10)	-0.0034(11)	0.034(4)
C(9a)	0.5673(3)	0.0667(11)	-0.3008(10)	0.049(5)
C(me1)	0.3104(3)	0.0648(12)	-0.1719(11)	0.068(6)
C(me2)	0.3935(4)	-0.1085(14)	0.3435(15)	0.059(6)
C(ome)	0.2563(5)	0.4219(14)	0.2389(18)	0.070(7)

TABLE 2 Fractional atomic coordinates for the hydrogen atoms

Atom	x	y	z	
H(01a)	0.618(4)	-0.180(11)	0.142(13)	0.08(3)
H(3a)	0.515(3)	-0.197(8)	0.280(9)	0.04(2)
H(6a)	0.444(2)	0.137(8)	-0.243(9)	0.02(2)
H(1m2)	0.349(4)	-0.069(14)	0.310(15)	0.14(2)
H(2m2)	0.408(5)	-0.069(15)	0.466(14)	0.14(2)
H(3m2)	0.394(4)	-0.236(14)	0.371(15)	0.14(2)
H(1om)	0.212(4)	0.471(11)	0.199(12)	0.10(2)
H(2om)	0.284(4)	0.516(11)	0.235(14)	0.10(2)
H(3om)	0.250(4)	0.335(12)	0.364(13)	0.10(2)
H(1m1)	0.327(4)	-0.048(13)	-0.259(15)	0.14(2)
H(2m1)	0.299(5)	0.138(15)	-0.251(17)	0.14(2)
H(3m1)	0.271(4)	-0.020(14)	-0.106(13)	0.14(2)
H(9a1)	0.547(4)	0.109(14)	-0.423(15)	0.14(2)
H(9a2)	0.588(5)	-0.023(14)	-0.348(16)	0.14(2)
H(9a3)	0.598(4)	0.159(14)	-0.262(15)	0.14(2)

TABLE 3 Anisotropic thermal parameters ( $\text{\AA}^2$ )

Atom	$U_{11}$	$U_{22}$	$U_{33}$	$U_{23}$	$U_{13}$	$U_{12}$
O(1a)	0.033(3)	0.069(4)	0.049(4)	0.012(3)	-0.003(3)	0.014(3)
N(1a)	0.031(3)	0.046(4)	0.044(4)	0.002(4)	-0.007(3)	0.005(3)
O(2b)	0.033(3)	0.064(4)	0.058(4)	-0.006(4)	-0.006(3)	0.015(3)
C(2a)	0.043(4)	0.042(5)	0.025(4)	0.002(4)	-0.003(4)	0.001(4)
C(3a)	0.047(5)	0.031(5)	0.044(5)	0.004(5)	-0.011(5)	0.009(4)
C(4a)	0.036(4)	0.033(4)	0.035(4)	-0.003(4)	-0.006(4)	0.006(4)
C(5a)	0.032(4)	0.040(5)	0.026(4)	-0.006(4)	-0.004(4)	0.001(4)
C(6a)	0.044(4)	0.032(5)	0.040(5)	0.003(5)	-0.014(5)	0.004(4)
C(7a)	0.032(4)	0.032(5)	0.040(4)	-0.005(4)	0.006(4)	-0.000(4)
C(8a)	0.036(4)	0.027(4)	0.039(4)	0.000(5)	-0.000(4)	-0.002(3)
C(9a)	0.044(4)	0.059(6)	0.045(5)	0.009(5)	0.006(4)	0.004(5)
C(me1)	0.058(5)	0.087(7)	0.059(5)	-0.025(6)	-0.025(5)	0.010(5)
C(me2)	0.055(5)	0.069(7)	0.053(5)	0.027(6)	0.011(6)	0.010(6)
C(ome)	0.057(5)	0.070(9)	0.082(7)	-0.025(8)	-0.002(6)	0.031(6)

TABLE 4 Bond lengths (Å)

O(1a) - C(4a)	1.366(8)	N(1a) - O(2b)	1.429(7)
N(1a) - C(8a)	1.278(10)	O(2b) - C(ome)	1.421(12)
C(2a) - C(3a)	1.388(10)	C(2a) - C(7a)	1.381(10)
C(2a) - C(me2)	1.533(12)	C(3a) - C(4a)	1.383(10)
C(4a) - C(5a)	1.391(10)	C(5a) - C(6a)	1.390(9)
C(5a) - C(9a)	1.497(9)	C(6a) - C(7a)	1.409(10)
C(7a) - C(8a)	1.488(9)	C(8a) - C(me1)	1.473(11)
O(1a) - H(o1a)	.91(9)	C(3a) - H(3a)	.99(6)
C(6a) - H(6a)	.91(6)	C(9a) - H(9a1)	.99(9)
C(9a) - H(9a2)	.87(9)	C(9a) - H(9a3)	.98(9)
C(me1) - H(1m1)	1.09(9)	C(me1) - H(2m1)	.81(9)
C(me1) - H(3m1)	1.13(9)	C(me2) - H(1m2)	.99(9)
C(me2) - H(2m2)	.94(9)	C(me2) - H(3m2)	.98(9)
C(ome) - H(1om)	1.03(8)	C(ome) - H(2om)	.91(9)
C(ome) - H(3om)	1.08(9)		

TABLE 5 Bond angles (°)

C(8a)-N(1a)-O(2b)	110.9(6)	C(ome)-O(2b)-N(1a)	109.1(6)
C(7a)-C(2a)-C(3a)	119.3(7)	C(me2)-C(2a)-C(3a)	119.2(7)
C(me2)-C(2a)-C(7a)	121.5(6)	C(4a)-C(3a)-C(2a)	121.3(7)
C(3a)-C(4a)-O(1a)	122.0(7)	C(5a)-C(4a)-O(1a)	116.9(6)
C(5a)-C(4a)-C(3a)	121.1(6)	C(6a)-C(5a)-C(4a)	116.8(6)
C(9a)-C(5a)-C(4a)	121.8(6)	C(9a)-C(5a)-C(6a)	121.5(6)
C(7a)-C(6a)-C(5a)	122.9(7)	C(6a)-C(7a)-C(2a)	118.5(6)
C(8a)-C(7a)-C(2a)	125.1(6)	C(8a)-C(7a)-C(6a)	116.4(6)
C(7a)-C(8a)-N(1a)	115.1(6)	C(me1)-C(8a)-N(1a)	124.7(6)
C(me1)-C(8a)-C(7a)	120.1(6)		
H(o1a)-O(1a)-C(4a)	114(5)	H(3a)-C(3a)-C(2a)	119(3)
H(3a)-C(3a)-C(4a)	119(3)	H(6a)-C(6a)-C(5a)	119(3)
H(6a)-C(6a)-C(7a)	118(3)	H(9a1)-C(9a)-C(5a)	116(5)
H(9a2)-C(9a)-C(5a)	115(7)	H(9a2)-C(9a)-H(9a1)	99(9)
H(9a3)-C(9a)-C(5a)	111(6)	H(9a3)-C(9a)-H(9a1)	106(9)
H(9a3)-C(9a)-H(9a2)	109(9)	H(1m1)-C(me1)-C(8a)	116(5)
H(2m1)-C(me1)-C(8a)	121(8)	H(2m1)-C(me1)-H(1m1)	105(9)
H(3m1)-C(me1)-C(8a)	104(5)	H(3m1)-C(me1)-H(1m1)	90(7)
H(3m1)-C(me1)-H(2m1)	115(9)	H(1m2)-C(me2)-C(2a)	108(6)
H(2m2)-C(me2)-C(2a)	112(6)	H(2m2)-C(me2)-H(1m2)	115(9)
H(3m2)-C(me2)-C(2a)	113(6)	H(3m2)-C(me2)-H(1m2)	110(8)
H(3m2)-C(me2)-H(2m2)	98(9)	H(1om)-C(ome)-O(2b)	105(5)
H(2om)-C(ome)-O(2b)	111(6)	H(2om)-C(ome)-H(1om)	106(7)
H(3om)-C(ome)-O(2b)	99(5)	H(3om)-C(ome)-H(1om)	109(7)
H(3om)-C(ome)-H(2om)	124(8)		

TABLE 6 Intermolecular distances (Å)

H(1om)...O(1a)	2.94	3	-1.0	0.0	0.0
N(1a) ...O(1a)	2.87	4	1.0	0.0	0.0
C(ome)...O(1a)	3.29	4	1.0	0.0	0.0
H(6a) ...O(1a)	2.87	4	1.0	0.0	-1.0
H(3m2)...O(1a)	2.99	4	1.0	-1.0	0.0
H(2om)...O(1a)	2.99	4	1.0	0.0	0.0
H(o1a)...N(1a)	1.98	4	1.0	-1.0	0.0
C(ome)...O(2b)	3.29	2	0.0	1.0	0.0
H(1m1)...O(2b)	2.94	2	0.0	0.0	-1.0
H(o1a)...O(2b)	2.94	4	1.0	-1.0	0.0
H(3a) ...C(2a)	2.88	4	1.0	-1.0	0.0
H(9a1)...C(3a)	2.94	4	1.0	0.0	-1.0
H(6a) ...C(4a)	2.95	4	1.0	0.0	-1.0
H(3m2)...C(4a)	2.93	4	1.0	-1.0	0.0
H(3a) ...C(6a)	3.03	4	1.0	-1.0	0.0
H(3a) ...C(7a)	2.80	4	1.0	-1.0	0.0
H(o1a)...C(8a)	2.98	4	1.0	-1.0	0.0
H(o1a)...C(ome)	2.85	4	1.0	-1.0	0.0

TABLE 7 Intramolecular distances (Å)

C(3a) ...O(1a)	2.40	C(5a) ...O(1a)	2.35
C(9a) ...O(1a)	2.80	H(3a) ...O(1a)	2.61
H(9a2)...O(1a)	2.72	H(9a3)...O(1a)	2.92
C(2a) ...N(1a)	3.06	C(6a) ...N(1a)	3.37
C(7a) ...N(1a)	2.34	C(me1)...N(1a)	2.44
C(me2)...N(1a)	3.19	C(ome)...N(1a)	2.32
H(1m2)...N(1a)	2.59	H(2om)...N(1a)	2.52
H(3om)...N(1a)	2.52	H(2m1)...N(1a)	2.77
H(3m1)...N(1a)	2.80	C(8a) ...O(2b)	2.23
C(me1)...O(2b)	2.63	H(1om)...O(2b)	1.96
H(2om)...O(2b)	1.95	H(3om)...O(2b)	1.92
H(2m1)...O(2b)	2.69	H(3m1)...O(2b)	2.73
C(4a) ...C(2a)	2.42	C(5a) ...C(2a)	2.82
C(6a) ...C(2a)	2.40	C(8a) ...C(2a)	2.55
H(3a) ...C(2a)	2.06	H(1m2)...C(2a)	2.07
H(2m2)...C(2a)	2.08	H(3m2)...C(2a)	2.12
C(5a) ...C(3a)	2.42	C(6a) ...C(3a)	2.73
C(7a) ...C(3a)	2.39	C(me2)...C(3a)	2.52
H(o1a)...C(3a)	2.50	H(2m2)...C(3a)	2.78
H(3m2)...C(3a)	2.77	C(6a) ...C(4a)	2.37
C(7a) ...C(4a)	2.78	C(9a) ...C(4a)	2.52
H(o1a)...C(4a)	1.93	H(3a) ...C(4a)	2.05
H(9a2)...C(4a)	2.76	H(9a3)...C(4a)	2.87
C(7a) ...C(5a)	2.46	H(6a) ...C(5a)	2.00
H(9a1)...C(5a)	2.13	H(9a2)...C(5a)	2.02



table 7 continued

H(9a3)...C(5a)	2.06	C(8a) ...C(6a)	2.46
C(9a) ...C(6a)	2.52	C(me1)...C(6a)	3.11
H(1m1)...C(6a)	3.03	H(9a1)...C(6a)	2.68
C(me1)...C(7a)	2.57	C(me2)...C(7a)	2.54
H(6a) ...C(7a)	2.00	H(1m2)...C(7a)	2.58
H(1m1)...C(7a)	2.74	C(me2)...C(8a)	3.04
C(ome)...C(8a)	3.46	H(6a) ...C(8a)	2.55
H(1m2)...C(8a)	2.55	H(1m1)...C(8a)	2.19
H(2m1)...C(8a)	2.01	H(3m1)...C(8a)	2.07
H(6a) ...C(9a)	2.66	H(6a) ...C(me1)	2.88
H(3a) ...C(me2)	2.66		

A5      Tables for  $[\text{Zn}(\text{L}15)(\text{NO}_2)(\text{H}_2\text{O})](\text{NO}_2)$ .

X-ray structure of  $[\text{Zn}(\text{L}15)(\text{NO}_2)(\text{H}_2\text{O})](\text{NO}_3)_2 \cdot$   
 $\text{aqua}(6,7,8,9,10,11,16,17,18,19\text{-decahydro-5H-}$   
 $\text{dibenzo[e,n]}[1,4,8,12]\text{tetra-azacyclopentadecine})\text{-}$   
 $\text{nitratozinc(II) nitrate}.$

Crystal data:  $\text{C}_{19}\text{H}_{28}\text{N}_6\text{O}_7\text{Zn}$ , Mwt = 517.8, monoclinic,  
space group  $\text{C2/c}$ ,  $a = 19.628(5) \text{ \AA}$ ,  $b = 7.670(2) \text{ \AA}$ ,  $c =$   
 $29.153(8) \text{ \AA}$ . Beta =  $99.22(2)^\circ$ ,  $U = 4331.4 \text{ \AA}^3$ ,  $D_c = 1.59$   
 $\text{g cm}^{-3}$ ,  $F_{000} = 2160$ .

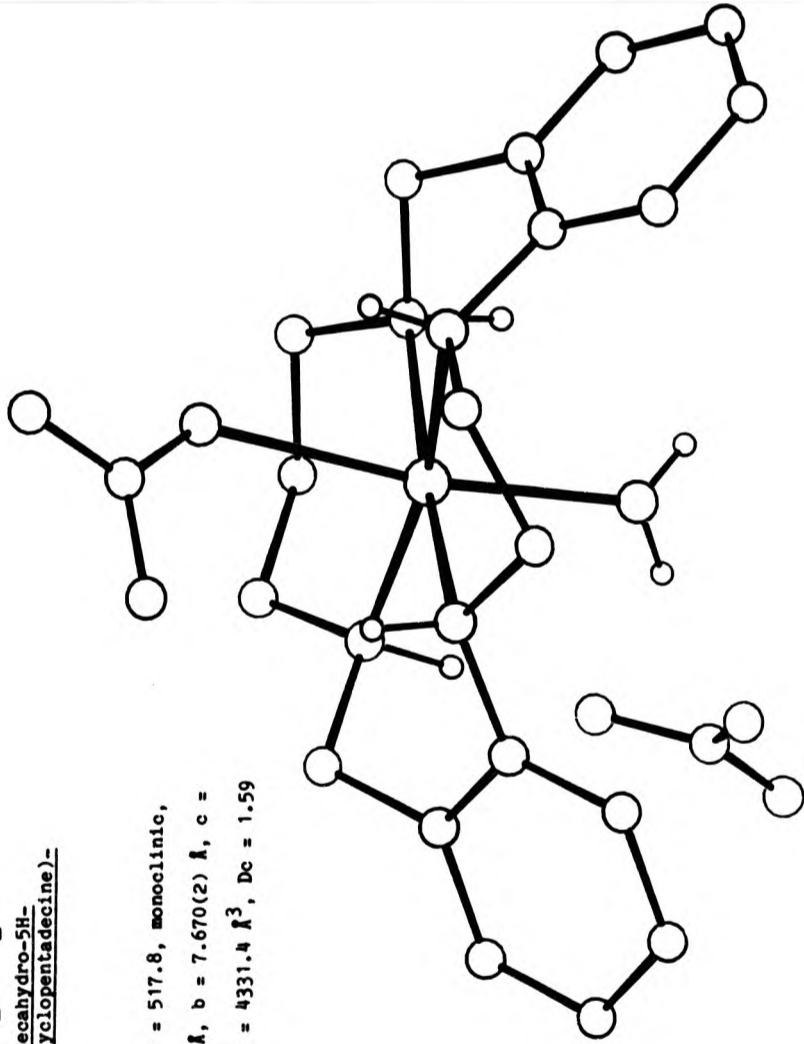


TABLE 1 Fractional atomic coordinates and thermal parameters ( $\text{\AA}^2$ )

Atom	x	y	z	U <sub>iso</sub> or U <sub>eq</sub>
Zn	0.09759(3)	-0.12514(9)	0.38326(2)	0.0328(4)
C(1a)	0.1454(3)	0.0627(8)	0.4744(2)	0.033(3)
N(1a)	0.0803(2)	-0.0217(6)	0.4518(1)	0.030(2)
C(2a)	0.0170(3)	0.0760(7)	0.4463(2)	0.026(3)
C(3a)	0.0140(3)	0.2498(8)	0.4583(2)	0.034(3)
C(4a)	-0.0498(3)	0.3345(7)	0.4535(2)	0.042(3)
C(5a)	-0.1097(3)	0.2455(9)	0.4349(2)	0.042(3)
C(6a)	-0.1059(3)	0.0754(9)	0.4211(2)	0.041(3)
C(7a)	-0.0427(3)	-0.0149(8)	0.4270(2)	0.032(3)
C(8a)	-0.0404(3)	-0.2019(8)	0.4120(2)	0.036(3)
N(2a)	-0.0036(2)	-0.2251(6)	0.3713(2)	0.030(2)
C(9a)	-0.0078(3)	-0.4103(8)	0.3554(2)	0.040(3)
C(9c)	0.0275(3)	-0.4385(9)	0.3123(2)	0.043(3)
C(9b)	0.1058(4)	-0.4363(8)	0.3221(2)	0.046(4)
N(2b)	0.1353(3)	-0.2589(6)	0.3302(2)	0.039(3)
C(8b)	0.2132(3)	-0.2651(8)	0.3383(2)	0.042(3)
C(7b)	0.2427(3)	-0.0846(7)	0.3361(2)	0.036(3)
C(6b)	0.2803(3)	-0.0422(9)	0.3013(2)	0.048(4)
C(5b)	0.3062(3)	0.1253(11)	0.2965(2)	0.055(4)
C(4b)	0.2927(3)	0.2567(10)	0.3272(2)	0.049(4)
C(3b)	0.2570(3)	0.2163(9)	0.3632(2)	0.041(3)
C(2b)	0.2329(3)	0.0460(8)	0.3683(2)	0.033(3)
N(1b)	0.1965(2)	-0.0010(6)	0.4060(1)	0.030(2)
C(1b)	0.1840(3)	0.1415(8)	0.4379(2)	0.035(3)
N(1)	0.1774(2)	-0.4161(6)	0.4608(2)	0.035(3)

table 1 continued

O(1)	0.1216(2)	-0.3693(6)	0.4354(1)	0.047(2)
O(2)	0.2327(2)	-0.3660(9)	0.4502(2)	0.080(4)
O(3)	0.1753(2)	-0.5115(6)	0.4940(1)	0.049(3)
N(2)	0.0864(3)	-0.9236(7)	0.2284(2)	0.039(3)
O(4)	0.1054(4)	-0.8230(9)	0.2610(2)	0.093(5)
O(5)	0.0746(3)	-0.8754(9)	0.1877(2)	0.080(4)
O(6)	0.0797(3)	-1.0798(8)	0.2363(2)	0.088(5)
O(w)	0.0674(2)	0.1095(5)	0.3449(1)	0.040(2)

TABLE 2 Fractional atomic coordinates for the hydrogen atoms

Atom	x	y	z
H(1a1)	0.1374	0.1439	0.5011
H(1a2)	0.1755	-0.0201	0.4906
HN(1a)	0.0791	-0.1196	0.4624
H(3a)	0.0592	0.3385	0.4759
H(4a)	-0.0517	0.4655	0.4582
H(5a)	-0.1541	0.2819	0.4272
H(6a)	-0.1483	-0.0047	0.4117
H(8a1)	-0.0132	-0.2690	0.4365
H(8a2)	-0.0865	-0.2565	0.4014
HN(2a)	-0.0333	-0.1468	0.3425
H(9a1)	0.0134	-0.4786	0.3844
H(9a2)	-0.0589	-0.4337	0.3453
H(9c1)	0.0043	-0.3399	0.2930
H(9c2)	0.0121	-0.5573	0.3019
H(9b1)	0.1246	-0.5188	0.3471
H(9b2)	0.1219	-0.4747	0.2922
HN(2b)	0.1219	-0.1759	0.3036
H(8b1)	0.2281	-0.3248	0.3116
H(8b2)	0.2249	-0.3321	0.3665
H(6b)	0.2784	-0.1210	0.2737
H(5b)	0.3338	0.1829	0.2691
H(4b)	0.3178	0.3789	0.3237
H(3b)	0.2513	0.3031	0.3935
HN(1b)	0.2176	-0.0877	0.4221
H(1b1)	0.2265	0.1927	0.4508

table 2 continued

H(1b2)	0.1575	0.2258	0.4170
H(0w1)	0.0770	0.1119	0.3146
H(0w2)	0.0287	0.1462	0.3385

TABLE 3 Anisotropic thermal parameters ( $\text{\AA}^2$ )

Atom	U11	U22	U33	U23	U13	U12
Zn	0.0328(4)	0.0312(4)	0.0343(4)	-0.0051(3)	0.0062(2)	-0.0012(3)
C(1a)	0.022(2)	0.046(3)	0.032(3)	0.001(2)	0.004(2)	0.001(2)
N(1a)	0.024(2)	0.034(3)	0.032(2)	0.001(2)	0.000(2)	-0.001(2)
C(2a)	0.025(3)	0.028(3)	0.025(3)	0.003(2)	0.004(2)	0.000(2)
C(3a)	0.037(3)	0.034(3)	0.032(3)	0.001(2)	0.007(2)	-0.000(3)
C(4a)	0.054(4)	0.027(3)	0.045(3)	0.003(3)	0.022(3)	0.001(3)
C(5a)	0.023(3)	0.045(4)	0.057(4)	0.006(3)	0.002(3)	0.005(3)
C(6a)	0.035(3)	0.049(4)	0.038(3)	0.002(3)	0.005(3)	-0.002(3)
C(7a)	0.030(3)	0.035(3)	0.029(3)	0.001(2)	0.000(2)	0.007(2)
C(8a)	0.034(3)	0.037(3)	0.038(3)	-0.002(3)	0.006(3)	0.001(2)
N(2a)	0.036(2)	0.021(2)	0.033(2)	-0.002(2)	0.000(2)	-0.001(2)
C(9a)	0.046(3)	0.033(3)	0.041(3)	-0.001(2)	0.005(3)	-0.009(3)
C(9c)	0.057(4)	0.033(3)	0.039(3)	-0.005(3)	0.002(3)	0.002(3)



Table 3 continued

C(9b)	0.063(4)	0.026(3)	0.049(4)	-0.003(3)	0.017(3)	0.003(3)
N(2b)	0.055(3)	0.027(2)	0.035(3)	-0.002(2)	0.015(2)	-0.001(2)
C(8b)	0.043(3)	0.038(3)	0.044(3)	0.000(3)	0.011(3)	0.017(3)
C(7b)	0.038(3)	0.027(3)	0.043(3)	0.001(2)	0.014(3)	0.007(2)
C(6b)	0.051(4)	0.051(4)	0.040(3)	0.000(3)	0.016(3)	0.007(3)
C(5b)	0.043(4)	0.082(5)	0.041(4)	0.014(4)	0.012(3)	-0.003(4)
C(4b)	0.041(3)	0.055(4)	0.049(4)	0.009(3)	0.011(3)	-0.013(3)
C(3b)	0.028(3)	0.053(4)	0.042(3)	-0.001(3)	0.008(2)	-0.002(3)
C(2b)	0.023(3)	0.043(3)	0.034(3)	0.002(3)	0.003(2)	0.003(2)
N(1b)	0.027(2)	0.030(2)	0.032(2)	0.005(2)	0.007(2)	0.004(2)
C(1b)	0.037(3)	0.036(3)	0.032(3)	-0.004(3)	0.009(2)	-0.004(3)
N(1)	0.037(3)	0.032(3)	0.037(3)	0.004(2)	-0.002(2)	0.008(2)
O(1)	0.038(2)	0.050(3)	0.053(3)	0.009(2)	-0.000(2)	0.002(2)
O(2)	0.036(3)	0.115(5)	0.090(4)	0.056(4)	0.010(3)	0.013(3)
O(3)	0.059(3)	0.042(3)	0.047(3)	0.009(2)	0.007(2)	0.001(2)
N(2)	0.040(3)	0.043(3)	0.035(3)	-0.001(2)	0.005(2)	-0.005(2)

table 3 continued

O(4)	0.147(6)	0.076(4)	0.058(4)	-0.020(3)	0.033(4)	-0.035(4)
O(5)	0.073(4)	0.128(6)	0.039(3)	0.029(3)	-0.003(3)	-0.015(4)
O(6)	0.127(6)	0.046(3)	0.091(5)	-0.001(3)	0.028(4)	-0.003(3)
O(w)	0.048(2)	0.033(2)	0.039(2)	0.003(2)	0.004(2)	0.007(2)

TABLE 4 Bond lengths (Å)

Zn	-N(1a)	2.227(5)	Zn	-N(2a)	2.104(5)
Zn	-N(2b)	2.089(5)	Zn	-N(1b)	2.168(4)
Zn	-O(1)	2.410(5)	Zn	-O(w)	2.151(4)
C(1a)	-N(1a)	1.488(7)	C(1a)	-C(1b)	1.525(9)
N(1a)	-C(2a)	1.438(7)	C(2a)	-C(3a)	1.381(8)
C(2a)	-C(7a)	1.402(7)	C(3a)	-C(4a)	1.396(9)
C(4a)	-C(5a)	1.391(8)	C(5a)	-C(6a)	1.371(9)
C(6a)	-C(7a)	1.406(8)	C(7a)	-C(8a)	1.502(9)
C(8a)	-N(2a)	1.496(8)	N(2a)	-C(9a)	1.492(7)
C(9a)	-C(9c)	1.544(10)	C(9c)	-C(9b)	1.518(10)
C(9b)	-N(2b)	1.483(8)	N(2b)	-C(8b)	1.510(8)
C(8b)	-C(7b)	1.506(8)	C(7b)	-C(6b)	1.386(10)
C(7b)	-C(2b)	1.407(9)	C(6b)	-C(5b)	1.397(11)
C(5b)	-C(4b)	1.401(11)	C(4b)	-C(3b)	1.388(10)
C(3b)	-C(2b)	1.405(9)	C(2b)	-N(1b)	1.450(7)
N(1b)	-C(1b)	1.481(8)	N(1)	-O(1)	1.271(6)
N(1)	-O(2)	1.238(7)	N(1)	-O(3)	1.219(7)
N(2)	-O(4)	1.234(8)	N(2)	-O(5)	1.227(7)
N(2)	-O(6)	1.231(8)			

TABLE 5 Bond angles (°)

N(2a) - Zn - N(1a)	90.2(2)	N(2b) - Zn - N(1a)	164.4(2)
N(2b) - Zn - N(2a)	97.8(2)	N(1b) - Zn - N(1a)	80.1(2)
N(1b) - Zn - N(2a)	170.1(2)	N(1b) - Zn - N(2b)	92.0(2)
O(1) - Zn - N(1a)	75.7(2)	O(1) - Zn - N(2a)	84.6(2)
O(1) - Zn - N(2b)	91.7(2)	O(1) - Zn - N(1b)	94.2(2)
O(w) - Zn - N(1a)	95.7(2)	O(w) - Zn - N(2a)	92.6(2)
O(w) - Zn - N(2b)	97.3(2)	O(w) - Zn - N(1b)	87.1(2)
O(w) - Zn - O(1)	170.9(2)	C(1b) - C(1a) - N(1a)	110.6(4)
C(1a) - N(1a) - Zn	107.9(3)	C(2a) - N(1a) - Zn	109.9(3)
C(2a) - N(1a) - C(1a)	119.2(4)	C(3a) - C(2a) - N(1a)	123.1(5)
C(7a) - C(2a) - N(1a)	115.9(5)	C(7a) - C(2a) - C(3a)	120.9(5)
C(4a) - C(3a) - C(2a)	119.9(5)	C(5a) - C(4a) - C(3a)	119.8(5)
C(6a) - C(5a) - C(4a)	119.9(5)	C(7a) - C(6a) - C(5a)	121.5(5)
C(6a) - C(7a) - C(2a)	117.8(5)	C(8a) - C(7a) - C(2a)	122.0(5)
C(8a) - C(7a) - C(6a)	120.2(5)	N(2a) - C(8a) - C(7a)	112.7(5)
C(8a) - N(2a) - Zn	112.9(3)	C(9a) - N(2a) - Zn	113.7(4)
C(9a) - N(2a) - C(8a)	110.4(5)	C(9c) - C(9a) - N(2a)	112.1(5)
C(9b) - C(9c) - C(9a)	114.8(5)	N(2b) - C(9b) - C(9c)	113.4(5)
C(9b) - N(2b) - Zn	113.2(4)	C(8b) - N(2b) - Zn	111.8(4)
C(8b) - N(2b) - C(9b)	110.8(5)	C(7b) - C(8b) - N(2b)	110.6(5)
C(6b) - C(7b) - C(8b)	120.0(6)	C(2b) - C(7b) - C(8b)	122.2(6)
C(2b) - C(7b) - C(6b)	117.8(5)	C(5b) - C(6b) - C(7b)	122.3(6)
C(4b) - C(5b) - C(6b)	119.3(7)	C(3b) - C(4b) - C(5b)	119.5(7)
C(2b) - C(3b) - C(4b)	120.4(6)	C(3b) - C(2b) - C(7b)	120.5(6)
N(1b) - C(2b) - C(7b)	117.7(5)	N(1b) - C(2b) - C(3b)	121.7(5)

table 5 continued

C(2b) -N(1b) -Zn	113.9(3)	C(1b) -N(1b) -Zn	106.6(3)
C(1b) -N(1b) -C(2b)	116.4(5)	N(1b) -C(1b) -C(1a)	107.3(5)
O(2) -N(1) -O(1)	118.3(5)	O(3) -N(1) -O(1)	119.9(5)
O(3) -N(1) -O(2)	121.8(5)	N(1) -O(1) -Zn	130.6(4)
O(5) -N(2) -O(4)	122.8(6)	O(6) -N(2) -O(4)	119.4(6)
O(6) -N(2) -O(5)	117.7(6)		

TABLE 6 Intermolecular distances (Å)

O(5) ...Zn	4.14	2	0.0	-1.0	0.0
O(3) ...C(1a)	3.35	1	0.0	-1.0	0.0
C(6a) ...C(1a)	3.43	-1	0.0	0.0	1.0
O(2) ...C(1a)	3.34	-1	0.5	-0.5	1.0
H(9a1)...C(3a)	3.00	1	0.0	-1.0	0.0
H(8a1)...C(3a)	3.07	-1	0.0	0.0	1.0
H(9a1)...C(4a)	2.91	1	0.0	-1.0	0.0
O(3) ...C(4a)	3.39	-1	0.0	0.0	1.0
O(3) ...C(5a)	3.31	-1	0.0	0.0	1.0
O(2) ...C(5a)	3.31	1	0.5	-0.5	0.0
H(1a1)...C(6a)	2.97	-1	0.0	0.0	1.0
O(5) ...C(6a)	3.35	2	0.0	-1.0	0.0
H(4a) ...C(8a)	2.91	1	0.0	1.0	0.0
O(5) ...N(2a)	3.37	2	0.0	-1.0	0.0
O(6) ...N(2b)	3.10	1	0.0	-1.0	0.0
H(9a2)...C(5b)	2.83	1	-0.5	-0.5	0.0
H(8a2)...C(4b)	2.94	1	-0.5	-0.5	0.0
H(6a) ...C(3b)	3.03	1	-0.5	-0.5	0.0
O(3) ...C(1b)	3.14	1	0.0	-1.0	0.0
O(3) ...C(1b)	3.28	-1	0.5	-0.5	1.0
H(1b2)...N(1)	3.03	1	0.0	1.0	0.0
H(3a) ...O(1)	2.90	1	0.0	1.0	0.0
H(5a) ...O(2)	2.68	1	-0.5	0.5	0.0
H(6a) ...O(2)	2.95	1	-0.5	0.5	0.0
H(1a2)...O(2)	2.45	-1	0.5	-0.5	1.0

table 6 continued

H(1a1)...0(3)	2.76	1	0.0	1.0	0.0
H(3a) ...0(3)	2.53	1	0.0	1.0	0.0
H(1b1)...0(3)	2.86	1	0.0	1.0	0.0
H(1b2)...0(3)	3.00	1	0.0	1.0	0.0
H(5a) ...0(3)	2.98	-1	0.0	0.0	1.0
H(1a2)...0(3)	2.90	-1	0.5	-0.5	1.0
H(1b1)...0(3)	2.69	-1	0.5	-0.5	1.0
HN(2b)...N(2)	2.92	1	0.0	1.0	0.0
H(Ow1)...N(2)	2.56	1	0.0	1.0	0.0
HN(2a)...N(2)	2.75	2	0.0	1.0	0.0
H(Ow2)...N(2)	2.79	2	0.0	1.0	0.0
H(4b) ...N(2)	3.01	2	0.5	1.5	0.0
O(w) ...0(4)	2.72	1	0.0	1.0	0.0
HN(2b)...0(4)	2.97	1	0.0	1.0	0.0
H(Ow1)...0(4)	1.81	1	0.0	1.0	0.0
H(Ow2)...0(4)	2.92	1	0.0	1.0	0.0
O(w) ...0(5)	2.80	2	0.0	1.0	0.0
HN(2a)...0(5)	2.35	2	0.0	1.0	0.0
H(Ow1)...0(5)	2.97	2	0.0	1.0	0.0
H(Ow2)...0(5)	2.90	2	0.0	1.0	0.0
H(4b) ...0(5)	2.89	2	0.5	1.5	0.0
HN(2b)...0(6)	2.13	1	0.0	1.0	0.0
H(Ow1)...0(6)	2.72	1	0.0	1.0	0.0
HN(2a)...0(6)	2.39	2	0.0	1.0	0.0
H(9c1)...0(6)	2.64	2	0.0	1.0	0.0
H(5b) ...0(6)	2.51	2	0.5	1.5	0.0
H(4b) ...0(6)	2.89	2	0.5	1.5	0.0
H(9c2)...0(w)	2.97	1	0.0	-1.0	0.0

TABLE 7 Intramolecular distances (Å)

C(1a) ...Zn	3.03	C(2a) ...Zn	3.03
C(3a) ...Zn	4.11	C(7a) ...Zn	3.32
C(8a) ...Zn	3.02	C(9a) ...Zn	3.03
C(9c) ...Zn	3.32	C(9b) ...Zn	3.00
C(8b) ...Zn	3.00	C(7b) ...Zn	3.37
C(3b) ...Zn	4.19	C(2b) ...Zn	3.06
C(1b) ...Zn	2.95	N(1) ...Zn	3.38
O(2) ...Zn	3.55	H(1a2)...Zn	3.35
HN(1a)...Zn	2.39	H(8a1)...Zn	3.07
HN(2a)...Zn	2.66	H(9a1)...Zn	3.18
H(9c1)...Zn	3.38	H(9b1)...Zn	3.27
HN(2b)...Zn	2.48	H(8b2)...Zn	3.06
HN(1b)...Zn	2.46	H(1b1)...Zn	3.82
H(1b2)...Zn	3.04	H(0w1)...Zn	2.69
H(0w2)...Zn	2.70	C(2a) ...C(1a)	2.52
C(3a) ...C(1a)	2.92	N(1b) ...C(1a)	2.42
HN(1a)...C(1a)	1.90	H(3a) ...C(1a)	2.71
HN(1b)...C(1a)	2.52	H(1b1)...C(1a)	2.09
H(1b2)...C(1a)	2.13	C(3a) ...N(1a)	2.48
C(7a) ...N(1a)	2.41	C(8a) ...N(1a)	2.83
N(2a) ...N(1a)	3.07	N(1b) ...N(1a)	2.83
C(1b) ...N(1a)	2.48	O(1) ...N(1a)	2.85
O(w) ...N(1a)	3.25	H(1a1)...N(1a)	2.10
H(1a2)...N(1a)	2.02	H(3a) ...N(1a)	2.90
H(8a1)...N(1a)	2.63	HN(1b)...N(1a)	3.00



table 7 continued

H(1b2)...N(1a)	2.72	C(4a) ...C(2a)	2.40
C(5a) ...C(2a)	2.78	C(6a) ...C(2a)	2.41
C(8a) ...C(2a)	2.54	N(2a) ...C(2a)	3.16
C(1b) ...C(2a)	3.36	O(w) ...C(2a)	3.28
H(1a1)...C(2a)	2.68	HN(1a)...C(2a)	1.94
H(3a) ...C(2a)	2.29	H(8a1)...C(2a)	2.72
C(5a) ...C(3a)	2.41	C(6a) ...C(3a)	2.77
C(7a) ...C(3a)	2.42	H(1a1)...C(3a)	2.67
H(4a) ...C(3a)	2.10	C(6a) ...C(4a)	2.39
C(7a) ...C(4a)	2.80	H(3a) ...C(4a)	2.13
H(5a) ...C(4a)	2.11	C(7a) ...C(5a)	2.42
H(4a) ...C(5a)	2.09	H(6a) ...C(5a)	2.13
C(8a) ...C(6a)	2.52	H(5a) ...C(6a)	1.87
H(8a2)...C(6a)	2.65	N(2a) ...C(7a)	2.50
HN(1a)...C(7a)	2.57	H(6a) ...C(7a)	2.05
H(8a1)...C(7a)	2.04	H(8a2)...C(7a)	2.13
HN(2a)...C(7a)	2.70	C(9a) ...C(8a)	2.45
O(1) ...C(8a)	3.40	HN(1a)...C(8a)	2.64
H(6a) ...C(8a)	2.60	HN(2a)...C(8a)	2.09
H(9a1)...C(8a)	2.56	H(9a2)...C(8a)	2.62
C(9c) ...N(2a)	2.52	C(9b) ...N(2a)	3.21
N(2b) ...N(2a)	3.16	O(1) ...N(2a)	3.04
O(w) ...N(2a)	3.08	HN(1a)...N(2a)	2.99
H(8a1)...N(2a)	1.97	H(8a2)...N(2a)	1.98
H(9a1)...N(2a)	2.00	H(9a2)...N(2a)	2.01
H(9c1)...N(2a)	2.47	C(9b) ...C(9a)	2.58
N(2b) ...C(9a)	3.23	O(1) ...C(9a)	3.17
H(8a1)...C(9a)	2.62	H(8a2)...C(9a)	2.50

table 7 continued

HN(2a)...C(9a)	2.10	H(9c1)...C(9a)	1.95
H(9c2)...C(9a)	2.01	H(9b1)...C(9a)	2.78
N(2b) ...C(9c)	2.51	HN(2a)...C(9c)	2.75
H(9a1)...C(9c)	2.19	H(9a2)...C(9c)	2.08
H(9b1)...C(9c)	2.10	H(9b2)...C(9c)	2.05
HN(2b)...C(9c)	2.78	C(8b) ...C(9b)	2.46
O(1) ...C(9b)	3.31	H(9a1)...C(9b)	2.78
H(9c1)...C(9b)	2.17	H(9c2)...C(9b)	2.06
HN(2b)...C(9b)	2.11	H(8b1)...C(9b)	2.61
H(8b2)...C(9b)	2.61	C(7b) ...N(2b)	2.48
C(2b) ...N(2b)	3.11	N(1b) ...N(2b)	3.06
O(1) ...N(2b)	3.23	O(w) ...N(2b)	3.18
H(9c1)...N(2b)	2.70	H(9b1)...N(2b)	2.07
H(9b2)...N(2b)	1.98	H(8b1)...N(2b)	2.05
H(8b2)...N(2b)	1.98	C(6b) ...C(8b)	2.50
C(2b) ...C(8b)	2.55	N(1b) ...C(8b)	2.88
O(2) ...C(8b)	3.32	H(9b1)...C(8b)	2.65
H(9b2)...C(8b)	2.61	HN(2b)...C(8b)	2.03
H(6b) ...C(8b)	2.68	HN(1b)...C(8b)	2.79
C(5b) ...C(7b)	2.44	C(4b) ...C(7b)	2.82
C(3b) ...C(7b)	2.44	N(1b) ...C(7b)	2.44
HN(2b)...C(7b)	2.51	H(8b1)...C(7b)	1.98
H(8b2)...C(7b)	2.15	H(6b) ...C(7b)	2.07
HN(1b)...C(7b)	2.63	C(4b) ...C(6b)	2.41
C(3b) ...C(6b)	2.77	C(2b) ...C(6b)	2.39
H(8b1)...C(6b)	2.44	H(5b) ...C(6b)	2.30
C(3b) ...C(5b)	2.41	C(2b) ...C(5b)	2.79
H(6b) ...C(5b)	2.05	H(4b) ...C(5b)	2.10

table 7 continued

C(2b) ...C(4b)	2.42	H(5b) ...C(4b)	2.07
H(3b) ...C(4b)	2.24	N(1b) ...C(3b)	2.49
C(1b) ...C(3b)	2.85	H(4b) ...C(3b)	2.18
HN(1b)...C(3b)	3.07	H(1b1)...C(3b)	2.72
H(1b2)...C(3b)	2.69	C(1b) ...C(2b)	2.49
O(w) ...C(2b)	3.25	H(8b2)...C(2b)	2.91
H(3b) ...C(2b)	2.12	HN(1b)...C(2b)	1.94
H(1b1)...C(2b)	2.68	H(1b2)...C(2b)	2.60
O(1) ...N(1b)	3.36	O(2) ...N(1b)	3.12
O(w) ...N(1b)	2.97	H(1a2)...N(1b)	2.57
H(8b2)...N(1b)	2.88	H(3b) ...N(1b)	2.62
H(1b1)...N(1b)	2.00	H(1b2)...N(1b)	1.95
O(w) ...C(1b)	3.26	H(1a1)...C(1b)	2.19
H(1a2)...C(1b)	2.00	HN(1a)...C(1b)	3.04
H(3b) ...C(1b)	2.35	HN(1b)...C(1b)	1.96
HN(1a)...N(1)	2.99	HN(1b)...N(1)	2.92
O(2) ...O(1)	2.15	O(3) ...O(1)	2.16
HN(1a)...O(1)	2.28	H(8a1)...O(1)	2.76
H(9a1)...O(1)	2.53	H(9b1)...O(1)	2.83
HN(1b)...O(1)	2.93	O(3) ...O(2)	2.15
H(8b2)...O(2)	2.44	HN(1b)...O(2)	2.29
O(5) ...O(4)	2.16	O(6) ...O(4)	2.13
H(9b2)...O(4)	2.82	O(6) ...O(5)	2.10
HN(2a)...O(w)	2.78	HN(2b)...O(w)	2.79
H(1b2)...O(w)	2.67		

A6     Tables for  $[\text{Cd}(\text{L}15)(\text{NO}_2)_2](\text{NO}_2)_2$ .

X-ray structure of  $[\text{Cd}(\text{L15})(\text{NO}_2)_2](\text{NO}_3)_2$ .

(6,7,8,9,10,11,16,17,18,19-decahydro-5H-dibenzo-  
[e,n][1,4,8,12]tetra-azacyclotetradecine)nitrate-  
cadmium(II) nitrate.

Crystal data:  $\text{C}_{19}\text{H}_{26}\text{N}_6\text{O}_6\text{Cd}$ , Mwt = 546.8, monoclinic,

space group  $\text{P}2_1/\text{c}$ ,  $a = 8.310(4) \text{ \AA}$ ,  $b = 18.945(5) \text{ \AA}$ ,

$c = 7.905(4) \text{ \AA}$ . Beta =  $100.09(2)^\circ$ ,  $V = 2224.5 \text{ \AA}^3$ ,

$D_c = 1.62 \text{ gm}^{-3}$ ,  $F_{000} = 1292$ .

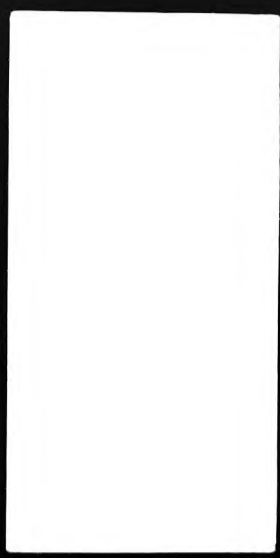
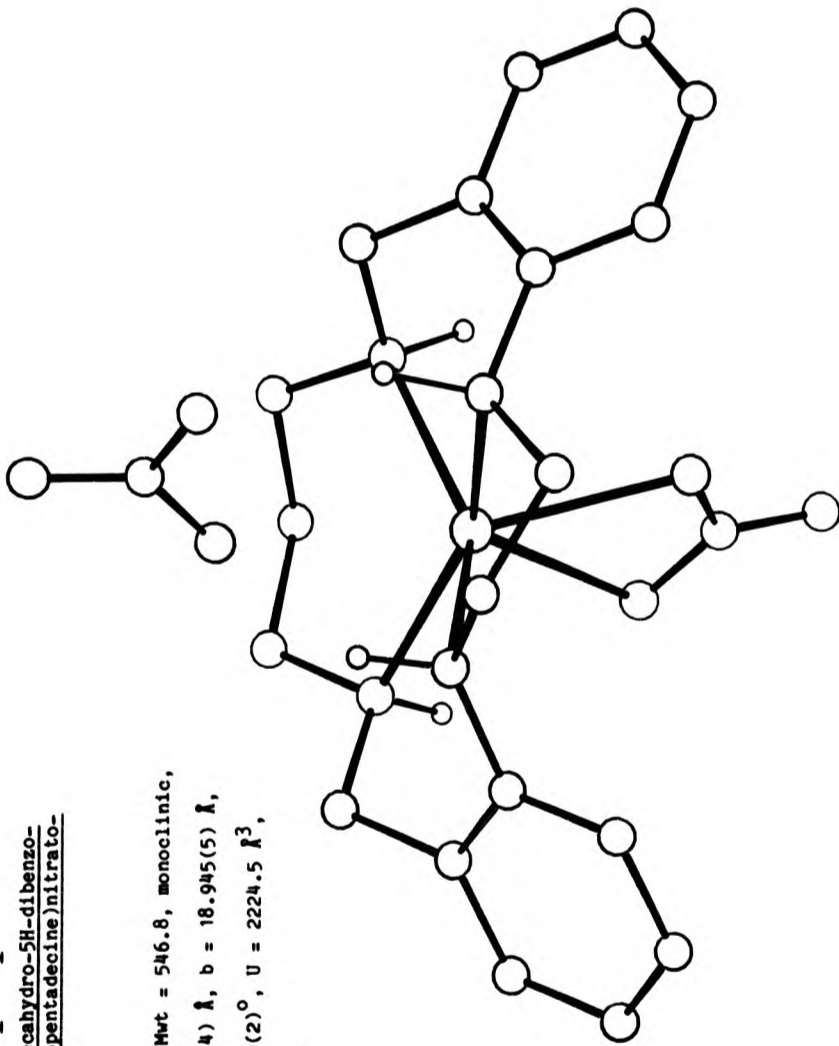


TABLE 1 Fractional atomic coordinates and thermal parameters ( $\text{\AA}^2$ )

Atom	x	y	z	Uiso or Ueq
Cd	0.01006(8)	0.15370(3)	0.12996(4)	0.0458(4)
N(1)	0.1814(9)	0.1300(4)	-0.0231(6)	0.055(5)
O(1)	0.2061(10)	0.1781(4)	0.0336(6)	0.111(6)
O(2)	0.0859(11)	0.0855(4)	-0.0088(5)	0.110(7)
O(3)	0.2469(9)	0.1294(4)	-0.0922(5)	0.085(5)
C(1a)	0.2512(11)	0.1839(5)	0.3291(6)	0.059(6)
N(1a)	0.1571(8)	0.1225(3)	0.2846(5)	0.049(4)
C(2a)	0.2260(11)	0.0548(4)	0.2733(6)	0.050(6)
C(3a)	0.3916(11)	0.0441(5)	0.2841(6)	0.062(6)
C(4a)	0.4503(12)	-0.0223(6)	0.2669(7)	0.075(7)
C(5a)	0.3453(13)	-0.0779(5)	0.2391(7)	0.072(7)
C(6a)	0.1812(13)	-0.0667(4)	0.2281(6)	0.062(6)
C(7a)	0.1158(11)	-0.0013(4)	0.2442(6)	0.047(5)
C(8a)	-0.0669(11)	0.0091(4)	0.2253(6)	0.047(5)
N(2a)	-0.1207(8)	0.0487(3)	0.1358(4)	0.045(4)
C(9a)	-0.2993(10)	0.0559(5)	0.1117(7)	0.060(6)
C(9c)	-0.3577(11)	0.1051(5)	0.0288(6)	0.055(6)
C(9b)	-0.3611(10)	0.1837(5)	0.0527(7)	0.057(6)
N(2b)	-0.2001(8)	0.2186(3)	0.0534(4)	0.047(4)
C(8b)	-0.1987(11)	0.2926(4)	0.0902(6)	0.054(6)
C(7b)	-0.0449(12)	0.3307(4)	0.0808(6)	0.054(6)
C(6b)	-0.0502(13)	0.3853(4)	0.0142(6)	0.062(7)
C(5b)	0.0901(16)	0.4183(5)	0.0007(7)	0.075(8)
C(4b)	0.2366(15)	0.4004(5)	0.0520(8)	0.077(8)
C(3b)	0.2489(12)	0.3477(5)	0.1198(6)	0.064(6)

table 1 continued

C(2b)	0.1084(12)	0.3148(4)	0.1370(6)	0.050(6)
N(1b)	0.1156(8)	0.2599(3)	0.2070(5)	0.047(4)
C(1b)	0.2751(12)	0.2393(5)	0.2598(7)	0.060(6)
K(2)	-0.2265(10)	0.2127(4)	0.3272(5)	0.053(5)
O(4)	-0.1869(8)	0.1656(3)	0.2762(5)	0.077(5)
O(5)	-0.1288(10)	0.2627(4)	0.3485(5)	0.085(5)
O(6)	-0.3480(9)	0.2104(5)	0.3603(6)	0.103(6)

TABLE 2 Fractional atomic coordinates for the hydrogen atoms

Atom	x	y	z
H(1a)	0.3558	0.1640	0.3714
H(1a2)	0.1916	0.2109	0.3877
HN(1a)	0.0573	0.1364	0.2790
H(3a)	0.4618	0.0885	0.3007
H(4a)	0.5587	-0.0333	0.2355
H(5a)	0.4086	-0.1261	0.2278
H(6a)	0.1348	-0.1182	0.2182
H(8a1)	-0.0873	0.0387	0.2869
H(8a2)	-0.1232	-0.0412	0.2256
HN(2a)	-0.1072	0.0227	0.0648
H(9a1)	-0.3517	0.0764	0.1611
H(9a2)	-0.3512	0.0191	0.1196
H(9c1)	-0.4642	0.0841	0.0023
H(9c2)	-0.3141	0.0947	-0.0367
H(9b1)	-0.4060	0.1933	0.1161
H(9b2)	-0.4462	0.2087	-0.0031
HN(2b)	-0.1769	0.2174	-0.0218
H(8b1)	-0.2007	0.2873	0.1593
H(8b2)	-0.3240	0.3116	0.0647
H(6b)	-0.1925	0.3845	-0.0267
H(5b)	0.0776	0.4649	-0.0539
H(4b)	0.3519	0.4326	0.0458
H(3b)	0.3360	0.3378	0.1750
HN(1b)	0.0127	0.2719	0.2436
H(1b1)	0.3747	0.2170	0.2159
H(1b2)	0.3266	0.2850	0.3014



TABLE 3 Anisotropic thermal parameters ( $\text{\AA}^2$ )

Atom	U11	U22	U33	U23	U13	U12
Cd	0.0443(4)	0.0381(3)	0.0551(4)	-0.0013(4)	0.0046(3)	-0.0023(4)
N(1)	0.046(5)	0.056(5)	0.063(6)	-0.015(4)	0.017(4)	-0.005(4)
O(1)	0.104(6)	0.116(6)	0.113(6)	-0.059(6)	0.043(5)	-0.034(5)
O(2)	0.139(8)	0.097(6)	0.094(6)	-0.023(5)	0.069(6)	-0.032(6)
O(3)	0.090(5)	0.086(5)	0.079(5)	-0.011(4)	0.040(4)	-0.009(4)
C(1a)	0.058(6)	0.060(6)	0.060(6)	-0.001(5)	-0.014(5)	-0.008(5)
N(1a)	0.043(4)	0.041(4)	0.062(5)	-0.006(4)	-0.005(4)	0.002(4)
C(2a)	0.053(6)	0.047(5)	0.050(5)	0.019(4)	0.010(5)	0.003(5)
C(3a)	0.057(6)	0.055(6)	0.075(7)	0.021(5)	0.016(5)	0.008(5)
C(4a)	0.065(7)	0.076(7)	0.084(8)	0.032(6)	0.034(6)	0.017(6)
C(5a)	0.069(8)	0.051(6)	0.096(8)	0.023(6)	0.023(7)	0.027(6)
C(6a)	0.088(8)	0.034(5)	0.063(6)	0.010(4)	0.023(6)	0.010(5)
C(7a)	0.059(6)	0.036(5)	0.047(5)	0.009(4)	0.008(5)	-0.004(5)

Table 3 continued

C(8a)	0.059(6)	0.030(4)	0.052(5)	0.007(4)	0.007(4)	-0.010(4)
N(2a)	0.042(4)	0.039(4)	0.055(4)	-0.007(3)	0.011(3)	-0.007(3)
C(9a)	0.034(5)	0.062(6)	0.084(7)	0.002(5)	0.019(5)	-0.018(5)
C(9c)	0.054(6)	0.060(6)	0.051(6)	-0.011(5)	-0.006(5)	-0.013(5)
C(9b)	0.033(5)	0.060(6)	0.079(7)	0.020(5)	0.004(5)	0.012(4)
N(2b)	0.047(4)	0.051(4)	0.041(4)	-0.001(3)	0.008(3)	0.004(4)
C(8b)	0.055(6)	0.044(5)	0.064(6)	-0.003(5)	0.007(5)	0.007(5)
C(7b)	0.071(7)	0.030(5)	0.062(6)	-0.014(4)	0.006(6)	-0.000(5)
C(6b)	0.093(8)	0.033(5)	0.059(6)	-0.007(5)	0.015(6)	0.002(6)
C(5b)	0.127(11)	0.035(5)	0.064(7)	-0.009(5)	0.026(7)	-0.022(7)
C(4b)	0.099(9)	0.051(6)	0.082(8)	-0.022(6)	0.028(7)	-0.035(7)
C(3b)	0.072(7)	0.055(6)	0.064(6)	-0.019(6)	0.011(5)	-0.028(6)
C(2b)	0.066(7)	0.036(5)	0.050(6)	-0.014(4)	0.013(5)	-0.009(5)
N(1b)	0.049(5)	0.039(4)	0.053(4)	-0.006(3)	0.005(4)	-0.002(4)
C(1b)	0.060(6)	0.049(6)	0.072(7)	-0.008(5)	-0.007(5)	-0.018(5)
N(2)	0.050(5)	0.062(5)	0.048(5)	-0.004(4)	-0.000(4)	-0.003(5)

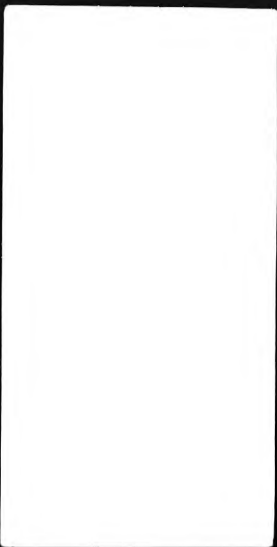


Table 3 continued

O(4)	0.089(5)	0.062(4)	0.080(5)	-0.033(4)	0.020(4)	-0.000(4)
O(5)	0.116(7)	0.058(4)	0.083(5)	-0.006(4)	0.031(5)	-0.010(5)
O(6)	0.046(4)	0.153(8)	0.110(6)	-0.043(6)	0.022(5)	-0.010(5)

TABLE 4 Bond lengths ( $\text{\AA}$ )

Cd	-O(1)	2.360(9)	Cd	-O(2)	2.544(8)
Cd	-N(1a)	2.412(6)	Cd	-N(2a)	2.275(6)
Cd	-N(2b)	2.257(6)	Cd	-N(1b)	2.387(6)
N(1)	-O(1)	1.214(12)	N(1)	-O(2)	1.201(12)
N(1)	-O(3)	1.212(12)	C(1a)	-N(1a)	1.483(11)
C(1a)	-C(1b)	1.483(14)	N(1a)	-C(2a)	1.426(11)
C(2a)	-C(3a)	1.372(13)	C(2a)	-C(7a)	1.417(12)
C(3a)	-C(4a)	1.387(14)	C(4a)	-C(5a)	1.381(14)
C(5a)	-C(6a)	1.362(15)	C(6a)	-C(7a)	1.387(12)
C(7a)	-C(8a)	1.507(13)	C(8a)	-N(2a)	1.487(10)
N(2a)	-C(9a)	1.470(10)	C(9a)	-C(9c)	1.523(12)
C(9c)	-C(9b)	1.529(13)	C(9b)	-N(2b)	1.490(11)
N(2b)	-C(8b)	1.498(11)	C(8b)	-C(7b)	1.494(14)
C(7b)	-C(6b)	1.405(12)	C(7b)	-C(2b)	1.415(13)
C(6b)	-C(5b)	1.366(17)	C(5b)	-C(4b)	1.350(16)
C(4b)	-C(3b)	1.385(14)	C(3b)	-C(2b)	1.384(14)
C(2b)	-N(1b)	1.440(11)	N(1b)	-C(1b)	1.460(11)
N(2)	-O(4)	1.235(11)	N(2)	-O(5)	1.251(11)
N(2)	-O(6)	1.190(12)			

TABLE 5 Bond angles (°)

O(2) -Cd -O(1)	49.4(3)	N(1a) -Cd -O(1)	107.3(3)
N(1a) -Cd -O(2)	116.1(2)	N(2a) -Cd -O(1)	125.2(3)
N(2a) -Cd -O(2)	76.7(3)	N(2a) -Cd -N(1a)	85.4(2)
N(2b) -Cd -O(1)	99.4(3)	N(2b) -Cd -O(2)	99.9(2)
N(2b) -Cd -N(1a)	143.6(2)	N(2b) -Cd -N(2a)	99.2(2)
N(1b) -Cd -O(1)	82.6(3)	N(1b) -Cd -O(2)	132.0(3)
N(1b) -Cd -N(1a)	72.2(2)	N(1b) -Cd -N(2a)	149.2(2)
N(1b) -Cd -N(2b)	87.5(2)	O(2) -N(1) -O(1)	116.8(9)
O(3) -N(1) -O(1)	120.6(9)	O(3) -N(1) -O(2)	122.5(8)
N(1) -O(1) -Cd	101.2(6)	N(1) -O(2) -Cd	92.2(6)
C(1b) -C(1a) -N(1a)	112.9(7)	C(1a) -N(1a) -Cd	110.3(5)
C(2a) -N(1a) -Cd	105.3(5)	C(2a) -N(1a) -C(1a)	124.3(7)
C(3a) -C(2a) -N(1a)	122.3(8)	C(7a) -C(2a) -N(1a)	117.2(8)
C(7a) -C(2a) -C(3a)	120.4(8)	C(4a) -C(3a) -C(2a)	119.4(8)
C(5a) -C(4a) -C(3a)	121.3(9)	C(6a) -C(5a) -C(4a)	118.9(9)
C(7a) -C(6a) -C(5a)	122.3(9)	C(6a) -C(7a) -C(2a)	117.8(8)
C(8a) -C(7a) -C(2a)	122.3(7)	C(8a) -C(7a) -C(6a)	119.9(7)
N(2a) -C(8a) -C(7a)	111.2(7)	C(8a) -N(2a) -Cd	113.6(4)
C(9a) -N(2a) -Cd	112.3(5)	C(9a) -N(2a) -C(8a)	112.9(7)
C(9c) -C(9a) -N(2a)	114.3(7)	C(9b) -C(9c) -C(9a)	115.9(7)
N(2b) -C(9b) -C(9c)	112.4(7)	C(9b) -N(2b) -Cd	112.3(5)
C(8b) -N(2b) -Cd	112.4(5)	C(8b) -N(2b) -C(9b)	111.7(7)
C(7b) -C(8b) -N(2b)	112.0(7)	C(6b) -C(7b) -C(8b)	119.4(8)
C(2b) -C(7b) -C(8b)	123.0(8)	C(2b) -C(7b) -C(6b)	117.6(9)
C(5b) -C(6b) -C(7b)	120.5(9)	C(4b) -C(5b) -C(6b)	121.2(9)

table 5 continued

C(3b) -C(4b) -C(5b)	121(1)	C(2b) -C(3b) -C(4b)	119.3(9)
C(3b) -C(2b) -C(7b)	120.3(8)	N(1b) -C(2b) -C(7b)	118.3(8)
N(1b) -C(2b) -C(3b)	121.2(8)	C(2b) -N(1b) -Cd	108.6(5)
C(1b) -N(1b) -Cd	104.0(5)	C(1b) -N(1b) -C(2b)	118.5(7)
N(1b) -C(1b) -C(1a)	108.7(8)	O(5) -N(2) -O(4)	117.6(9)
O(6) -N(2) -O(4)	123.0(9)	O(6) -N(2) -O(5)	119.3(9)

TABLE 6 Intermolecular distances ( $\text{\AA}$ )

HN(2a)...N(1)	3.00	-1	0.0	0.0	0.0
H(1a2)...O(1)	2.96	-2	0.0	1.0	1.0
N(2a)...O(2)	3.17	-1	0.0	0.0	0.0
HN(2a)...O(2)	2.22	-1	0.0	0.0	0.0
H(9c1)...O(3)	2.68	1	-1.0	0.0	0.0
H(8a2)...O(3)	2.61	-1	0.0	0.0	0.0
H(9a2)...O(3)	2.99	-1	0.0	0.0	0.0
C(1b)...O(3)	3.31	-2	0.0	1.0	1.0
H(1b2)...O(3)	2.40	-2	0.0	1.0	1.0
O(6)...C(1a)	3.32	1	-1.0	0.0	0.0
C(5b)...N(1a)	3.34	-2	0.0	1.0	0.0
H(5b)...N(1a)	3.01	-2	0.0	1.0	0.0
H(5b)...C(2a)	2.98	-2	0.0	1.0	0.0
H(9a1)...C(3a)	3.06	1	-1.0	0.0	0.0
H(9a1)...C(4a)	3.06	1	-1.0	0.0	0.0
H(9a2)...C(4a)	3.00	1	-1.0	0.0	0.0
H(4b)...C(4a)	3.02	2	1.0	0.0	0.0
H(9c2)...C(5a)	2.89	-1	0.0	0.0	0.0
O(5)...C(6a)	3.42	2	0.0	0.0	0.0
H(5b)...C(7a)	3.05	-2	0.0	1.0	0.0
H(4a)...C(9a)	2.85	1	1.0	0.0	0.0
O(5)...N(2b)	3.12	-2	0.0	1.0	1.0
O(6)...N(2b)	3.13	-2	0.0	1.0	1.0
O(6)...C(8b)	3.32	-2	0.0	1.0	1.0
H(5b)...C(6b)	2.91	-1	0.0	1.0	0.0

table 6 continued

N(2) ...C(6b)	3.38	-2	0.0	1.0	1.0
C(5b) ...C(5b)	3.44	-1	0.0	1.0	0.0
H(5b) ...C(5b)	2.79	-1	0.0	1.0	0.0
O(6) ...C(1b)	3.26	1	-1.0	0.0	0.0
HN(2b)...N(2)	2.51	-2	0.0	1.0	0.0
H(7b) ...N(2)	2.77	-2	0.0	1.0	0.0
H(7b) ...O(4)	2.99	-2	0.0	1.0	0.0
H(6a) ...O(5)	2.45	2	0.0	-1.0	0.0
HN(2b)...O(5)	2.01	-2	0.0	1.0	0.0
H(1a) ...O(6)	2.64	1	1.0	0.0	0.0
H(3a) ...O(6)	2.84	1	1.0	0.0	0.0
H(1b1)...O(6)	2.82	1	1.0	0.0	0.0
H(9b2)...O(6)	2.72	-2	0.0	1.0	0.0
HN(2b)...O(6)	2.43	-2	0.0	1.0	0.0
H(8b2)...O(6)	2.94	-2	0.0	1.0	0.0
H(7b) ...O(6)	2.61	-2	0.0	1.0	0.0



TABLE 7 Intramolecular distances (Å)

N(1) ...Cd	2.85	O(3) ...Cd	4.06
C(1a) ...Cd	3.24	C(2a) ...Cd	3.11
C(3a) ...Cd	4.10	C(7a) ...Cd	3.40
C(8a) ...Cd	3.18	C(9a) ...Cd	3.14
C(9c) ...Cd	3.28	C(9b) ...Cd	3.14
C(8b) ...Cd	3.15	C(7b) ...Cd	3.44
C(3b) ...Cd	4.19	C(2b) ...Cd	3.16
C(1b) ...Cd	3.08	N(2) ...Cd	3.88
O(4) ...Cd	2.89	O(5) ...Cd	4.09
H(8a1)...Cd	3.33	HN(2a)...Cd	2.77
H(9a1)...Cd	3.44	H(9c2)...Cd	3.46
H(9b1)...Cd	3.51	HN(2b)...Cd	2.73
H(8b1)...Cd	3.15	HN(1b)...Cd	2.77
H(1b1)...Cd	3.29	O(2) ...O(1)	2.06
O(3) ...O(1)	2.11	C(2b) ...O(1)	3.16
N(1b) ...O(1)	3.13	C(1b) ...O(1)	3.40
H(1b1)...O(1)	2.84	O(3) ...O(2)	2.12
N(2a) ...O(2)	3.00	HN(2a)...O(2)	2.39
C(2a) ...C(1a)	2.57	C(3a) ...C(1a)	3.01
N(1b) ...C(1a)	2.39	HN(1a)...C(1a)	1.88
H(3a) ...C(1a)	2.60	HN(1b)...C(1a)	2.71
H(1b1)...C(1a)	2.16	H(1b2)...C(1a)	2.07
C(3a) ...N(1a)	2.45	C(7a) ...N(1a)	2.43
C(8a) ...N(1a)	2.87	N(2a) ...N(1a)	3.18
N(1b) ...N(1a)	2.83	C(1b) ...N(1a)	2.47

table 7 continued

O(4) ...N(1a)	2.96	H(1a) ...N(1a)	2.04
H(1a2)...N(1a)	2.22	H(3a) ...N(1a)	2.58
H(8a1)...N(1a)	2.58	H(1b1)...N(1a)	2.84
C(4a) ...C(2a)	2.38	C(5a) ...C(2a)	2.78
C(6a) ...C(2a)	2.40	C(8a) ...C(2a)	2.56
N(2a) ...C(2a)	3.20	H(1a) ...C(2a)	2.63
HN(1a)...C(2a)	2.10	H(3a) ...C(2a)	2.03
H(8a1)...C(2a)	2.66	C(5a) ...C(3a)	2.41
C(6a) ...C(3a)	2.76	C(7a) ...C(3a)	2.42
H(1a) ...C(3a)	2.64	H(4a) ...C(3a)	2.22
C(6a) ...C(4a)	2.36	C(7a) ...C(4a)	2.77
H(3a) ...C(4a)	2.15	H(5a) ...C(4a)	2.06
C(7a) ...C(5a)	2.41	H(4a) ...C(5a)	1.97
H(6a) ...C(5a)	1.88	C(8a) ...C(6a)	2.51
N(2a) ...C(6a)	3.41	H(5a) ...C(6a)	2.20
H(8a2)...C(6a)	2.57	N(2a) ...C(7a)	2.47
HN(1a)...C(7a)	2.72	H(6a) ...C(7a)	2.26
H(8a1)...C(7a)	2.04	H(8a2)...C(7a)	2.10
HN(2a)...C(7a)	2.93	C(9a) ...C(8a)	2.46
O(4) ...C(8a)	3.25	HN(1a)...C(8a)	2.68
H(6a) ...C(8a)	2.95	HN(2a)...C(8a)	2.28
H(9a1)...C(8a)	2.71	H(9a2)...C(8a)	2.58
C(9c) ...N(2a)	2.51	C(9b) ...N(2a)	3.34
O(4) ...N(2a)	3.11	HN(1a)...N(2a)	2.85
H(8a1)...N(2a)	2.15	H(8a2)...N(2a)	2.14
H(9a1)...N(2a)	2.08	H(9a2)...N(2a)	1.97
H(9c2)...N(2a)	2.84	C(9b) ...C(9a)	2.59
N(2b) ...C(9a)	3.33	O(4) ...C(9a)	3.16

table 7 continued

H(8a1)...C(9a)	2.82	H(8a2)...C(9a)	2.71
HN(2a)...C(9a)	1.94	H(9c1)...C(9a)	1.97
H(9c2)...C(9a)	2.24	H(9b1)...C(9a)	2.75
N(2b) ...C(9c)	2.51	HN(2a)...C(9c)	2.58
H(9a1)...C(9c)	1.97	H(9a2)...C(9c)	2.08
H(9b1)...C(9c)	2.17	H(9b2)...C(9c)	2.12
HN(2b)...C(9c)	2.77	C(8b) ...C(9b)	2.47
O(4) ...C(9b)	3.30	H(9a1)...C(9b)	2.55
H(9c1)...C(9b)	2.15	H(9c2)...C(9b)	2.19
HN(2b)...C(9b)	2.11	H(8b1)...C(9b)	2.69
H(8b2)...C(9b)	2.44	C(7b) ...N(2b)	2.48
C(2b) ...N(2b)	3.20	N(1b) ...N(2b)	3.21
O(4) ...N(2b)	3.33	H(9c2)...N(2b)	2.76
H(9b1)...N(2b)	2.12	H(9b2)...N(2b)	2.07
H(8b1)...N(2b)	2.00	H(8b2)...N(2b)	2.06
C(6b) ...C(8b)	2.50	C(2b) ...C(8b)	2.56
N(1b) ...C(8b)	2.91	H(9b1)...C(8b)	2.62
H(9b2)...C(8b)	2.75	HN(2b)...C(8b)	2.18
H(7b) ...C(8b)	2.42	HN(1b)...C(8b)	2.59
C(5b) ...C(7b)	2.41	C(4b) ...C(7b)	2.78
C(3b) ...C(7b)	2.43	N(1b) ...C(7b)	2.45
HN(2b)...C(7b)	2.72	H(8b1)...C(7b)	2.03
H(8b2)...C(7b)	2.32	H(7b) ...C(7b)	2.06
HN(1b)...C(7b)	2.56	C(4b) ...C(6b)	2.37
C(3b) ...C(6b)	2.77	C(2b) ...C(6b)	2.41
H(8b2)...C(6b)	2.87	H(5b) ...C(6b)	2.17
C(3b) ...C(5b)	2.38	C(2b) ...C(5b)	2.75
H(7b) ...C(5b)	2.40	H(4b) ...C(5b)	2.18

table 7 continued

C(2b) ...C(4b)	2.39	H(5b) ...C(4b)	2.20
H(3b) ...C(4b)	2.17	N(1b) ...C(3b)	2.46
C(1b) ...C(3b)	2.85	H(4b) ...C(3b)	2.18
H(1b1)...C(3b)	2.94	H(1b2)...C(3b)	2.84
C(1b) ...C(2b)	2.49	H(8b1)...C(2b)	2.69
H(3b) ...C(2b)	1.92	HN(1b)...C(2b)	2.01
H(1b1)...C(2b)	2.96	H(1b2)...C(2b)	2.77
O(5) ...N(1b)	3.11	H(1a2)...N(1b)	2.72
HN(1a)...N(1b)	2.64	H(8b1)...N(1b)	2.65
H(3b) ...N(1b)	2.46	H(1b1)...N(1b)	2.28
H(1b2)...N(1b)	2.07	H(1a) ...C(1b)	2.16
H(1a2)...C(1b)	2.14	HN(1a)...C(1b)	2.71
H(3b) ...C(1b)	2.33	HN(1b)...C(1b)	2.24
HN(1a)...N(2)	2.95	H(8b1)...N(2)	2.83
HN(1b)...N(2)	2.74	O(5) ...O(4)	2.13
O(6) ...O(4)	2.13	HN(1a)...O(4)	2.10
H(8a1)...O(4)	2.54	H(9a1)...O(4)	2.58
H(9b1)...O(4)	2.72	H(8b1)...O(4)	2.84
HN(1b)...O(4)	2.70	O(6) ...O(5)	2.11
H(1a2)...O(5)	2.80	H(8b1)...O(5)	2.72
HN(1b)...O(5)	2.07		

A7      Tables for [Cd(L,15b)(NO<sub>2</sub>)](NO<sub>2</sub>)<sub>2</sub>.

X-ray structure of [Cd(L15b)(NO<sub>3</sub>)<sub>2</sub>](NO<sub>3</sub>)<sub>2</sub>

(5,11-di-n-butyl-7,8,9,10,11,16,17,18,19-decahydro-5H-dibenzo[e,n][1,4,8,12]tetra-azacyclotetradecine)-nitrate cadmium(II) nitrate.

Crystal data: C<sub>27</sub>H<sub>42</sub>N<sub>6</sub>O<sub>6</sub>Cd, Mwt = 659.1, monoclinic,

space group, P2<sub>1</sub>/n, a = 16.487(3) Å, b = 23.196(4) Å,

c = 7.905(4) Å. Beta = 98.799(3)°, U = 2987.6 Å<sup>3</sup>,

D<sub>c</sub> = 1.46 gcm<sup>-3</sup>, F<sub>000</sub> = 1368.

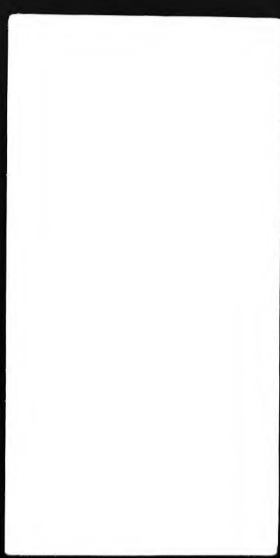
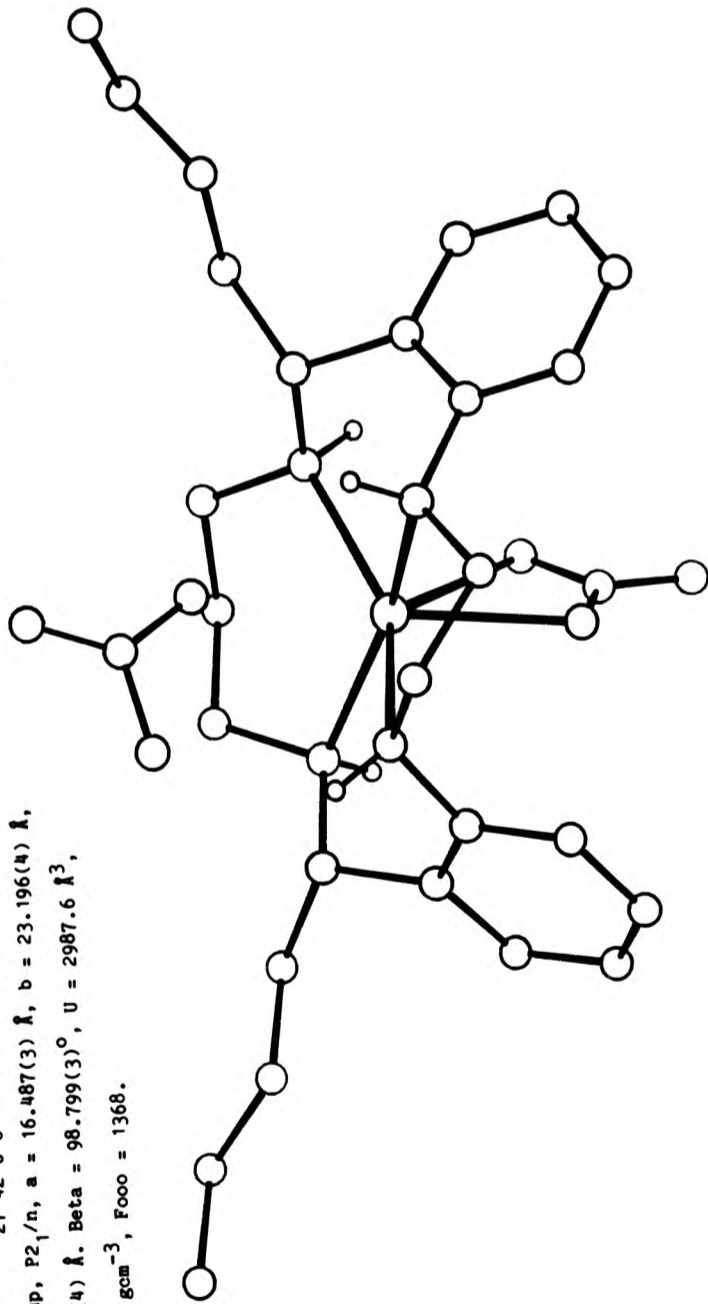


TABLE 1 Fractional atomic coordinates and thermal parameters ( $\text{\AA}^2$ )

Atom	x	y	z	$U_{\text{iso}}$ or $U_{\text{eq}}$
Cd	0.13796(4)	0.22712(3)	0.12722(8)	0.0477(4)
N(1a)	0.2396(4)	0.2031(3)	-0.0316(8)	0.048(4)
N(1b)	0.1764(4)	0.3173(3)	0.0080(9)	0.053(4)
N(2a)	0.0824(4)	0.1381(3)	0.0726(9)	0.053(5)
N(2b)	0.0281(4)	0.2746(3)	0.1940(8)	0.049(4)
C(1a)	0.2934(5)	0.2527(4)	-0.0205(12)	0.057(6)
C(1b)	0.2454(5)	0.3061(4)	-0.0863(12)	0.062(6)
C(9a)	-0.0069(5)	0.1414(4)	0.0244(14)	0.066(7)
C(9c)	-0.0469(5)	0.1812(4)	0.1402(14)	0.077(7)
C(9b)	-0.0462(5)	0.2457(4)	0.1065(14)	0.065(6)
C(8a)	0.1290(5)	0.1079(4)	-0.0496(12)	0.054(6)
C(8b)	0.0331(5)	0.3377(3)	0.1582(12)	0.050(6)
C(10b)	-0.0394(5)	0.3702(4)	0.2136(12)	0.060(6)
C(11b)	-0.0405(5)	0.4343(4)	0.1689(13)	0.062(6)
C(12b)	-0.1207(6)	0.4632(4)	0.1923(14)	0.079(7)
C(13b)	-0.1212(7)	0.5285(4)	0.1439(17)	0.091(9)
C(10a)	0.0903(6)	0.0504(4)	-0.1107(14)	0.083(8)
C(11a)	0.1318(7)	0.0205(5)	-0.2542(16)	0.115(10)
C(2a)	0.2709(5)	0.1494(4)	0.0350(11)	0.048(2)
C(3a)	0.3511(5)	0.1449(4)	0.1103(12)	0.059(2)
C(4a)	0.3790(6)	0.0937(4)	0.1844(14)	0.078(3)
C(5a)	0.3283(6)	0.0476(5)	0.1826(14)	0.076(3)
C(6a)	0.2465(6)	0.0515(4)	0.1057(12)	0.066(3)
C(7a)	0.2177(5)	0.1028(4)	0.0292(11)	0.054(2)
C(2b)	0.1852(5)	0.3504(4)	0.1593(12)	0.052(2)

table 1 continued

C(3b)	0.2616(6)	0.3689(4)	0.2380(12)	0.059(3)
C(4b)	0.2691(6)	0.3953(4)	0.3965(13)	0.066(3)
C(5b)	0.2029(6)	0.4023(4)	0.4759(14)	0.070(3)
C(6b)	0.1270(5)	0.3851(3)	0.3997(12)	0.056(2)
C(7b)	0.1165(5)	0.3588(3)	0.2405(11)	0.046(2)
C(12a)	0.0963(13)	-0.0227(9)	-0.3502(30)	0.096(7)
C(13a)	0.1290(15)	-0.0381(11)	-0.5119(36)	0.131(9)
C(12c)	0.1225(12)	0.0460(8)	-0.3922(27)	0.091(6)
C(13c)	0.1437(14)	0.0049(10)	-0.5514(32)	0.097(7)
O(1a)	0.2405(5)	0.2349(3)	0.3632(10)	0.088(5)
O(1b)	0.2576(4)	0.1942(4)	0.6094(9)	0.091(5)
O(1c)	0.1546(5)	0.1744(4)	0.4255(10)	0.103(6)
N(1n)	0.2185(5)	0.2018(4)	0.4687(12)	0.064(6)
O(2a)	0.0696(5)	0.2311(4)	-0.2083(10)	0.094(6)
O(2b)	0.0494(5)	0.3177(5)	-0.2894(13)	0.122(8)
O(2c)	-0.0042(5)	0.2497(5)	-0.4505(11)	0.136(8)
N(2n)	0.0375(6)	0.2630(6)	-0.3218(15)	0.091(8)
HN(1a)	0.21630	0.19680	-0.14150	0.0500
HN(1b)	0.14240	0.34010	-0.06080	0.0500
HN(2a)	0.10380	0.11810	0.17490	0.0500
HN(2b)	0.02990	0.27170	0.31280	0.0500



TABLE 2 Fractional atomic coordinates for the hydrogen atoms

Atom	x	y	z
H(1a1)	0.3191	0.2591	0.1122
H(1a1)	0.3423	0.2453	-0.0945
H(1b1)	0.2225	0.3001	-0.2206
H(1b2)	0.2856	0.3432	-0.0705
H(9a1)	-0.0185	0.1601	-0.1021
H(9a2)	-0.0340	0.0990	0.0215
H(9c1)	-0.1092	0.1671	0.1415
H(9c2)	-0.0115	0.1751	0.2656
H(9b1)	-0.0993	0.2648	0.1489
H(9b2)	-0.0494	0.2521	-0.0297
H(8a1)	0.1229	0.1333	-0.1653
H(8b1)	0.0249	0.3444	0.0214
H(3a)	0.3922	0.1811	0.1086
H(4a)	0.4419	0.0902	0.2462
H(5a)	0.3517	0.0077	0.2411
H(6a)	0.2058	0.0149	0.1047
H(3b)	0.3153	0.3616	0.1778
H(4b)	0.3285	0.4108	0.4555
H(5b)	0.2107	0.4221	0.6010
H(6b)	0.0744	0.3914	0.4638
H(101)	-0.0974	0.3515	0.1576
H(102)	-0.0318	0.3658	0.3511
H(111)	-0.0278	0.4402	0.0400
H(112)	0.0055	0.4563	0.2576
H(121)	-0.1305	0.4624	0.3242

table 2 continued

H(122)	-0.1677	0.4380	0.1154
H(131)	-0.1807	0.5465	0.1535
H(132)	-0.1114	0.5292	0.0120
H(133)	-0.0742	0.5536	0.2208
H(103)	0.0987	0.0217	-0.0018
H(104)	0.0255	0.0560	-0.1550
H(113)	0.1936	0.0120	-0.1919
H(114)	0.0958	0.0369	-0.1616

TABLE 3 Anisotropic thermal parameters ( $\text{\AA}^2$ )

Atom	$U_{11}$	$U_{22}$	$U_{33}$	$U_{23}$	$U_{13}$	$U_{12}$
Cd	0.0437(3)	0.0530(4)	0.0463(4)	-0.0004(5)	0.0075(2)	0.0003(4)
N(1a)	0.047(4)	0.061(5)	0.035(4)	-0.003(4)	0.004(4)	-0.001(4)
N(1b)	0.053(4)	0.052(4)	0.053(5)	0.017(4)	0.017(4)	0.019(4)
N(2a)	0.059(5)	0.050(4)	0.049(5)	-0.009(4)	0.007(4)	-0.003(4)
N(2b)	0.053(4)	0.057(4)	0.039(4)	0.002(4)	0.009(3)	0.001(4)
C(1a)	0.053(5)	0.069(6)	0.049(6)	0.006(5)	0.016(5)	0.002(5)
C(1b)	0.059(6)	0.068(6)	0.059(6)	0.006(6)	0.019(5)	0.009(5)
C(9a)	0.043(5)	0.069(6)	0.086(8)	-0.023(6)	0.005(5)	-0.011(5)
C(9c)	0.054(6)	0.081(8)	0.095(9)	-0.035(7)	0.029(6)	-0.027(5)
C(9b)	0.039(5)	0.079(7)	0.078(7)	-0.026(5)	0.007(5)	0.000(5)
C(8a)	0.053(5)	0.064(6)	0.044(6)	-0.018(5)	0.000(5)	0.001(5)
C(8b)	0.045(5)	0.049(6)	0.055(6)	0.005(5)	0.009(5)	0.011(4)
O(1a)	0.106(6)	0.094(6)	0.063(5)	0.021(5)	0.004(4)	-0.010(5)

Table 3 continued

O(1b)	0.080(5)	0.156(7)	0.037(4)	0.011(4)	-0.006(4)	0.006(5)
O(1c)	0.098(6)	0.140(7)	0.070(6)	0.013(5)	-0.007(5)	-0.011(6)
N(1n)	0.057(6)	0.087(7)	0.047(6)	-0.009(5)	-0.004(5)	0.013(5)
O(2a)	0.110(6)	0.108(6)	0.063(5)	0.018(5)	-0.016(4)	0.027(5)
O(2b)	0.101(6)	0.152(8)	0.114(8)	0.047(7)	-0.002(6)	0.011(7)
O(2c)	0.084(5)	0.265(14)	0.060(5)	-0.022(7)	-0.016(5)	0.038(7)
N(2n)	0.062(6)	0.126(10)	0.085(8)	0.008(8)	0.013(6)	0.025(7)
C(10b)	0.056(6)	0.061(6)	0.065(7)	0.001(5)	0.015(5)	0.012(5)
C(11b)	0.056(6)	0.064(6)	0.065(7)	0.005(5)	0.016(5)	0.010(5)
C(12b)	0.063(6)	0.098(8)	0.077(8)	-0.001(6)	0.023(6)	0.031(6)
C(13b)	0.091(8)	0.064(7)	0.117(12)	0.001(8)	0.029(8)	0.026(6)
C(10a)	0.092(8)	0.075(7)	0.083(8)	-0.035(6)	-0.003(7)	0.010(6)
C(11a)	0.102(9)	0.149(10)	0.094(10)	-0.062(9)	0.004(8)	0.044(8)

TABLE 4 Bond lengths (Å)

Cd -N(1a)	2.310(7)	Cd -N(1b)	2.418(7)
Cd -N(2a)	2.274(7)	Cd -N(2b)	2.251(7)
Cd -O(1a)	2.325(7)	Cd -O(1c)	2.633(8)
N(1a) -C(1a)	1.446(11)	N(1a) -C(2a)	1.418(11)
N(1b) -C(1b)	1.475(12)	N(1b) -C(2b)	1.410(11)
N(2a) -C(9a)	1.465(10)	N(2a) -C(8a)	1.497(12)
N(2b) -C(9b)	1.472(10)	N(2b) -C(8b)	1.496(11)
C(1a) -C(1b)	1.520(12)	C(9a) -C(9c)	1.520(15)
C(9c) -C(9b)	1.520(13)	C(8a) -C(7a)	1.505(11)
C(8a) -C(10a)	1.524(13)	C(8b) -C(7b)	1.510(11)
C(8b) -C(10b)	1.532(13)	C(2a) -C(3a)	1.368(12)
C(2a) -C(7a)	1.390(12)	C(3a) -C(4a)	1.373(14)
C(4a) -C(5a)	1.355(15)	C(5a) -C(6a)	1.395(13)
C(6a) -C(7a)	1.386(13)	C(2b) -C(3b)	1.386(12)
C(2b) -C(7b)	1.398(13)	C(3b) -C(4b)	1.383(14)
C(4b) -C(5b)	1.348(15)	C(5b) -C(6b)	1.363(12)
C(6b) -C(7b)	1.385(12)	O(1a) -N(1n)	1.230(13)
O(1b) -N(1n)	1.210(11)	O(1c) -N(1n)	1.233(12)
O(2a) -N(2n)	1.219(14)	O(2b) -N(2n)	1.303(17)
O(2c) -N(2n)	1.179(13)	C(10b) -C(11b)	1.526(13)
C(11b) -C(12b)	1.519(13)	C(12b) -C(13b)	1.561(15)
C(10a) -C(11a)	1.573(17)	C(11a) -C(12a)	1.337(25)
C(11a) -C(12c)	1.230(24)	C(12a) -C(13a)	1.50(4)
C(12c) -C(13c)	1.66(3)		

TABLE 5 Bond angles (°)

N(1b) - Cd - N(1a)	75.0(2)	N(2a) - Cd - N(1a)	89.0(3)
N(2a) - Cd - N(1b)	146.5(2)	N(2b) - Cd - N(1a)	157.2(2)
N(2b) - Cd - N(1b)	86.4(2)	N(2b) - Cd - N(2a)	100.0(3)
O(1a) - Cd - N(1a)	87.5(3)	O(1a) - Cd - N(1b)	92.5(2)
O(1a) - Cd - N(2a)	116.5(3)	O(1a) - Cd - N(2b)	106.7(3)
O(1c) - Cd - N(1a)	112.9(3)	O(1c) - Cd - N(1b)	138.9(2)
O(1c) - Cd - N(2a)	74.4(3)	O(1c) - Cd - N(2b)	89.7(3)
O(1c) - Cd - O(1a)	49.8(3)	C(1a) - N(1a) - Cd	105.4(5)
C(2a) - N(1a) - Cd	105.3(5)	C(2a) - N(1a) - C(1a)	119.3(6)
C(1b) - N(1b) - Cd	108.3(5)	C(2b) - N(1b) - Cd	98.0(5)
C(2b) - N(1b) - C(1b)	122.5(7)	C(9a) - N(2a) - Cd	111.2(5)
C(8a) - N(2a) - Cd	108.4(5)	C(8a) - N(2a) - C(9a)	116.8(7)
C(9b) - N(2b) - Cd	108.0(5)	C(8b) - N(2b) - Cd	111.4(5)
C(8b) - N(2b) - C(9b)	115.0(6)	C(1b) - C(1a) - N(1a)	110.2(7)
C(1a) - C(1b) - N(1b)	111.8(8)	C(9c) - C(9a) - N(2a)	112.8(7)
C(9b) - C(9c) - C(9a)	118.5(9)	C(9c) - C(9b) - N(2b)	113.2(7)
C(7a) - C(8a) - N(2a)	109.4(7)	C(10a) - C(8a) - N(2a)	112.5(8)
C(10a) - C(8a) - C(7a)	113.3(7)	C(7b) - C(8b) - N(2b)	107.9(6)
C(10b) - C(8b) - N(2b)	111.1(7)	C(10b) - C(8b) - C(7b)	114.7(7)
C(3a) - C(2a) - N(1a)	120.1(8)	C(7a) - C(2a) - N(1a)	118.6(7)
C(7a) - C(2a) - C(3a)	121.2(8)	C(4a) - C(3a) - C(2a)	119.4(9)
C(5a) - C(4a) - C(3a)	120.8(9)	C(6a) - C(5a) - C(4a)	120(1)
C(7a) - C(6a) - C(5a)	119.2(9)	C(2a) - C(7a) - C(8a)	121.5(8)
C(6a) - C(7a) - C(8a)	119.6(8)	C(6a) - C(7a) - C(2a)	118.8(8)
C(3b) - C(2b) - N(1b)	121.2(8)	C(7b) - C(2b) - N(1b)	118.7(7)

table 5 continued

C(7b)-C(2b)-C(3b)	119.7(8)	C(4b)-C(3b)-C(2b)	119.5(9)
C(5b)-C(4b)-C(3b)	120.6(9)	C(6b)-C(5b)-C(4b)	121(1)
C(7b)-C(6b)-C(5b)	120.7(9)	C(2b)-C(7b)-C(8b)	120.4(8)
C(6b)-C(7b)-C(8b)	120.9(8)	C(6b)-C(7b)-C(2b)	118.7(7)
N(1n)-O(1a)-Cd	104.0(6)	N(1n)-O(1c)-Cd	88.7(6)
O(1b)-N(1n)-O(1a)	122.9(9)	O(1c)-N(1n)-O(1a)	117.5(8)
O(1c)-N(1n)-O(1b)	119.6(9)	O(2b)-N(2n)-O(2a)	114(1)
O(2c)-N(2n)-O(2a)	127(1)	O(2c)-N(2n)-O(2b)	118(1)
C(11b)-C(10b)-C(8b)	113.2(8)	C(12b)-C(11b)-C(10b)	112.4(8)
C(13b)-C(12b)-C(11b)	111.8(8)	C(11a)-C(10a)-C(8a)	114.0(9)
C(12a)-C(11a)-C(10a)	123(1)	C(12c)-C(11a)-C(10a)	115(1)
C(12c)-C(11a)-C(12a)	83(1)	C(13a)-C(12a)-C(11a)	119(2)
C(13c)-C(12a)-C(11a)	91(1)	C(13c)-C(12a)-C(13a)	33(1)
C(13c)-C(12a)-C(12c)	53(1)	C(13c)-C(12c)-C(11a)	113(2)
C(13c)-C(12c)-C(12a)	72(1)	C(12c)-C(13c)-C(12a)	55(1)
C(12c)-C(13c)-C(13a)	103(2)		

TABLE 6 Intermolecular distances (Å)

O(1b) ...N(1a)	2.91	1	0.0	0.0	1.0
O(2c) ...N(2b)	3.00	1	0.0	0.0	-1.0
O(1b) ...C(1a)	3.20	1	0.0	0.0	1.0
O(2c) ...C(1a)	3.30	-2	0.0	1.0	0.0
O(1b) ...H(1a1)	2.80	1	0.0	0.0	1.0
O(2c) ...H(1a1)	2.61	-2	0.0	1.0	0.0
O(1b) ...H(1b1)	2.90	1	0.0	0.0	1.0
H(4b) ...C(9a)	2.94	-2	1.0	1.0	1.0
C(4b) ...H(9c1)	2.95	-2	1.0	1.0	1.0
O(2c) ...H(9c2)	2.82	1	0.0	0.0	-1.0
O(1b) ...H(9b1)	2.52	-2	1.0	1.0	1.0
O(2b) ...C(3a)	3.36	-2	0.0	1.0	0.0
H(102)...C(3a)	3.03	-2	0.0	1.0	1.0
O(2b) ...H(3a)	2.59	-2	0.0	1.0	0.0
O(2c) ...H(3a)	2.44	-2	0.0	1.0	0.0
N(2n) ...H(3a)	2.71	-2	0.0	1.0	0.0
O(2b) ...H(4a)	2.82	-2	0.0	1.0	0.0
H(121)...C(5a)	3.02	-2	0.0	1.0	1.0
C(5b) ...H(5a)	3.04	2	0.0	0.0	0.0
C(13c)...H(6a)	3.06	1	0.0	0.0	-1.0
C(4b) ...H(6a)	2.80	2	0.0	0.0	0.0
C(13a)...C(3b)	3.47	2	0.0	-1.0	-1.0
C(13a)...H(3b)	2.89	2	0.0	-1.0	-1.0
C(13b)...H(5b)	2.91	-1	0.0	1.0	1.0
O(2b) ...C(6b)	3.33	1	0.0	0.0	-1.0



table 6 continued

O(2b) ...H(6b)	2.67	1	0.0	0.0	-1.0
N(1n) ...O(1b)	2.18	1	0.0	0.0	-1.0
H(101)...O(1b)	2.59	-2	0.0	1.0	0.0
C(12c)...O(1c)	3.38	1	0.0	0.0	-1.0
N(2n) ...O(2c)	2.10	1	0.0	0.0	1.0
O(2c) ...N(2n)	2.88	1	0.0	0.0	1.0

TABLE 7 Intramolecular distances (Å)

C(1a) ...Cd	3.03	H(1a1)...Cd	3.10
C(1b) ...Cd	3.20	H(1b1)...Cd	3.68
C(9a) ...Cd	3.12	H(9a1)...Cd	3.31
C(9c) ...Cd	3.25	H(9c2)...Cd	3.09
C(9b) ...Cd	3.05	H(9b2)...Cd	3.20
C(8a) ...Cd	3.09	H(8a1)...Cd	3.16
C(8b) ...Cd	3.13	H(8b1)...Cd	3.33
C(2a) ...Cd	3.01	C(3a) ...Cd	4.02
C(7a) ...Cd	3.31	C(2b) ...Cd	2.96
C(3b) ...Cd	3.90	C(7b) ...Cd	3.22
O(1b) ...Cd	4.09	N(1n) ...Cd	2.88
O(2a) ...Cd	2.72	O(2b) ...Cd	3.99
N(2n) ...Cd	3.77	N(2n) ...Cd	2.74
N(2n) ...Cd	3.02	N(2n) ...Cd	2.63
N(2n) ...Cd	2.68	N(1b) ...N(1a)	2.88
N(2a) ...N(1a)	3.21	H(1a1)...N(1a)	2.06
H(1a1)...N(1a)	2.08	C(1b) ...N(1a)	2.43
H(1b1)...N(1a)	2.69	C(8a) ...N(1a)	2.85
H(8a1)...N(1a)	2.61	C(3a) ...N(1a)	2.41
H(3a) ...N(1a)	2.64	C(7a) ...N(1a)	2.41
O(1a) ...N(1a)	3.20	O(2a) ...N(1a)	3.01
N(2b) ...N(1b)	3.20	C(1a) ...N(1b)	2.48
H(1a1)...N(1b)	2.73	H(1b1)...N(1b)	2.10
H(1b2)...N(1b)	2.08	C(8b) ...N(1b)	2.84
H(8b1)...N(1b)	2.59	C(3b) ...N(1b)	2.44

Table 7 continued

H(3b) ...N(1b)	2.68	C(7b) ...N(1b)	2.41
O(2a) ...N(1b)	3.02	O(2b) ...N(1b)	2.90
H(9a1)...N(2a)	2.06	H(9a2)...N(2a)	2.11
C(9c) ...N(2a)	2.49	H(9c2)...N(2a)	2.49
C(9b) ...N(2a)	3.31	H(8a1)...N(2a)	2.09
C(2a) ...N(2a)	3.18	C(6a) ...N(2a)	3.35
C(7a) ...N(2a)	2.45	O(1c) ...N(2a)	2.98
O(2a) ...N(2a)	3.08	C(10a)...N(2a)	2.51
H(103)...N(2a)	2.78	H(104)...N(2a)	2.69
H(114)...N(2a)	3.02	C(9a) ...N(2b)	3.38
C(9c) ...N(2b)	2.50	H(9c2)...N(2b)	2.49
H(9b1)...N(2b)	2.09	H(9b2)...N(2b)	2.08
H(8b1)...N(2b)	2.11	C(2b) ...N(2b)	3.18
C(6b) ...N(2b)	3.33	C(7b) ...N(2b)	2.43
C(10b)...N(2b)	2.50	H(101)...N(2b)	2.71
H(102)...N(2b)	2.71	H(1b1)...C(1a)	2.13
H(1b2)...C(1a)	2.14	C(2a) ...C(1a)	2.47
C(3a) ...C(1a)	2.81	H(3a) ...C(1a)	2.44
C(2b) ...C(1a)	3.34	C(3b) ...C(1a)	3.47
H(3b) ...C(1a)	2.97	O(1a) ...C(1a)	3.31
O(1b) ...C(1a)	1.96	C(1b) ...H(1a1)	2.13
C(2a) ...H(1a1)	2.71	C(3a) ...H(1a1)	2.70
C(3b) ...H(1a1)	2.94	O(1a) ...H(1a1)	2.59
C(1b) ...H(1a1)	2.14	C(2a) ...H(1a1)	2.78
C(3a) ...H(1a1)	2.83	C(2b) ...C(1b)	2.53
C(3b) ...C(1b)	2.93	H(3b) ...C(1b)	2.57
O(2a) ...C(1b)	3.39	O(2b) ...C(1b)	3.39
O(2b) ...C(1b)	2.61	O(2b) ...C(1b)	1.91

table 7 continued

C(12c)...H(8a1)	2.71	C(2b) ...C(8b)	2.52
C(6b) ...C(8b)	2.52	H(6b) ...C(8b)	2.71
H(101)...C(8b)	2.17	H(102)...C(8b)	2.09
C(11b)...C(8b)	2.55	H(111)...C(8b)	2.69
H(112)...C(8b)	2.92	H(112)...C(8b)	2.68
H(112)...C(8b)	1.97	C(2b) ...H(8b1)	2.70
C(7b) ...H(8b1)	2.14	O(2b) ...H(8b1)	2.63
C(10b)...H(8b1)	2.07	C(11b)...H(8b1)	2.69
H(3a) ...C(2a)	2.13	C(4a) ...C(2a)	2.37
C(5a) ...C(2a)	2.74	C(6a) ...C(2a)	2.39
O(1a) ...C(2a)	3.36	O(1a) ...C(2a)	1.89
H(4a) ...C(3a)	2.13	C(5a) ...C(3a)	2.37
C(6a) ...C(3a)	2.77	C(7a) ...C(3a)	2.40
C(7a) ...C(3a)	3.00	C(4a) ...H(3a)	2.13
H(5a) ...C(4a)	2.11	C(6a) ...C(4a)	2.39
C(7a) ...C(4a)	2.76	C(5a) ...H(4a)	2.11
H(6a) ...C(5a)	2.16	C(7a) ...C(5a)	2.40
C(6a) ...H(5a)	2.15	C(10a)...C(6a)	2.87
H(103)...C(6a)	2.55	C(11a)...C(6a)	3.25
H(113)...C(6a)	2.55	H(114)...C(6a)	3.03
H(114)...C(6a)	2.94	C(7a) ...H(6a)	2.14
C(10a)...H(6a)	2.49	C(11a)...H(6a)	2.91
C(10a)...C(7a)	2.53	H(103)...C(7a)	2.70
C(11a)...C(7a)	3.11	H(113)...C(7a)	2.73
H(114)...C(7a)	2.78	H(114)...C(7a)	2.56
H(114)...C(7a)	2.38	H(3b) ...C(2b)	2.14
C(4b) ...C(2b)	2.39	C(5b) ...C(2b)	2.75
C(6b) ...C(2b)	2.39	O(1a) ...C(2b)	3.19

table 7 continued

O(1a) ...C(2b)	1.79	H(4b) ...C(3b)	2.13
C(5b) ...C(3b)	2.37	C(6b) ...C(3b)	2.75
C(7b) ...C(3b)	2.41	O(1a) ...C(3b)	3.30
O(1a) ...C(3b)	2.91	C(4b) ...H(3b)	2.14
H(5b) ...C(4b)	2.10	C(6b) ...C(4b)	2.36
C(7b) ...C(4b)	2.76	C(5b) ...H(4b)	2.11
H(6b) ...C(5b)	2.12	C(7b) ...C(5b)	2.39
C(6b) ...H(5b)	2.12	C(10b)...C(6b)	2.93
H(102)...C(6b)	2.63	C(11b)...C(6b)	3.27
H(112)...C(6b)	2.71	C(7b) ...H(6b)	2.13
C(10b)...H(6b)	2.56	C(11b)...H(6b)	2.94
C(10b)...C(7b)	2.56	H(102)...C(7b)	2.72
C(11b)...C(7b)	3.10	H(112)...C(7b)	2.93
H(112)...C(7b)	2.52	H(112)...C(7b)	2.59
O(1b) ...O(1a)	2.14	O(1c) ...O(1a)	2.11
O(1c) ...O(1b)	2.11	C(12c)...O(1c)	2.41
O(2b) ...O(2a)	2.12	O(2c) ...O(2a)	2.15
N(2n) ...O(2a)	2.53	N(2n) ...O(2a)	2.96
O(2c) ...O(2b)	2.13	N(2n) ...O(2b)	2.25
H(111)...C(10b)	2.15	H(112)...C(10b)	2.14
C(12b)...C(10b)	2.53	H(121)...C(10b)	2.83
H(122)...C(10b)	2.66	H(122)...C(10b)	2.62
C(11b)...H(101)	2.13	C(12b)...H(101)	2.64
C(11b)...H(102)	2.13	C(12b)...H(102)	2.88
H(121)...C(11b)	2.17	H(122)...C(11b)	2.08
C(13b)...C(11b)	2.55	H(132)...C(11b)	2.71
H(133)...C(11b)	2.87	C(12b)...H(111)	2.16
C(13b)...H(111)	2.76	C(12b)...H(112)	2.07

table 7 continued

C(13b)...H(112)	2.72	H(131)...C(12b)	2.17
H(132)...C(12b)	2.11	H(133)...C(12b)	2.23
C(13b)...H(121)	2.11	C(13b)...H(122)	2.23
H(113)...C(10a)	2.11	C(12a)...C(10a)	2.56
C(12c)...C(10a)	2.37	C(12c)...C(10a)	2.73
C(11a)...H(103)	2.15	C(12a)...H(103)	2.94
C(11a)...H(104)	2.19	C(12a)...H(104)	2.76
C(12c)...H(104)	2.65	C(13a)...C(11a)	2.44
C(13c)...C(11a)	2.41	C(12a)...H(113)	2.04
C(13a)...H(113)	2.84	C(12c)...H(113)	1.98
C(13c)...H(113)	2.84	C(12a)...H(114)	2.03
C(12c)...H(114)	1.95	C(12c)...C(13a)	2.18

A8      Tables for L15b.

X-ray structure of 'free' ligand L15b  
5,11-di-n-butyl-6,7,8,9,10,11,16,17,18,19-  
decahydro-5H-dibenzof[e,n][1,4,8,12]tetra-  
azacycllopentadecine.

Crystal data:  $C_{27}H_{42}N_4$ , Mwt = 422.67, triclinic,  
space group  $P\bar{1}$ ,  $a = 11.305(3)$  Å,  $b = 11.031(3)$  Å,  
 $c = 10.947(2)$  Å. Alpha =  $109.44(6)^\circ$ , Beta =  $84.66(7)^\circ$ ,  
gamma =  $87.13(7)^\circ$ ,  $U = 1276.97$  Å<sup>3</sup>,  $D_c = 1.096$  gcm<sup>-3</sup>,  
 $F_{000} = 464$ .

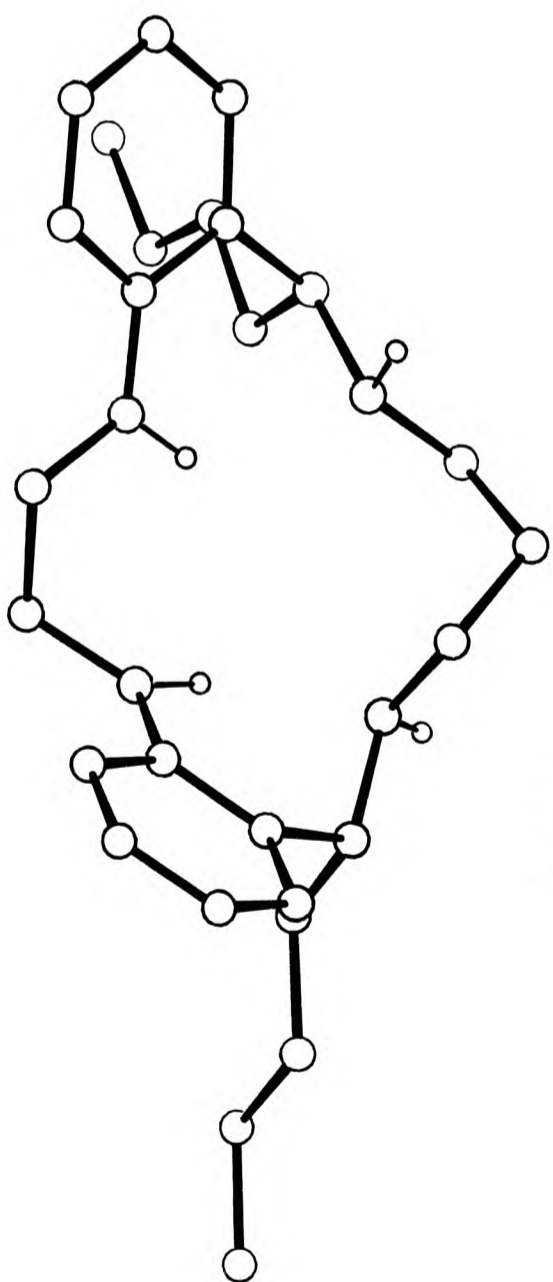




TABLE 1 Fractional atomic coordinates and thermal parameters ( $\text{\AA}^2$ ).

Atom	x	y	z	$U_{\text{iso}}$ or $U_{\text{eq}}$
N(2a)	1.0805(3)	0.5655(4)	-0.2311(4)	0.053(3)
N(2b)	0.8128(4)	0.7136(4)	-0.0415(4)	0.050(3)
N(1a)	1.2006(4)	0.7415(4)	-0.0476(4)	0.052(3)
N(1b)	0.9747(3)	0.8740(4)	0.1129(4)	0.054(3)
C(1a)	1.1962(4)	0.8276(5)	0.0863(4)	0.053(3)
C(1b)	1.0902(4)	0.9260(4)	0.1170(5)	0.053(3)
C(9a)	0.9670(4)	0.5498(5)	-0.2862(4)	0.058(3)
C(9c)	0.8787(4)	0.4985(5)	-0.2064(5)	0.058(3)
C(9b)	0.8536(4)	0.5790(5)	-0.0616(4)	0.052(3)
C(8a)	1.1832(4)	0.5880(5)	-0.3128(4)	0.050(3)
C(8b)	0.7370(4)	0.7784(5)	0.0848(4)	0.050(3)
C(10a)	1.1605(4)	0.7130(5)	-0.3423(5)	0.059(3)
C(11a)	1.2565(5)	0.7240(5)	-0.4471(5)	0.063(3)
C(12a)	1.2438(5)	0.8467(6)	-0.4755(6)	0.086(4)
C(13a)	1.3381(6)	0.8592(6)	-0.5771(6)	0.102(5)
C(10b)	0.6853(4)	0.9099(5)	0.0875(4)	0.053(3)
C(11b)	0.5752(4)	0.9644(5)	0.1867(5)	0.056(3)
C(12b)	0.5296(4)	1.0973(5)	0.1906(5)	0.062(3)
C(13b)	0.4177(5)	1.1546(6)	0.2865(6)	0.080(4)
C(2a)	1.2984(4)	0.6592(4)	-0.1148(4)	0.045(1)
C(3a)	1.4034(4)	0.6495(5)	-0.0579(5)	0.057(1)
C(4a)	1.5023(4)	0.5723(5)	-0.1320(5)	0.066(1)
C(5a)	1.5012(5)	0.5032(5)	-0.2605(5)	0.069(1)
C(6a)	1.3970(4)	0.5094(5)	-0.3175(5)	0.060(1)
C(7a)	1.2946(4)	0.5832(4)	-0.2480(4)	0.047(1)

table 1 continued

C(2b)	0.9189(4)	0.8380(4)	0.2124(4)	0.044(1)
C(3b)	0.9722(4)	0.8537(4)	0.3277(5)	0.055(1)
C(4b)	0.9123(4)	0.8198(5)	0.4280(5)	0.063(1)
C(5b)	0.8035(4)	0.7702(5)	0.4160(5)	0.066(1)
C(6b)	0.7505(4)	0.7551(5)	0.3019(5)	0.056(1)
C(7b)	0.8068(4)	0.7886(4)	0.2001(4)	0.045(1)

TABLE 2 Fractional atomic coordinates for the hydrogen atoms.

Atom	x	y	z
H(a1)	1.1896	0.7734	0.1523
H(a2)	1.2768	0.8768	0.0964
H(b1)	1.0969	0.9764	0.0476
H(b2)	1.0911	0.9939	0.2142
H(9a1)	0.9306	0.6439	-0.2815
H(a2)	0.9807	0.4865	-0.3866
H(9c1)	0.9159	0.4038	-0.2139
H(9c2)	0.7955	0.4902	-0.2485
H(9b1)	0.9340	0.5774	-0.0158
H(9b2)	0.7848	0.5378	-0.0166
H(8a)	1.1948	0.5133	-0.4075
H(8b)	0.6639	0.7211	0.0931
H(1a1)	1.0743	0.7144	-0.3771
H(1a2)	1.1613	0.7940	-0.2536
H(2a1)	1.2522	0.6448	-0.5364
H(2a2)	1.3427	0.7170	-0.4136
H(3a1)	1.1585	0.8518	-0.5113
H(3a2)	1.2450	0.9255	-0.3851
H(4a1)	1.3177	0.9516	-0.5880
H(4a2)	1.3378	0.7834	-0.6699
H(4a3)	1.4251	0.8568	-0.5443
H(1b1)	0.6620	0.9008	-0.0084
H(1b2)	0.7533	0.9765	0.1121
H(2b1)	0.5974	0.9704	0.2822
H(2b2)	0.5058	0.8999	0.1601

table 2 continued

H(3b1)	0.5090	1.0907	0.0944
H(3b2)	0.5993	1.1612	0.2179
H(4b1)	0.3873	1.2507	0.2914
H(4b2)	0.4414	1.1571	0.3806
H(4b3)	0.3473	1.0915	0.2596
H(3a)	1.4074	0.7031	0.0438
H(4a)	1.5817	0.5657	-0.0860
H(5a)	1.5801	0.4454	-0.3176
H(6a)	1.3964	0.4543	-0.4195
H(3b)	1.0586	0.8909	0.3388
H(4b)	0.9522	0.8338	0.5171
H(5b)	0.7592	0.7439	0.4942
H(6b)	0.6650	0.7155	0.2923
H(N2a)	1.1042	0.4941	-0.2154
H(N2b)	0.7652	0.7168	-0.1002
H(N1a)	1.1232	0.7196	-0.0620
H(N1b)	0.9421	0.8425	0.0390

TABLE 3 Anisotropic thermal parameters ( $\text{\AA}^2$ ).

Atom	$U_{11}$	$U_{22}$	$U_{33}$	$U_{23}$	$U_{13}$	$U_{12}$
N(2a)	0.044(2)	0.074(3)	0.042(2)	0.024(2)	-0.010(2)	-0.010(2)
N(2b)	0.049(3)	0.062(3)	0.038(2)	0.016(2)	-0.009(2)	-0.006(2)
N(1a)	0.043(3)	0.078(3)	0.037(3)	0.012(2)	-0.012(2)	-0.005(2)
N(1b)	0.045(2)	0.077(3)	0.040(2)	0.028(2)	-0.010(2)	-0.024(2)
C(1a)	0.049(3)	0.069(4)	0.042(3)	0.020(3)	-0.014(2)	-0.018(3)
C(1b)	0.058(3)	0.053(3)	0.049(3)	0.018(3)	-0.008(3)	-0.015(3)
C(9a)	0.049(3)	0.087(4)	0.038(3)	0.008(3)	-0.011(2)	-0.007(3)
C(9c)	0.051(3)	0.071(4)	0.052(3)	0.005(3)	-0.010(3)	-0.013(3)
C(9b)	0.054(3)	0.056(3)	0.046(3)	0.014(3)	-0.002(2)	-0.007(3)
C(8a)	0.056(3)	0.063(3)	0.032(3)	0.016(3)	-0.003(2)	-0.009(3)
C(8b)	0.045(3)	0.063(3)	0.042(3)	0.021(3)	-0.006(2)	-0.008(2)
C(10a)	0.058(3)	0.075(4)	0.043(3)	0.025(3)	-0.009(3)	-0.001(3)
C(11a)	0.081(4)	0.068(4)	0.038(3)	0.021(3)	-0.011(3)	-0.011(3)

table 3 continued

C(12a)	0.095(4)	0.086(5)	0.077(4)	0.046(4)	-0.025(4)	-0.011(4)
C(13a)	0.140(6)	0.091(5)	0.077(5)	0.048(4)	0.002(4)	-0.015(4)
C(10b)	0.049(3)	0.065(3)	0.045(3)	0.025(3)	-0.007(2)	-0.001(2)
C(11b)	0.051(3)	0.062(4)	0.054(3)	0.022(3)	-0.004(3)	-0.005(3)
C(12b)	0.066(3)	0.066(4)	0.055(3)	0.022(3)	-0.006(3)	0.004(3)
C(13b)	0.082(4)	0.073(4)	0.084(4)	0.023(4)	0.006(4)	0.012(3)

TABLE 4 Bond lengths (Å).

N(2a) - C(9a)	1.462(6)	N(2a) - C(8a)	1.482(6)
N(2b) - C(9b)	1.470(7)	N(2b) - C(8b)	1.489(5)
N(1a) - C(1a)	1.451(5)	N(1a) - C(2a)	1.375(5)
N(1b) - C(1b)	1.450(6)	N(1b) - C(2b)	1.388(7)
C(1a) - C(1b)	1.510(6)	C(9a) - C(9c)	1.517(8)
C(9c) - C(9b)	1.529(6)	C(8a) - C(10a)	1.532(8)
C(8a) - C(7a)	1.510(7)	C(8b) - C(10b)	1.526(7)
C(8b) - C(7b)	1.526(7)	C(10a) - C(11a)	1.543(7)
C(11a) - C(12a)	1.490(9)	C(12a) - C(13a)	1.514(9)
C(10b) - C(11b)	1.527(6)	C(11b) - C(12b)	1.514(8)
C(12b) - C(13b)	1.528(7)	C(2a) - C(3a)	1.406(7)
C(2a) - C(7a)	1.425(6)	C(3a) - C(4a)	1.382(6)
C(4a) - C(5a)	1.360(7)	C(5a) - C(6a)	1.392(8)
C(6a) - C(7a)	1.383(6)	C(2b) - C(3b)	1.412(7)
C(2b) - C(7b)	1.405(6)	C(3b) - C(4b)	1.402(8)
C(4b) - C(5b)	1.371(7)	C(5b) - C(6b)	1.400(8)
C(6b) - C(7b)	1.395(7)		

TABLE 5 Bond angles ( $^{\circ}$ )

C(8a) - N(2a) - C(9a)	116.9(4)	C(8b) - N(2b) - C(9b)	113.4(4)
C(2a) - N(1a) - C(1a)	123.9(4)	C(2b) - N(1b) - C(1b)	123.7(4)
C(1b) - C(1a) - N(1a)	109.3(4)	C(1a) - C(1b) - N(1b)	115.3(4)
C(9c) - C(9a) - N(2a)	110.7(4)	C(9b) - C(9c) - C(9a)	115.5(4)
C(9c) - C(9b) - N(2b)	111.8(5)	C(10a) - C(8a) - N(2a)	111.6(4)
C(7a) - C(8a) - N(2a)	108.9(4)	C(7a) - C(8a) - C(10a)	113.6(4)
C(10b) - C(8b) - N(2b)	109.1(4)	C(7b) - C(8b) - N(2b)	111.2(4)
C(7b) - C(8b) - C(10b)	112.3(4)	C(11a) - C(10a) - C(8a)	111.5(4)
C(12a) - C(11a) - C(10a)	114.4(4)	C(13a) - C(12a) - C(11a)	114.9(5)
C(11b) - C(10b) - C(8b)	113.6(4)	C(12b) - C(11b) - C(10b)	112.0(5)
C(13b) - C(12b) - C(11b)	113.9(5)	C(3a) - C(2a) - N(1a)	122.3(4)
C(7a) - C(2a) - N(1a)	119.0(4)	C(7a) - C(2a) - C(3a)	118.6(4)
C(4a) - C(3a) - C(2a)	120.3(4)	C(5a) - C(4a) - C(3a)	121.6(5)
C(6a) - C(5a) - C(4a)	118.9(5)	C(7a) - C(6a) - C(5a)	122.2(4)
C(2a) - C(7a) - C(8a)	120.7(4)	C(6a) - C(7a) - C(8a)	120.9(4)
C(6a) - C(7a) - C(2a)	118.3(4)	C(3b) - C(2b) - N(1b)	120.7(4)
C(7b) - C(2b) - N(1b)	119.9(4)	C(7b) - C(2b) - C(3b)	119.4(5)
C(4b) - C(3b) - C(2b)	119.4(4)	C(5b) - C(4b) - C(3b)	121.4(5)
C(6b) - C(5b) - C(4b)	119.1(5)	C(7b) - C(6b) - C(5b)	121.3(4)
C(2b) - C(7b) - C(8b)	123.5(5)	C(6b) - C(7b) - C(8b)	117.0(4)
C(6b) - C(7b) - C(2b)	119.4(4)		



TABLE 6 Intermolecular distances (Å).

Hb(1) ...N(1b)	2.92	-1	2.0	2.0	0.0
C(3b) ...H(9c1)	2.87	-1	2.0	1.0	0.0
H(3b2)...C(11a)	3.07	-1	2.0	2.0	0.0
H(5a) ...C(11a)	3.02	-1	3.0	1.0	-1.0
C(3b) ...H(3a1)	2.87	1	0.0	0.0	1.0
C(4b) ...H(3a1)	2.93	1	0.0	0.0	1.0
C(2b) ...H(3a2)	3.07	-1	2.0	2.0	0.0
C(2a) ...H(3b2)	2.83	-1	2.0	2.0	0.0
C(7a) ...H(3b2)	3.05	-1	2.0	2.0	0.0
H(5b) ...C(13b)	2.85	-1	1.0	2.0	1.0
H(6b) ...C(5a)	3.08	-1	2.0	1.0	0.0
C(6b) ...C(6a)	3.48	-1	2.0	1.0	0.0
H(6b) ...C(6a)	2.70	-1	2.0	1.0	0.0
H(N2a)...C(5b)	3.07	-1	2.0	1.0	0.0
H(N2a)...C(6b)	2.95	-1	2.0	1.0	0.0

TABLE 7 Intramolecular distances (Å).

N(1a) ...N(2a)	2.80	H(9a1)...N(2a)	2.07
H(a2) ...N(2a)	2.10	C(9c) ...N(2a)	2.45
H(9c1)...N(2a)	2.68	C(9b) ...N(2a)	2.99
H(9b1)...N(2a)	2.71	H(8a) ...N(2a)	2.11
C(10a)...N(2a)	2.49	H(1a1)...N(2a)	2.65
H(1a2)...N(2a)	2.80	C(2a) ...N(2a)	2.95
C(7a) ...N(2a)	2.43	H(N1a)...N(2a)	2.17
N(1b) ...N(2b)	2.87	C(9a) ...N(2b)	3.01
H(9a1)...N(2b)	2.68	C(9c) ...N(2b)	2.48
H(9c2)...N(2b)	2.77	H(9b1)...N(2b)	2.09
H(9b2)...N(2b)	2.08	H(8b) ...N(2b)	2.11
C(10b)...N(2b)	2.46	H(1b1)...N(2b)	2.52
H(1b2)...N(2b)	2.84	C(2b) ...N(2b)	3.05
C(7b) ...N(2b)	2.49	H(N1b)...N(2b)	2.13
N(1b) ...N(1a)	2.97	H(a1) ...N(1a)	2.09
H(a2) ...N(1a)	2.07	C(1b) ...N(1a)	2.41
H(b1) ...N(1a)	2.62	C(8a) ...N(1a)	2.87
C(10a)...N(1a)	3.21	H(1a2)...N(1a)	2.58
C(3a) ...N(1a)	2.44	H(3a) ...N(1a)	2.69
C(7a) ...N(1a)	2.41	H(N1b)...N(1a)	3.02
C(1a) ...N(1b)	2.50	H(a1) ...N(1b)	2.75
H(b1) ...N(1b)	2.05	H(b2) ...N(1b)	2.05
C(8b) ...N(1b)	2.94	C(10b)...N(1b)	3.32
H(1b2)...N(1b)	2.70	C(3b) ...N(1b)	2.43
H(3b) ...N(1b)	2.68	C(7b) ...N(1b)	2.42

table 7 continued

H(N1a)...N(1b)	2.52	H(b1) ...C(1a)	2.12
H(b2) ...C(1a)	2.12	C(2a) ...C(1a)	2.49
C(3a) ...C(1a)	2.94	H(3a) ...C(1a)	2.62
C(2b) ...C(1a)	3.29	C(3b) ...C(1a)	3.41
H(3b) ...C(1a)	2.89	H(N1a)...C(1a)	1.95
H(N1b)...C(1a)	2.97	C(1b) ...H(a1)	2.14
C(2a) ...H(a1)	2.89	C(2b) ...H(a1)	3.07
C(3b) ...H(a1)	2.88	C(1b) ...H(a2)	2.13
C(2a) ...H(a2)	2.70	C(3a) ...H(a2)	2.75
C(2b) ...C(1b)	2.50	C(3b) ...C(1b)	2.91
H(3b) ...C(1b)	2.58	H(N1a)...C(1b)	2.44
H(N1b)...C(1b)	2.07	C(2b) ...H(b2)	2.66
C(3b) ...H(b2)	2.63	H(9c1)...C(9a)	2.10
H(9c2)...C(9a)	2.13	C(9b) ...C(9a)	2.58
H(9b1)...C(9a)	2.86	C(8a) ...C(9a)	2.51
H(8a) ...C(9a)	2.73	C(10a)...C(9a)	3.05
H(1a1)...C(9a)	2.64	H(N2a)...C(9a)	1.96
H(N2b)...C(9a)	2.99	C(9c) ...H(9a1)	2.12
C(9b) ...H(9a1)	2.81	C(8a) ...H(9a1)	2.86
C(10a)...H(9a1)	2.83	C(9c) ...H(a2)	2.15
C(8a) ...H(a2)	2.67	H(9b1)...C(9c)	2.14
H(9b2)...C(9c)	2.14	H(N2a)...C(9c)	2.54
H(N2b)...C(9c)	2.52	C(9b) ...H(9c1)	2.12
C(9b) ...H(9c2)	2.13	C(8b) ...C(9b)	2.47
H(8b) ...C(9b)	2.67	C(7b) ...C(9b)	3.00
H(N2b)...C(9b)	1.96	H(N1b)...C(9b)	3.01
C(8b) ...H(9b1)	2.92	C(7b) ...H(9b1)	2.91
C(8b) ...H(9b2)	2.52	C(7b) ...H(9b2)	3.03

table 7 continued

H(1a1)...C(8a)	2.14	H(1a2)...C(8a)	2.14
C(11a)...C(8a)	2.54	H(2a1)...C(8a)	2.78
H(2a2)...C(8a)	2.72	C(2a) ...C(8a)	2.55
C(6a) ...C(8a)	2.52	H(6a) ...C(8a)	2.71
H(N2a)...C(8a)	1.91	H(N1a)...C(8a)	2.65
C(10a)...H(8a)	2.08	C(11a)...H(8a)	2.62
C(6a) ...H(8a)	2.58	C(7a) ...H(8a)	2.12
H(1b1)...C(8b)	2.13	H(1b2)...C(8b)	2.12
C(11b)...C(8b)	2.55	H(2b1)...C(8b)	2.76
H(2b2)...C(8b)	2.80	C(2b) ...C(8b)	2.58
C(6b) ...C(8b)	2.49	H(6b) ...C(8b)	2.66
H(N2b)...C(8b)	1.90	H(N1b)...C(8b)	2.51
C(10b)...H(8b)	2.13	C(11b)...H(8b)	2.64
C(6b) ...H(8b)	2.49	C(7b) ...H(8b)	2.10
H(2a1)...C(10a)	2.15	H(2a2)...C(10a)	2.14
C(12a)...C(10a)	2.55	H(3a1)...C(10a)	2.77
H(3a2)...C(10a)	2.74	C(2a) ...C(10a)	3.26
C(6a) ...C(10a)	3.49	C(7a) ...C(10a)	2.55
H(N1a)...C(10a)	3.03	C(11a)...H(1a1)	2.15
C(12a)...H(1a1)	2.81	C(11a)...H(1a2)	2.15
C(12a)...H(1a2)	2.77	C(2a) ...H(1a2)	2.94
C(7a) ...H(1a2)	2.73	H(3a1)...C(11a)	2.09
H(3a2)...C(11a)	2.09	C(13a)...C(11a)	2.53
H(4a2)...C(11a)	2.82	H(4a3)...C(11a)	2.80
C(7a) ...C(11a)	3.12	C(12a)...H(2a1)	2.10
C(13a)...H(2a1)	2.76	C(12a)...H(2a2)	2.09
C(13a)...H(2a2)	2.75	C(6a) ...H(2a2)	2.88
C(7a) ...H(2a2)	2.73	H(4a1)...C(12a)	2.10

table 7 continued

H(4a2)...C(12a)	2.16	H(4a3)...C(12a)	2.14
C(13a)...H(3a1)	2.11	C(13a)...H(3a2)	2.13
H(2b1)...C(10b)	2.14	H(2b2)...C(10b)	2.13
C(12b)...C(10b)	2.52	H(3b1)...C(10b)	2.73
H(3b2)...C(10b)	2.74	C(2b) ...C(10b)	3.26
C(6b) ...C(10b)	3.44	C(7b) ...C(10b)	2.54
H(N2b)...C(10b)	2.47	H(N1b)...C(10b)	2.91
C(11b)...H(1b1)	2.14	C(12b)...H(1b1)	2.76
C(11b)...H(1b2)	2.13	C(12b)...H(1b2)	2.72
C(2b) ...H(1b2)	2.87	C(7b) ...H(1b2)	2.63
H(3b1)...C(11b)	2.12	H(3b2)...C(11b)	2.12
C(13b)...C(11b)	2.55	H(4b2)...C(11b)	2.72
H(4b3)...C(11b)	2.78	C(7b) ...C(11b)	3.22
C(12b)...H(2b1)	2.13	C(13b)...H(2b1)	2.79
C(6b) ...H(2b1)	2.95	C(7b) ...H(2b1)	2.89
C(12b)...H(2b2)	2.13	C(13b)...H(2b2)	2.77
H(4b1)...C(12b)	2.20	H(4b2)...C(12b)	2.10
H(4b3)...C(12b)	2.14	C(13b)...H(3b1)	2.13
C(13b)...H(3b2)	2.13	H(3a) ...C(2a)	2.16
C(4a) ...C(2a)	2.42	C(5a) ...C(2a)	2.80
C(6a) ...C(2a)	2.41	H(N2a)...C(2a)	2.98
H(N1a)...C(2a)	2.03	H(4a) ...C(3a)	2.13
C(5a) ...C(3a)	2.39	C(6a) ...C(3a)	2.76
C(7a) ...C(3a)	2.43	C(4a) ...H(3a)	2.13
H(5a) ...C(4a)	2.12	C(6a) ...C(4a)	2.37
C(7a) ...C(4a)	2.79	C(5a) ...H(4a)	2.11
H(6a) ...C(5a)	2.13	C(7a) ...C(5a)	2.43
C(6a) ...H(5a)	2.15	C(7a) ...H(6a)	2.13

table 7 continued

H(N2a)...C(7a)	2.45	H(N1a)...C(7a)	2.66
H(3b) ...C(2b)	2.17	C(4b) ...C(2b)	2.43
C(5b) ...C(2b)	2.81	C(6b) ...C(2b)	2.42
H(N1b)...C(2b)	1.91	H(4b) ...C(3b)	2.15
C(5b) ...C(3b)	2.42	C(6b) ...C(3b)	2.78
C(7b) ...C(3b)	2.43	C(4b) ...H(3b)	2.15
H(5b) ...C(4b)	2.13	C(6b) ...C(4b)	2.39
C(7b) ...C(4b)	2.79	C(5b) ...H(4b)	2.12
H(6b) ...C(5b)	2.14	C(7b) ...C(5b)	2.44
C(6b) ...H(5b)	2.16	C(7b) ...H(6b)	2.15
H(N1b)...C(7b)	2.47		

**Dislocation Discrimination: The Interaction of Zinc(II) and Cadmium(II) with Dibenzo-substituted Macrocyclic and Open-chain Tetra-amines**

Kenneth R. Adam,<sup>a</sup> Christopher W. G. Ansell,<sup>b</sup> Keith P. Dancy,<sup>b</sup> Laurel A. Drummond,<sup>b</sup> Anthony J. Leong,<sup>a</sup> Leonard F. Lindoy,<sup>a\*</sup> and Peter A. Tasker<sup>b\*†</sup>

<sup>a</sup> Department of Chemistry and Biochemistry, James Cook University, Queensland 4811, Australia

<sup>b</sup> School of Chemistry, Polytechnic of North London, London N7 8DB, U.K.

Thermodynamic stabilities have been determined for zinc(II) and cadmium(II) complexes of a series of macrocyclic and open-chain tetra-amines; for the 14- to 16-membered macrocyclic systems a dislocation in the stability pattern occurs for zinc(II) at the 16-membered ring complex while, for cadmium(II), the dislocation occurs at the 15-membered ring species resulting in an enhanced stability difference [Zn<sup>II</sup>>Cd<sup>II</sup>] for the complexes of this latter ring.

---

### Dislocation Discrimination: The Interaction of Zinc(II) and Cadmium(II) with Dibenzo-substituted Macrocyclic and Open-chain Tetra-amines

Kenneth R. Adam,<sup>a</sup> Christopher W. G. Ansell,<sup>b</sup> Keith P. Dancy,<sup>b</sup> Laurel A. Drummond,<sup>b</sup> Anthony J. Leong,<sup>a</sup> Leonard F. Lindoy,<sup>a\*</sup> and Peter A. Tasker<sup>b,\*†</sup>

<sup>a</sup> Department of Chemistry and Biochemistry, James Cook University, Queensland 4811, Australia

<sup>b</sup> School of Chemistry, Polytechnic of North London, London N7 8DB, U.K.

Thermodynamic stabilities have been determined for zinc(II) and cadmium(II) complexes of a series of macrocyclic and open-chain tetra-amines; for the 14- to 16-membered macrocyclic systems a dislocation in the stability pattern occurs for zinc(II) at the 16-membered ring complex while, for cadmium(II), the dislocation occurs at the 15-membered ring species resulting in an enhanced stability difference [Zn<sup>II</sup>>Cd<sup>II</sup>] for the complexes of this latter ring.

Selective complex formation by macrocyclic ligands is of considerable current interest.<sup>1-3</sup> As part of a wider programme in this area, we have previously investigated a little-studied discrimination mechanism termed 'dislocation discrimination'.<sup>4</sup> Such discrimination involves the occurrence of a dislocation in the complexation behaviour of a particular metal ion along a series of closely related ligands.

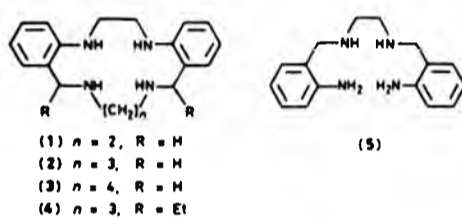
In a previous study,<sup>5</sup> we have investigated the complexation of Zn<sup>II</sup> and Cd<sup>II</sup> by 17- to 19-membered O<sub>2</sub>N<sub>2</sub>-donor macrocycles. Along these respective complex series, a dislocation in the expected log<sub>10</sub>K values occurs for the Cd<sup>II</sup> complex of the 19-membered ring whereas no similar dislocation is apparent along the Zn<sup>II</sup> series. This different complexation behaviour for Zn<sup>II</sup> and Cd<sup>II</sup> has been demonstrated to provide a basis for discriminating between these ions. Further, with these ligands, the 'natural' stability order of Zn<sup>II</sup>>Cd<sup>II</sup> found for simple polyamine ligands<sup>6</sup> is reversed for the complexes of the 17- and 18-membered rings but reverts to the normal order for the complexes of the 19-membered ring.

We now report a new example of dislocation discrimination involving Zn<sup>II</sup> and Cd<sup>II</sup> complexes of the smaller (N<sub>4</sub>-donor) macrocycles (1)-(3)‡ which contain 14- to 16-membered rings, the macrocycles (1)-(3) were obtained by reduction of their corresponding di-imine precursors.<sup>7</sup> Stability patterns for the Zn<sup>II</sup> and Cd<sup>II</sup> complexes were determined potentiometrically (pH titration in 95% methanol) and are given in Figure 1. For Zn<sup>II</sup>, the 14- and 15-membered rings yield log<sub>10</sub>K values which are quite similar whereas there is a sudden drop in stability for the complex of the 16-membered ring. The behaviour for Cd<sup>II</sup> is quite different: in this case a dislocation in stability occurs between the 14- and 15-membered rings with the value for the 15-membered ring complex being lower than expected. The stability then increases for the 16-

‡ (1) 5,6,7,8,9,10,15,16,17,18-decahydrodibenzo[e,m][1,4,8,11]-tetra-azacyclotetradecine; (2) 6,7,8,9,10,11,16,17,18,19-decahydro-5H-dibenzo[e,n][1,4,8,12]tetra-azacyclopentadecine; (3) 5,6,7,8,9,10,11,12,17,18,19,20-dodecahydrodibenzo[e,o][1,4,6,13]-tetra-azacyclohexadecine; (4) 5,11-dithyl-6,7,8,9,10,11,16,17,18,19-decahydro-5H-dibenzo[e,n][1,4,8,12]tetra-azacyclopentadecine; (5) N,N'-bis-(o-aminobenzyl)ethylenediamine; (6) N,N'-bis-(p-(amino-methyl)phenyl)ethylenediamine

\* Present address: Research Department, Imperial Chemical Industries plc, Organics Division, P.O. Box No. 42, Hexagon House, Blackley, Manchester M3 3DA, U.K.





(5)

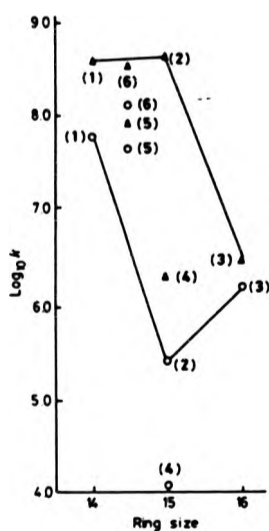
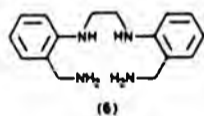


Figure 1.  $\log_{10}K$  values for formation of the 1:1 complexes of  $Zn^{II}$  and  $Cd^{II}$  with (1)–(6). The stabilities were obtained potentiometrically in 95% methanol ( $I = 0.1 M$ ,  $Et_4NClO_4$ ) at 25 °C. All values are the mean of between 2 and 5 individual determinations at varying metal:ligand ratios. In all cases individual  $\log_{10}K$  values fell within 0.1 of the mean (and usually within 0.05).  $\Delta$ ,  $Zn^{II}$ ;  $\circ$ ,  $Cd^{II}$ .

membered ring species. Thus, relative to the 14-membered and 16-membered ring systems, the 15-membered ring shows enhanced recognition for  $Zn^{II}$  over  $Cd^{II}$ .

In order to probe the generality of this enhanced recognition for  $Zn^{II}$ , the stabilities of the  $Zn^{II}$  and  $Cd^{II}$  complexes of the corresponding 15-membered diethylated (*meso*) derivative (4)<sup>†</sup> were determined. Although both  $\log_{10}K$  values are lower than those for the unsubstituted 15-membered macrocycle (2), the diethyl derivative still maintains the discrimination observed for the parent ring. The lower  $\log_{10}K$  values obtained with the disubstituted macrocycle presumably reflect the effect of increased steric hindrance on complexation; nevertheless, the stability difference for  $Zn^{II}$  and  $Cd^{II}$  is clearly not markedly dependent on the presence or absence of diethyl substituents.

In parallel experiments, the interaction of the above ions with the open-chain ligands (5)<sup>‡</sup> and (6)<sup>‡</sup> was investigated. Both ligands can be considered to be analogues of the 15 membered macrocycle (2). For each open-chain system, the  $\log_{10}K$  values are unremarkable (see Figure 1) with the respective  $Zn^{II}$  complexes being only slightly more stable than the corresponding  $Cd^{II}$  species. Thus, the discrimination observed for the 15-membered ring (2) clearly depends on its cyclic nature; nevertheless, the behaviour does not constitute ring-size discrimination of the most common type.<sup>1,2</sup> The latter solely involves the match or otherwise of the metal-ion for the radius of the available macrocyclic hole.

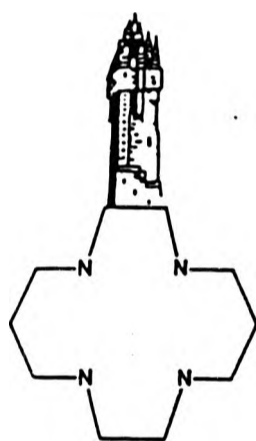
In contrast to the stability pattern for the  $Zn^{II}$  complexes of (1)–(3), the complexes of the larger  $Cd^{II}$  ion show decreased stability as the ring size increases from 14 to 15 members (even though the stability again rises as the hole size is further increased in the 16-membered ring). The enhanced discrimination ability shown by the 15-membered ring thus appears to be a consequence of the different dislocation patterns which occur when these cyclic ligands interact with  $Zn^{II}$  and  $Cd^{II}$ . Overall, the study thus documents a new example of dislocation discrimination: a discrimination mechanism of potential importance to a number of other metal-containing chemical and biochemical systems.

We thank the S.E.R.C. and I.C.I. (U.K.) for a Co-operative Research Grant as well as the Australian Research Grants Scheme and the Australian Institute of Nuclear Science and Engineering for assistance.

Received, 6th December 1985; Com 1730

#### References

- R. M. Izatt, J. S. Bradshaw, S. A. Nielsen, J. D. Lamb, and J. J. Christensen, *Chem. Rev.*, 1985, **85**, 271.
- K. Henrick, P. A. Tasker, and L. F. Lindoy, *Prog. Inorg. Chem.*, 1985, **33**, 1.
- K. R. Adam, K. P. Dancy, B. A. Harrison, A. J. Leong, L. F. Lindoy, M. McPartlin, and P. A. Tasker, *J. Chem. Soc., Chem. Commun.*, 1983, 1351.
- K. R. Adam, A. J. Leong, L. F. Lindoy, H. C. Lip, B. W. Skelton, and A. H. White, *J. Am. Chem. Soc.*, 1983, **105**, 4645.
- P. G. Owston, R. Peters, E. Ramsammy, P. A. Tasker, and J. Trotter, *J. Chem. Soc., Chem. Commun.*, 1980, 1218.
- K. Henrick, P. M. Judd, P. G. Owston, R. Peters, P. A. Tasker, and R. W. Turner, *J. Chem. Soc., Chem. Commun.*, 1983, 1253.
- C. W. G. Ansell, M. McPartlin, P. A. Tasker, and A. Thambythurai, *Polyhedron*, 1983, **2**, 83.



**POSTERS AND LECTURE ABSTRACTS**

**3rd EUROPEAN SYMPOSIUM ON  
MACROCYCLIC COMPOUNDS**

**1984**

**AUGUST 29, 30, 31**

**UNIVERSITY OF STIRLING  
SCOTLAND**

## B 25

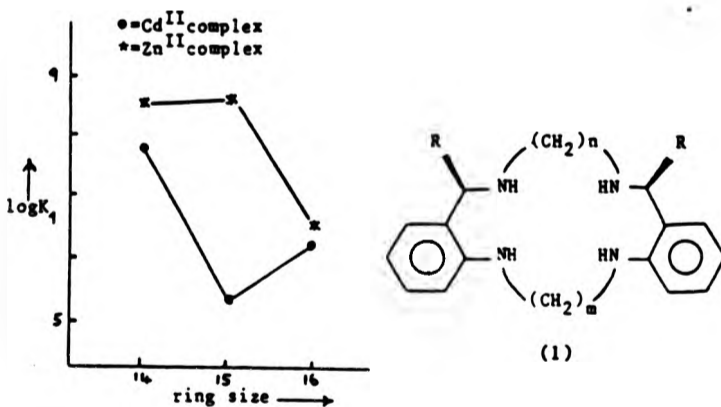
### A STRUCTURAL BASIS FOR ZINC/CADMIUM DISCRIMINATION BY QUADRIDENTATE NITROGEN LIGANDS.

Laurel A Drummond,<sup>a</sup> Keith P Dancey,<sup>a</sup> Antony J Leong,<sup>b</sup> Leonard F Lindoy,<sup>b</sup> Mary McPartlin,<sup>a</sup> and Peter A Tasker.<sup>a</sup>

a. School of Chemistry, The Polytechnic of North London, London N7 8DB.

b. Dept. of Chemistry and Biochemistry James Cook University, Townsville 4811 Australia.

Selective complex formation by macrocyclic compounds is currently being considered for industrial and biochemical uses. As part of a wider programme we have recently considered design of ligands which discriminate between Zn(II) and Cd(II).<sup>1</sup> An empirical approach has been used which involves assessing how discrimination ( $\Delta \log K_1$ ) varies as a function of a given type of ligand structural parameter, eg. ring-size (see figure).



Once the optimum value of this parameter has been ascertained, variation of another type of structural parameter (eg. the size of peripheral groups such as R in 1) is considered, to further enhance discrimination, i.e. to obtain larger values of  $\Delta \log K_1$ . Interpretation of the variations of discrimination within such ligand-series has required detailed structural analysis (usually X-ray structure determination). Data of this kind will be presented and the evidence for "structural dislocation" within the series of M<sub>4</sub>-ligands will be considered. A series of ligands (1) with different alkyl substituents (R) can be conveniently prepared by stereoselective C-alkylation of the related diimine.

#### References:

1. K.R.Adam, K.P.Dancey, B.A.Harrison, A.J.Leong, L.F.Lindoy, M.McPartlin and P.A.Tasker, *J.Chem.Soc., Chem.Commun.*, 1983 1351.

Contribution from the Department of Chemistry, Polytechnic of North London, London N7 8DB, United Kingdom, and the Department of Chemistry and Biochemistry, James Cook University of North Queensland, Queensland 4811, Australia

## Studies of Macrocyclic Ligand Hole Sizes. 2.<sup>1</sup> X-ray Structures of the Nickel Chloride Complexes of Analogous 15-Membered Macrocycles Containing O<sub>2</sub>N<sub>2</sub>-, N<sub>4</sub>-, and S<sub>2</sub>N<sub>2</sub>-Donor Sets

LAUREL A. DRUMMOND,<sup>2a</sup> KIM HENRICK,<sup>2a</sup> MARY J. L. KANAGASUNDARAM,<sup>2a</sup> LEONARD F. LINDOY,<sup>2b</sup> MARY McPARTLIN,<sup>2a</sup> and PETER A. TASKER<sup>2a\*</sup>

Received February 26, 1982

X-ray diffraction structures of the nickel chloride complexes of the N<sub>4</sub>-donor and S<sub>2</sub>N<sub>2</sub>-donor macrocycles 3,4,9,10-dibenzo-1,5,8,12-tetraazacyclopentadecane (N<sub>4</sub>-mac) and 3,4,9,10-dibenzo-1,12-diaza-5,8-dithiacyclopentadecane (S<sub>2</sub>N<sub>2</sub>-mac) have been obtained and compared with the previously determined structure of the analogous complex of the O<sub>2</sub>N<sub>2</sub> macrocycle 3,4,9,10-dibenzo-1,12-diaza-5,8-dioxacyclopentadecane (O<sub>2</sub>N<sub>2</sub>-mac). All complexes contain corresponding 15-membered macrocyclic rings and show trans-chloro, pseudooctahedral coordination geometries with the X<sub>2</sub>N<sub>2</sub>-donor (X = O, N, S) sets being nearly planar. In each complex the nickel atom lies in the hole of the macrocycle, with both aromatic rings confined to the same side of the respective donor atom planes when X = O or S and to opposite sides when X = N. A general procedure for estimating the match of a metal ion for a particular macrocyclic ring is described: the hole size given by the mean distance of the donor atom positions from their centroid is "corrected" for the mean covalent radii of the donor atom types present to yield the apparent cavity available to the metal ion. This is then compared with the covalent radius of the metal ion involved. The results for the present systems suggest that all three macrocycles fit high-spin nickel well. Even though the radius of the sulfur donors is considerably larger than those of oxygen or nitrogen, this difference appears to be largely compensated by the greater "circumference" of the inner ring in the sulfur-containing macrocycle (resulting from the presence of four long C-S bonds) so that the cavity presented to nickel remains nearly ideal. [Ni(N<sub>4</sub>-mac)Cl<sub>2</sub>]: space group P2<sub>1</sub>/c, a = 12.151 (3) Å, b = 18.934 (6) Å, c = 11.253 (2) Å, β = 115.98 (8)°, R = 0.059 for 1459 four-circle diffraction data with I > 2σ(I). [Ni(S<sub>2</sub>N<sub>2</sub>-mac)Cl<sub>2</sub>]: space group P2<sub>1</sub>/n, a = 19.334 (4) Å, b = 13.128 (9) Å, c = 7.999 (1) Å, β = 99.05 (3)°, R = 0.032 for 4127 four-circle diffraction data with I > 3σ(I).

### Introduction

As part of a series of studies involving the design and synthesis of macrocyclic ligands of potential use as metal ion selective reagents, the solution behavior of a variety of such ligands toward a number of transition-metal ions has been investigated.<sup>2-9</sup> Particular attention has been given to a search for macrocycle hole-size discrimination effects, and for example, such effects were observed in the kinetic and thermodynamic behavior of a series of nickel complexes of 14- to 17-membered O<sub>2</sub>N<sub>2</sub>-donor macrocycles.<sup>3,8</sup> In parallel to these studies, X-ray diffraction structural determinations of selected compounds have also been performed.<sup>3,4,7,9</sup> Of particular interest have been the hole sizes of the respective macrocycles and their relationship to the observed metal ion chemistry; in these studies the radius of the hole defined by the O<sub>2</sub>N<sub>2</sub>-donor sets was calculated as the mean distance of the positions of the donor atoms from their centroid. A previous study<sup>3</sup> has shown that substitution of two imine linkages for two secondary amine linkages in the 16-membered O<sub>2</sub>N<sub>2</sub>-donor ring leads to only a very minor reduction in the cavity size available to nickel when allowance is made for the effectively smaller radius of sp<sup>2</sup> nitrogen over sp<sup>3</sup> nitrogen.

Up to the present, little structural information is available on the effects of variation of donor atom type on hole size

Table I. Crystal Data and Selected<sup>a</sup> Details of Structure Determinations of [Ni(N<sub>4</sub>-mac)Cl<sub>2</sub>] and [Ni(S<sub>2</sub>N<sub>2</sub>-mac)Cl<sub>2</sub>]

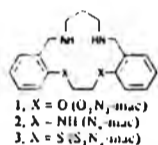
	[Ni(N <sub>4</sub> -mac)Cl <sub>2</sub> ]	[Ni(S <sub>2</sub> N <sub>2</sub> -mac)Cl <sub>2</sub> ]
mol formula <sup>b</sup>	C <sub>20</sub> H <sub>22</sub> Cl <sub>2</sub> N <sub>4</sub> Ni	C <sub>20</sub> H <sub>22</sub> Cl <sub>2</sub> N <sub>2</sub> S <sub>2</sub> Ni
M <sub>r</sub>	524.99	474.17
space group	P2 <sub>1</sub> /c	P2 <sub>1</sub> /n
a/Å	12.151 (3)	19.334 (3)
b/Å	18.934 (6)	13.128 (9)
c/Å	11.253 (2)	7.991 (2)
d/deg	115.98 (8)	99.05 (3)
Z	4	4
θ range/deg <sup>c</sup>	3-25	3-25
V/F <sub>0</sub> /(V/F <sub>0</sub> ) <sup>d</sup> for data used in refinement	4	6
no. of data in refinement	1459	4127
R = Σ F <sub>o</sub> - F <sub>c</sub>   / ΣF <sub>o</sub> <sup>e</sup>	0.059	0.032
R <sub>w</sub> <sup>f</sup> = [Σw( F <sub>o</sub> - F <sub>c</sub>  ) <sup>2</sup> / ΣwF <sub>o</sub> <sup>2</sup> ] <sup>1/2</sup>	0.059	0.036

<sup>a</sup> Further information is available in the supplementary material, Table 1S. <sup>b</sup> The N<sub>4</sub>-mac complex contains a CH<sub>2</sub>Cl<sub>2</sub> solvate molecule. This shows complex disorder near an inversion center. Two sites are represented by atoms C(1a), C(1b), C(1c), and C(1d). C(1a), C(1b), C(1c), and C(1d) in Table II with site occupation factors 0.59 and 0.22, respectively. A third site (occupation factor 0.19) has its C atom coincident with C(1a) and its Cl atoms coincident with C(1c) and C(1d), related to C(1a) in Table II by 1 + x, 1 - y, -z. Refinement with this model was accomplished by adjusting the site occupation factors for C(1a) and C(1b) (see Table II) to take account of the overlaid third site. <sup>c</sup> Intensity measurements were made on a Philips PW1100 diffractometer using Mo Kα radiation. <sup>d</sup> The function minimized was Σw(|F<sub>o</sub> - F<sub>c</sub>|)<sup>2</sup> where w = 1/(σ(F<sub>o</sub>))<sup>2</sup>. <sup>e</sup> R<sub>w</sub> = [Σw(|F<sub>o</sub> - F<sub>c</sub>|)<sup>2</sup> / ΣwF<sub>o</sub><sup>2</sup>]<sup>1/2</sup>.

within a given macrocyclic ligand framework. In an attempt to redress this deficiency, the X-ray structures of three high-spin nickel complexes of type [Ni(mac)Cl<sub>2</sub>] (macrocyclic (mac) = 1-3) are now compared.<sup>10</sup>

(10) Details of the structure of [Ni(O,N-mac)Cl<sub>2</sub>] have been published previously,<sup>3</sup> and a full report of the corresponding dithiocarbamate complex has also appeared. See Battaglia, L. P.; Corradi, A. B.; Mapiña, A. *Inorg. Chim. Acta* 1980, 39, 211.

- (1) Part I: Goodwin, H. J.; Henrick, K.; Lindoy, L. F.; McPartlin, M.; Tasker, P. A. *Inorg. Chem.* 1982, 21, 3261.
- (2) (a) Polytechnic of North London. (b) James Cook University of North Queensland.
- (3) Ekstrom, A.; Lindoy, L. F.; Lip, H. C.; Smith, R. J.; Goodwin, H. J.; McPartlin, M.; Tasker, P. A. *J. Chem. Soc., Dalton Trans.* 1979, 1027.
- (4) Adam, K. R.; Anderregg, G.; Lindoy, L. F.; Lip, H. C.; McPartlin, M.; Rea, J. H.; Smith, R. J.; Tasker, P. A. *Inorg. Chem.* 1980, 19, 2956.
- (5) Lindoy, L. F.; Lip, H. C.; Rea, J. H.; Smith, R. J.; Henrick, K.; McPartlin, M.; Tasker, P. A. *Acta Cryst.* 1980, 36, 360.
- (6) Anderregg, G.; Ekstrom, A.; Lindoy, L. F.; Smith, R. J. *J. Am. Chem. Soc.* 1980, 102, 2670.
- (7) Ekstrom, A.; Lindoy, L. F.; Smith, R. J. *Inorg. Chem.* 1980, 19, 724.
- (8) Adam, K. R.; Anderregg, G.; Henrick, K.; Lindoy, L. F.; Lip, H. C.; McPartlin, M.; Smith, R. J.; Tasker, P. A., to be submitted for publication in *Inorg. Chem.*
- (9) Adam, K. R.; Lindoy, L. F.; Lip, H. C.; Rea, J. H.; Shelton, B. W.; White, A. H. *J. Chem. Soc., Dalton Trans.* 1981, 74.
- (10) Lindoy, L. F.; Smith, R. J. *Inorg. Chem.* 1981, 20, 1314.



#### Experimental Section

Blue crystals of  $[Ni(S_2N_2\text{-mac})Cl_2]^{17}$  were obtained on recrystallization of this complex from methanol.  $[Ni(N_4\text{-mac})Cl_2]^{11}$  was recrystallized from dichloromethane to yield blue crystals. Crystal data and details of the structure determinations are summarized in Table I. Further details are given in the supplementary material together with additional data for  $[Ni(O_2N_2\text{-mac})Cl_2]$ . Atomic fractional coordinates and isotropic thermal parameters in the former two complexes are listed in Table II.

Hydrogen atoms attached to carbon atoms were included in calculated positions (Table 2S, supplementary material) and refined with common thermal parameters. Hydrogen atoms attached to nitrogen atoms (Table 1S, supplementary material) were inserted in positions found in difference-Fourier maps. Their positional and isotropic thermal parameters were refined for  $[Ni(S_2N_2\text{-mac})Cl_2]$ . However, only a common isotropic thermal parameter for aryl hydrogens was refined for  $[Ni(N_4\text{-mac})Cl_2]$ .

#### Results and Discussion

In accordance with the evidence from other physical measurements, the X-ray structural determinations indicate that the  $N_4$ -donor and  $S_2N_2$ -donor complexes have *trans*-dichloro structures, which are related to that found previously for  $[Ni(O_2N_2\text{-mac})Cl_2]$ .<sup>3</sup> In all three complexes the coordination geometries are best described as distorted octahedral (Figure 2a-c). A comparison of selected bond lengths and angles for the complexes is given in Table III and Figure 3; torsion angles in the inner great rings are compared in Table 7S (supplementary material). The distortions from octahedral symmetry are reflected by the considerable variation of bond lengths and angles, which occur about the nickel atom in each complex. The  $N_4$ -donor complex has pseudo-two-fold symmetry whereas the other two complexes show approximate mirror symmetry; the lengths of most of the chemically equivalent bonds in the two halves (a and b) of each molecule are the same within experimental error (see Table III). Exceptions to this are the Ni-O lengths in  $[Ni(O_2N_2\text{-mac})Cl_2]$  and the Ni-S lengths in  $[Ni(S_2N_2\text{-mac})Cl_2]$  where the bonds differ by 0.102 and 0.046 Å, respectively (see Figure 3). Related variations in Ni-O bond lengths were also found in the nickel bromide complex of the analogous 16-membered  $O_2N_2$  macrocycle.<sup>1,12</sup> In the  $(O_2N_2\text{-mac})$  and  $(S_2N_2\text{-mac})$  ligands the gauche conformation of the ethane linkage in the five-membered chelate rings coupled with the saddle-shaped conformation of the macrocycles (vide infra) require the pairs of Ni-O or Ni-S bonds to be nonequivalent. In all these mixed-donor systems, the ether and thioether donor atoms are expected to bind more weakly to nickel than the nitrogen donors. As a consequence, any cumulative ring strain in the complexes arising from the presence in each of three six-membered fused rings might be expected to be accommodated by variation of the bond lengths and/or angles in the remaining (five-membered) chelate ring incorporating the oxygen or sulfur donors. Such an effect appears to be a source of the unequal bond lengths mentioned above. In addition, the conformations of the five-membered rings in  $[Ni(O_2N_2\text{-mac})Cl_2]$  or  $[Ni(S_2N_2\text{-mac})Cl_2]$  each have an uneven distribution of the ethane bridge with respect to the

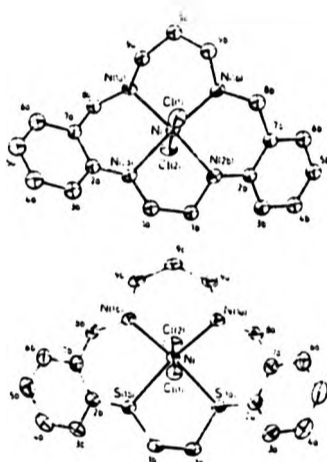


Figure 1. Views of  $[Ni(N_4\text{-mac})Cl_2]$  and  $[Ni(S_2N_2\text{-mac})Cl_2]$  showing atom labels and thermal ellipsoids (30% probability).

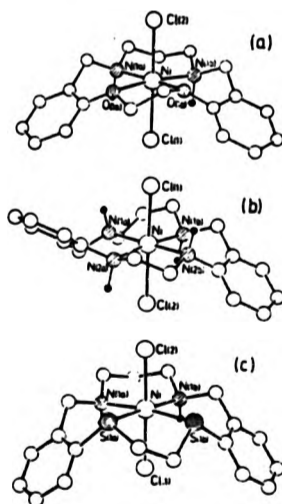


Figure 2. Comparative views of the macrocycle conformations in (a)  $[Ni(O_2N_2\text{-mac})Cl_2]$ , (b)  $[Ni(N_4\text{-mac})Cl_2]$ , and (c)  $[Ni(S_2N_2\text{-mac})Cl_2]$ .

donor atom planes of the respective macrocycles. Each bridge is bent away from the normal gauche arrangement toward an envelope conformation. In contrast, the five-membered ring in  $[Ni(N_4\text{-mac})Cl_2]$  is much closer to a regular gauche arrangement.

The axial Ni-Cl bonds in the  $(S_2N_2\text{-mac})$  complex show a small but significant difference in length. The longer bond is observed for Cl(1), which experiences the shortest intramolecular contacts: Cl(1)-H(1Na), 2.60; Cl(1)-H(1Nb), 2.70; Cl(1)-H(1b2), 2.77 Å; cf. Cl(2)-H(9b1), 2.85 Å. A similar situation was reported<sup>1</sup> for nonequivalent *trans*-Ni-Br

(11) Owsen, P. G.; Peters, K.; Tasker, P. A., unpublished work.

(12) Even greater variations of metal-ether oxygen bond lengths occur in cis complexes of related ligands. See Armstrong, I. G.; Lindsay, L. F.; McParlin, M.; Mosker, G. M.; Tasker, P. A. *Inorg Chem* 1977, 16, 1645; Lalancette, K. A.; Mackay, D. J.; Lorey, W. F. *Inorg Chem* 1976, 15, 545.

Macrocyclic Ligand Hole Sizes

Table II. Fractional Atomic Coordinates and Thermal Parameters/A<sup>2</sup> for [Ni(N<sub>2</sub>-mac)Cl<sub>2</sub>] and [NiS<sub>2</sub>N<sub>2</sub>-mac]Cl<sub>2</sub>

atom	x	y	z	U(iso) or U(eq)
[Ni(N <sub>2</sub> -mac)Cl <sub>2</sub> ]				
Ni(1)	0.09036 (14)	0.15576 (8)	0.24698 (16)	0.0327 (8)
Cl(1)	0.1925 (3)	0.1421 (2)	0.4893 (3)	0.032 (2)
Cl(2)	-0.0147 (3)	0.1532 (1)	0.0029 (3)	0.042 (2)
N(1a)	-0.0078 (8)	0.2419 (5)	0.2589 (8)	0.033 (6)
N(2a)	-0.0509 (8)	0.0829 (4)	0.2357 (9)	0.037 (6)
N(1b)	0.2288 (8)	0.2192 (4)	0.2418 (9)	0.037 (6)
N(2b)	0.1842 (8)	0.0610 (4)	0.2429 (8)	0.032 (6)
C(1a)	0.0087 (11)	0.0135 (6)	0.2717 (12)	0.044 (3)
C(2a)	-0.1292 (10)	0.1916 (6)	0.2942 (11)	0.039 (3)
C(3a)	-0.1647 (11)	0.0538 (6)	0.3645 (11)	0.051 (3)
C(4a)	-0.2438 (11)	0.0750 (6)	0.4178 (13)	0.057 (4)
C(5a)	-0.2850 (11)	0.1416 (6)	0.4025 (12)	0.058 (4)
C(6a)	-0.2494 (10)	0.1915 (6)	0.3356 (12)	0.052 (4)
C(7a)	-0.1733 (10)	0.1726 (5)	0.2762 (11)	0.038 (3)
C(8a)	-0.1393 (10)	0.2262 (6)	0.2010 (11)	0.042 (3)
C(9a)	0.0176 (10)	0.3051 (5)	0.1998 (11)	0.044 (3)
C(9c)	0.1445 (9)	0.3339 (6)	0.2777 (11)	0.045 (3)
C(9b)	0.2505 (10)	0.2814 (6)	0.3310 (12)	0.049 (3)
C(1b)	0.0939 (9)	0.0029 (3)	0.2099 (11)	0.041 (3)
C(2b)	0.2587 (10)	0.0626 (6)	0.1704 (11)	0.036 (3)
C(3b)	0.2504 (10)	0.0101 (6)	0.0814 (12)	0.045 (3)
C(4b)	0.3207 (11)	0.0140 (6)	0.0121 (12)	0.052 (4)
C(5b)	0.3985 (11)	0.0698 (6)	0.0355 (12)	0.052 (3)
C(6b)	0.4092 (11)	0.1227 (6)	0.1231 (12)	0.052 (3)
C(7b)	0.3367 (10)	0.1197 (6)	0.1903 (6)	0.038 (3)
C(8b)	0.3471 (10)	0.1803 (6)	0.2858 (12)	0.049 (3)
C(1a) <sup>#</sup>	-0.4649 (21)	0.3656 (13)	0.2721 (25)	0.058 (7)
C(1b) <sup>#</sup>	-0.4130 (9)	0.3722 (6)	0.1501 (11)	0.144 (4)
C(2a) <sup>#</sup>	-0.4207 (7)	0.3398 (4)	0.3871 (8)	0.101 (2)
C(2b) <sup>#</sup>	-0.5143 (23)	0.4229 (13)	0.1948 (27)	0.124 (9)
C(3a) <sup>#</sup>	-0.4459 (28)	0.3477 (17)	0.2220 (34)	0.139 (11)
C(4a) <sup>#</sup>	-0.4955 (11)	0.4645 (5)	0.0480 (11)	0.125 (4)
[NiS <sub>2</sub> N <sub>2</sub> -mac]Cl <sub>2</sub>				
Ni	0.19433 (1)	0.18633 (2)	-0.10657 (3)	0.0307 (1)
Cl(1)	0.18409 (3)	0.05734 (4)	0.11032 (7)	0.0388 (3)
Cl(2)	0.20368 (4)	0.31382 (4)	-0.32211 (8)	0.0511 (4)
S(1a)	0.12648 (3)	0.31748 (5)	0.02249 (8)	0.0395 (3)
S(1b)	0.29038 (3)	0.26935 (4)	0.07769 (8)	0.0377 (3)
N(1a)	0.1028 (1)	0.1232 (1)	-0.2379 (2)	0.036 (1)
N(1b)	0.2610 (1)	0.0849 (1)	-0.2046 (2)	0.034 (1)
C(1b)	0.2474 (1)	0.2892 (2)	0.2634 (3)	0.049 (1)
C(2b)	0.3487 (1)	0.1673 (2)	0.1403 (3)	0.036 (1)
C(3b)	0.3779 (1)	0.1518 (2)	0.3098 (3)	0.043 (1)
C(4b)	0.4281 (1)	0.0770 (2)	0.3504 (4)	0.052 (2)
C(5b)	0.4490 (1)	0.0182 (2)	0.2256 (4)	0.056 (2)
C(6b)	0.4183 (1)	0.0310 (2)	0.0583 (4)	0.051 (1)
C(7b)	0.3679 (1)	0.1065 (2)	0.0117 (3)	0.040 (1)
C(8b)	0.3355 (1)	0.1173 (2)	-0.1720 (3)	0.043 (1)
C(9b)	0.2396 (1)	0.0618 (2)	-0.3874 (3)	0.043 (1)
C(9c)	0.1668 (1)	0.0192 (2)	-0.4277 (3)	0.044 (1)
C(1a)	0.1846 (1)	0.3550 (2)	0.2150 (3)	0.053 (2)
C(2a)	0.0554 (1)	0.2451 (2)	0.0758 (3)	0.040 (1)
C(3a)	0.0333 (1)	0.2494 (2)	0.2328 (4)	0.052 (1)
C(4a)	-0.0277 (2)	0.1985 (2)	0.2564 (4)	0.063 (2)
C(5a)	-0.0654 (2)	0.1432 (2)	0.1274 (4)	0.064 (2)
C(6a)	-0.0421 (1)	0.1365 (2)	-0.0286 (4)	0.054 (2)
C(7a)	0.0179 (1)	0.1885 (2)	-0.0567 (3)	0.042 (1)
C(8a)	0.0385 (1)	0.1847 (2)	-0.2318 (3)	0.043 (1)
C(9a)	0.1074 (1)	0.0926 (2)	-0.4150 (3)	0.045 (1)

<sup>#</sup> Site occupation factors for these atoms are given in Table I.

bonds in a complex of a related 16-membered ring

In all three complexes the four donor atoms of the respective macrocycles are close to planar. The maximum deviation of the nitrogen atoms from the equatorial plane in [Ni(N<sub>2</sub>-mac)Cl<sub>2</sub>] is 0.06 Å. For the O<sub>2</sub>N<sub>2</sub> and S<sub>2</sub>N<sub>2</sub> systems the maximum deviations of the donor atoms are 0.06 and 0.05 Å, respectively.

The Ni-N bond lengths in the three complexes (Figure 3) all fall within the range of 2.03-2.16 Å observed for the co-

Inorganic Chemistry, Vol. 21, No. 11, 1982 3925

Table III. Selected<sup>a</sup> Bond Lengths/Å and Angles/Deg in the Complexes [Ni(N<sub>2</sub>-mac)Cl<sub>2</sub>] and [NiS<sub>2</sub>N<sub>2</sub>-mac]Cl<sub>2</sub>

	[Ni(N <sub>2</sub> -mac)Cl <sub>2</sub> ]		[NiS <sub>2</sub> N <sub>2</sub> -mac]Cl <sub>2</sub>	
	X = N(2a) or N(2b)	X = S(1a) or S(1b)	part a	part b
Distances <sup>b</sup>				
Ni-Cl(1)	2.465 (3)	2.453 (1)		
Ni-Cl(2)	2.471 (3)	2.429 (1)		
Ni-N(1)	2.059 (10)	2.089 (10)	2.082 (2)	2.089 (2)
Ni-X	2.162 (10)	2.138 (9)	2.485 (1)	2.438 (1)
C(1)-C(1)'	1.49 (2)		1.491 (4)	
C(1)-X	1.47 (1)	1.48 (1)	1.824 (3)	1.830 (3)
X-C(2)	1.42 (2)	1.46 (2)	1.777 (3)	1.771 (2)
C(2)-C(7)	1.43 (2)	1.39 (2)	1.399 (3)	1.397 (3)
C(7)-C(8)	1.49 (1)	1.54 (2)	1.514 (4)	1.509 (3)
C(8)-N(1)	1.47 (1)	1.49 (2)	1.490 (3)	1.486 (3)
N(1)-C(9)	1.47 (2)	1.49 (2)	1.487 (3)	1.486 (3)
C(9)-C(9c)	1.50 (1)	1.53 (2)	1.515 (3)	1.502 (4)
Angles <sup>b</sup>				
C(1)-Ni-C(2)	172.8 (1)		179.6 (1)	
Cl(1)-Ni-X	90.0 (3)	85.5 (3)	94.5 (1)	91.2 (1)
Cl(1)-Ni-N(1)	92.1 (3)	94.0 (3)	85.7 (1)	87.0 (1)
Cl(2)-Ni-X	84.9 (3)	88.9 (2)	85.4 (1)	89.2 (1)
Cl(2)-Ni-N(1)	93.2 (2)	90.6 (3)	93.9 (1)	93.1 (1)
X-Ni-X'	83.1 (4)		80.9 (1)	
X-Ni-N(1)	92.4 (4)	92.2 (4)	91.3 (1)	93.2 (1)
X-Ni-N(1)'	173.6 (4)	174.9 (4)	173.9 (1)	171.3 (1)
N(1)-Ni-N(1)'	92.5 (4)		94.7 (1)	
C(1)-C(1)-X	111 (1)	111.9 (9)	115.5 (2)	109.1 (2)
C(1)-X-Ni	105.8 (7)	106.5 (7)	104.0 (1)	98.8 (1)
C(1)-X-C(2)	116 (1)	116.7 (9)	109.8 (1)	103.2 (1)
C(2)-X-Ni	119.7 (7)	117.4 (6)	102.0 (1)	102.9 (1)
X-C(2)-C(7)	117 (1)	118 (1)	115.5 (2)	117.1 (2)
C(2)-C(7)-C(8)	123 (1)	122 (1)	122.5 (2)	122.9 (2)
C(7)-C(8)-N(1)	113.8 (8)	113.3 (8)	113.0 (2)	112.7 (2)
C(8)-N(1)-Ni	111.1 (6)	112.1 (7)	114.6 (1)	113.0 (1)
C(8)-N(1)-C(9)	111.6 (8)	107.8 (7)	110.7 (2)	110.0 (2)
C(9)-N(1)-Ni	112.0 (8)	109.9 (8)	114.4 (2)	114.0 (1)
N(1)-C(9)-C(9c)	113.4 (8)	112.3 (8)	113.2 (2)	113.1 (2)
C(9)-C(9c)-C(9)	117.8 (9)		116.3 (2)	

<sup>a</sup> Complete lists of bond lengths and angles are given in the supplementary material (Tables 45 and 55). <sup>b</sup> Primes denote atoms from the alternative part of the molecule. Atom C(9c) is the central atom of the trimethylene bridge.

ordinate bonds from neutral sp<sup>3</sup>-hybridized N atoms in high-spin nickel complexes of macrocyclic ligands.<sup>1</sup> In each complex, the corresponding pairs of Ni-N bonds are equal within experimental error. In [Ni(N<sub>2</sub>-mac)Cl<sub>2</sub>] the nickel is closer to the benzylamino nitrogens, N(1a) and N(1b), than to the anilino nitrogens, N(2a) and N(2b). The difference of 0.07 Å between the lengths (mean values) of the two Ni-N bond types appears to be a consequence of the smaller chelate ring containing N(2a) and N(2b), which defines a relatively unfavorable N-Ni-N bond angle (82°). A related situation exists in the other two complexes, where the angles subtended by the donor atoms of each five-membered chelate ring at nickel are both considerably less than 90°. In the O<sub>2</sub>N<sub>2</sub> and S<sub>2</sub>N<sub>2</sub>-donor complexes the O-Ni and S-Ni bond lengths each fall in the respective ranges of 1.99-2.31 Å (Ni-O)<sup>1</sup> and 2.38-2.53 Å (Ni-S),<sup>11</sup> found for related bonds to high-spin

- (13) Loub, J.; Podlshova, J. *Inorg. Nucl. Chem. Lett.* 1971, 7, 409. Podlshova, J.; Loub, J.; Novak, C. *Acta Crystallogr., Sect. B* 1972, 28, 1623. Loun, R.; Metz, B.; Weiss, R. *Ibid.* 1974, 30, 774. Obodovskaya, A. E.; Shkol'nikova, L. M.; Zavadnik, V. E.; Annev, N. V. R.; Kuchin, S. G.; Kogan, V. A.; Oupov, O. A. *Koord. Khim.* 1976, 2, 197. Delaunay, J.; Kappenstein, C.; Hugel, R. *Acta Crystallogr., Sect. B* 1976, 32, 2341. Bngel, E. M.; Moeckler, G. M.; Sinn, E. *Inorg. Chem.* 1977, 16, 467. Delaunay, J.; Kappenstein, C.; Hugel, R. *P. J. Chem. Res., Microsyn* 1978, 48, 891. Katarah, C.; Tasker, P. A.; Trotter, J. *J. Chem. Soc., Dalton Trans.* 1978, 1057. Choong, W.; Stephenson, N. C.; Ali, M. A.; Malik, M. A.; Phillips, D. *J. Aust. J. Chem.* 1978, 31, 1199. Loun, R.; Agans, Y.; Weiss, R. *Acta Crystallogr., Sect. B* 1979, 35, 2905.

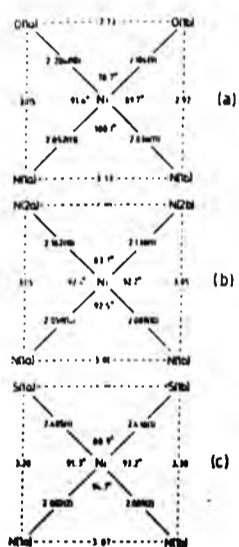


Figure 3. Comparison of bond lengths/Å and angles/deg within the donor atom planes of the macrocycles in (a)  $[\text{Ni}(\text{O}_2\text{N}_2\text{-mac})\text{Cl}_2]$ , (b)  $[\text{Ni}(\text{N}_2\text{-mac})\text{Cl}_2]$ , and (c)  $[\text{Ni}(\text{S}_2\text{N}_2\text{-mac})\text{Cl}_2]$ . The e.s.d.'s for ligand bond and bond angles in parts a, b, and c are  $\leq 0.01$ ,  $\leq 0.01$ ,  $\leq 0.004$  Å and  $\leq 0.5$ ,  $\leq 0.4$ ,  $\leq 0.1^\circ$ , respectively.

Table IV. Calculated Values for the Hole Sizes of the Coordinated Macrocycles

complex	$D_A/\text{Å}$ , diameter of macrocyclic hole (un-corrected) <sup>a</sup>	$R_A/\text{Å}$ , "apparent" radius of metal ion cavity <sup>b</sup>
$[\text{Ni}(\text{O}_2\text{N}_2\text{-mac})\text{Cl}_2]^c$	4.18	1.35 <sup>d</sup>
$[\text{Ni}(\text{N}_2\text{-mac})\text{Cl}_2]$	4.22	1.39
$[\text{Ni}(\text{S}_2\text{N}_2\text{-mac})\text{Cl}_2]$	4.54	1.39

<sup>a</sup> Calculated as twice the mean distance of the donor atom positions from their centroid. <sup>b</sup> Derived from the calculated diameter by correcting for the mean of the covalent radii of the donor atoms present, i.e.,  $R_A = D/2 - r_d$ , where  $r_d$  = "modified covalent radius" of donor(i) calculated from data in the Cambridge Crystallographic Data Centre files (see text and ref 20). <sup>c</sup> Identical values were obtained for  $[\text{Ni}(\text{O}_2\text{N}_2\text{-mac})(\text{NCS})_2]$ . <sup>d</sup> The Pauling radius for high-spin  $\text{Ni}(\text{II})$  is 1.39 Å.

nickel in other complexes.

The macrocycles in the  $\text{O}_2\text{N}_2$  and  $\text{S}_2\text{N}_2$  complexes both have a "saddle-shaped" configuration (see Figure 2). This "saddle-shaped" distortion from planarity is more marked in the  $\text{S}_2\text{N}_2$  complex in which the benzylamino chelate rings are inclined at 19 and 17° to the same side of the coordination plane (cf. 13 and 11° on the  $\text{O}_2\text{N}_2$  complex).<sup>14,15</sup> and the aliphatic chelate rings are inclined at 19 and 16° to the other side of the coordination plane (cf. 8 and 11° on the  $\text{O}_2\text{N}_2$  complex).<sup>14</sup> In these two complexes, the hydrogen atoms

attached to the two nitrogens forming the six-membered trimethylene chelate ring are orientated toward the same side of the chelate ring, and a chair conformation occurs in each case.

In contrast, in the coordinated macrocycle in  $[\text{Ni}(\text{N}_2\text{-mac})\text{Cl}_2]$ , the hydrogen atoms attached to adjacent nitrogen donors fall alternatively on opposed sides of the donor atom plane. This gives rise to a "skew-boat"<sup>16</sup> conformation for the six-membered chelate ring incorporating N(1a) and N(1b) and leads to the benzylamino chelate rings adopting a "step-shaped"<sup>17</sup> configuration, being inclined at 8 and 11° to opposite sides of the coordination plane. The different conformations of the aliphatic bridges in the three complexes are manifest by the different torsion angles (Table 7S (supplementary material)), particularly about the C(1)-X and C(9)-C(9c) bonds.

A comparison of the respective macrocyclic donor atom planes is given in Figure 3. The relative macrocyclic hole sizes, calculated as twice the mean distance of the donor atoms from their centroid, are tabulated in Table IV. It is apparent that the hole sizes in the  $\text{O}_2\text{N}_2$  and  $\text{N}_2$  systems are quite similar, and this is not unexpected in view of the similarity of the covalent radii of oxygen and nitrogen. Defined in this way, the hole size in the  $\text{S}_2\text{N}_2$  system is much larger, and this can in part be ascribed to the larger covalent radius of thioether sulfur, which leads to the introduction of four long sulfur-carbon bonds in the macrocyclic ring. Relative to the mean C(1)-O and mean C(2)-O bond lengths in  $[\text{Ni}(\text{O}_2\text{N}_2\text{-mac})\text{Cl}_2]$ , the corresponding mean C-S bond lengths in  $[\text{Ni}(\text{S}_2\text{N}_2\text{-mac})\text{Cl}_2]$  are longer by 0.37 and 0.41 Å, respectively, in good agreement with the difference of 0.38 Å between the Pauling covalent radii<sup>18</sup> for sulfur (1.04 Å) and oxygen (0.66 Å). Thus the "circumference" of the macrocyclic great ring is effectively increased, and this is reflected by the larger bites of the chelate rings containing sulfur donors (Figure 3).

Since the nonequivalent donor atoms in the three macrocycles have different covalent radii, it is clearly not appropriate to compare directly the hole sizes given in Table IV when attempting to predict the "fit" of each ring for the nickel ion. Allowance for the respective donor atom radii must first be made. Estimates of the required radii have been obtained: data in the Cambridge Crystallographic Data Centre files (accessed via the CSSR programs)<sup>19</sup> were used to obtain the mean lengths of bonds between high-spin nickel and ether, thioether, and secondary-amine donor functions, and 1.39 Å (the Pauling covalent radius of nickel)<sup>18</sup> was subtracted from each mean. The following values were obtained: O, 0.76 Å (based on 12 bonds);<sup>1</sup> N(sp<sup>3</sup>), 0.72 Å (based on 89 bonds);<sup>1</sup> S, 1.05 Å (based on 17 bonds).<sup>13</sup> Since these "modified covalent radii" values are derived solely from high-spin nickel complexes containing donor types similar to those in the complexes under study, their use for hole-size estimation was considered more appropriate than any of the published covalent radii.<sup>20</sup>

(16) Buckingham, D. A.; Seargeon, A. M. *Top. Stereochem.* 1971, 6, 219.

(17) The very different macrocyclic conformations in  $[\text{Ni}(\text{N}_2\text{-mac})\text{Cl}_2]$  and  $[\text{Ni}(\text{O}_2\text{N}_2\text{-mac})\text{Cl}_2]$  or  $[\text{Ni}(\text{S}_2\text{N}_2\text{-mac})\text{Cl}_2]$  parallel similar conformational differences observed by X-ray for a number of transition-metal complexes of the related, open-chain tetradentate ligand *N,N'*-cylindrene(methylideneamino). For this latter ligand system, the frequency with which both structural types occur strongly suggests that the energy difference between them is small. The ethylene bridge between the two sp<sup>3</sup> nitrogen atoms has an envelope conformation when the complex has a symmetrical saddle (or umbrella) shape, but a gauche conformation when a symmetrical steep geometry occurs. See: Callagran, M.; Nardin, G.; Randuccion, L. *Coord. Chem. Rev.* 1972, 7, 385. Mason, H. S.; Walters, T. N. *Ibid.* 1975, 17, 137.

(18) Pauling, L. "The Nature of the Chemical Bond", 3rd ed.; Cornell University Press: Ithaca, NY, 1960.

(19) Details are given in ref 4.

(14) Similar values are observed<sup>14</sup> in  $[\text{Ni}(\text{O}_2\text{N}_2\text{-mac})(\text{NCS})_2]$ .

(15) Angles of the benzene rings a and b to the respective macrocyclic donor planes:  $[\text{Ni}(\text{O}_2\text{N}_2\text{-mac})\text{Cl}_2]$ , 38 and 39°;  $[\text{Ni}(\text{S}_2\text{N}_2\text{-mac})\text{Cl}_2]$ , 31 and 49°;  $[\text{Ni}(\text{N}_2\text{-mac})\text{Cl}_2]$ , 33 and 41°.

For an estimation of a radius for the cavity occupied by the nickel in each complex, a general procedure of subtracting the mean of the "modified covalent radii" of all the donor atoms from the uncorrected radius of the macrocyclic hole was employed. While obviously such a procedure has its limitations, it does have the virtue of being applicable to a range of macrocyclic complexes and allows comparisons even when different types and/or numbers of donor atoms are present or irregular coordination geometries occur.<sup>21</sup> No other simple semiquantitative procedure for comparing the hole sizes from crystallographic data in such complexes appears to have been proposed previously.

The radii ( $R_A$ ) of the apparent cavities occupied by nickel, for each of the present complexes calculated as above, are listed in Table IV. Both the  $N_4$ - and  $S_2N_2$ -donor complexes give values that are identical with the Pauling radius for octahedral nickel of 1.39 Å while the value of 1.35 Å for the  $O_2N_2$ -donor complex is only slightly less than this radius.<sup>22</sup> It is apparent that the cavities in all three macrocyclic complexes are close to ideal for high-spin nickel. Previously it has been postulated that, along a series of saturated tetraaza macrocycles of increasing ring size, it is the 15-membered macrocycle that will provide the ring of best fit for high-spin nickel.<sup>23</sup> Hence, it is not unexpected that the present 15-membered  $N_4$  macrocycle also provides a ring of nearly optimum size for this ion, especially since the X-ray structural data confirm the absence of any major strain in the various chelate rings of the nickel complex.

Since the hole size in the free  $O_2N_2$  macrocycle in a "planar" configuration has been shown to be the same as that in  $[Ni(O_2N_2\text{-mac})Cl_2]$  and  $[Ni(O_2N_2\text{-mac})NCS_2]$ ,<sup>21</sup> it seems unlikely that undue strain is present in the chelated rings of

this macrocycle even though some conformational changes do occur on coordination. Indeed, along the series of 14- to 17-membered  $O_2N_2$  macrocycles, both the kinetic and thermodynamic stabilities of the nickel complexes reach a maximum at the 16-membered macrocycle although the values for the 15-membered ring system are only slightly lower.<sup>24</sup> This evidence suggests that both ring sizes fit high-spin nickel well, with the optimum hole size perhaps falling between the holes provided by these two ring sizes.

Clearly, for  $[Ni(S_2N_2\text{-mac})Cl_2]$ , the cavity occupied by nickel is again nearly ideal. However, whether the hole size occurring in the macrocycle corresponds to the "natural" (that is, least strained) value or whether some ring expansion (with an accompanying increase in energy) has occurred on incorporation of the nickel atom is difficult to answer in the absence of other studies. Nevertheless, there is little evidence for the presence of marked additional chelate ring strain in this complex, and this suggests that the enlarged macrocyclic ring "circumference"<sup>24</sup> discussed previously is quite effective in compensating for the larger covalent radii of the sulfur donors.

#### Concluding Remarks

The procedure described provides a means of obtaining a generalized picture of hole sizes in macrocyclic systems for comparison purposes. Although it may well be of wider applicability, its use for comparing the present closely related macrocyclic complexes seems particularly appropriate. The results indicate that substitution of two ether oxygens or two thioether sulfurs for two  $sp^3$  nitrogens in the 15-membered  $N_4$  macrocycle gives new macrocycles that are also capable of providing nearly ideal cavities for high-spin nickel(II). Although such cavities could differ from the "natural" hole in the metal-free system, there is little evidence that this is an important consideration for the present complexes.

**Acknowledgment.** K.H., M.M., and P.A.T. thank the Science Research Council (U.K.) for diffractometer equipment and computing facilities. L.F.L. thanks the Australian Research Grants Committee for support, the Australian Institute of Nuclear Science and Engineering for a travel grant, and Professor J. Lewis for assistance during a period spent at the University Chemical Laboratory, Cambridge, U.K.

Registry No.  $Ni(N_4\text{-mac})Cl_2$ , 82891-97-2;  $Ni(S_2N_2\text{-mac})Cl_2$ , 76137-02-5.

**Supplementary Material Available:** Further details of the structure determinations together with listings of interatomic bond lengths and angles, least-squares planes and deviations, structure factors, and data for  $[Ni(O_2N_2\text{-mac})Cl_2]$  additional to those published previously<sup>1</sup> (50 pages). Ordering information is given on any current masthead page.

(20) The "modified covalent-radius" values obtained for N (0.72 Å) and S (1.05 Å) are quite close to the corresponding Pauling covalent radii of 0.70 and 1.04 Å whereas the value for O (0.76 Å) is larger than the Pauling radius of 0.66 Å. The latter value was originally derived from carbon-oxygen bond lengths in organic compounds. However, all three radii correspond reasonably well to other values (based solely on bond lengths in compounds containing homonuclear bonds) of 0.74 (for both O and N) and 1.04 Å (for S). See: Sharpe, A. G. *Inorganic Chemistry*; Longmans, Green and Co.: New York, 1980; pp 127-129.

(21) Tasker, P. A.; Trotter, J.; Landoy, L. F. *J. Chem. Res., Miniprint* 1981, 3834.

(22) An alternative procedure involving subtraction of the donor atoms' "modified covalent radii" from the corresponding observed metal-donor bond lengths and then taking the mean value of the lengths, which remains as the radius ( $R$ ) of the metal ion cavity, gives virtually identical results:  $[Ni(O_2N_2\text{-mac})Cl_2]$ ,  $R = 1.36$  Å;  $[Ni(N_4\text{-mac})Cl_2]$ ,  $R = 1.39$  Å;  $[Ni(S_2N_2\text{-mac})Cl_2]$ ,  $R = 1.38$  Å. However, this procedure is not applicable to metal-free macrocycles. In contrast, the procedure outlined in the main text does not suffer from this disadvantage and thus allows direct comparison of the hole sizes in metal-free macrocycles and their metal complexes.

(23) Busch, D. H. *Acc. Chem. Res.* 1978, 11, 392 and references therein.

(24) As evidenced by the increased donor atom bites involving the sulfur donors.





THE BRITISH LIBRARY DOCUMENT SUPPLY CENTRE

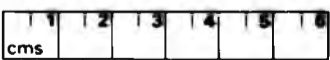
**TITLE** STRUCTURAL BASIS FOR THE DESIGN OF SELECTIVE COMPLEXING AGENTS FOR TRANSITION METALS. ....

**AUTHOR** Laurel .A. Drummond

**INSTITUTION and DATE** NORTH LONDON POLYTECHNIC  
C N A A 1989

Attention is drawn to the fact that the copyright of this thesis rests with its author.

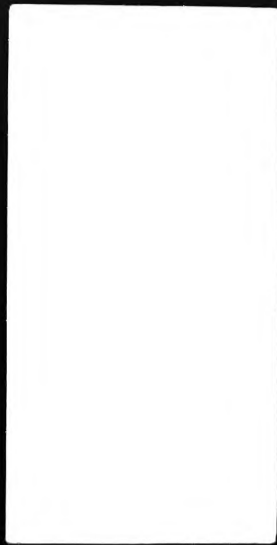
This copy of the thesis has been supplied on condition that anyone who consults it is understood to recognise that its copyright rests with its author and that no information derived from it may be published without the author's prior written consent.



THE BRITISH LIBRARY  
DOCUMENT SUPPLY CENTRE  
Boston Spa, Wetherby  
West Yorkshire  
United Kingdom

REDUCTION X 20

CAMERA 5



**DX**



**87720**

